THE HSV U_L17 PROTEIN: ITS ROLE IN CAPSID ASSEMBLY, TEGUMENTATION, AND INTRANUCLEAR CAPSID MOBILITY

A Dissertation

Presented to the Faculty of the Graduate School

of Cornell University

in Partial Fulfillment of the Requirements for the Degree of

Doctor of Philosophy

by

Luella D. Scholtes

August 2009

THE HSV U_L17 PROTEIN: ITS ROLE IN CAPSID ASSEMBLY, TEGUMENTATION, AND INTRANUCLEAR CAPSID MOBILITY

Luella D. Scholtes, Ph. D.

Cornell University 2009

Employing a novel anti-pU_L17 antibody I have resolved details of the physical relationship between the minor capsid protein, pU_L17, and the herpes simplex virus (HSV-1) capsid and tegument layers. I helped demonstrate that pU_L17 binds externally and multivalently to the capsid, fulfilling a structural role and potentially explaining its function in DNA encapsidation as well.

Immunoprecipitation assays illustrated interactions of pU_L17 with capsid proteins VP5 and pU_L25 as well as tegument proteins VP11/12 and VP13/14. A pU_L17/ pU_L25 capsid-independent complex was detected upon capsid-deficient infection. In wild-type infection, this complex could also be detected independently of capsid. Immunofluorescence studies revealed pU_L17 and pU_L25 co-localization in wild-type infection; moreover, proper localization was co-dependent. While pU_L25-deficient infection yielded a unique mis-localization of pU_L17, the mis-localization phenotype of pU_L25 in the absence of pU_L17 resembled pU_L25 mis-localization without VP23 and VP5.

Deletion of capsid proteins but not all DNA cleavage and packaging proteins increased cytoplasmic concentrations of pU_L25 and pU_L17 though overall protein levels appeared depressed in immunostaining. This observation coupled with poor pU_L25 immunoprecipitation from these mutant viruses, suggests that pU_L25/pU_L17 may undergo conformational changes.

Also, cytoplasmic localization of pU_L25 seems to occur at least in part through Crm-1 nuclear export machinery.

Additional immunoprecipitation studies revealed interactions with VP11/12 and VP13/14. pU_L17 was in turn immunoprecipitated with anti-VP13/14 antibody. Nickel matrix purification of pU_L17 from a pU_L17 C-terminal His-tagged virus also enhanced VP13/14 co-elution independently of VP16. A VP13/14 and pU_L17 immunofluorescence time course demonstrated co-localization in the replication compartment, cytoplasm, and both nuclear and plasma membranes. VP11/12 may mediate cytoplasmic VP13/14-pU_L17 interaction. Upon transfection VP13/14 and pU_L17 were found to co-localize in cytoplasmic puncta only when VP11/12 was expressed.

I also probed for functional roles of pU_L17 including intranuclear capsid transport, DNA-binding, and ATP hydrolysis. All essential encapsidation proteins, including pU_L17 were assayed by time-lapse microscopy for effects on intranuclear motility of GFP-VP26-labeled capsids. No single protein was concluded to deter capsid dynamics, indicating intranuclear capsid movement does not reflect encapsidation and does not require encapsidation proteins. Additionally, pU_L17 was found to bind to pac-1-containing DNA and may have ATPase activity.

BIOGRAPHICAL SKETCH

In 1996 as an undergraduate student at Washington University, Luella Scholtes began her research career studying genetics of plant pathogenesis in Dr. Barbara Kunkel's laboratory. She received a Bachelor of Arts degree from Washington University in 1997 and continued her studies for the following two years in Saint Louis University's Cellular and Molecular Regulation Master's degree program where she researched plant-nematode molecular interactions under the Chairman of the Department of Biology, Dr. Robert Bolla. In 1999, she carried on research in parasitology studying Leishmania at Washington University's School of Medicine under the guidance of Dr. Stephen Beverley, Chairman of the Department of Molecular Microbiology. She arrived at Cornell University in 2002 in pursuit of her Ph.D. from the department of Microbiology under the mentorship of Dr. Joel Baines and completed her Ph.D. work in 2009.

This work would not have been possible without the support and encouragement of my husband, family, and friends. Most especially I would like to recognize my parents who have made many sacrifices throughout their lives to allow me opportunities that they themselves never had.

ACKNOWLEDGEMENTS

I would like to thank the NIH, for the Virology Training Grant which supported many years of this work as well as Dr. Colin Parrish and Sachiko Funaba for their efforts in maintaining this support.

TABLE OF CONTENTS

LIST OF FIGURES

LIST OF TABLES

LIST OF ABBREVIATIONS

3-OST	3-O-sulfotransferase
^{32}P	radioactive phosphorous isotope
^{35}S	radioactive sulfur isotope
A	alanine
A	adenine
AMP-PNP	adenosine 5'-(β,γ-imido) tri-phosphate
ATP	adenosine tri-phosphate
BAC	bacterial artificial chromosome
BDM	2,3-butanedione monoxime
BFLA	bafilomycin A
BHV/BoHV	bovine herpes virus
bps	base pairs
BSA	bovine serum albumin
C	carboxyl
C3(b)	complement protein
$CaCl_2$	calcium chloride
CCSC	C-capsid specific complex
cDNA	complementary deoxyribonucleic acid
CHO	Chinese hamster ovary
CKII	casein kinase II
Cm	chloramphenicol
CMV	cytomegalovirus
CNS	central nervous system
Cos	cohesive

CPE	cytopathic effects
CS	chondroitin sulfate
D	aspartate
dH_2O	distilled water
DIG	detergent insoluble glycolipid
DMEM	Dulbecco's modified Eagle's medium
DNA	deoxyribonucleic acid
DR	direct repeat
DTT	dithiolthreitol
E	glutamic acid
E. Coli	*Escherichia coli*
EBV	Epstein-Barr virus
ECL	electrochemiluminescence
EDTA	ethylenediaminetetraacetic acid
EHV	equine herpes virus
EM	electron microscopy
EMSA	electrophoretic mobility shift assay
ER	endoplasmic reticulum
FACS	fluorescence-activated cell sorter
FITC	fluorescein isothiocynate
Fig	figure
fmole	femtomole
G	glycine
G	guanine
g-	glycoprotein
GAG	glycosaminoglycan

GFP	green fluorescent protein
gp	gene product
GST	glutathione-S transferase
H (2A, 3, 4)	histone (2A, 3, 4)
HA	hemagglutinin
His	histidine
HIV	human immune-deficiency virus
HR	heptad repeat
HRP	horse radish peroxidase
HS	heparan sulfate
HSV (1/2)	herpes simplex virus (serotype 1/2)
Hve (A/B/C)	herpesvirus entry protein (A/B/C)
HVEM	herpes virus entry mediator
Hyg	hygromycin
ICP	infected cell protein
Ig	immunoglobulin
IHF	integration host factor
INM	inner nuclear membrane
IR	inner repeat
ITLV	infectious laryngotracheitis virus
K	lysine
Kan	kanamycin
kb	kilobase
KCl	potassium chloride
K_d	dissociation constant
kD(a)	kilodalton

KSHV	Karposi’s sarcoma herpes virus
L	leucine
LAP	lamin-associated protein
LAT	latency activated transcript
LMN (A/C)	lamin (A/C)
M	Molar
MALDI-TOF MS	matrix-associated laser desorption Ionization-time of flight mass spectrometry
MAP	microtubule associated protein
MDV	Marek’s disease virus
Mg^{2+}	magnesium
MHC	major histocompatibility complex
ml	milliliter
mM	millimolar
MOI	multiplicity of infection
M_r	relative molecular weight
mRNA	messenger ribonucleic acid
mw	molecular weight
N	amino
NaCl	sodium chloride
NaH_2PO_4	sodium phosphate (monobasic)
Na_2HPO_4	sodium phosphate (dibasic)
Na_3VO_4	sodium vanadate
NBCS	newborn calf serum
ND10	nuclear domain 10
Ni++	nickel

Ni-NTA	nickel-nitrotriacetic acid
NLS	nuclear localization signal
nM	nanomolar
nm	nanometer
NPC	nuclear pore complex
ORF	open reading frame
Ori (S/L)	origin of replication (S/L)
ONM	outer nuclear membrane
p	probability
pac	packaging
PAGE	polyacrylamide gel electrophoresis
PBS(T)	phosphate buffered saline (with Tween)
PFD	pro-fusion domain
PFU	plaque-forming units
PG	phosphoglycan
pH	power of hydrogen
PI-3	phospho-inositol-3
PK (A/C)	protein kinase (A/C)
pmole	picomole
PMSF	phenymethanesulphonylfluoride
PNK	polynucleotide kinase
PRR1	poliovirus-related receptor 1
PrV	pseudorabies virus
R	purine
RFP	red fluorescent protein
RIPA	radioimmunoprecipitation assay

RNA	ribonucleic acid
rpm	revolutions per minute
RSC	rabbit skin cell
SDS	sodium dodecyl sulfate
STE	sodium Tris EDTA
T	threonine
T	thymine
TAE	Tris-acetate EDTA
TBE	Tris boric acid EDTA
TAP	tandem-affinity purification
TGN	trans-Golgi network
TLC	thin-layer chromatography
TLR	toll-like receptor
TNFR	tumor necrosis factor receptor
TR	terminal repeat
U_b	unique region b
U_c	unique region c
U_L	unique sequence long
U_S	unique sequence short
μg	microgram
μm	micrometer
V	volts
vhs	virus host shut-off
VP	viral protein
VSV	vesicular stomatitis virus
VZV	varicella-zoster virus

w/v	weight/volume
Zn^{2+}	zinc

LIST OF SYMBOLS

α	alpha/ immediate-early
α	anti-
β	beta/ early
δ	delta
Δ	deletion
γ	gamma/ late
λ	lambda phage
‘	prime
%	percent
^{0}C	degrees Celsius
-	null
Å	angstrom
^{R}	resistant

PREFACE

“Life is like a box of chocolates, Forrest, you never know what you are going to get…” *-Forrest Gump, 1995*

Thinking back on when I began my dissertation research project with very few clues in the literature, many more questions than answers, and no experience in virology, it is amazing to see both the scientific and personal evolution and development that has taken place.

When choosing to work on pU_L17, I remember being drawn by the adventure of not knowing where this project would take me. Like being given only a handful of pieces to an intricate puzzle, it is difficult to guess what form will actually take place. Determining the roles that this protein plays has certainly been challenging. The nearly unrestricted possibilities of investigation allowed me to ask a wide variety of questions. Although many of these pursuits were unsuccessful, in the end we have formed new ideas about the structural and functional roles of pU_L17 and the process has been invaluable to my development.

Science research really is like a box of chocolates, and in the pages that follow I have selected my favorite varieties to share.

CHAPTER I:

INTRODUCTION

Introduction:

Viruses of the herpesviridae can infect both humans and animals. HSV-1, or herpes simplex virus serotype 1, is a member of the alpha herpesvirus subfamily of the Herpesviridae family. They are divided into three classes: the alpha-, beta- and gammaherpesviruses. The alphaherpesviruses are characterized by their destruction of their host cell (CPE, cytopathic effects including multi-nucleated giant cells) and can form syncytia, or fused cells, in certain cell lines that is mediated by insertion of viral proteins into the host cell plasma membrane (104, 225). Members of each class can infect humans, namely: (alphaherpesviruses) HSV-1, HSV-2, and varicella zoster virus (VZV); (betaherpesviruses) roseolovirus and cytomegalo virus (CMV); (gammaherpesviruses) Epstein-Barr virus (EBV) and Karposi's Sarcoma herpesvirus (KSHV).

Clinical Effects:

Clinical symptoms of HSV infection range from oral and genital lesions to corneal blindness and encephalitis. Most commonly HSV-1 causes oral herpetic lesions in contrast to the primarily urogenital lesions seen from HSV-2 infection. However, the two viruses are remarkably similar in sequence and it is clear that cross-transmission occurs (68); HSV-1 can be isolated from urogenital lesions and HSV-2 is sometimes found in oral lesions .

Initially, HSV targets mucosal epithelial cells in which a lytic cycle of infection takes place. Progeny of the lytic round of infection are either released into the extracellular space, or are transmitted directly through a cell-cell spread mechanism into neighboring epithelial cells. Extracellular particles may re-infect locally or at a distance from their origin. Released virus particles target either more epithelial cells for additional rounds of lytic infection, or neurons, the cellular reservoir for latent HSV infection. Once harbored in a neuron, HSV can either remain latent, or can spread through the CNS through synaptically-linked neurons. Transneuronal spread through the CNS may cause fatal, HSV-induced encephalitis.

Herpesviruses are unique in establishing a true molecular latency in infected neurons. The molecular mechanism of HSV latency is poorly understood; however, it is clear that viral transcription is nearly completely abolished save LATs, or latency associated transcripts. These transcripts along with the immediate early protein, ICP0, play a role in re-activation to a lytic infection from the latent state.

Virion organization:

All herpesviruses share the same general architecture; the virion is composed of four main layers: envelope, tegument, capsid, and genome (Figure 1.1). The outermost layer is a lipid bi-layer envelope that the virion acquires as it leaves an infected cell. The envelope contains a variety of virally encoded glycoproteins that are crucial for the virion's ability to enter another cell. Beneath the envelope lies an asymmetric, proteinaceous layer unique to herpes viruses coined the tegument. Proteins in this compartment

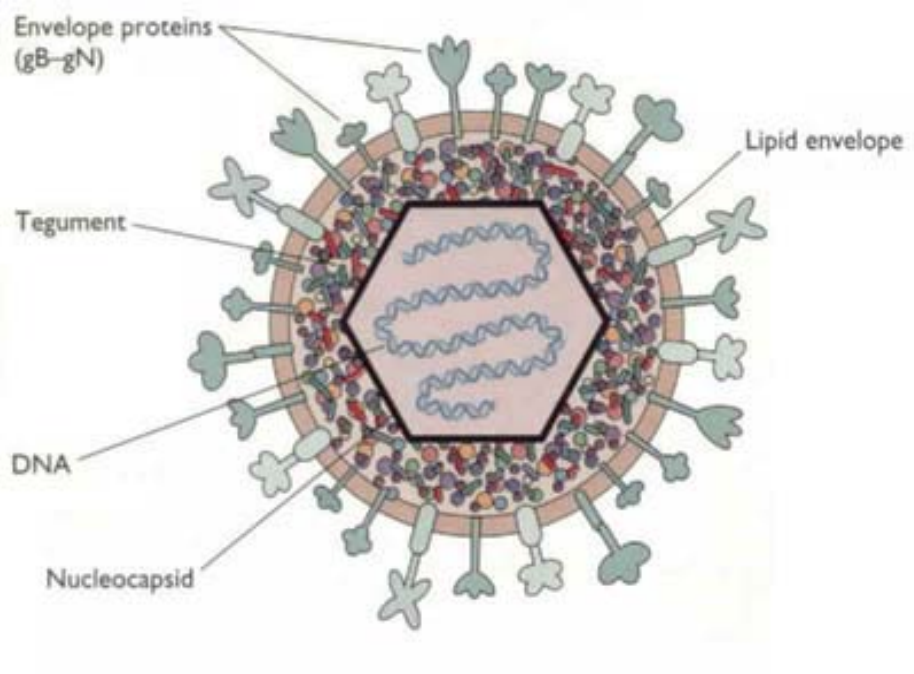

Figure 1.1 Conserved structure of Herpesviridae virions. Virions consist of four main layers: envelope, tegument, capsid, and genome. (Taken from http://bioinfo.bact.wisc.edu/themicrobialworld/hsv1struc.jpg)

perform a wide range of functions that enhance success of replication. Much of the virus' strategic actions such as giving preference to viral gene expression over that of the host and evading immune system detection are carried out by these proteins. The tegument lies between the envelope and the capsid. The capsid is a structure used to transport the genetic material of herpesviruses to and from their location of replication, the nucleus. The central domain is exclusively made up of a double-stranded DNA genome which encodes all the proteins essential for infection.

Genome:

The highly-structured 152 kilobase-pair HSV genome is divided into 2 unique coding regions coined the unique long (U_L) stretching 108 kilobase pairs and the unique short (U_S) containing 13 kilobase pairs (Figure 1.2). Each of these regions is flanked by inverted repeats. Repeated sequences flanking the U_L and U_S components are designated the IR_L and IR_S for inner repeats long and short. This terminology is necessary to distinguish the inner repeats from a separate set of repeated sequences, the terminal repeats, TR_L and TR_S that are located at the outermost regions of the genome. It is not entirely clear in exactly what manner HSV uses these many repeated sequences, but it is proposed that the inner repeats and terminal repeats offer HSV a recombination competent landscape, which may play a crucial role in the virus' replication strategy.

Another repeat-containing region called the *a* sequence has a more clearly understood role in HSV replication. The *a* sequence separates the inner repeats, IR_L and IR_S, and is also partially present at each of the terminal

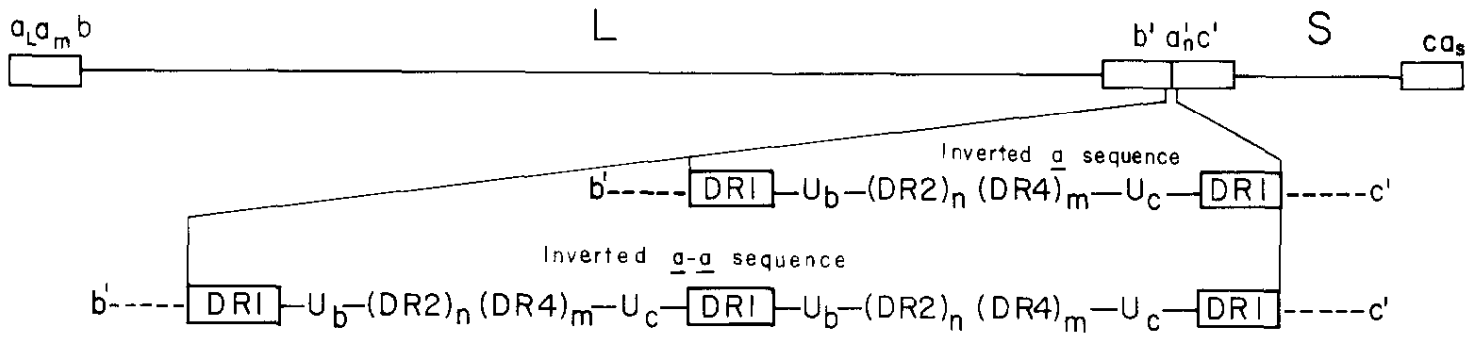

Figure 1.2 Schematic layout of HSV genome. Two unique regions (L=long, S=short) of coding sequence are separated by internal repeats and flanked by terminal repeats (open boxes). The “a” sequence lies between the internal repeats, DR, direct repeat; U_b and U_c unique regions containing pac1 and pac2, respectively (168)

ends (168). A 20 base pair direct repeat (DR1) defines the ends of the *a* sequence (168). A sequences also contain two regions of unique sequence U_b and U_c that are divided by a series of directly repeated sequence. Within the unique stretches of the *a* sequence there are two distinct packaging elements (pac sites), pac1 present in U_b and pac2 in U_c (60, 232). Electrophoretic mobility-shift assays using a U_b oligonucleotide as probe DNA suggest that a putative HSV terminase protein, pU_L28, recognizes and binds to single-stranded pac1 DNA (2). This interaction is specific for pac1 as samples using a U_c fragment containing pac2 are not altered in electrophoretic mobility (2). Mutant U_c oligonucleotides failed to bind to, or bound less efficiently to purified U_L28 protein, demonstrating specific recognition of the pac1 sequence within the U_c oligonucleotide. Additional experiments found this protein-DNA interaction to be DNA structure specific as only the more slowly migrating DNA species indicative of structured DNA were altered when protein was added (2). This evidence supports the hypothesis that pU_L 28 recognizes a specific HSV sequence to aid in proper cleavage of concatemeric genomic DNA at a single genome-length and subsequent packaging into capsids. Although the exact roles of HSV's many repeats are not known, it is likely that studies of these genomic structural elements will further elucidate HSV's mechanism of genomic replication.

Entry/attachment:

After HSV virions exit an infected cell, they target another epithelial cell by attaching to host cell-surface glycosaminoglycans (GAGs) that serve as receptors and support fusion to the host membrane. The mechanisms of

attachment and fusion (penetration) make use of host cell receptors and co-receptors, respectively, which are contacted by viral envelope glycoproteins (Figure 1.3). There is redundancy in these interactions contributed by both the virus and the host cell making if difficult to identify essential components of attachment. The HSV virion displays 12 glycoproteins on its surface, many of which facilitate entry (reviewed in (30, 108, 116, 204). GAG chains are commonly found on various cell surface proteoglycans (PG) thus presenting HSV with multiple attachment receptors. For example, the GAG chains of both heparin sulfate (HS) and chondroitin sulfate (CS) can function in HSV cell surface attachment (153). Cells devoid of all GAGs show lower infectivity, but still do not completely abolish HSV entry, highlighting HSV's mechanistic versatility (226).

The kinetics of HSV entry initially determined that the process could be broken down into at least three phases: initial attachment, stable attachment, and penetration (155). Attachment stages can be differentiated from penetration by temperature control. Attachment, unlike penetration, still occurs at 4^0C, leaving virions in an arrested state on the host cell surface. Extracellular, unattached virions can be inactivated by low pH and washed away. Studies deleting either viral glycoprotein gC or gB showed decreased attachment and infectivity, and deletion of both gC and gB severely hampered infectivity (91, 134, 227). It has been proposed that attachment through gC and gB functions primarily to bring the viral envelope into close enough proximity to the host cell membrane to allow for penetration.

Substantial evidence shows gC binds to heparan sulfate to initiate attachment. Heparan sulfate or heparin was first determined to be the receptor of HSV-1 and HSV-2 in assays that blocked infection by competing

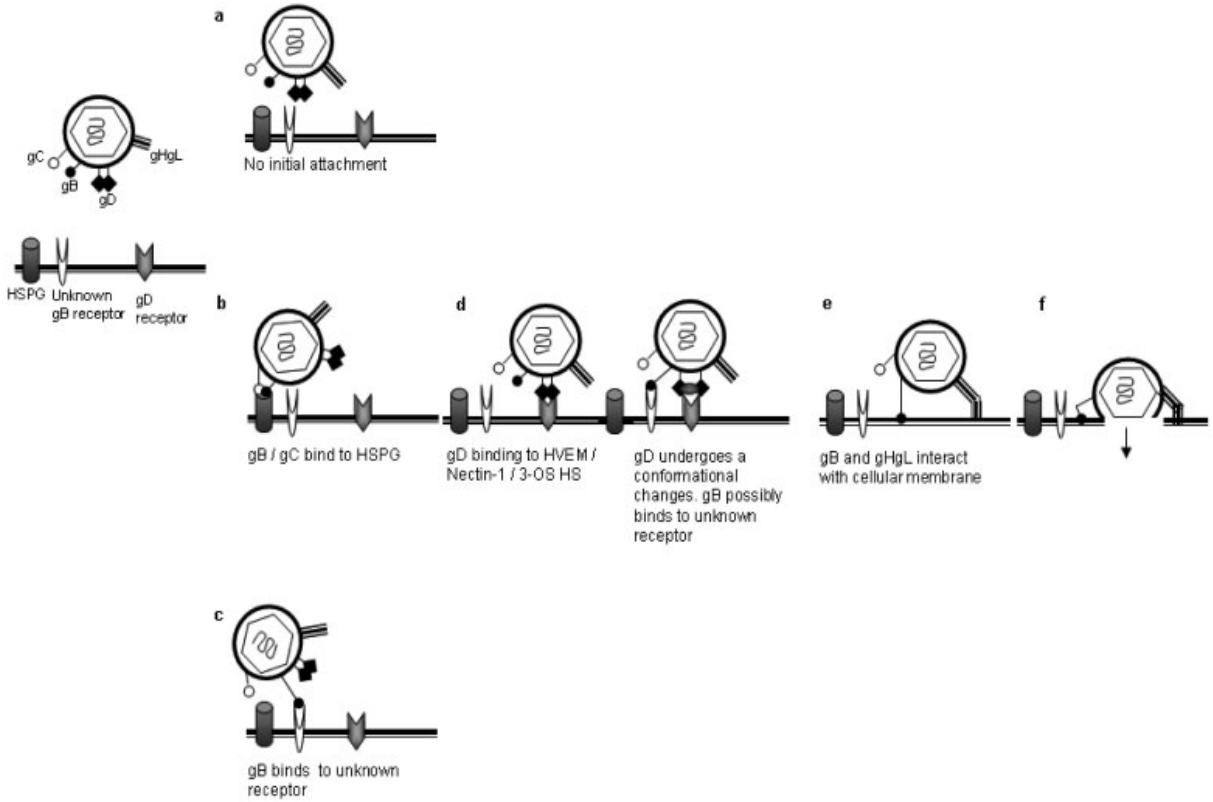

Figure 1.3 Protein-binding interactions in attachment and penetration. Non-specific attachment through gB/gC binding HSPGs (b) is followed by a more specific binding of gD and gB to host-cell receptors (c, d), and the virion is brought closer to the membrane to become fusion competent with gH/gL binding (204).

for heparan sulfate binding (276). Subsequent studies used Chinese hamster ovary (CHO) cells that are deficient in the synthesis of GAGs to assay HSV attachment (142). Virus binding to these mutant cells was severely impaired (219). Glycoprotein C has been shown to bind heparin. Virions deficient in gC showed decreased ability to bind heparan sulfate receptors at the cell surface. Of those particles that could bind, penetration was also impaired (111, 227, 256). Additionally, *in vitro* affinity chromatography experiments determined that both gC and gB can bind heparin Sepharose (112). Binding is thought to occur through electrostatic interactions between positively-charged glycoprotein domains and negatively-charged heparan sulfate moieties. Mutational studies mapped the heparin binding domain of gC to charged amino acid residues in an antigenic site (152, 255). An antigenic region, determined by reactivity to various monoclonal antibodies, is externally displayed, thus it must be accessible in the proteins native form, making this portion of the protein a likely candidate for receptor binding. Mutations of specific amino acids within two distinct regions of gC decreased attachment, and synthetic peptides of the two regions also inhibited infection (255).

Glycoprotein C can also bind C3b, a component of the host immune response complement pathway (84). Infection with HSV induces the display of complement C3 receptor, on epithelial cell surfaces (46). C3b receptors are normally present on human blood cell surfaces and function to inhibit complement activation through accelerating the decay of C3b convertase enzymes or to opsonize pathogens targeted with C3b. Binding of gC to C3b appears to occur independently of entry and is thought to promote immune evasion by neutralizing C3b.

Glycoprotein B has similar properties to gC in that it can also bind to HSPG. Although gC plays a significant role, some infectivity remains upon infection with a gC null virus, indicating that HSV has other sources of attachment. Upon glycoprotein C-null virus infection, absence of heparan sulfate was found to further attenuate infectivity, thus it was determined that HSV was able to bind multiple attachment proteins (110). Deletion analysis of gB revealed an N-terminal poly-lysine rich domain critical for interaction of gB with heparan sulfate (134). Additionally, double mutant recombinant viruses (gC-/gB-) are more severely attenuated than either single mutant (110, 134). Since the effects of gC and gB are additive, these results argue for independent functions of both glycoproteins. Although the contribution of gC in HSV-1 attachment appears to be more significant than gB, the reverse importances of the roles for these proteins have been shown upon HSV-2 infection (43, 134).

The role of gB in HSV attachment is less clear than that of gC. Studies show that gB, unlike gC, is essential for HSV infection despite the dispensable role of heparan sulfate in infection (29). Therefore, gB must also have a role outside of its interactions with HSPG or CSPG because both proteoglycans are not essential for HSV entry. A compilation of data suggests gB may bind another, yet unidentified receptor (20). Soluble HSPG analogs were used to competitively block binding and cell lines lacking either HSPG only or HSPG and CSPG were also assayed for binding. In both cases, the abrogation was enough to block attachment of gC completely; however, blockage of gB attachment was incomplete (20). It is possible that gB's binding to HSPG might preface a second interaction with a more specific receptor, or gB may just have the ability to bind multiple receptors.

Curiously, gB fractionates into detergent-insoluble glycolipid-enriched (DIG) membranes called lipid rafts. Lipid rafts are cholesterol-rich microdomains of the plasma membrane that function to organize membrane proteins and perform signal transduction in response to external stimuli. The possibility that HSV uses lipids rafts in entry has been suggested (31); however, studies failed to show any known HSV penetration receptors (HVEM or nectin-1) or other HSV glycoproteins (gC, gD, gH) in DIG fractions (21). The search to identify another receptor for gB to explain its essential role in HSV replication and clarify its interactions with lipid rafts is still underway.

Entry/penetration:

Attachment is the first step in entry, and is thought to cause a loose association between the viral envelope and the host cell membrane, possibly the result of the virion tumbling around the host cell surface. Following attachment, a more specific interaction between viral fusion protein gD and a host cell co-receptor promotes penetration, the second stage of viral entry, via envelope fusion to the plasma membrane. The mechanism of entry is still not entirely clear because, like attachment, penetration is also complicated by multiple mechanisms, the redundancy of HSV glycoprotein functions, and the variety of cells that can be infected.

gD has several receptors; the two best-studied that allow entry in all clinical isolates tested (129) are HVEM (Herpes Virus Entry Mediator) or HveA (herpesvirus entry protein A) and nectin-1 or HveC (herpesvirus entry protein C). The original receptor names, TNFRSF14 and poliovirus receptor-related protein 1 (PRR1), were based on protein family membership, but have since been renamed HVEM (HveA) and nectin-1 (HveC), respectively. HVEM

(HveA), a member of the tumor necrosis factor receptor (TNFR) family mediates entry of most strains of HSV-1 and HSV-2 (170). In contrast, nectin-1 (HveC), a cell-cell adhesion protein and a member of the (IG) immunoglobulin superfamily, appears more permissive, as it promotes fusion of many alpha herpes viruses including HSV-1, HSV-2, BHV, and PrV (51, 92). HveC binds to each gD species with different affinity (51). Curiously, the HVEM (HveA) and nectin-1 (HveC) receptor proteins are structurally unrelated and their expression patterns are distinct. Although both are expressed in epithelial cells and fibroblasts, only nectin-1 is present on neurons, arguing for the importance of nectin-1 as the HSV receptor on neuronal cells. HVEM (HveA) is expressed on other cell types such as liver, lung, kidney, spleen, and peripheral blood leukocytes, but any role for these cells in HSV infection is not yet clear. However, it has been suggested that HVEM's lymphoid tropism may aid HSV in preventing apoptosis (91).

A third receptor, nectin-2 (HveB) another member of the immunoglobin superfamily, binds HSV, but unlike the aforementioned receptors, nectin-2 differentiates between HSV-1 and HSV-2, allowing HSV-2 fusion in all strains but only limited HSV-1 fusion (267). Nectin-2, like nectin-1, also binds PrV gD but unlike nectin-1 does not bind BHV gD (267) and certain gD amino-terminal point mutants, rid1 and rid2 bind exclusively to nectin-2 . Nectin-2 also has a splice variant (nectin-2 delta) in which the ectodomain is identical to nectin-2 but the transmembrane and cytoplasmic domains are altered. The nectin-2 delta isoform, unlike the full-length nectin-2, also allows binding of BHV (161). gD amino-terminal point mutants such as rid1 and rid2 can enter only through interactions with nectin-2 (170).

A fourth, non-protein receptor of gD, sulfate-modified heparan sulfate, was identified when a cDNA screen showed 3-O-sulfotransferase-3_B was capable of conferring susceptibility to CHO (Chinese hamster ovary) cells, which are naturally resistant to HSV infection (221, 249). Multiple isoforms of 3-OST-3 from mouse or human can render CHO cells susceptible, indicating that a 3-O-sulfate modification of HS by multiple enzymes is sufficient to allow entry. An oligosaccharide library derived from 3-OST modified HS was reacted with gD to reveal one particular octasaccharide of HS critical for the interaction (146). The K_d determined for the octasaccharide's interaction with gD was 10-fold higher than that of complete HS with gD, possibly due to multiple gD binding sites (146). The crystal structure of gD supports this result and proposes two potential binding sites for 3-O-sulfated HS, one very near the HveA binding site (33). Others confirmed a role of 3-O-sulfated HS in HSV entry demonstrating cell-cell fusion in a luciferase reporter gene fusion assay using glycoproteins B, D, H, and L (248). Taken together, these data indicate that 3-O-sulfated HS can be sufficient as a receptor for HSV fusion despite not being essential for entry.

gD is also essential for HSV entry (143). Infection is blocked in the presence of either soluble gD or anti-gD antibodies. Conceptually, the sequence of the gD ectodomain can be divided into two functional domains, the N (amino)-terminal domain containing receptor binding sites (amino acids 1-260) and the C (carboxy)-terminal pro-fusion domain (PFD) encompassing amino acids 260-310. In pull-down experiments using a GST (glutathione S-transferase) tagged pro-fusion domain, multiple sites in the carboxy terminal half (PFD) of gD were concluded to interact with a truncated amino-terminus of gD in the absence of gD receptor binding (89). However, GST-gD PFD was

not able to pull-down longer truncations of gD, presumably because they retained internal PFD that were blocking accessibility of GST-gD. The presence of either HVEM or nectin-1 soluble receptor precluded the self-interaction of gD, leading to the hypothesis that gD folds back on itself forming a “closed” structure, which has since been confirmed by structural data (33) (Figure 1.4). In the presence of receptor, a conformational change is triggered such that gD self-interactions are lost in exchange for receptor-binding interactions (89). Thus it has been suggested that this “open” conformation of gD may trigger fusion between HSV envelop and the host cell plasma membrane.

Crystal structures of both gD alone as well as gD bound to HVEM have been determined, and comparison indicates a conformational change occurs upon binding (33). This is a common trend in virology throughout many viruses including influenza, HIV, and Ebola, which all encode similar fusion peptides that are triggered during fusion to undergo a conformational change (reviewed in (270)). In gD an amino-terminal region containing the receptor binding domain remains flexible in the unbound state but changes into a hairpin loop with a long alpha helix when gD was bound to HveA (33). However, a mutant gD with an engineered di-sulfide bond intended to stabilize the hairpin loop structure was insufficient to induce fusion indicating that additional factors are needed (50). This suggests that either gD is not the fusogenic molecule of HSV, or that it acts in concert with another essential glycoprotein either gH/gL or gB to initiate fusion.

Despite the revelation of gD’s structure and the HVEM binding site, the exact nectin-1 binding domain remained elusive. It is clear that the binding domains of HVEM and nectin-1 are overlapping, since each receptor in soluble

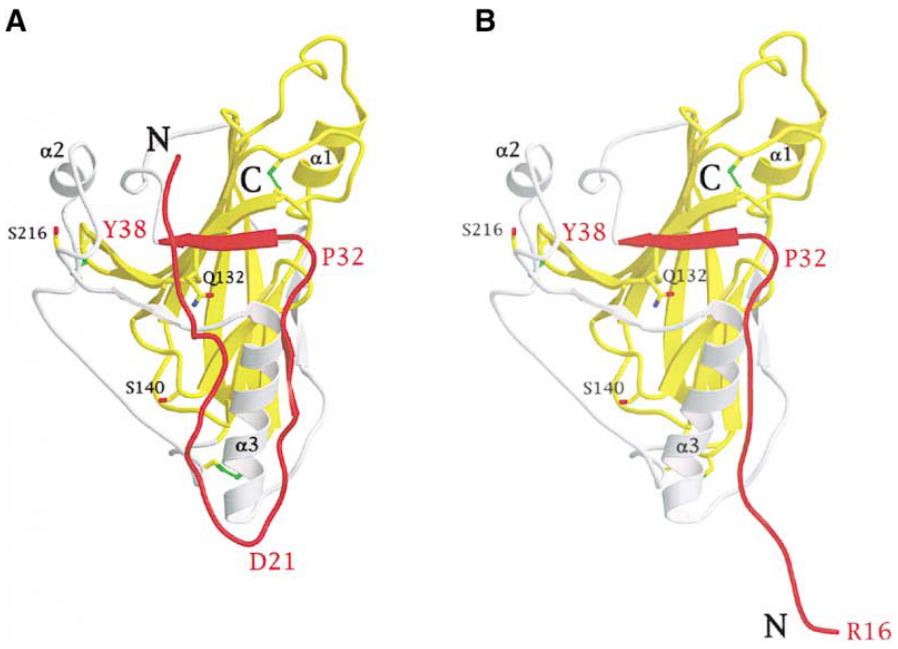

Figure 1.4 Conformational change in gD N terminus. (A) hairpin loop shown in red is in "closed" conformation in receptor-bound conditions. (B) "open" conformation of gD in unliganded state (33)

.

form can block entry through the other. Also, some gD monoclonal antibodies can prevent binding by both receptors. However, other gD monoclonal antibodies will specifically block HVEM or nectin-1, indicating that although these two receptors may share overlapping binding domains on gD, at least part of the binding sites is distinct. Connolly et al propose a nectin-1 specific interaction region of gD (50). Point mutations of gD at amino acid 38 and at other amino acids positioned locally on the same surface disrupted nectin-1 binding. This proposed “hot spot” for nectin-1 binding is located adjacent to the HVEM binding site of gD (50).

The minimal set of glycoproteins required for HSV fusion is composed of gB, gD, gH and gL. However, in the absence of any one of the proteins binding still occurs, presumably through gC, but penetration does not. In infected cells, gH and gL form a heterodimer in which each in the absence of the other is not trafficked properly to ultimately be displayed at the plasma membrane, or incorporated into exiting virions (117, 125). The transmembrane domain of gH, retains the protein in the ER in the absence of gL; whereas gL is secreted without gH. The interaction domain of each of these proteins has been mapped, and not surprisingly, mutants of gL that disrupt the gH binding domain are deficient in penetration. However, deletions of gL outside of the gH-binding region which retained gH-gL protein-protein interactions yet failed in fusion assays elucidated a proposed chaperone domain in gL (125). Thus, the current model suggests after protein synthesis, gH and gL interact so that gL can ensure proper folding of gH. Glycoprotein H, in turn, anchors the complex to cytoplasmic membranes where upon budding, both are integrated onto the virion so that they can aid in penetration of the virion into another cell.

Immunoprecipitation studies found that a complex containing gB, gD, gH, and gL and HVEM receptor could be detected only transiently after infection. At zero minutes post infection, the complex could not be immunoprecipitated, and similarly, by 30 minutes post infection the complex had dissociated (94). Transfection of expression plasmids of gD, gB, gH, and gL demonstrated that this complex could be reconstituted in the absence of any other viral proteins (7). Immunoprecipitation studies from infection with recombinant viruses deleted for each of the essential entry glycoproteins or from selective transfection of various expression plasmids attempted to order the sequence of protein interactions. Both experimental approaches concluded that interaction of gD with HVEM receptor initiated complex formation and was paramount for other protein-protein interactions (7, 94). Following gD recognition of receptor, gB is added, and subsequent to and dependent on gB integration, gH and gL are incorporated to complete the complex (94).

Recent evidence suggests either gB or gH, rather than gD, is the HSV fusion protein and that gD's role is primarily in attachment. Currently, most reports claim gH as HSV's candidate fusion protein; support for this is drawn from many properties of gH. The ectodomain of gH has a hydrophobic alpha helix located internally in the peptide that is positionally conserved in all herpesviruses (95). Furthermore, a swapping experiment replacing the entire HSV gH protein with the gH protein of VZV sustains viral replication, indicating the functional conservation as well (95). Additionally, mutations within this alpha helix confer loss of infectivity and loss of cell-cell syncytia formation. Also, supplementing defective gH with gp41 or G, the HIV or VSV fusion protein, respectively, partially restores infectivity (95).

One of the strongest pieces of evidence suggesting gH bears the fusion peptide, is its ability to form a coiled-coil structure through heptad repeats (Figure 1.5) (96). In addition to the conformational change of fusion proteins previously discussed with respect to gD, another canonical structural feature of class 1 viral fusion proteins is the formation of an alpha-helical coiled-coil through protein multimerization. Influenza virus, for example, uses a trimer of coiled-coil hemagglutinin (HA) alpha helices in the form of a hairpin to effectively form a six-helix bundle (28).

Peptide modeling predicted amino acid substitutions of two residues of heptad repeat 1 (HR1), E450G and L453A, would abolish coiled-coil formation. This virus created by site-directed mutagenesis demonstrated loss of infectivity, inability to complement a gH deletion, and cell-cell fusion despite proper functioning of gL as indicated by heterodimer formation, gH folding, and gH localization (96). Similar mutational analyses were later done with a second, downstream heptad repeat 2 (HR2); mutations created based off of a model design to either increase or decrease the likelihood of coiled-coil formation. The effects of the alterations on fusion paralleled the proteins ability to form the structure (97). Synthetic peptides mimicking HR1 and HR2 were found to bind one another; moreover, competition with HR1 or HR2 peptides inhibited fusion in a dose-dependent manner, though curiously the HR1 synthetic peptide induced inhibition was specific for HSV-1 and had no effect on HSV-2 infection (97). This inhibition of infection could be reversed with the simultaneous presence of both HR1 and HR2 synthetic peptides (97).

Taken together, these data indicate the coiled-coil formation of HR1 and HR2 is independently important for infectivity. Additionally, HR1 and HR2 most likely interact with one another. Individual gH HR sequences may form

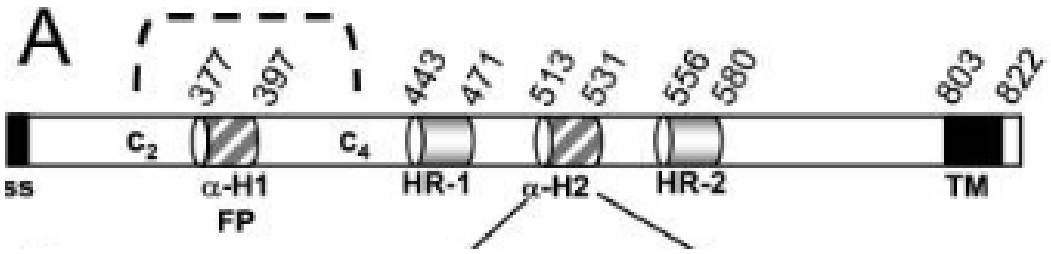

Figure 1.5 Arrangement of primary amino acid sequence of gH. SS, signal sequence; C, cysteine; HR, heptad repeat; TM, transmembrane domain; FP, candidate internal fusion peptide (93)

.

coiled coils that can structurally result in a hairpin loop. Whether gH's self-interactions are capable of creating a canonical six-helix bundle, or whether interactions with another glycoprotein, perhaps the hairpin of gD, are necessary to complete HSV fusion machinery remains unclear. Yet it is certain that the complexity of glycoproteins needed to execute fusion, gB, gD, gH and gL, makes HSV different from other class 1 fusion viruses.

Most recently, the structure of gB suggests that the gB ectodomain shares structural properties with the fusion protein G of Vesicular Stomatitis Virus (VSV) (Figure 1.6), a rhabdovirus with a single stranded RNA genome, as well as the fusogenic gp64 protein of Baculovirus, thus leading to its designation as a class III fusion protein (105). Historically, fusion proteins were divided into either class I fusion peptides or class II fusion peptides. Class I fusion proteins are characterized by their conserved three-stranded coiled-coil "spike" structure and amino-terminal fusion peptides. In contrast, class II fusion proteins are structurally less pronounced and maintain a single internal fusion loop. The newest category of fusion protein merges qualities of both class I and class II proteins. Class III proteins form three-stranded coiled coils but also carry an internal fusion loop; however, the hydrophobic fusion loops of class III proteins vary slightly from class II in that they are bipartite.

Previous studies have shown that gB interacts with cells through a receptor that is independent of HS and CS, and bound gB protein is sufficient to block subsequent entry (20). Mutations in the potential internal fusion loop of gB were found to block or impair entry to cells just like the wild-type gB protein, implying the receptor binding domain was not altered upon mutation of the potential fusion loop (105). However, these fusion loop mutant gB proteins

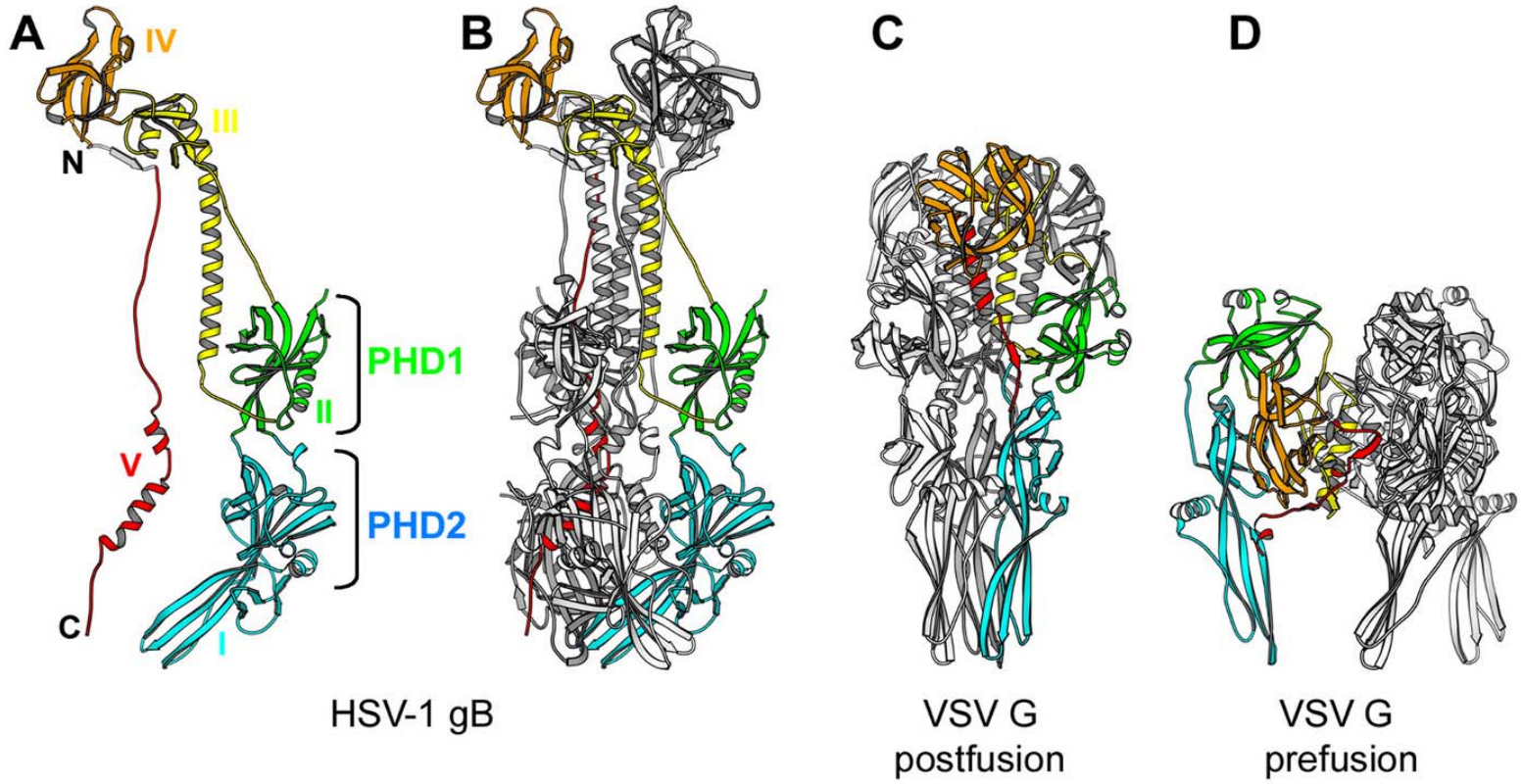

Figure 1.6 Structural similarity between HSV gB and VSV G proteins. Three-dimensional ribbon diagrams of monomeric (A) and trimeric (B) ectodomain of HSV gB protein (aa 111-725); VSV G protein post-fusion (C) and pre-fusion (D) (108).

could not bind liposomes (105). These data suggest that gB, like gH, may also be an HSV fusion protein. Whether or not these two proteins act in concert, or individually remain unknown.

The field of HSV entry is further complicated by the debate on where penetration takes place. Originally, dogma based on electron micrographs presented HSV fusion solely at the plasma membrane (88) (Figure 1.7). A more recent study performing cryo-electron tomography has documented fusion intermediates thus providing a clearer picture of envelope fusion (154). Although the plasma membrane undoubtedly can be a site of penetration, other studies indicate that this simplistic viewpoint does not represent a complete perspective on HSV entry pathways. Many variables such as the cell type, energy requirements, and pH determine the use of different pathways of virus uptake.

Electron micrographs of enveloped HSV particles in cytoplasmic, vesicular compartments less than 30 minutes after infection, strongly argue that HSV can make use of the endocytic pathway (187) (Figure 1.8). Entry by endocytosis may also be called internalization, a stage that is temporally and spatially distinct from penetration. Internalized particles have been taken up within the cell, but still technically reside in an extracellular environment within vesicles. Cytoplasmic, endocytosed virions have been readily observed in HeLa cells and CHO cells bearing nectin-1, and also occasionally found in Vero cells, albeit at a much lower frequency (187). The endocytic pathway as a route of entry clearly appears to be cell type-specific as cytoplasmic, naked capsids are not observed in HeLa and nectin-1 expressing CHO cells, and conversely most virus entry in Vero cells results in naked capsids, indicative of

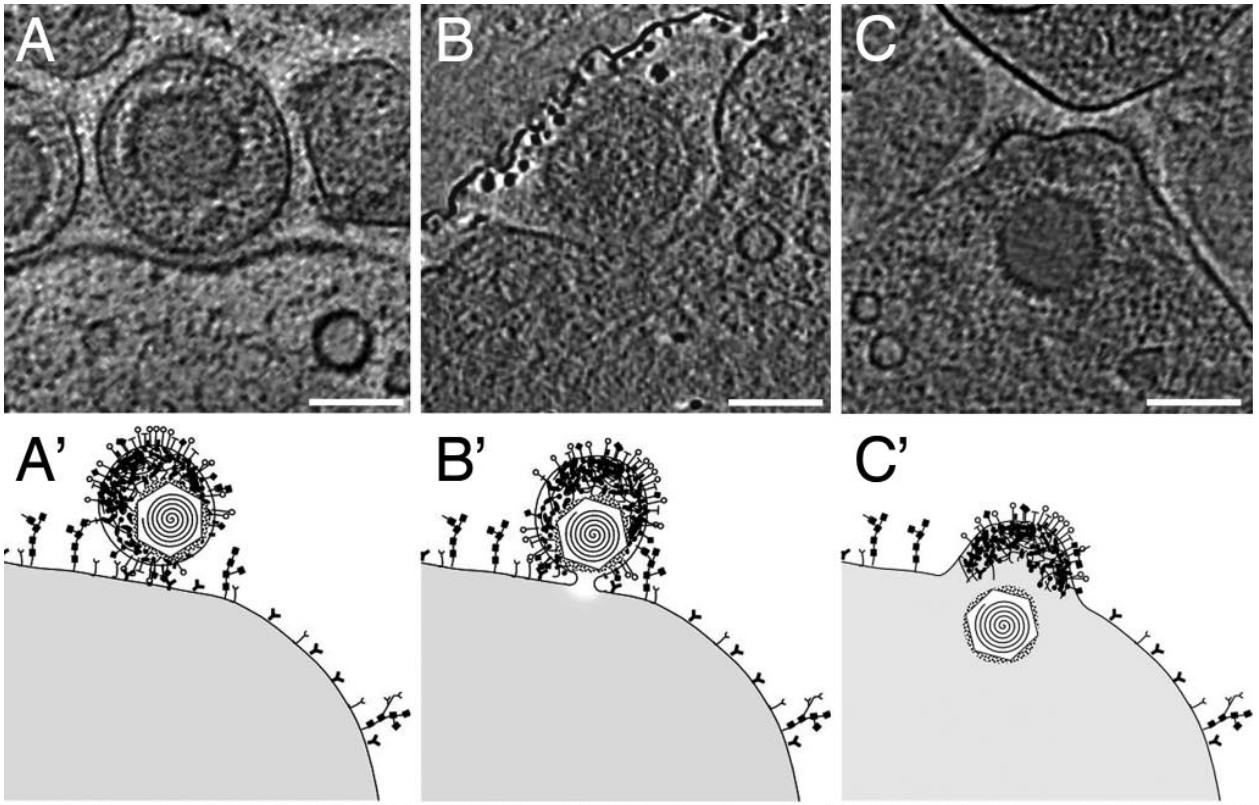

Figure 1.7 Virion entry by fusion at the plasma membrane (154).

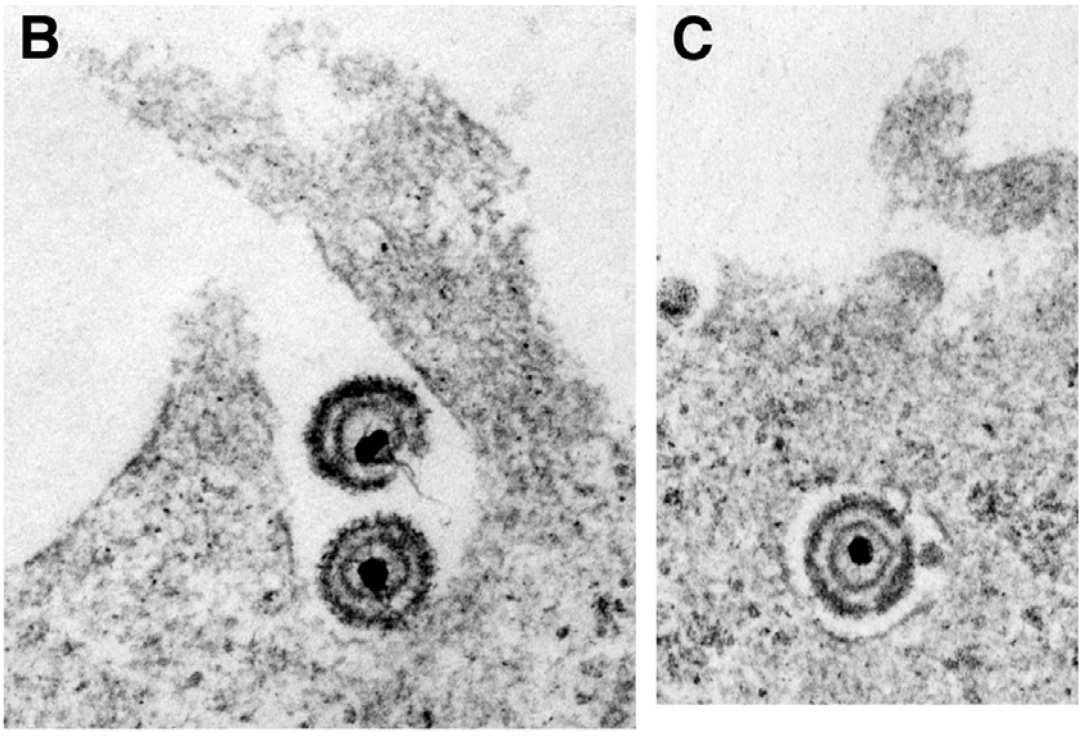

Figure 1.8 Virion entry by endocytosis (187).

fusion at the plasma membrane (88). Endocytosis of HSV into cells appears to occur very quickly. In protease protection assays accessible virus had a half-life of only 9 minutes, and within 30 minutes, nearly all virus was endocytosed (188). Concomitant envelope loss was also shown (188).

Endocytosis of HSV into HeLa and CHO cells does not require gD but does require compartment acidification. In the absence of gD-receptor binding and penetration, CHO cells still take up particles though these are sent to the lysosome for degradation. Thus gD/ligand binding is not required for endocytosis (187). To determine whether or not acidification of the endocytic vesicle was needed for viral fusion, cells were treated with bafilomycin A, buffering weak base ammonium chloride, or the ionophore monensin, all of which disrupt organelle acidification. Under these conditions, penetration was again blocked (187, 188). It still remains unclear as to whether or not endocytosis of HSV is clathrin-mediated. Other viral glycoprotein mutants were analyzed for functional differences between the entry and endocytic pathways, but gC was still found to be non-essential and gB, gD, gH, and gL were required suggesting a similar mechanism of penetration in both direct fusion and the endocytic pathway of viral entry (188).

In vitro binding requirements of HSV have also been investigated using binding assays in which liposomes are tested for fusion to HSV by characteristic migration in a sucrose gradient. These studies have also determined that mildly acidic pH (5.0-5.3) is necessary for virions to bind HVEM-bearing liposomes (268). When the assay was performed at neutral pH virtually undetectable levels of fusion were observed resulting in all liposomes present in the top fraction of the sucrose gradient (268).

Unexpectedly, nectin-1 proved ineffective in mediating binding in all assays regardless of conditions (268).

In order to address the biological significance of HSV endocytosis in relevant primary cells, neurons and epidermal keratinocytes have been studied. Only in keratinocytes, not neurons, did HSV enter through the endocytic pathway (186). Internalization could be disrupted by lysosomotrophic agents suggesting that low-pH is a prerequisite for entry in these cells (186) . Treatment with isoflavone genistein, an inhibitor of cellular protein tyrosine kinases reduced transport of endocytosed HSV indicating a signaling requirement for capsid transport (186). It is not surprising that neurons do not demonstrate the same need, as fusion has been shown to occur at the plasma membrane in these cells (151).

Milne et al. recently proposed a third, pH–independent endocytic route of internalization. Employing mouse cancer cells (B78H1 cells) which normally do not express any HSV receptors and a derived B78C10 cell line expressing the human nectin-1 protein, the role of gB in entry was assayed. Virus was applied to both cell types, cross-linked with BS3 (an agent not permeable to the plasma membrane), and immunoprecipitated with anti-gB antibody. Entry, as determined by protection from the cross linking agent, was determined to be both receptor (nectin-1) dependent and energy dependent (167). Ultrastructural images demonstrated internalization of particles in membrane invaginations specifically with B78C10 (receptor-expressing) not B78H1 cells (167). These data are similar to those of Nicola et al., who first reported endocytic uptake of HSV (187). In contrast to the findings of Nicola et al, however, fusion after endocytosis was bafilomycin A1 (BFLA) and ammonia chloride-resistant suggesting internalization in these cells proceeds in a pH-

independent manner (167). Whether penetration occurs in the endocytic vesicles or at a later stage such as in the phagolysosome has not been directly addressed, although the lack of low pH requirement for fusion argues that fusion may occur relatively early in the endocytic pathway.

Capsid transport:

Membrane fusion, or penetration, releases the capsid and allows tegument proteins to be exposed to the cytosol. The tegument layer is composed of approximately 20 structural proteins including VP1/2 (U_L36), pU_L37, VP11/12 (U_L46), VP13/14 (U_L47), VP16 (U_L48), VP22 (U_L49), pU_S3 (U_S3) and pU_L17 (U_L17) (214, 235). Electron microscopic time course studies showed a collection of densely staining material, proposed to arise from tegument proteins, formed at the cytoplasmic surface of the plasma membrane, near naked capsids after entry (224). It's thought that most tegument proteins dissociate from the capsid upon entry (164). The mechanism and regulation of tegument protein dissociation is poorly understood but has been hypothesized to occur through dephosphorylation events. Phosphorylation of virion-associated tegument proteins VP1/2, VP13/14, VP16, and VP22 was observed for each protein with at least one of the following kinases: CKII, PKA, or PKC (171). In a PrV correlative motion study, analysis by sequential imaging was used to compare positioning of capsids labeled with RFP-VP16 to any signal arising from individually labeled GFP-tegument proteins (150) (Figure 1.9). By this method, it was concluded that outer tegument proteins VP16, VP13/14, and VP22 dissociate from the capsid within an hour of entering sensory neurons (150). In contrast, both RFP-pU_L36 and RFP-pU_L37 were associated with the capsid through axon

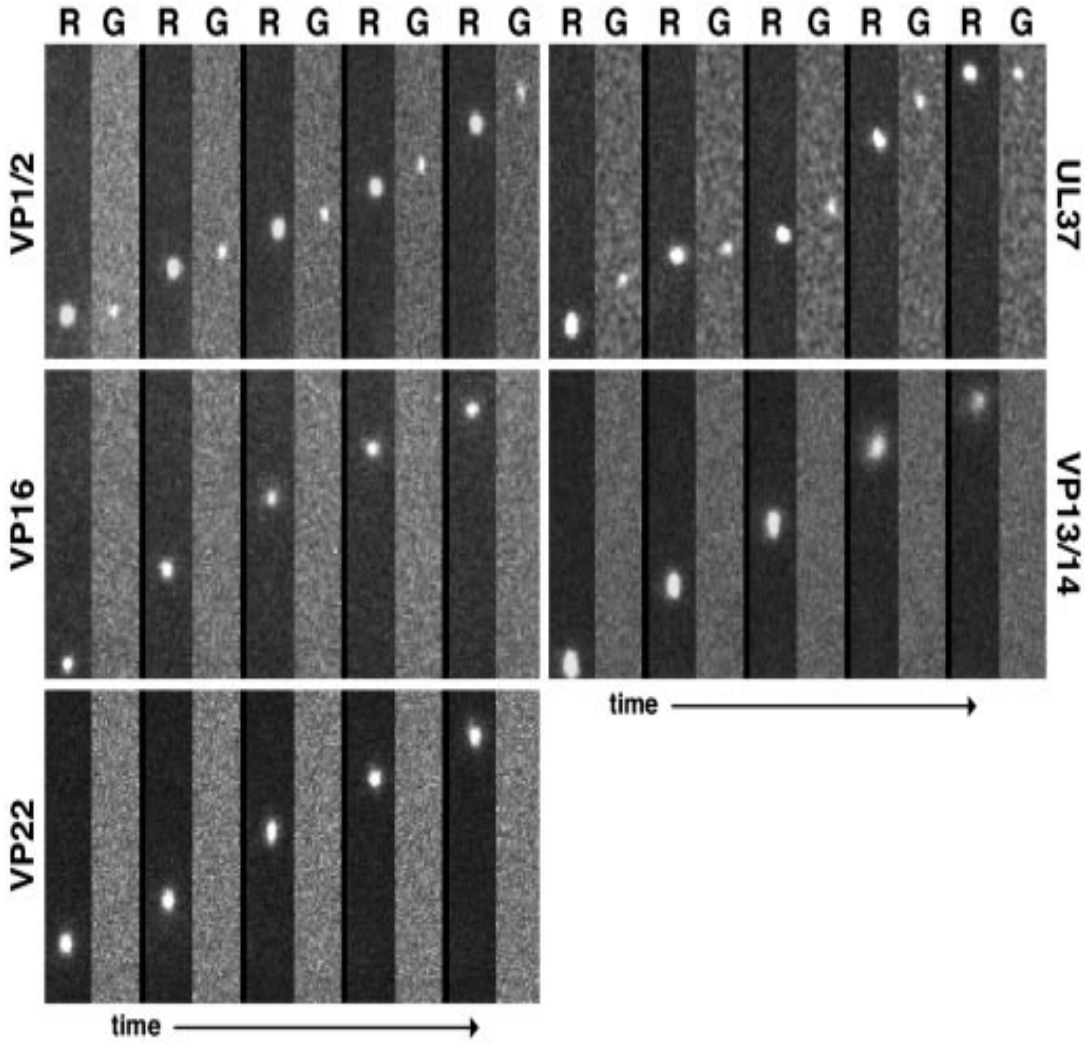

Figure 1.9 Correlative motion analysis. PrV GFP-fusion tegument proteins and RFP-labeled capsids demonstrate retention of VP1/2 and U_L37 protein and dissociation of VP16, VP13/14, and VP22. (R=RFP, capsid; G=GFP, tegument protein) (150)

transport (150). Tegument protein labeling via immunoelectron microscopy corroborated and expanded these results to demonstrate the loss of pU_L11 and retention of pU_S3 (101). These experiments clearly highlight the temporal/special specificity of tegument dissociation.

Released tegument proteins are free to diffuse throughout the cytosol or may be targeted to particular cellular locations. Many of these proteins serve regulatory functions of gene expression which will be discussed later. Conversely, tegument proteins that remain capsid-bound are needed for transport through the cytoplasm or to gain access to the nucleus.

The capsid-bound tegument proteins attach to microtubules and take advantage of a host cell transport motor, dynein, to bring the capsid to the microtubule organizing center (66, 224). The capsid's association with microtubules was first demonstrated by immunofluorescence microscopy staining for capsid and tubulin proteins (224). Signal from anti-capsid antibodies was consistently found approximately 50 nm from the microtubule (224). This correlation supports the prediction that HSV utilizes host cell motor proteins for cytoplasmic transport.

Less is known about the transport of particles entering the host cell through endocytosis. It is presumed that HSV uses a hybrid of transport mechanisms, trafficking of the endosome as well as capsid transport subsequent to penetration, both of which employ dynein-mediated anterograde transit on microtubules. When cells were treated with wortmannin, a phospho-inositol-3 (PI3) kinase inhibitor, capsids from endocytosed particles failed to reach the nucleus whereas capsids in Vero cells (in which HSV enters by envelope fusion at the plasma membrane) were

distributed at the periphery of the nucleus (188). This suggests a role for the cellular kinase in transport of endocytosed particles.

It is believed that capsids dock at the nuclear pore within two hours of entry (224). By electron microscopy, the naked capsid has been observed tethered to the nuclear pore complex (NPC) through cytosolic fibers (224). The capsid, averaging 125 nm in diameter (216), is too large to enter through the nuclear pore complex, which excludes particles greater than 26 nm; therefore the capsid must trigger an uncoating event while docked at the NPC to release and inject the double-stranded DNA genome into the nucleus, leaving the empty capsid in the cytoplasm. Two HSV proteins that have been shown to interact with each other (49), VP1/2, encoded by the U_L36 open reading frame, and pU_L25, have also been implicated in uncoating the genome. Infection with temperature-sensitive mutants of each of these proteins halted the release of the genome as did treatment with a serine-cysteine protease inhibitor (14, 121, 199). Additionally, pU_L25 interacts with nuclear pore proteins (nucleoporins), CAN/Nup214 and hCG1, which may act as receptors to tether the capsid at the NPC (193). pU_L36 has been shown to be proteolytically cleaved around the time of entry and thus it may act as the substrate for the required serine-cysteine protease (121).

Transcription and replication:

Shortly after infection, HSV proteins set up a replication compartment in the nucleus to host viral DNA replication and capsid assembly that is defined by localization of replication proteins such as ICP8 the ssDNA binding protein. This compartment forms from multiple sites adjacent to ND10 structures that grow and converge (242). The replication compartment becomes large,

encompassing most of the nucleus, with a lobed, asymmetric design. As infection progresses the infected nucleus increases two-fold in size, a process that is dependent upon expression of two HSV late genes, U_L31 and U_L34 (169, 223). Possibly as a consequence of replication compartment expansion, host chromatin is condensed and displaced to the periphery of the nucleus (169). Marginalized chromatin is a potential barrier that capsids must overcome to egress from the nucleus.

After viral DNA enters the nucleus it initiates a transcriptional cascade that is designed to promote, in order, the transcription of regulatory proteins, replication proteins, and structural proteins (reviewed in (235)). A transcription transactivator protein, VP16, present in the HSV virion initiates transcription of 5 immediate early genes, ICP0, ICP4, ICP22, ICP27 and ICP47 (15). Unlike the other immediate early genes, ICP47, does not appear to be a major transcriptional regulator, but instead acts to down-regulate MHC class I presentation of viral antigen as a means of immune system evasion (280). Many of the immediate early proteins are multifunctional; together they act to regulate and co-ordinate viral transcription of immediate early (α), early (β), and late (γ) genes.

Upon transcription of early genes synthesis of new viral DNA takes place in the replication compartment (56, 200). HSV replication is a complicated process that is still not fully understood. The HSV genome contains 3 origins of replication, two copies of an OriS sequence and one copy of an OriL sequence; however, in cultured cells both OriS sites are dispensable (118). Despite HSV having access to host machinery for double-stranded DNA replication, the virus still encodes a helicase (U_L5), an origin-binding protein (U_L9), a primase (U_L52), a DNA polymerase (U_L30), a

processivity factor (U_L41), and a single-stranded DNA binding protein (U_L29, ICP8), so it is clear that its replication strategy is different from that of the host. Initial DNA replication is thought to use a theta structure and subsequent rounds of replication mimic some bacteriophage by using a rolling circle mechanism (24). Additionally, it is proposed that DNA recombination events play a role in replication, through the combination of an alkaline nuclease (U_L12) and the single-stranded DNA binding protein (U_L29, ICP8) that act in a similar fashion to the phage λ Red recombination system (205). The product of replication is known to be a concatemer of many genomes connected end-to-end in both linear and branched arrangements.

Capsid assembly:

Only after new DNA has been synthesized are late genes transcribed efficiently. The transcription of late genes promotes the production of structural components necessary to build the icosahedral capsid. Capsid assembly takes place in the nucleus with the aid of a scaffolding protein, pre-VP22a (U_L26.5, ICP35), around which 11 pentamers and 150 hexamers of VP5 (U_L19, ICP5) and one dodecamer of pU_L6 all associate to form a T=16 icosahedral shell (216, 288) (Figure 1.10). Limiting concentrations of pre-VP22a protein can result in a decrease in the capsid size (181).

Transient co-expression of the major capsid and scaffolding proteins suggests the two associate in the cytoplasm to promote transport of VP5 into the nucleus (185). After entry into the nucleus, VP5 monomers self-assemble into multimers. The multimers are in two forms, pentamers and hexamers, both of which are integrated into the capsid shell (253, 262). Preassembled structures called triplexes each composed of a single VP19C (U_L38) and two

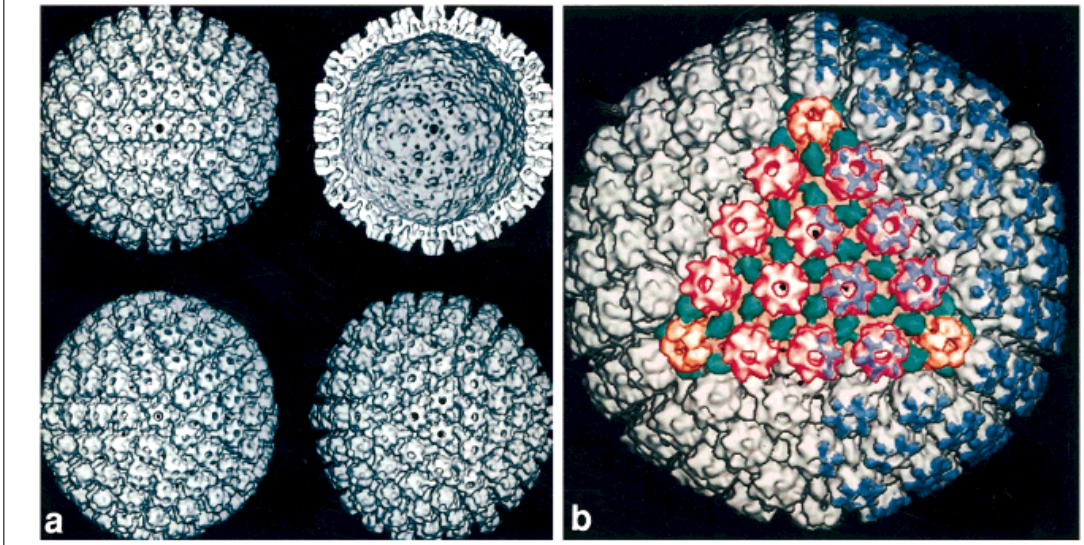

Figure 1.10 Three-dimensional HSV capsid reconstruction. Resolution at 2.5 nm. (a) Views looking from various points of symmetry. (b) Capsid proteins are false colored such that VP5 molecules are red (hexons) and orange (pentons), triplex complexes (containing 2 copies of VP23 and a single copy of VP19c) are green, and VP26 (blue) capping the tops of hexons is shown only on the right half of the capsid (116)

.

molecules of VP23 (U_L18) link the VP5 hexamers (183, 228, 251). The scaffold, VP5, and triplex proteins are the minimum set of proteins required to make capsids (Figure 1.11). Each of these proteins has been expressed in baculovirus and co-infection with these expression vectors is sufficient to build HSV capsids (116, 239). Additionally, it has been shown that capsids can assemble in vitro from mixed cell lysates from the individual baculoviruses (180).

VP21 and VP24, auto-proteolytic products of the U_L26 (protease) gene, and VP26 (the product of U_L35) complete the capsid, although these proteins are not essential for assembly in the baculovirus system (116, 239) (Figure 1.12). VP26 molecules adorn the top of the VP5 hexamers, protruding outward from the capsid (287). Neither capsid assembly nor tegumentation require the presence of VP26 (42), although viral propagation is more efficient with VP26 (239, 244).

Capsid assembly results in an immature form called the procapsid. Procapsids differ from the mature form, known as C capsids, in that (i) they are more round, not angular, in structure (ii) the non-proteolytically processed scaffolding protein is retained in their shells, and (iii) the genome has not been packaged (reviewed in (116)). Mutations in proteins necessary for DNA packaging have allowed two distinct capsid types, A and B, either precursors or abortive forms of the maturation process, to be identified (3, 132, 158, 195, 196, 218, 241, 243, 281). The scaffold protein, pre-VP22a, in A capsids is cleaved by a U_L26-encoded protease yielding VP22a and a 25 aa peptide, which are expelled, but no genome is inserted, thus resulting in an empty, angularized capsid. In contrast, in B capsids the pU_L26 protease again

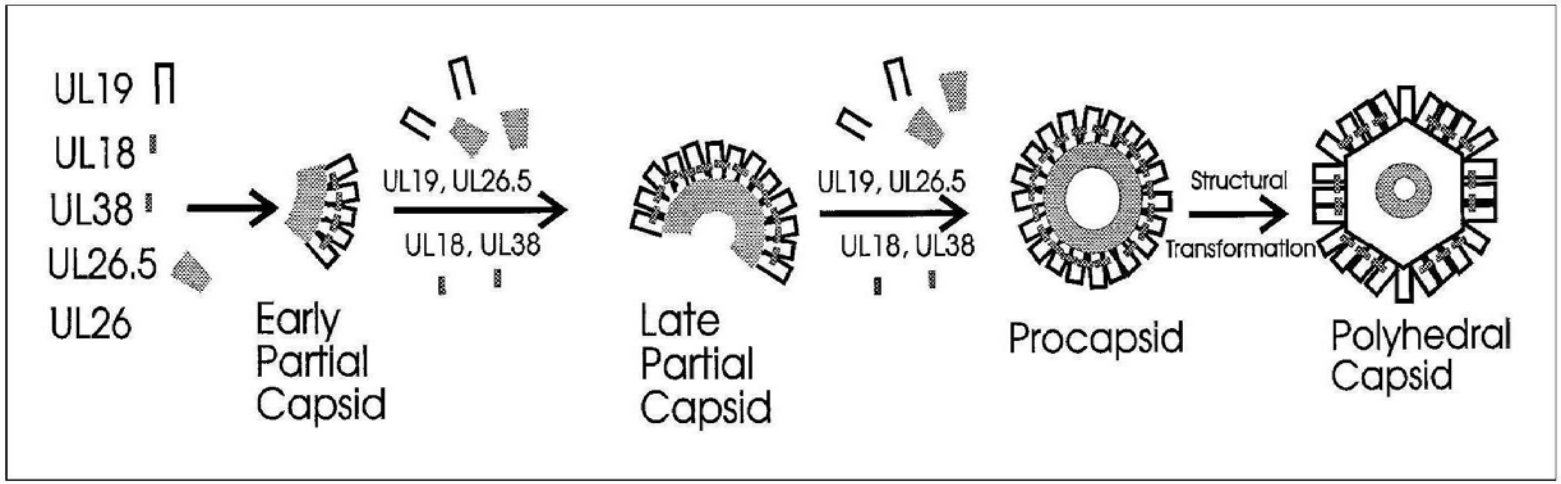

Figure 1.11 Capsid Assembly

Triplex proteins encoded by U_L18 (VP23) and U_L38 (VP19c) connect multimers of the major capsid protein (U_L19, VP5) to form a shell surrounding a $U_L26.5$-encoded scaffold protein (116). The structure is built from a nucleation point and continues until it completes a sphere

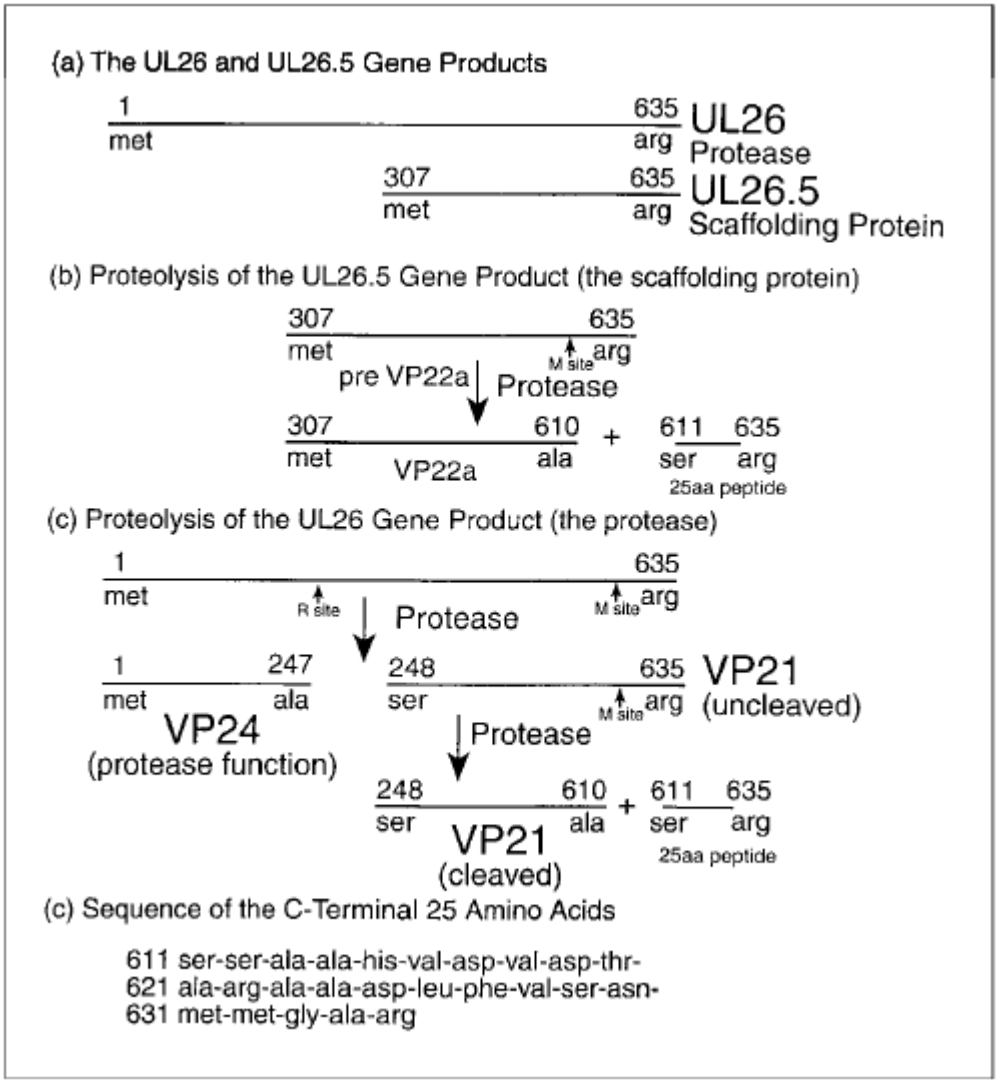

Figure 1.12 Proteolytic processing of U_L26 and $U_L26.5$ gene products (116).

cleaves the scaffold, but VP22a is retained, leaving no opportunity for DNA packaging to occur (98, 178). Of all of the capsid forms, C capsids are preferentially recognized at the inner nuclear membrane and undergo primary envelopment (196). The site of capsid assembly and DNA packaging is controversial. It has been hypothesized to occur in nuclear compartments called assemblons that are defined as peripheral nuclear aggregates containing capsid proteins including ICP35, ICP5 and VP19c (266), as well as throughout the replication compartment (132).

DNA encapsidation:

Capsids must encounter the genomic concatemer located in the replication compartment for the process of DNA cleavage and packaging to take place. New capsids are pre-formed and subsequently packed with DNA. HSV-1 is considered to be an example of sequential rather than concerted packaging and assembly. There are seven viral proteins (pU_L6, pU_L15, pU_L17, pU_L25, pU_L28, pU_L32, and pU_L33) that are essential to form correctly encapsidated HSV genomes. Deletion or truncation of any of these packaging proteins apparently does not disturb capsid construction or replication of new viral genomes; however, these mutants fail to incorporate nascent viral genome into capsids, and all except the U_L25 mutant fail to sever the replication concatemer into single-unit genomes (3, 132, 158, 195, 241, 243, 281).

Bacteriophage double-stranded DNA encapsidation:

Similar cleavage and packaging mechanisms are understood for double-stranded DNA bacteriophages such as P22, T4, T7, and λ. Since

phage generally utilize simpler mechanisms than eukaryotic viruses, most studies of packaging mechanisms have been performed on phage. Although there are many virus-specific variations, the fundamental strategies provided by early phage packaging research have largely directed HSV cleavage and packaging models. Like HSV, phage also use a protein complex referred to as the terminase that works in combination with the portal, a multimer present on only one vertex of the capsid shell, to bind DNA, translocate the genome, and cleave the encapsidated genome from the concatemeric replication product.

In Salmonella P22 phage, gene product 3 (gp3) and gene product 2 (gp2) are thought to constitute the small and large subunits of the packaging terminase, respectively. gp3 recognizes a 22 base pair "pac" site on P22 genomic DNA to initiate packaging (35, 275). Electron microscopy studies show gp3 self-assembles into a nonameric ring with a channel that non-specifically binds to the DNA backbone through electrostatic interactions (177). The other terminase component, gp2, provides both endonuclease activity and also the motor force to drive the packaging reaction via ATP hydrolysis. It was hypothesized that a symmetry mismatch between the portal protein, gp1, and the five-fold symmetry axis of the capsid shell may be exploited to provide packaging force through portal rotation with respect to the capsid (109, 119). However, subsequent studies with another T-even bacteriophage, T4, have strongly refuted this model. First, T4 portal fusion mutants designed to prevent rotation failed to inhibit phage assembly (16). Second, the resolved structure of the T4 packaging ATPase was observed to be similar to that of other helicases, which suggests that DNA translocation may be a repeated process of binding and releasing the DNA (236). This is

often referred to as the inch-worm model. Translocation of the genome continues uni-directionally and is processive.

Bacteriophage T4, also carries out strictly headful packaging of new genomes through the use of a two-part terminase complex; in this phage DNA packaging is not terminated or initiated by recognition of specific DNA sequence. Instead, the terminase large subunit, gp17, is responsible for random cleavage of the genomic DNA (22). Purified gp17 protein has been shown to possess single-stranded DNA binding, double-stranded DNA binding and endonuclease activity; the presence of Mg2+ and gp16 control the mutual exclusion of these two properties (4, 5, 83). The gp17 protein also binds to the capsid portal (gp20)(144), and generates the force behind the packaging reaction via hydrolysis of ATP (139). The terminase small subunit, gp16, does not hydrolyze ATP (145), but enhances the ATPase activity of gp17 (139, 203).

In contrast, in T7, a T-odd phage, packaging studies give no indication of headful packaging. Instead, cleavage takes place at uniquely recognized terminal genomic sites and the placement of the sequence in the concatemer dictates the length of the genome inserted into the capsid. T7 cleavage is executed in a staggered fashion in the genomic junction region of the concatemer leaving terminal 5’ overhangs of DNA. Each end is then filled by DNA polymerase using the shorter 3’ strand as a primer for synthesis resulting in a completely double-stranded genome with duplication of directly repeating terminal ends. Although it is through another mechanism, the end result is similar to packaging 102% of the genomic DNA length as seen with T4 phage.

Phage λ, has yet another mechanism for DNA cleavage and packaging. Phage λ's cleavage and packaging mechanism is arguably more similar to that

of T7 in that a particular 200 base pair region defined as a CosN site is the target of cleavage. The λ terminase is composed of the two proteins gpNu1 (small subunit) and gpA (large subunit) that form a hetero-oligomer. First, gpNu1 binds a 16 base pair repeated sequence, the R element, that is present in three copies in a cosB site sub-region to initiate the packaging reaction (220). Then the dimer of gpNu1 interacts with its terminase counterpart, gpA (250). Sequence-specific binding of gpNu1 positions gpA so that it may introduce two site-specific symmetric nicks 12 base pairs apart at the cosN cleavage site (114). Terminase binding to the R element through gpNu1 is augmented by ATPase activity in contrast to the strict requirement of ATP for gpA to recognize the cosN site (113). The cleavage and packaging mechanisms of phage lambda are unique in that the cleavage reaction is supported by a host (E. coli) protein IHF, or Integration Host Factor (128). It seems this protein is exploited by λ phage to bind and bend the phage DNA at the cos site, possibly priming it for cleavage or for gpNu1 recognition.

The endonucleolytic activity of gpA (212) with the aid of gpA's helicase ability removes preceding bases in the 12 base pair cosN region, thereby generating single-stranded 5' overhangs, or "sticky" ends. These ends have also been called "cos" ends for their cohesive property because cleavage of two consecutive cos sites in the concatemer creates unpaired overhangs that complement one another and can re-ligate. Both terminase proteins possess ATPase activity. gpA uses ATP hydrolysis to promote both its endonucleolytic cleavage and helicase functions. It is still unclear in what manner the ATP hydrolysis of gpNu1 is used. It has been shown that gpA also interacts with gpB, the portal protein, to initiate the packaging reaction (279).

Although many viruses share the common need to package concatemeric DNA and most retain homologous functional properties of terminase proteins, there clearly are many different mechanisms by which this can be achieved. Each of the four bacteriophages mentioned above appears to have both similar and unique properties in its cleavage and packaging strategies. P22 and T4, for example, use a “headful” packaging mechanism. After initiation of DNA translocation, these phage continue to package DNA beyond the length of a single genome until the capsid head has reached maximum capacity. For P22, this results in approximately 104% of the genome being incorporated into each new virion (34). By introducing more than a single unit-length genome into the capsid, this mechanism may provide a safety net in the duplicated terminal sequence to compensate for any incomplete coding sequences or missing promoter regions potentially generated from cleavage. T4 is considered to use a strictly headful mechanism since no sequence markers for packaging have been reported. In contrast, P22 also uses headful packaging, as indicated by the length of packaged DNA, yet this phage has pac sites for terminase recognition. With this headful packaging strategy, the portal (gp3 and gp20, respectively) serves not only as the DNA conduit, but also as a pressure sensor to monitor the capsid head’s capacity. The headful DNA packaging model is also supported by a three-dimensional asymmetrical reconstruction of the crystal structure of P22 DNA encapsidation. The structure indicates that packaged DNA is coiled against the coat protein in the phage head interior and presses against the portal protein, potentially providing the signal that the capsid is full (133, 177). This is in contrast to T7 and lambda phage packaging in which both termini of

the genome are specifically marked with direct repeats or cos sites to ensure encapsidation of an appropriate size DNA molecule (119).

HSV DNA encapsidation proteins:

Unlike its phage counterparts, the HSV terminase may be composed of more than two viral proteins. In HSV three proteins, pU_L15, pU_L28, and pU_L33, form a packaging terminase complex (19). Protein-protein interactions among these terminase proteins have been more clearly defined through co-immunoprecipitation experiments. The results indicate that pU_L15 and pU_L33 are incapable of interacting directly with each other, even though both pU_L33 and pU_L15 can each directly interact with pU_L28 (277). Therefore, it seems that the association of pU_L15 with pU_L33 can only be observed through interactions with pU_L28 (277). The protein complex is formed in the cytoplasm, and transport of pU_L15/ pU_L28 into the nucleus appears to be dependent upon a pU_L15 nuclear localization signal (278). pU_L28 and pU_L15 are suggested to serve the respective roles of DNA binding and energy production necessary for DNA encapsidation to parallel phage terminase systems. The role of pU_L33, however, is less clear, although it has been demonstrated to strengthen the interaction between pU_L15 and pU_L28 and thus may serve as an accessory component to the complex (277).

In vitro, pU_L28 binds the single-stranded, structured pac1 sites in a sequence-specific manner (2). Nascent genomes are first cleaved at the U_L terminus; this is the genomic end which first enters the capsid through the dodecameric ring of pU_L6 (32, 182, 252). This combined with the understanding of the atypical DNA binding-properties of pU_L28 lends to the

hypothesis that pU_L28 recognizes the pac1 site at the U_S terminal end and is responsible for this second cleavage event of the packaging reaction.

Additionally pU_L15 shares homology with the ATPase domain of T4 terminase protein gp17 (54). The putative ATPase domain of pU_L15 is predicted by two conserved nucleotide binding protein motifs, GKT and DE, coined Walker A and B boxes respectively (67, 265).

Of HSV packaging proteins, pU_L6 was found to form a portal through which the nascent genome can enter the capsid. Electron microscopy studies showed that pU_L6 formed a ring and was most commonly found only on a single vertex of capsids (182). Quantitative western blots and scanning transmission electron microscopy indicated a 12-mer forms the pU_L6 ring (182). Additionally, pU_L6 has been shown to interact with at least two of the HSV terminase proteins, pU_L15 and pU_L28 (278). It is widely accepted that genomic HSV DNA enters the capsid through the portal ring, however, any additional mechanical roles of pU_L6 in capacity sensing, energy generation, or DNA binding are currently unclear. A three-dimensional asymmetric reconstruction of P22 phage shows the structure of the virion at 17 angstroms (133). Although this is a relatively low-resolution structure determination, the asymmetric reconstruction provides information about the unique vertex of the portal, which is eliminated when icosahedral averaging is used to derive the structure. This asymmetric structure containing the portal (gp1) in the context of the virion reveals significant conformational differences from the crystal structure of the portal alone. It appears as if the conformational change in gp1 may be an indicator of a fully packaged virion. In HSV it is unclear if pac site recognition is all that is needed to maintain uniform insertion of complete

genomes into capsid or if pU_L6 may additionally serves as a headful packaging indicator.

Thus, the roles of four of the seven genes essential for proper HSV DNA cleavage and packaging can be attributed to the roles these proteins play in forming the terminase and portal structures; each have analogs in phage packaging mechanisms. However, homologs of the remaining 3 remaining essential genes, U_L32, U_L25, and U_L17 exist only in other herpesviruses and their functions in DNA encapsidation have yet to be clearly defined.

Similar to the other HSV packaging proteins, pU_L32 is essential for construction of C capsids (132). The primary sequence of U_L32 predicts putative N-linked glycosylation sites, and aspartyl protease and zinc-binding motifs (39). Although no biochemical function of this protein has yet to be reported, purified, native, U_L32 protein as well as a Histidine-tagged U_L32 protein expressed in baculovirus were both capable of binding zinc (39). Deletion of this gene results in the production of only B capsids, does not alter the rate of viral DNA replication, and does not allow for the cleavage of the genomic concatemers (132). Originally pU_L32 was reported to localize exclusively to the cytoplasm (39), which obscures any direct role of this protein in cleavage and packaging, but in later studies performed with an antibody against a tagged fusion U_L32 protein, both in infected and transfected cells some pU_L32 was found in the nucleus although the predominant staining of pU_L32 still remained cytoplasmic (132). The nuclear pU_L32 was present within the replication compartment but absent from presumed nucleoli. Deletion of U_L32 caused mislocalization of assembled capsids early in infection (132). This lead to the hypothesis that pU_L32 was needed for capsid localization to the replication compartment. In the proposed (Weller) model, pre-assembled

capsids are brought to the replication compartment either by a direct or indirect interaction with pU_L32 in order for cleavage and packaging to occur in the replication compartment (132). This is in direct opposition to the model proposed by Ward et al that suggested capsid maturation and packaging occurs in assembly structures located at the periphery of the replication compartment (266).

pU_L25 and pU_L17 are present on the external face of C capsids in a proposed heterodimer coined the C Capsid-Specific Complex (CCSC) (254). This structure, present on C capsids, extends radially from each of the five-fold points of symmetry of VP5 pentons passing between hexons of VP5 and above triplex complexes (254)(fig 1.13).

pU_L25 like the other cleavage and packaging proteins is essential for optimal formation of C capsids, however, U_L25 stands alone in that deletion of this gene results in a higher ratio of A to B capsids (158). Additionally, upon deletion of U_L25 HSV still retains its ability to cleave concatemeric DNA (158) and allows for some DNA packaging to occur, though much less efficiently (approximately 20-fold) compared to wild-type HSV-1 infection (231). Genomes propagated in U_L25 deletion virus-infected cells undergo cleavage at both genomic termini, but in southern blots of DNAse-resistant viral DNA the two ends are disproportionally represented indicating the U_S terminus specifically is degraded presumably from failure to be encapsidated (231). These data suggest that pU_L25 plays a later role in cleavage and packaging than do the other proteins of this class. It has been proposed that pU_L25 may act as a gate to close the portal after packaging in order to keep the genome contained within the capsid.

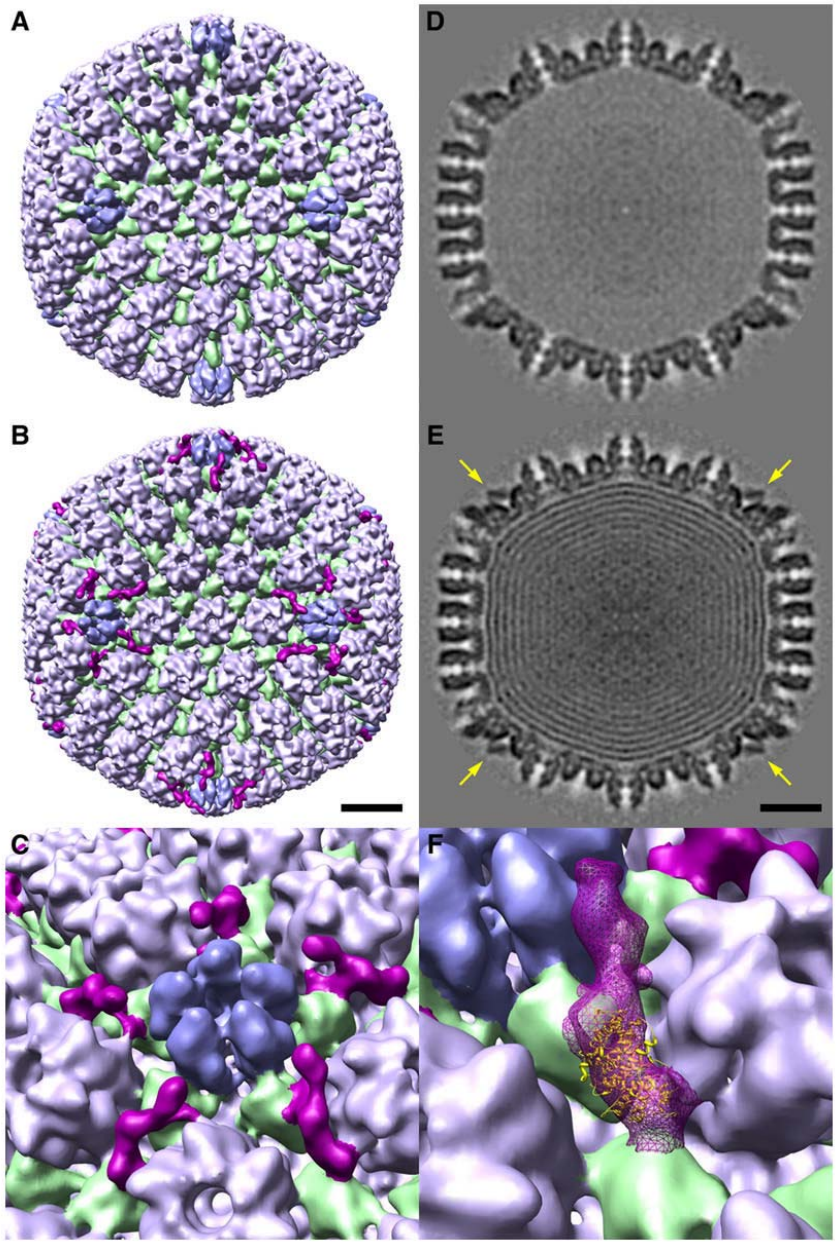

Figure 1.13 The C-Capsid Specific Complex. CyroEM and three-dimensional reconstruction of the pU_L17/pU_L25 heterodimer (magenta) present on C capsids (B, C, E, F) but not A capsids (A, D). Panel F shows the optimal fit of a pU_L25 fragment in ribbon structure within the heterodimer (254).

In another alphaherpesvirus, pseudorabies virus (PrV), the U_L25 gene product is not required for DNA cleavage or encapsidation, yet, the protein is absolutely essential for viral replication (124). DNA-containing C capsids are retained in the nucleus upon infection with pU_L25-lacking PrV (124). Instead of being required for cleavage and packaging, electron microscopy of PrV U_L25- infection shows an accumulation of nucleocapsids throughout the nucleus and at the inner nuclear membrane as well as a void of cytoplasmic capsids and extracellular virions all indicating pU_L25 is necessary for nuclear egress (124). The presence of light particles in the cytoplasm also ensures that the effect is specific to primary envelopment as secondary envelopment is still functional in the absence of pU_L25. The different phenotype of the PrV mutant compared to its HSV homolog may reflect subtle differences in replication strategy between these viruses. Presumably, this indicates that pU_L17 in PrV is capable of sealing the packaged capsid independent of pU_L25, and that pU_L25 may recognize markers for primary envelopment. Whether or not the same role for pU_L25 in primarily envelopment exists in HSV infection has not been clearly established, although it has been shown as an attachment point for the inner tegument proteins (49).

HSV pU_L25 is not associated with the procapsid and may be added on to maturing capsids in a pU_L17-dependent manner (245). Purified U_L25 protein was able to bind to U_L25-null capsids (179). Studies analyzing protein components of B capsids purified from U_L17-null virus infection showed depleted levels of pU_L25 suggesting that pU_L17 is required for efficient incorporation of pU_L25 in B capsids (245). The reciprocal experiment detecting protein levels of pU_L17 present on B capsids from U_L25- infection resulted in a two-fold reduction of pU_L17 (245). Combined, these data lead to

the hypothesis that pU_L25 may stabilize pU_L17's association with capsids. However, it is not clear why pU_L17 stabilization through pU_L25 would be necessary since pU_L17 associates with the procapsid prior to addition of pU_L25 in capsid maturation (246). Regardless, these effects suggest roles for pU_L25 and pU_L17 in capsid structure and maturation that may produce indirect effects on the cleavage and packaging process.

The mechanisms of regulation of DNA packaging, tegumentation, and nuclear egress remain elusive. However, studies investigating the quantity of pU_L25 and pU_L17 assembled onto various capsid types as well as into the virion suggest that both proteins are continually built upon the capsid, and capsid-bound protein concentrations may aid to regulate these processes. Protein levels of assembled pU_L25 have been shown to be minimal on procapsids, intermediate on B capsids, and highest on C capsids with an overall 15-fold difference between procapsids and C capsids (217). In a separate study, quantitative western blot analysis indicated approximately 20 copies of pU_L25 were present per single B capsid, 45 copies per A capsid, and 75 copies per C capsid (179). When the incorporation of pU_L17 protein was analyzed, both A and B capsids were determined to have similar amounts of pU_L17 whereas C capsids indicated approximately two-fold increase (246). The addition of pU_L25 and pU_L17 correlates with the CCSC (pU_L17/pU_L25) being detectable by cryoelectron microscopy specifically on C capsids, not on A capsids (179, 246, 254) in which pU_L25 may be less uniformly structured.

The gene most recently shown to be essential for DNA cleavage and packaging, U_L17, is an open reading frame that is predicted to encode a protein of 74,577 daltons (703 amino acids) and that resides in the intron of UL15 (214). U_L17 has no significant homology to any other cellular or viral

proteins other than U_L17 homologs of other herpesviruses. The first antibody to pU_L17, a polyclonal rabbit antibody from DNA immunization reported by Salmon et al reacted with two proteins with molecular weights of 72,000 daltons and 77,000 daltons. Subsequently another polyclonal rabbit antibody from a fusion protein immunization that reacted only with a viral protein of 78,000 daltons was reported (99). These data suggest that pU_L17 protein exists in multiple forms in infected cells.

pU_L17 was observed to be essential for viral replication based on the evidence that U_L17 deletion mutants could not form viral plaques on wild-type (Vero) cells (11). Since U_L17 lies within the intron of another essential gene, U_L15, deletion of U_L17 proves an additional challenge. A U_L17 mutant virus replacing U_L15 exon I with the entire cDNA was constructed in order to control for effects on splicing of U_L15 (214). Although mutants of U_L17 were unable to grow on wild-type (Vero) cells, these mutants sustained growth on cells designated G5 that were derived from transformed Vero cells engineered to incorporate a 16.2 kb EcoRI fragment containing viral genes U_L16 to U_L21 from the KOS strain of HSV-1 (62). When compared to another mutant bearing a premature stop codon in U_L17 made in the wild-type virus, supplementing with the U_L15 cDNA made no difference in the mutant phenotype of U_L17.

Cells infected with a U_L17 deletion virus were shown to be deficient in cleavage of concatemeric DNA by BamHI southern blot probed with an S fragment probe (214). This probe will bind to the US terminal BamHI fragment (“S”) generated only in cleaved genomic DNA. In uncleaved, concatemeric DNA this probe will instead recognize the larger, uncleaved S-P fragment. U_L17-null virus grown on complementing cells (providing pU_L17 in trans)

restored the cleavage required to regenerate the S fragment (214). With this method, Salmon et al showed both that cleavage was prevented in U_L17-null infected cells, but also that replication of genomic DNA remained unaltered (214).

A defect in genomic DNA packaging was also confirmed by thin-section electron microscopy of U_L17-null infected cells (214). Akin to most other cleavage and packaging mutants, deletion of U_L17 caused accumulation of B capsids only. However, deletion of U_L17 produced aggregates of capsids at the periphery of the nucleus, a unique phenotype (241) revealed by immunostaining with a monoclonal antibody, 8F5, that specifically recognizes an epitope on hexons of assembled capsid (253). In contrast to capsids in wild-type infected cells where mature capsids are dispersed throughout the replication compartment, the capsid aggregates formed upon U_L17-null infection were excluded from the replication compartment (241). From these data, pU_L17 has been proposed to transport capsids from assemblons to the replication compartment.

The cellular localization of the U_L17 protein in HSV-1 and HSV-2 has been assayed by indirect immunofluorescence with two different antibodies both against a U_L17-His fusion proteins (99) (figure 3.4). In one report pU_L17 co-localized with VP5 and ICP35 to assemblons at late times in infection (99) in contrast to the punctate localization throughout the replication compartment presented in this work (figure 3.4).

Egress pathway debate:

After mitigating the lamina barrier, capsids must pass through both the inner and outer nuclear membrane. Multiple, diverse pathways of egress have

been hypothesized and a sustained debate ensued. The most evidence has accumulated for the de-envelopment/re-envelopment pathway which will be discussed in greater detail below in “Nuclear Egress/Primary Envelopment and “Nuclear Egress/Secondary Envelopment” (Fig 1.14). This route of egress was originally proposed by Stackpole in the late 1960’s but because of its complexity was not embraced at the time (229). In this model, capsids bud through the inner nuclear membrane (INM) obtaining a primary envelope as they enter into the periplasmic space. Exit from this space is thought to occur through a fusion event of the primary envelope with the outer nuclear membrane (ONM) (de-envelopment). This route of nuclear egress produces unenveloped, cytoplasmic capsids. Stackpole hypothesized these unenveloped cytoplasmic capsids would subsequently obtain their final, secondary envelope (re-envelopment) by budding through a cytoplasmic membrane such as the Golgi or an endosome (163) and ultimately HSV virions exit the cell through the secretory pathway. This model suggests that a primary tegument is acquired in budding at the inner nuclear membrane, but the final tegument is built in the cytoplasm rather than the nucleus.

There three main alternative pathways have been proposed. The first variation of the de-envelopment/re-envelopment pathway suggests capsids bud through the inner nuclear membrane and these enveloped capsids leave the perinuclear space in an outer nuclear membrane-derived vesicle (102) (Figure 1.14, Figure 1.15). In this model, the outer nuclear membrane and virion envelope fuse to release unenveloped capsids into the cytoplasm, where they can bud into trans-Golgi network cisternae and exit through the secretory system. This pathway variant is the most closely related to the

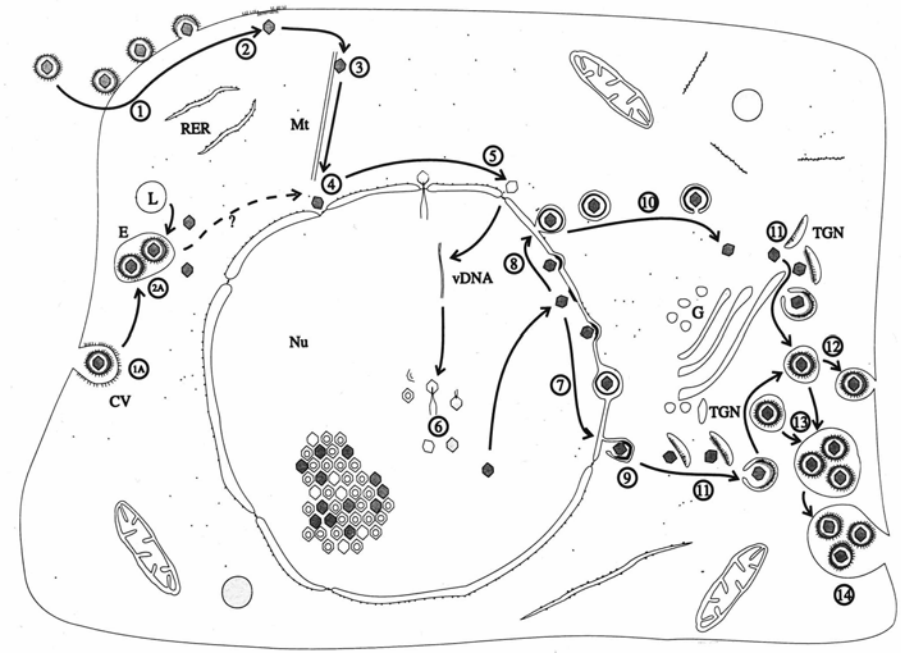

.

Figure 1.14 Two pathways of egress with 2-step envelopment

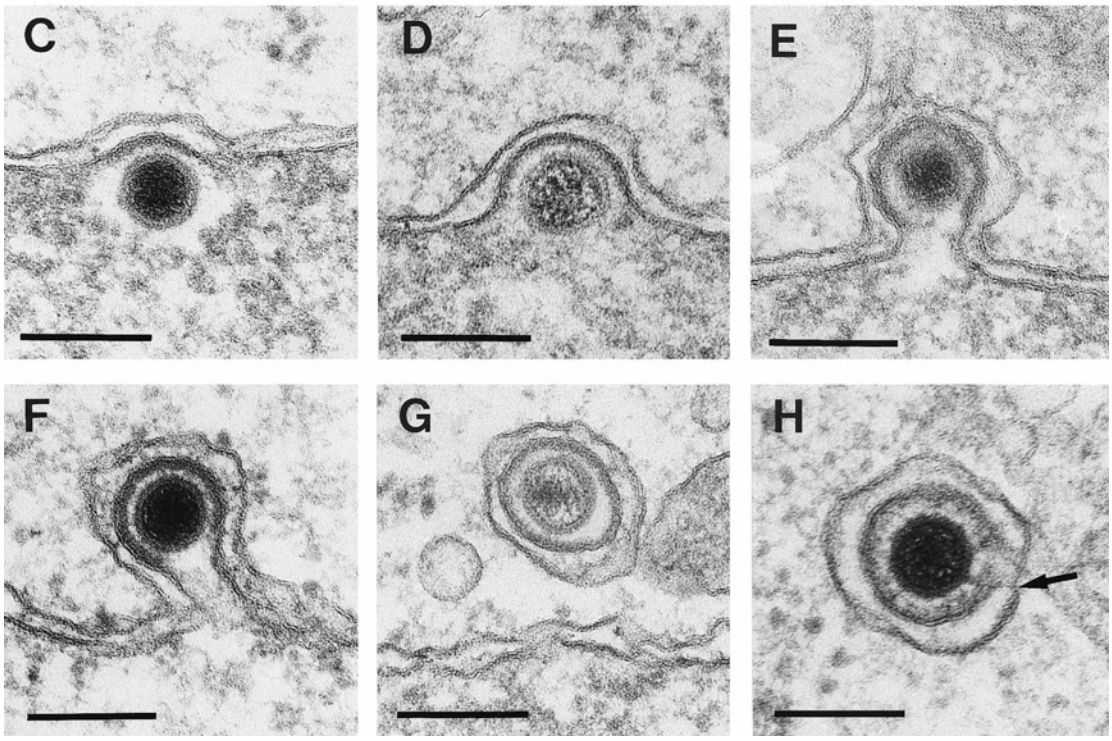

Figure 1.15 Electron micrographs of capsid egress forming a double-membrane vesicle. Budding through the inner and outer nuclear membrane in concert (C-F). Vesicularization at the outer leaflet of the nuclear membrane (G). Potential fusion between the PrV envelope and outer vesicular membrane (H) (102).

accepted de-envelopment/re-envelopment pathway in that it also suggests two steps of envelopment.

Data arguing for another route of egress through dilated nuclear pores have been presented (271). This model proposes a pathway in which holes large enough for the passage of capsids (>140nm) exist in the nuclear membrane late in infection (271, 272). This route offers capsid egress without requiring inner or outer nuclear membrane interactions. In quantitative analysis of electron micrographs, Wild et al. found capsids were readily capable of budding into any membrane from the cytoplasmic side, whereas the occurrence of nuclear capsids budding into the inner nuclear membrane was rarely observed (271). Using fast freezing electron microscopy preparation, HSV capsids were seen in the openings of dilated nuclear pores (271) (Figure 1.16). Also, HSV budding into the perinuclear space was reported to originate from both the nuclear as well as the cytoplasmic side. In the dilated nuclear pore model, Wild et al propose HSV uses two pathways to obtain an envelope. Naked cytoplasmic capsids can either bud into Golgi cisternae, or bud back into the periplasmic space, which is continuous with the ER and Golgi, or into another part of this continuum. Thickening of the nuclear membrane proximal to the capsid was found to correlate with budding. This was observed in both the inner (rarely) and outer nuclear membrane, arguing capsids can bud from either the nuclear or cytoplasmic side into the perinuclear space (140). The thickening of the outer nuclear membrane was not attributed to the remains of a primary envelope after fusion because the length of thickened membrane was insufficient to cover the perimeter of the HSV capsid.

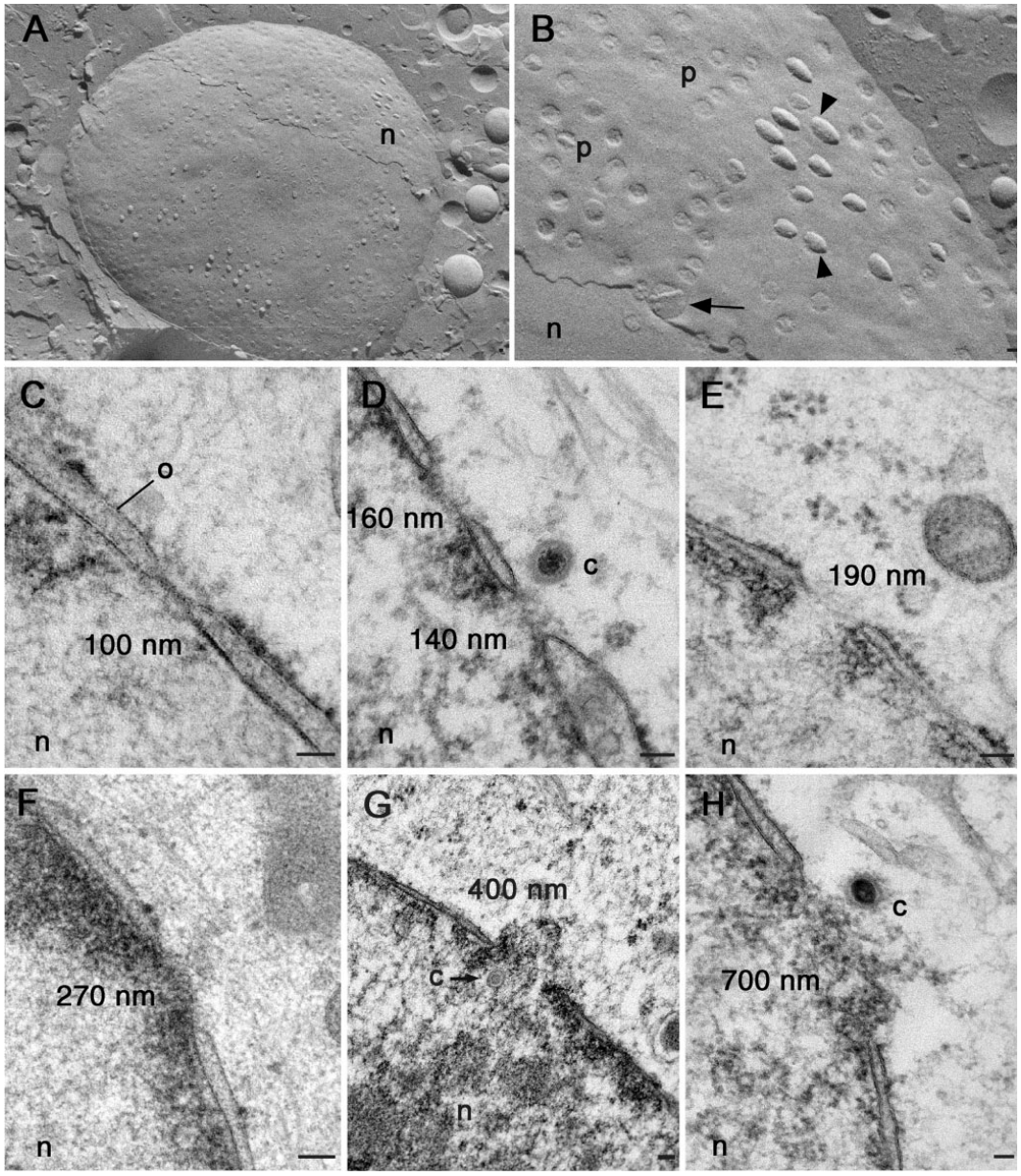

Figure 1.16 Capsid passage through nuclear pores. Cryo-FESEM (A-B) TEM images of capsids in proximity to various-sized dilated nuclear pores in BoHV-infected MDBK cells (C-H) n=nucleus, c=cytoplasm (271).

Intracisternal passage of capsids to the Golgi is supported by the presence of capsids within the RER cisternae. However, if these enveloped capsids are fusion competent as indicated by the presence of gB, gC and gD in the perinuclear capsids, then another protein(s) must be preventing fusion during intralumenal transport. It has been speculated that gK, gM, U_L20, pU_L31, or pU_L34 might serve this anti-fusogenic role.

A third alternate route of egress that held popularity for some time also suggested that only a single step of envelopment was necessary for egress. This model proposed capsids were enveloped at the inner nuclear membrane and then passed through the perinuclear space/ER continuum into the Golgi. This model also requires that the membrane originally obtained from budding at the inner nuclear membrane is maintained and the capsid leaves through the secretory system. Simplicity made this proposed pathway attractive, and experimental support came from the finding that perinuclear virions were infectious and that the Golgi was required for virion egress (257). However, for the following reasons there is currently little backing for this pathway and some of the alternatives described above.

Firstly, cytoplasmic capsids, both enveloped and unenveloped, have been observed by electron microscopy. Also through live cell microscopy, capsid transport on neuronal axons as well as through the cytoplasm of infected mammalian cells has been observed. Only one of the three alternate pathways presented, direct egress to the cytoplasm through the nuclear pore, anticipates the existence of unenveloped particles throughout the cytoplasm.

Secondly, many other reports have failed to notice the dilated nuclear pores that Wild presents, and capsid envelopment has been documented in the vicinity of intact nuclear pores (166). In Wild's study nuclear pore size

variation ranged from 140 nm to 1900 nm late in bovine herpesvirus (BoHV-1) infection of MDCK cells and often showed nuclear membrane extensions (blebbing) associated with the expanded pores (271). Such gross alterations of the nuclear membrane suggest fixation artifacts although the authors did not see dilated nuclear pores in uninfected cells indicating the effects were specific to infection. Due to the rapid disintegration of infected MDCK cells, the authors prepared rapid-freeze substitution EM samples of infected cells and uninfected cells and examined them at low temperatures (140). This technique offers better preservation of membranes and high temporal and special resolution through arresting cellular processes in nanoseconds. Only infected cells demonstrated the enlarged nuclear pores and therefore the phenomenon was attributed specifically to cytopathic effects and not to a technical artifact.

Thirdly, budding was seen, albeit at a low frequency, upon MDCK infection with BoHV-1 despite the presence of expanded nuclear pores. Electron micrographs of HSV also provide clear images of capsids budding through the inner nuclear membrane and into the perinuclear space in close proximity to seemingly intact nuclear pores (162). The low frequency of budding observed in Wild's assay may reflect the rapidity with which INM budding is executed rather than its likelihood. Perinuclear enveloped particles have also been seen fusing to the outer nuclear membrane (100).

Of the alternate pathways, only the INM/ONM double membrane particle is proposed to go through two steps of envelopment. All of the single-step routes of transport imply tegument is assembled as the capsid fulfills its only budding step or within the ER-Golgi. However, this model fails to explain why (i) tegument proteins have a cytoplasmic distribution, (ii) the phospholipid

content of virions differs from that of perinuclear particles (163, 258), and (iii) proteins such as pU_L31 and pU_L34 have been detected in perinuclear virions but not in final virions.

Much of the confusion over the mechanism of egress is a result of technical limitations. Although electron microscopy offers a clear picture of ultrastructural localization at a given point in time, it does not offer any information about directional progression through time. In a snap-shot view a particle budding towards the nucleus from the cytoplasm appears identical to a particle leaving the nucleus after fusion or de-envelopment. Also, observing only a single point in time, it is not possible to differentiate between successful and aberrant particles. Although a number of studies have been published, a consensus of the route of HSV egress still has not been reached. Perhaps egress is more complex than expected in that multiple pathways exist to maximize viral success in various cell types or environments.

Nuclear egress/primary envelopment:

The most popular model of HSV capsid egress involves INM budding, de-envelopment at the ONM, and re-envelopment in the Golgi or other cytoplasmic membrane (Figure 1.14). Other alphaherpes virus including PrV, ITLV (infectious laryngotracheitis virus), and EHV (equine herpes virus) are thought to use this pathway. It suggests that a primary tegument is acquired in budding at the inner nuclear membrane, but the final tegument is built in the cytoplasm rather than the nucleus.

Since C capsids are preferentially enveloped at the inner nuclear membrane, it is clear that something must distinguish these from other immature A and B capsids that remain within the nucleus, and yet this

mechanism is still unknown. It is unclear whether a capsid component or proteins in the tegument are involved in the process of assembly or whether they are only added to capsids after nuclear egress and envelopment (164, 165, 266). However, recent studies suggest that some tegument proteins may be added to the capsid within the nucleus. U_S3 has been shown on both perinuclear and extracellular virions (209). Additionally, the pU_L36 and pU_L37 tegument proteins have recently been found to co-purify with intranuclear capsids, and pU_L41 has been detected on intranuclear B and C capsids (27, 202). Moreover, despite its cytoplasmic localization, the VP11/12 (U_L46) tegument protein was found to interact with purified nucleocapsids as well as to fractionate with capsids when virions were stripped of their envelopes, suggesting its interaction with the capsid (174).

Capsids that are selected for nuclear exit must pass first through a layer of condensed host chromatin, then through a network of nuclear structural proteins, and finally through two layers (inner and outer) of nuclear membrane to finally arrive in the cytoplasm. Immunofluorescence studies assaying chromatin distribution late in infection found that host cell chromatin (as indicated by an antibody against histone H1) became fragmented in the nuclear periphery by 18 hours post infection, forming channels into which ICP8 (infected cell protein 8), a marker of HSV replication compartments, extended (222). No co-localization between the chromatin and replication compartment markers was seen, suggesting discrete compartmentalization. This led to the hypothesis that after marginalizing host cell chromatin, HSV also manipulates the compacted structures at the nuclear periphery to allow capsids access to the inner nuclear membrane. When two HSV late genes, U_L31 and U_L34, were each singly deleted from the virus, infections no longer exhibited nuclear

expansion nor produced channels in the condensed chromatin; instead, a continuous layer of chromatin lined the inner rim of the nuclear membrane (222). Repair of the missing gene into each of these mutant viruses restored the fragmentation of chromatin late in infection, indicating the observed phenotypes were specific for the mutations created. Taken together, these data suggest pU_L31 and pU_L34 actively manipulate the distribution of marginalized chromatin late in infection to allow passage of capsids toward the inner nuclear membrane (222).

Chromatin is only one of many barriers obstructing the capsids access to the nuclear membrane. Structural proteins, such as lamins, normally offer mechanical support to maintain the integrity, size, and shape of the nucleus. Lamins self-associate in multiple ways. First, they have a coiled-coil domain that facilitates dimer formation. Second, these dimeric, skeletal proteins are linked in a head-to-tail fashion to create a support network of filaments that lie interior to the inner nuclear membrane. There are three lamin genes expressed in vertebrates, LMNB1, LMNB2, and LMNA. LMNB1 encodes only a single gene product, lamin B1. In contrast, LMNB2 encodes both lamin B2 and B3 proteins, and LMNA produces four lamins proteins, A, AΔ10, C1 and C2, through alternate splicing of the LMNA transcript (115). Each of these products can be categorized as one of two types of lamins, A or B type. Studies transfecting truncated lamin A show disruption of lamin A/C localization but not of lamin B, suggesting that the two types of lamins are independent (115).

It has been proposed that the lamin network, the lamina, must be disassembled or disrupted by exiting nucleocapsids to permit egress (192). Lamins are only a subset of the structural proteins present in the complex

lamina that includes emerin and other lamin binding proteins such as lamin-associated protein (LAP2) and lamin B receptor. Capsid penetration of this complex layer uses components of a cellular system intended for lamina disruption. Normal host cell processes such as mitosis and apoptosis also require dismantling of the nuclear lamina; disassembly can be accomplished in various ways. In mitosis, induced host cell kinases such as (cdc2) can phosphorylate components of the lamina (lamin proteins and LAPs, including emerin) to promote the necessary reversible filament depolymerization (77, 81, 106). In contrast, apoptosis utilizes both depolymerization by PKCδ and caspase 6 cleavage to permanently destroy the nuclear lamina (52).

In order to transport capsids out of the nucleus, HSV induces progressive lamin disruption which can be seen in lamin A/C immunostaining. Mock-infected cells show smooth, uniform lamin A/C staining surrounding the nucleus, but infected cells reveal punctate staining leaving gaps along the nuclear rim. Redistribution of LAP2 as well as lamin A/C was observed late in infection and this allowed expansion of the replication compartment to the nuclear membrane (222). Two protein products of HSV late genes, pU_L31 and pU_L34, both present only on the perinuclear virion (209) were found to be essential for this redistribution to occur (222).

U_L34 encodes a type II membrane phosphoprotein that upon infection or transfection resides in the nuclear envelope. pU_L31 is a nuclear matrix-associated phosphoprotein (40); however, its membrane localization in infected and transfected cells is influenced by the presence of pU_L34 (208). In the absence of pU_L34, pU_L31 is entirely mis-localized and stains predominantly within the nucleus. In contrast, in the absence of pU_L31, some pU_L34 can still be detected at the nuclear rim, but pU_L34 is also spread out in

the replication compartment, and in the perinuclear region. Direct interaction of the two proteins *in vitro* has been shown with GST-fusion pull down experiments and co-localization assays (208). The region containing amino acids 137-181 in the U_L34 protein is essential for this interaction with pU_L31 (141).

In addition to each of the U_L31 and U_L34 proteins influencing the localization of the other, the nuclear membrane localization of both proteins can also be altered by a viral kinase encoded by U_S3. In the absence of pU_S3, pU_L31 and pU_L34 form punctate accumulations along the nuclear rim (208). Like pU_L31 and pU_L34, pU_S3 is also present in the inner nuclear membrane, closely associated with pU_L34 (209). pU_S3 exerts its kinase activity on both U_L31 and U_L34 proteins as well as other, unrelated viral proteins such as pU_S9 and ICP22 and many other cellular substrates including emerin and lamins (122, 136, 172). It is thought that lamin A/C phosphorylation by pU_S3 regulates lamina disruption through conformational changes thus in effect perforating the barrier to capsid egress (23, 172, 207). Studies in PrV revealed that capsids accumulate within nuclear membrane invaginations in cells infected with the U_S3-null virus (264). Thus far, phosphorylation of pU_S9 and ICP22 by pU_S3 has not shown any relevance to inner nuclear membrane recognition for capsid budding. Instead, these pU_S3 substrates most likely aid in other pU_S3 functions such as capsid de-envelopment at the outer nuclear membrane or prevention of apoptosis.

Remarkably, despite their roles in gaining access to the nuclear membrane, neither pU_L31 nor pU_L34 is strictly essential for replication though both U_L31 and U_L34 deletion viruses produce many fewer virions. U_L34 deletion virus is attenuated at least 3 orders of magnitude for growth when

compared to wild-type viral titers (211). Deletion of U_L31 lowered virus output by 1-3 logs depending on the cell line (41). Specifically, electron microscopy revealed that either U_L31 or U_L34 deletion viruses produce an accumulation of unenveloped capsids at the interior of the nuclear membrane (208). These observations also suggest pU_L31 and pU_L34 are crucial for nuclear egress.

Tegument:

The tegument, analogous to the matrix of other viruses, is an asymmetrical network of at least 20 proteins with various functions (162). The innermost layer, the layer most proximal to the capsid shell, is composed of the product of HSV's largest ORF, U_L36, which encodes VP1/2 (159), pU_L37, and pU_S3; these are believed to be the first tegument proteins added to the capsid (285). The external capsid proteins, pU_L17 and pU_L25, may also be considered part of the tegument. This conclusion is supported by the presence of pU_L17 in "light" particles which contain tegument proteins but lack capsids (214). De-envelopment of the perinuclear virion results in cytoplasmic capsids which appear "naked" by electron microscopy. Although they do not posses enough tegument to visualize, these capsids contain U_L36, U_L37, and U_S3 proteins as detected by immunogold electron microscopy (85). The distribution of U_L36 protein around the capsid may reflect the symmetry of the icosahedral capsid by association with the VP26-less pentons, although this symmetry is lost in more capsid-distal layers of the tegument (285).

Physical interaction of the U_L36 and U_L37 gene products has been documented upon infection with PrV through immunoprecipitation studies and in both PrV and HSV yeast-two hybrid screens (123, 263). The interaction, confirmed by reciprocal immunoprecipitations, was mapped to the N terminus

of pU_L36 (123). Both pU_L36 and pU_L37 are essential virion proteins. Despite successful C capsid formation and nuclear egress, ultrastructural studies of a U_L36-null infection demonstrated the accumulation of cytoplasmic capsids and abrogated production of enveloped virions (65). Incorporation of U_L37 protein in the tegument was found to be independent of pU_L36 (123). More recently live-cell microscopy studies using a U_L37-GFP recombinant virus indicate pU_L37 is trafficked to the Golgi in a pU_L36-dependent, capsid-independent, manner (64). These results suggest interplay between pU_L36 and pU_L37 is necessary for Golgi-recruitment of pU_L37 possibly defining a crucial role for pU_L37 in cytoplasmic envelopment.

Beyond the inner layer the organization of the tegument becomes much less ordered and less well understood. Two independent yeast two-hybrid screens have been performed to reveal structural interactions creating the network of tegument proteins (138, 263). This quest is encumbered by the redundancy and flexibility of the tegument. Reports indicate that deletion of the tegument protein VP22 creates a void in which other tegument as well as cellular proteins are over-represented in the virion presumably as a compensatory mechanism (61). Whether reported tegument interactions are merely structural or whether they have functionally relevant purposes is still largely unknown.

The functions of many tegument proteins appear to be redundant. No single tegument-glycoprotein interaction appears to be essential for assembly of the tegument; in fact, a PrV virus with U_L46, U_L47, U_L48, and U_L49 all deleted can replicate although level of replication is impaired (86). Viruses deficient in either U_L46 or U_L49 were unattenuated; however, deletion of U_L47 or U_L48 impaired replication (85, 126). Not only are some tegument proteins

redundant in function, their interactions with glycoproteins may also share redundancy further complicating the study of secondary envelopment. Studies deleting both gM and gE found infection was only mildly hampered (26).

HSV tegument proteins are diverse, serving roles in viral transcriptional regulation, degradation of mRNA, inter- and intra-cellular trafficking, and induction of the NFkappaB pathway. One aspect all tegument proteins share is the potential to function immediately upon cell entry instead of relying on productive transcription and synthesis. This suggests that tegument proteins may have either early or high priority functions in terms of replication. However, the function of many tegument proteins remains an enigma at the present.

For example, one tegument protein, VP16 (U_L48), is known to promote transcription of viral genes. Although VP16 itself is not a transcription factor in that the protein is not capable of binding DNA directly, it promotes transcription through the assistance and interactions with the cellular protein, Oct-1, that recognizes a specific immediate early gene promoter sequence. The consensus sequence, TAATGARAT, is recognized by Oct-1 which in combination with VP16 forms a complex (157, 189, 198). Transactivation of a CAT construct linked to a TAATGARAT promoter element has demonstrated the recognition sequence alone is sufficient for activation (90).

Another tegument protein with an established functional role in infection is pU_L41, also coined vhs for virion host cell shut-off protein. This protein appears to degrade or destabilize both viral and host mRNAs early in infection thereby shutting down protein synthesis so that cellular translation machinery can be used primarily by viral transcripts. Early reports using a U_L41 mutant suggested that this protein is necessary for incorporation of the transactivator,

VP16, into the virion (201). A VP16-binding domain was mapped to 20 particular amino acids of vhs in a yeast-two hybrid assay (215). Clearly, however, interaction between these two proteins does not occur exclusively through this domain; in more recent studies deletion of the VP16 binding domain in vhs did not preclude co-immunoprecipitation from infected cells and only made a modest decrease in the amount of vhs assembled into the virion (233).

The U_L49 tegument protein, VP22, is not essential in HSV, but in Marek's disease virus (MDV) is indispensible (70). In HSV, VP22 has been demonstrated to co-localize and co-purify with the HSV major transcriptional regulator, VP16 (U_L48) through its activation domain (73, 173, 190). In a complex with VP16, VP22 also works indirectly with vhs to regulate viral gene expression. In the absence of VP16/VP22, vhs protein levels produced from solo transfection were lower compared to levels after co-transfection of VP16/VP22 with vhs (237). Despite the difference in protein levels, amount of vhs mRNA was equivalent in the single and co-transfection samples, indicating ample transcription of vhs, but the vhs protein is unstable without VP16 and VP22 (237). Thus VP22, like VP16, may play role in regulating the ribonuclease activity of vhs which is strong early in infection and inhibited late in infection, thus explaining why VP22 is needed for mRNA accumulation of specific viral proteins (71, 131).

Additionally, VP22 may aid in transport of virus particles both intra- and inter-cellularly. Since it was found to hyperacetylate and rearrange microtubules into thick, resilient bundles, VP22 has been suggested to be a microtubule associated protein (MAP) (74). Independent of the HSV virion, VP22 has also been reported to spread from one cell to another (75),

however, later reports suggest the uptake of VP22 may be influenced by fixation parameters (149).

The pU_L37 tegument protein has been shown to induce NFkappa activation (147). The host cell uses the NFkappaB pathway to respond to many stimuli. NFkappaB translocates to the nucleus or is “activated” when its repressor IkappaB is phosphorylated. The phosphorylation event induces dissociation of IkappaB from NFkappaB thus exposing the NLS of NFkappaB. Upon HSV infection two distinct phases of reduction of IkappaB and NFkappaB activation can be detected. The first is virus-independent and co-incidental with infection and may be the result of gD signaling through TLR2; the second is virus dependent and starts between 5-6 hours post-infection (6). In a proteome-wide screen of 70 ORFs, the tegument protein pU_L37 demonstrated the strongest ability to activate NFkappaB (147). This function was also determined to be TLR-independent (147).

Secondary envelopment/cellular egress:

Many outer tegument proteins interact with the cytoplasmic tails of glycoproteins present in cytoplasmic membranes which act as targets for sites of secondary envelopment. Many organelle membranes have been proposed as secondary envelopment sites including the endoplasmic reticulum-Golgi intermediate, the Golgi, the trans-Golgi network (TGN), aggresomes, tegusomes, endosomes, and multi-vesicular bodies. However, more recent reports support the TGN as the most likely candidate. Infection with a temperature-sensitive protease mutant to block capsid egress, targeted glycoproteins gD, gE, gH, gI and gL specifically to the TGN at the restrictive temperature, which is in congruence with the idea that the TGN is the primary

site of secondary envelopment (257). With a shift to the permissive temperature the egress block was reversed and capsids were found to co-localize with viral glycoproteins at the TGN (257).

Some direct tegument-glycoprotein interactions have been reported, for example, the tegument protein VP16 (U_L48) has been shown to interact in the cytoplasm with the gH glycoprotein using a GST-fusion of VP16. This interaction was further substantiated with the *in vivo* co-immunoprecipitation of the two proteins (103). Curiously, the PrV homolog of U_L49 has not been shown to interact with gD; rather, yeast two hybrid studies suggest that in PrV this tegument protein can interact with gM and gE glycoproteins (87).

The functional redundancy of tegument proteins and membrane-bound glycoproteins complicates the study of secondary envelopment. Analysis of a single outer tegument protein, VP22 (U_L49), and its multiple interactions with glycoproteins provides an excellent example of redundancy involved in the mechanism for secondary envelopment. Using an *in vitro* assay, VP22 was shown to interact with the cytoplasmic tail of gD in two separate studies, one reacting cellular extracts with a GST-gD fusion protein and the second using tandem-affinity purified (TAP) cytoplasmic gD tail to capture VP22(44, 79). However, VP22 is also capable of interacting with the cytoplasmic tail of gE (79, 234).

During secondary envelopment the virus particle obtains its final membrane from the compartment into which it buds. Virus export to the extracellular space continues through the secretory system.

Cytoplasmic capsid transport:

Cytoplasmic, anterograde transport of exiting virus particles occupying cytoplasmic compartments appears also to be mediated by microtubules. Using cytoplasmic organelles purified by sucrose-gradient that contain GFP-VP26 recombinant HSV, time-lapse microscopy demonstrated ATP-dependent, microtubule-based transport. Movement rates along microtubules were calculated to average approximately 0.58 um/second (137). In these studies, two types of motion were observed, short distance with highly variable speed and long distance with constant speed. When kinesin motor inhibitors were used such as AMP-PNP (adenosine 5'-(β, γ-imido) tri-phosphate) and vanadate only the constant-speed, long-distance moving particles were stopped (137). This argues that progressive anterograde transport of HSV is through kinesin motor transport on microtubules. The force behind the other class of saltatory moving particles remains unknown.

Roles of the U_L17 protein:

In the chapters that follow I explore structural and functional roles of the essential HSV protein pU_L17. Electron microscopy indicates pU_L17 is multivalently present on the external surface of the HSV capsid. Biochemical and immunofluorescent studies support the Trus et al hypothesis that pU_L17 and pU_L25 form a heterodimer on the capsid (254). pU_L17 also appears to have DNA-binding properties similar to pU_L25 (191). Consistent with its capsid surface positioning, pU_L17 also appears to interact with tegument proteins VP11/12 and VP13/14. Both pU_L17 and pU_L25 as well as every other DNA cleavage and packaging protein are not essential to the intranuclear

dynamics of capsids despite potential ATPase activity displayed with purified U_L17 protein.

CHAPTER II:

The Herpes Simplex Virus 1 DNA packaging proteins encoded by U_L15, U_L17, U_L28, and U_L33 are located on the external surface of the viral capsid

Portions of this chapter are published in **Wills, E., L. Scholtes, and J. D. Baines.** 2006. Herpes simplex virus 1 DNA packaging proteins encoded by U_L6, U_L15, U_L17, U_L28, and U_L33 are located on the external surface of the viral capsid. J Virol **80:**10894-9.

Abstract:

Herpes simplex virus capsids were purified and were reacted with antibodies directed against the portal protein encoded by U_L6, the putative terminase components encoded by U_L15, U_L28, and U_L33, the minor capsid proteins encoded by U_L17 and U_L33 protein, and the major scaffold protein ICP35. The presence of bound antibodies in intact and sectioned capsids was revealed by immunoelectron microscopy. Epitopes of the scaffold protein, ICP35, were more readily reactive after capsids were embedded and sectioned, indicating that, as expected, this protein was located exclusively within the capsid interior. Epitopes of pU_L6, pU_L17, pU_L33 and pU_L15 were present at the capsid surface as revealed by the immunoreactivity of intact capsids reacted with antibodies directed against these proteins. Epitopes of pU_L15 were also recognized in sectioned capsids suggesting that portions of this protein were present at both the capsid exterior and interior.

Introduction:

Capsids form in the nuclei of cells infected with all herpesviruses. Herpes simplex virus capsid pentons and hexons form spontaneously from five and six molecules of ICP5 respectively; these capsomeres are linked by triplexes consisting of two molecules of VP23 and one molecule of VP19C to form a porous procapsid (183, 228, 251). ICP5 is also associated with ICP35 that forms an internal shell or scaffold within the procapsid. The procapsid is believed to give rise to the three other types of capsids seen in HSV-infected cells, designated A, B, and C. All of these differ internally but contain identical outer shells as determined by cryoelectron microscopy (180, 216, 288). Type B capsids retain the scaffold internal to the outer shell, type A capsids only

contain the outer shell, and type C capsids lack the internal scaffold but contain viral DNA (98). Type C capsids then bud from the nuclear membrane in a reaction termed primary envelopment (163, 210).

One of the vertices of A, B, and C capsids is biochemically and structurally unique and has been designated the portal vertex. Thus, the U_L6 encoded protein (pU_L6) forms a dodecameric ring with an internal diameter of at least 65 Å, i.e. sufficiently wide to accommodate DNA as it is packaged into the capsid (252). Critical to the discovery of the portal was the observation that an antibody to the C-terminus of pU_L6 recognized epitopes on a single vertex of type B capsids, thus showing that at least the C-terminus of pU_L6 is located at the capsid exterior in a position to access incoming viral DNA (182, 241).

It has also been shown that HSV-1 B capsids contain a number of capsid proteins in addition to pU_L6, ICP5, and ICP35. These include approximately 1.2 copies of pU_L15, 2.4 copies of pU_L28, 40 copies of pU_L25, and an undetermined number of copies of pU_L17 and pU_L33 (17, 18, 99, 194, 213, 246, 283). By analogy to extensive studies of bacteriophage capsid assembly, one might predict that some of these minor capsid proteins would be involved in processing concatemeric DNA and threading the DNA into the portal through the hydrolysis of ATP (36). Such a complex, termed the terminase, remains somewhat enigmatic in HSV, but a variety of indirect evidence suggests that it comprises at least the U_L15, U_L28, and U_L33 proteins. Specifically, (i) all three proteins are among seven required for viral DNA packaging (3, 197, 243), (ii) the U_L15 protein contains a conserved P-loop ATPase motif and mutation of this motif precludes DNA packaging (54, 282), (iii) the U_L28 protein can specifically bind DNA sequences known to be

required for correct cleavage of concatemeric viral DNA (2), (iv) the U_L15, U_L28, and U_L33 proteins interact in vitro and can be purified from lysates of infected cells by co-immunoprecipitation (1, 19, 127), (v) in vitro, both pU_L28 and pU_L15 can interact with the portal protein encoded by U_L6 (269).

Although it is also required for DNA packaging, the precise function of pU_L17 is unknown (214). Analysis of a U_L17 deletion mutant revealed alteration of the normal intranuclear distributions of capsids, and a number of viral proteins including pU_L6, ICP35, and ICP5 (241). These observations suggest that U_L17 protein is involved in capsid assembly, the reorganization of the infected cell nucleus, or directly or indirectly in capsid or protein transport within the nucleus. Relevant to this last possibility is the observation that HSV capsids are actively transported in the nucleus and this transport is both energy and actin-dependent (82).

The hypotheses that the U_L15, U_L28, and U_L33 proteins form the HSV terminase, and pU_L17 acts directly or indirectly to mediate transport of capsids within the nucleoplasm predict that at least portions of these proteins would localize on the external surfaces of capsids. This study was undertaken to test this possibility.

Production and specificity of novel chicken antiserum against pU_L17:

Because a previously described pU_L17 antibody produced using a DNA vaccine did not recognize small quantities of U_L17 protein (214) (data not shown), pU_L17 was fused to DNA encoding a 6X Histidine tag and a recombinant baculovirus was generated that expressed the fusion protein. The U_L17 fusion protein was purified from lysates of insect cells infected with the recombinant baculovirus by affinity chromatography on Ni++-containing

Sepharose beads as described previously (18). Immunization of chickens with the purified fusion protein was followed by purification of IgY from the eggs of immunized hens.

To test the antisera for specificity, Hep-2 cells were mock infected or infected with HSV-1 (F) or a U_L17 null virus at an MOI of 5 pfu per cell. Lysates from approximately 1.3 $x10^6$ cells were prepared by denaturation and boiling in 1% SDS and 5 mM beta mercaptoethanol. Denatured proteins were electrophoretically separated on an 8% SDS polyacrylamide gel and transferred electrically to a nitrocellulose membrane. The nitrocellulose membrane was blocked overnight at 4^oC in PBS supplemented with 5.0% milk and 0.2% Tween-20. The membrane was rinsed twice with room temperature PBS and 0.2% Tween-20 and was further blocked by immersion in a 1:10 dilution of Block Hen (Aves labs) for 15 minutes. Polyclonal anti-pU_L17 IgY was diluted 1:500,000 into PBS with 1% BSA and 0.2% Tween-20 and applied overnight. After extensive washes in PBS containing 0.2% Tween-20, the membrane was incubated with horseradish peroxidase-conjugated anti-chicken antibody diluted 1:5,000 in PBS containing 5.0% milk and 0.5% Tween-20. Bound IgY was detected using a five minute incubation with ECL Plus reagents (Amersham) and flash exposure to Fuji autoradiographic film.

As shown in Figure 2.1, the anti-pU_L17 antiserum recognized a 79,000 apparent M_r protein that was not present in lysates of mock infected Hep2 cells or cells that were infected with the U_L17 deletion virus. This size is consistent with a previous study reporting an apparent M_r of 77,000 in virions (214). We did not detect the previously reported 72,000 apparent M_r protein that was previously identified in virion lysates by mass spectrometry,

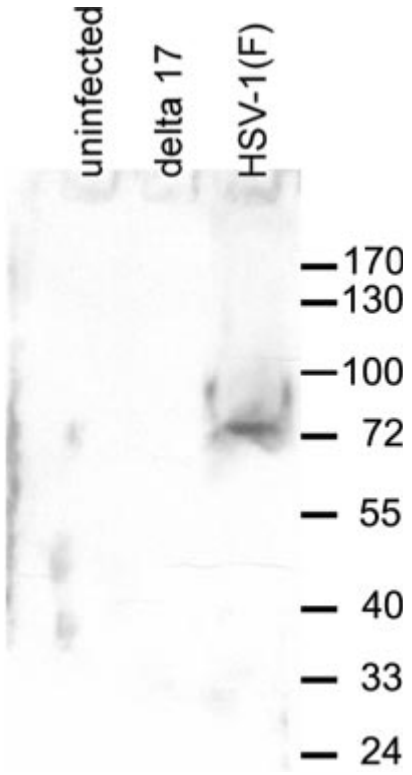

Figure 2.1. Chicken anti-pU_L17 antibody immunoblotting. Digitally scanned image of immunoblot of lysates of infected and uninfected cells reacted with pU_L17 specific antiserum. Lysates of cells that were uninfected (left lane) or infected with a U_L17 deletion virus (center lane), or wild type virus HSV-1(F) (right lane) were electrophoretically separated on an SDS polyacrylamide gel, transferred to nitrocellulose and reacted with purified IgY obtained from a chicken immunized with purified pU_L17. Bound IgY was revealed as indicated in the text.

suggesting that the smaller protein may be highly enriched in virion preparations (214).

Immunogold labeling of wild type and mutant capsids:

Using standard procedures, capsids were purified from nuclear lysates of cells infected with wild type HSV-1(F), and viruses respectively lacking the U_L6, U_L15, U_L17, U_L28 and U_L33 genes (10, 53, 195, 213, 243). Capsids were either attached to Formvar carbon-coated electron microscopic grids, or were placed into microdialysis tubes (200 μm diameter), subsequently embedded in LRWhite and sliced with a diamond knife into 60 nm sections that were then placed on EM grids.

Previously described rabbit antisera directed against pU_L6, pU_L15, pU_L28 and pU_L33 were prepared by adsorption against capsids purified from Vero cells infected with 5.0 PFU/ml of the appropriate viral null mutant (8, 10, 195, 206, 240, 241, 243). The adsorbed antisera were then diluted 1:50 in PBS supplemented with 1% triton-100 and 1% fish gelatin and applied directly to the EM grids, followed by extensive washing. Experiments performed with the pU_L17-specific chicken IgY were similar except that the antibody was not preadsorbed and was diluted 1:5,000 for reaction with capsids. As a control, the capsid samples were also reacted separately with a polyclonal antiserum directed against the internal scaffold protein ICP35 (48) (NC 3-4) (kindly provided by Roselyn Eisenberg and Gary Cohen). Bound immunoglobulins remaining after the washing were recognized by goat anti-rabbit immunoglobulin conjugated to 12 nm gold beads, or goat anti-chicken IgY conjugated to 12 nm gold beads. After further washing, the grids were viewed in a Philips 201 electron microscope after counterstaining with 2% aqueous

uranyl acetate and 0.5% Reynold's lead citrate. Capsids were scored as positively immunolabeled only when a gold bead was observed in direct association with an observed capsid.

The results are summarized in table 2.1, and representative examples of immunostained capsids are shown in Figure 2.2.

Examination of at least 400 capsids in each treatment group revealed the following:

(i) Background levels of immunostaining with the pU_L15, pU_L17, pU_L28 and pU_L33-specific antisera, as revealed by the number of appropriate mutant capsids bearing gold beads, was significantly below (All P values < 0.001 as assessed with the Fisher exact T test) similarly stained wild type HSV-1(F) capsids.

(ii) As shown previously (182), pU_L6-specific epitopes were recognized on the surface of the capsid inasmuch as significantly more ($P < 0.001$) gold beads were present in intact wild type capsids reacted with the pU_L6-specific antiserum than were present in capsids lacking pU_L6. These epitopes were detected more frequently in intact capsids than in sectioned capsids ($p < 0.001$) suggesting that the bulk of the epitopes were available primarily for reaction at the capsid surface rather than internal to the capsid shell. Approximately 16.3% (53 of 325) of capsids were labeled suggesting either that the immunogold staining was insensitive and did not detect portal protein in many capsids, or that many capsids lack portals. Biochemical studies showing that populations of B capsids have on average 14.8 +/- 2.6 copies of pU_L6 per capsid (182), coupled with the high likelihood that the portal ring contains 12 copies of pU_L6 (252), argue against the latter possibility.

Table 2.1. Capsids were purified from cells infected with wild type viruses or viruses lacking the indicated open reading frames. In some experiments (intact), capsids were attached to grids and reacted with the indicated antibodies. In other experiments capsids were embedded and sectioned, followed by reaction of the thin sections with the indicated antibodies. The number of immunolabeled capsids vs. number of capsids examined is indicated and the resulting percentage of labeled capsids shown.

[1]The amount of immunoreactivity with a given antibody was greater ($P < 0.001$) in wild type capsids than in the corresponding deletion mutant capsids.

[2]The immunoreactivity of sectioned capsids was greater than intact capsids ($p < 0.001$)

[3]Immunoreactivity of intact capsids was greater than sectioned capsids ($p < 0.001$)

[4] Immunoreactivity of intact capsids was greater than sectioned capsids ($p = 0.01$)

[5]Immunoreactivity of sectioned capsids vs. intact capsids ($p = 0.06$)

All P values were obtained with Fisher's exact T test

.

Table 2.1. Percent capsids Immunolabeled with monospecific antisera

Antibody	Virus	Intact	Sectioned
ICP35	HSV-1(F)	(18/1007) 1.8%[2]	(115/413) 27.8%[2]
pU_L6[1]	HSV-1(F)	(53/325) 16.3%[3]	(48/1181) 4.0%[3]
pU_L6	U_L6-	(4/945) 0.4%	(3/929) 0.3%
pU_L17[1]	HSV-1(F)	(97/714) 13.5%[3]	(134/2447) 5.4%[3]
pU_L17	U_L17-	(0/1000) 0.0%	(2/969) 0.2%
pU_L33[1]	HSV-1(F)	(25/281) 8.8%[3]	(35/1644) 2.1%[3]
pU_L33	U_L33-	(9/1155) 0.8%	(4/1042) 0.3%
pU_L28[1]	HSV-1(F)	(33/378) 8.7%[4]	(43/960) 4.4%[4]
pU_L28	U_L28-	(8/1074)) 0.7%	(3/973) 0.3%
pU_L15C[1]	HSV-1(F)	(40/847) 4.7%[5]	(35/595) 5.8%[5]
pU_L15C	U_L15-	(6/571) 1.0%	(2/1000) 0.7%

Figure 2.2. Capsid electron micrographs labeled with various antibodies. Capsids were purified from cells infected with HSV-1(F). These were attached to copper mesh grids (left column), or were embedded in Lowicryl and sectioned (right column). Each row shows intact capsids and thin sections reacted with antisera directed against the indicated proteins. Bound immunoglobulin was identified by reaction with appropriate antisera conjugated to 12 nm gold beads. Arrowheads indicate gold beads associated with capsids.

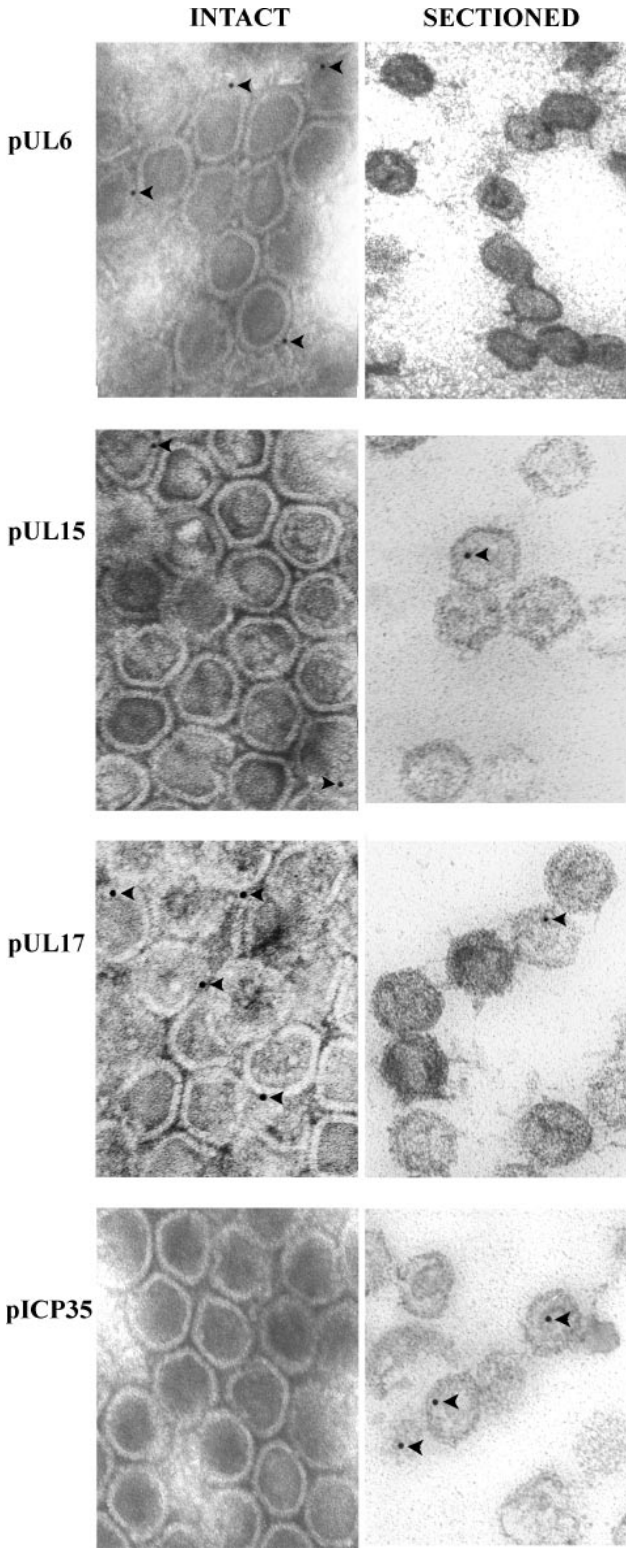
INTACT
SECTIONED
pUL6
pUL15
pUL17
pICP35

(iii) As expected, the ICP35-specific antiserum did not recognize the external surface of capsids to an appreciable extent inasmuch as only 18 capsids were labeled with the NC 3-4 antibody of 1007 examined (1.8%). Upon sectioning the capsids however, ICP35-specific epitopes were rendered significantly more immunoreactive with the antiserum ($P < 0.001$) as revealed by an increased number of labeled sectioned capsids [115 (28%) of 413 sectioned capsids]. These observations indicated that, as expected, ICP35 was present in the capsid interior rather than the capsid surface, and verified that the inner surfaces of unsectioned capsids were sequestered from the applied antibodies under the experimental conditions.

(iv) Epitopes from pU_L17, pU_L28 and pU_L33 localized at the surface of the capsid as revealed by immunoreactivity of intact capsids significantly above background levels obtained upon reaction with the corresponding deletion virus capsids. (All P values were less than 0.001 by Fischer's exact T test.) In all three cases, although immunoreactivity was present in sectioned HSV-1(F) capsids, the level of immunoreactivity was significantly less than that obtained using intact capsids, presumably because a given thin section contains only a limited portion of the capsid surface. More capsids (13%) labeled with the pU_L17-specific antibody than with either the pU_L28 or pU_L33 specific antibodies (8.7% and 8.9%, respectively).

(v) Antisera directed against C-terminal epitopes of pU_L15 were recognized on the external surface of capsids as revealed by increased immunoreactivity of intact capsids over that of pU_L15 negative capsids. Unlike the case with pU_L6, pU_L33, pU_L28 and pU_L17-specific antibodies, however, immunoreactivity of the pU_L15-specific antibody was increased in sectioned capsids, but the observed increase over immunoreactivity obtained with

unsectioned capsids was not statistically significant (p = 0.06). Because so little of the surface of the capsid is available for reaction in a thin section, the preservation of reactivity in sectioned capsids suggests that pU_L15 C-terminal epitopes are available on both the surface and within the capsid interior. Thus, pU_L15 is apparently located in a position such that some epitopes exterior and some epitopes exposed to the capsid interior. Alternatively, multiple copies of pU_L15 may be present at different locations within the capsid. Assuming that all B capsids are biochemically identical (an assumption that has not been tested), the observation that each B capsid contains only 1.2 copies of pU_L15 (18) argues against this possibility.

Rabbit skin cells infected with wild-type virus at an MOI of 5 were embedded and thin-sectioned (as described above). Immunolabeling with anti-pU_L17 antisera diluted 1:100 and subsequently reacted with a 1:50 dilution of goat anti-chicken IgY conjugated to 12 nm gold beads. Immunostaining revealed multiple binding sites on individual intranuclear capsids (Figure 2.3). Thus we were also able to conclude that multiple epitopes of pU_L17 are present on the surface of intranuclear capsids. We conclude from these data that at least some epitopes of pU_L6, pU_L15, pU_L17, pU_L28, and pU_L33 are located at the capsid surface. The data also suggest that some epitopes in the C-terminus of pU_L15 are sequestered from antibody unless the capsids are sectioned. One model, consistent with previous observations showing that A capsids contain approximately 12 copies pU_L15 but less than one copy of pU_L28 (18), is that pU_L15 is more intimately associated with the capsid whereas pU_L28 is more peripheral. Whether or not this conclusion is correct, the localization of portions of pU_L15, pU_L17, pU_L28 and pU_L33 at the capsid surface places these proteins in a position to engage

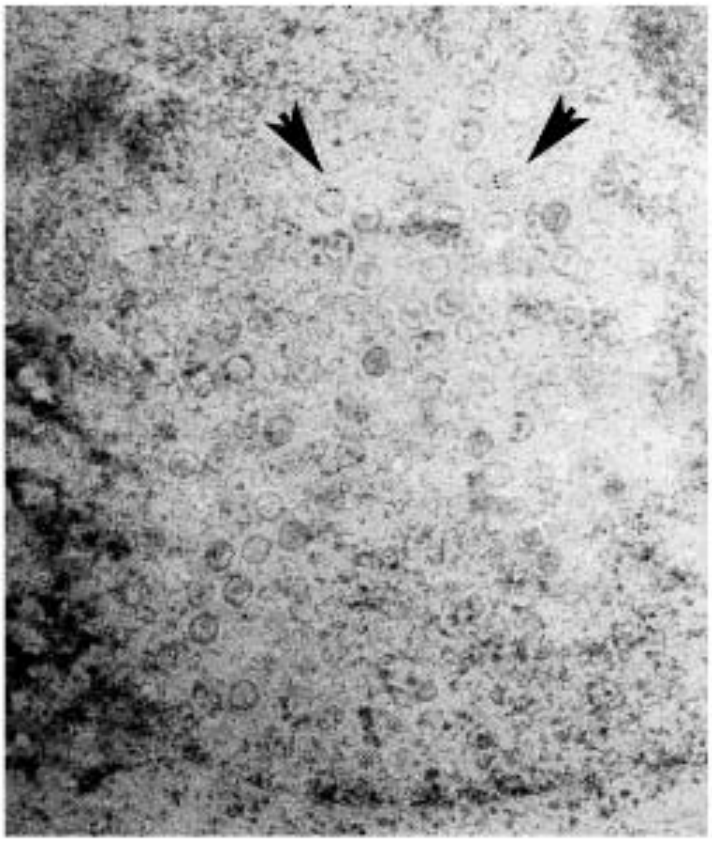

Figure 2.3 ImmunoEM labeling of pU_L17 upon infection. Capsids were observed with multiple beads indicating multiple sites of occupancy on the capsid surface.

DNA as it is being packaged. Alternatively, such a position might serve to engage molecular motors for capsid transport either within the nucleoplasm, or along microtubules in the cytoplasm.

Acknowledgements:

These studies were supported by public health service grant R01 GM 50740 from the National Institutes of Health.

CHAPTER III:

Effects of major capsid proteins, capsid assembly, and DNA cleavage and packaging on the pU_L17/pU_L25 complex of herpes simplex virus 1

Abstract:

The U_L17 and U_L25 proteins of herpes simplex virus 1 (HSV-1) are located at the external surface of capsids and are essential for DNA packaging and DNA retention in the capsid, respectively. The current studies were undertaken to determine how these proteins become associated with capsids by examining their interactions in cells infected with wild-type, VP5-null, VP23-null, U_L15-null and U_L32-null viruses. We found that pU_L17 and pU_L25 co-immunoprecipitated from cells infected with wild type virus whereas the major capsid protein, VP5, did not co-immunoprecipitate with these proteins. In addition, pU_L17 (i) co-immunoprecipitated with pU_L25 in the presence or absence of VP5 (ii) did not co-immunoprecipitate efficiently with pU_L25 in the absence of the triplex protein VP23, (iii) required pU_L25 for proper solubilization and localization within the replication compartment, (iv) was essential to the nuclear retention of pU_L25 and (v) required capsid proteins VP5 and VP23 for nuclear localization and normal levels of immunoreactivity in an indirect immunofluorescence assay. Proper intranuclear localization of pU_L25 required pU_L17, pU_L32, and the major capsid proteins VP5 and VP23, but not the DNA packaging protein pU_L15. The data suggest that VP23 and VP5 induce conformational changes in pU_L17/ pU_L25, exposing epitopes that are otherwise partly masked in infected cells. These conformational changes can occur in the absence of DNA packaging. The data indicate that the pU_L17/ pU_L25 complex requires multiple viral proteins and functions for proper localization and biochemical behavior in the infected cell.

Introduction:

Immature herpes simplex virus capsids, like those of all herpesviruses, consist of two protein shells. The outer shell comprises 150 hexons, composed of six copies of VP5, and 11 pentons, each containing five copies of VP5 (216, 286). One vertex of five-fold symmetry is composed of 12 copies of the protein encoded by U_L6 and serves as the portal through which DNA is inserted (182). The pentons and hexons are linked together by more than 320 triplexes composed of 2 copies of the U_L18 gene product, VP23, and 1 copy of the U_L38 gene product, VP19C (183, 288). Each triplex arrangement has two arms contacting neighboring VP5 subunits (288). The internal shell of the capsid consists primarily of more than 1,200 copies of the scaffold protein ICP35 (VP22a) (183), and a smaller number of protease molecules encoded by the U_L26 open reading frame which self-cleaves to form VP24 and VP21 derived from the amino and carboxyl termini, respectively (55, 59). The outer shell is virtually identical in the three capsid types found in HSV infected cells, termed types A, B, and C (98). It is believed that all three are derived from the immature procapsid (184). Type C capsids contain DNA in place of the internal shell; type B contain both shells, and type A consist only of the outer shell (98). Only C capsids go on to become infectious virions (80).

The outer shell also contains minor capsid proteins derived from the U_L25 and U_L17 open reading frames (99, 245). These proteins are located on the external surface of the viral capsid and are believed to form a heterodimer arranged as a linear structure, termed the C capsid specific complex (CCSC), located between pentons and hexons of C capsids (254). This is consistent with the observation that levels of pU_L25 are increased in C capsids as opposed to B capsids (217). On the other hand, other studies have indicated

that at least some pU_L17 and pU_L25 associate with all capsid types, and pU_L17 can associate with enveloped light particles, which lack capsids but contain a number of viral structural proteins (245, 246). How the U_L17 and U_L25 proteins attach to capsids is not currently known although the structure of the CCSC suggests extensive contacts with triplexes (254). It is also unclear when pU_L17 and pU_L25 become incorporated into the capsid during the assembly pathway. Less pU_L25 associates with pU_L17(-) capsids suggesting that the two proteins bind capsids either cooperatively or sequentially, although this could also be consequential to the fact that less pU_L25 associates with capsids lacking DNA (245).

Both pU_L25 and pU_L17 are necessary for proper nucleocapsid assembly, but their respective deletion generates different phenotypes. Deletion of pU_L17 precludes DNA packaging and induces capsid aggregation in the nuclei of infected cells suggesting a critical early function (214, 241), whereas deletion of pU_L25 precludes retention of full length cleaved DNA within the capsid (47, 158, 231), thus suggesting a function late in the assembly pathway.

The current studies were undertaken to determine how pU_L17 and pU_L25 associate with capsids by studying their interactions in the presence and absence of other capsid proteins.

Materials and Methods:

Cell Lines and Viruses- Vero and Hep2 cells were obtained from the American Type culture association and were propagated in DMEM supplemented with 10% newborn calf serum (NBCS) and antibiotics as described previously (278).

A U_L18 deletion virus (delta 18) virus was constructed to remove the entire open reading frame of U_L18 and replace it with an FRT-flanked Kanamycin resistance (Kan^R) cassette as follows. A gene encoding Kan^R was PCR amplified with the following primers containing sequences homologous to the flanking regions U_L18 ORF and Kan^R cassette: (del18F, #64) CCCCCGTGGGTCTAGCCGGGCCGTGTAGGCTGGAGCTGCTTC; (del18R, #65) CCCTGCCGCGTGGATCGGCGCCATTCCGGGGATCCGTCGAC (Kan^R homology underlined). Amplicons were transformed into EL250 cells containing a chloramphenicol–resistant (Cm^R), wild-type HSV-1(F) BAC and Cm^R/Kan^R recombinants were selected on agar plates (238). Extracted BAC DNA was transfected with SuperFect (Qiagen) into and propagated on G5 cells complementing the HSV genome U_L16 to U_L21 region (62). Stocks were obtained from G5 cells infected at an MOI of 0.01 and grown in 890 cm^2 roller bottles.

Delta 17 (described in Chapter IV) and delta 25 (KUL25NS)(158) viruses were described previously and contain a Kanamycin cassette inserted into U_L17 and stop codon inserted into U_L25, respectively. Delta 17 and delta 25 were grown on CV1-17 and 8-1 cells complementing U_L17 and U_L25, respectively (158). Stocks were obtained from cells infected at an MOI of 0.01 and grown in 890 cm^2 roller bottles.

To rescue the U_L17 deletion, the delta 17 BAC and a U_L17-expression vector (pRB457) were co-transfected into non-complementing (Vero) cells. After plaques had begun to spread 10 days post transfection virus was harvested. Several plaques from this virus preparation yielded plaques on Vero cells. For stock preparation after a second round of plaque picking, Vero cells were infected with the virus at 0.01 PFU/cell. The repaired virus,

designated pU_L17R, was verified both by its competency to infect non-complementing cells and by expression of pU_L17 as assessed by immunoblotting.

Immunoprecipitation Assay - Vero cells in 10 cm or 15 cm dishes were infected with various viruses at 5 PFU per cell and incubated at 37^0C. Sixteen hours following infection, cells were removed by scraping, transferred to 15 ml conical tubes, and pelleted at 4000 rpm in an Eppendorf 5810R centrifuge with an A-4-62 rotor at 4^0C. Supernatants were discarded and pellets were resuspended in 5 ml PBS with Complete protease inhibitors (Roche). Again, samples were centrifuged at 4000 rpm at 4^0C for 10 minutes and supernatants were decanted. Cell pellets were stored at -80^0C overnight. After thawing, the infected-cell pellets were lysed in RIPA buffer (1.0% NP40, 0.25% sodium deoxycholate, 50 mM Tris-HCl pH 7.4, 150mM NaCl, 1mM EDTA pH 8.0, 1 μg/ml aprotinin, 1 μg/ml leupeptin, 1 μg/ml pepstatin, 1mM PMSF, 1mM Na_3VO_4) on ice for at least 20 minutes. Infected-cell lysates were centrifuged to pellet insoluble material at 4^0C for 10 minutes in a microcentrifuge and supernatants were transferred to new tubes. One twentieth of each soluble lysate volume was removed and combined with 2x SDS-PAGE (100mM Tris-HCl pH 6.8, 4.0% SDS, O.2% bromophenol blue, 20% glycerol, 200mM fresh DTT) to assess protein expression in the lysates. The remaining lysate was pre-cleared by reaction with normal mouse IgG with constant rotation at 4^0C for 30-60 minutes after which Gamma Bind G beads (GE lifesciences) in a 50% PBS slurry was added. The mixture was then constantly rotated at 4^0C for 1 hour after which samples were centrifuged for 5 minutes at 4^0C to remove the beads, normal mouse IgG, as well as any proteins capable of non-

specific binding. Pre-cleared lysates were then reacted with the target antibody (anti-pU_L25 or anti-pU_L17) for 30-60 minutes at 4^0C with constant rotation before Gamma Bind G beads were added. (Immunoprecipitation with anti-pU_L17 required an additional incubation with a rabbit anti-IgY bridging antibody to adhere to the Bind G beads (as described in Chapter IV) The beads were then allowed to react with antibody complexes for 2 hours at 4^0C with constant rotation, after which time they were pelleted at 4^0C for 5 minutes, resuspended in RIPA solution, and rotated for 10 minutes at 4^0C. This washing step was repeated three more times before elution of proteins by boiling in 2x SDS-PAGE denaturation buffer for 5 minutes. Soluble lysate samples and immunoprecipitation samples were electrophoretically separated on an 10% polyacrylamide gel and transferred to nitrocellulose at 30V for 5 hours at 4^0C.

Transfections- Adherent Hep2 cells were transfected with the indicated expression plasmids using Lipofectamine 2000 (Invitrogen) according to the protocol of the manufacturer.

Immunofluorescence Assay (IFA) – Hep2 cells were seeded onto glass coverslips and cultured in DMEM with 10% supplemental NBCS (newborn calf serum). Cells were either transfected in Opti-MEM (Invitrogen) media or infected with 5 PFU per cell using low serum-containing media (1% NBCS). At various times following transfection or infection, cells were briefly washed with PBS and fixed with 3% paraformaldehyde in PBS for 15 minutes at room temperature. Fixed cells were washed with PBS before quenching autofluorescence with a 15 minute incubation in 50 mM ammonium chloride.

Cells were then washed with PBS and permeabilized for 5 minutes in 1.0% Triton X-100, washed again with PBS, and then incubated for 30 minutes in PBS with 1.0% BSA, 5% donkey serum, and 5% human serum to block non-specific antibody binding. Primary antibody was diluted in blocking solution at the following concentrations: anti-pU_L17 between 1:1,000 and 1:500, anti-pU_L25 (25E10) 1:200, anti-capsid 8F5 monoclonal antibody (253) 1:100. After reaction of the primary antibodies with the fixed, permeabilized cells for 45 minutes unbound antibody was removed by washing in PBS. The coverslips were then reacted for 45 minutes with the indicated fluorescent-conjugated secondary antibodies diluted 1:1,000 in blocking solution. Subsequently, cells were washed extensively with PBS, dipped briefly in dH_20 to remove any excess salt, and mounted on glass slides with Vectashield mounting media. Mounted coverslips were sealed with nail polish.

Immunoblotting – Immunoblots were blocked in PBST with 5% milk for 20-30 minutes and rinsed with PBST. Primary antibodies were diluted in PBST with 1%BSA to the following concentrations (anti-pU_L17, 1:10,000; anti-pU_L25, 1:1,000; anti-VP5 (Virusys), 1: 500; anti-VP23 (NC-5), 1:2,000; anti-VP19C (NC-2). (NC-2 and NC-5 antibodies were gifts from Gary Cohen and Roselyn Eisenberg). Excess antibody was removed with 3, 10 minute washed in PBST. Horseradish peroxidase-conjugated secondary antibodies were diluted 1:5,000 in to PBST with 5% milk and allowed to react with immunoblots for at least 1 hour. Excess antibody was again removed with PBST washes and conjugate-binding was detected with Pierce chemiluminescent ECL and subsequent exposure to x-ray film. Bound antibody was stripped from membranes with 2% SDS and 0.71% β-mercaptoethanol in 62.5 mM Tris pH

6.8 at 50^0C for 15-20 minutes and membranes were washed extensively with PBST before reprobing.

Results:

pU_L17 and pU_L25 interact in the absence of assembled capsids:

In preliminary studies we found that pU_L17 co-immunoprecipitated with VP5, which was not surprising given several lines of evidence indicating pU_L17 associates with capsids. In this study, we wanted to further investigate the relationship between pU_L17 and nucleocapsid assembly of HSV.

First, we sought to determine whether pU_L17 interacted with all or a subset of major capsid constituents. To this end, cells were infected with HSV-1(F), and deletion mutants lacking functional U_L17 (delta 17), U_L25 (delta 25), U_L18 (delta 18; VP23), U_L19 (delta 19; VP5) or U_L32 (delta 32). The infected cells were lysed at 16 hours post-infection and lysates were subjected to immunoprecipitation with anti-pU_L17 antibody and a rabbit anti-IgY bridging antibody (described in Chapter IV). Immunoprecipitated material and aliquots of soluble cell lysates were electrophorectically separated on a denaturing polyacrylamide gel, transferred to nitrocellulose, and probed with antibodies to pU_L17, the major capsid protein VP5, triplex proteins VP23 and VP19C, and the minor capsid protein pU_L25.

As shown in figure 3.1 A, pU_L17 was immunoprecipitated specifically from lysates of cells infected with HSV-1(F), delta 25, delta 18, delta 19 and delta 32 at levels that reflect their relative amounts in the respective cell lysates. The absence of a signal from the immunoprecipitation with a delta 17 virus indicated that the signal examined represented U_L17 protein.

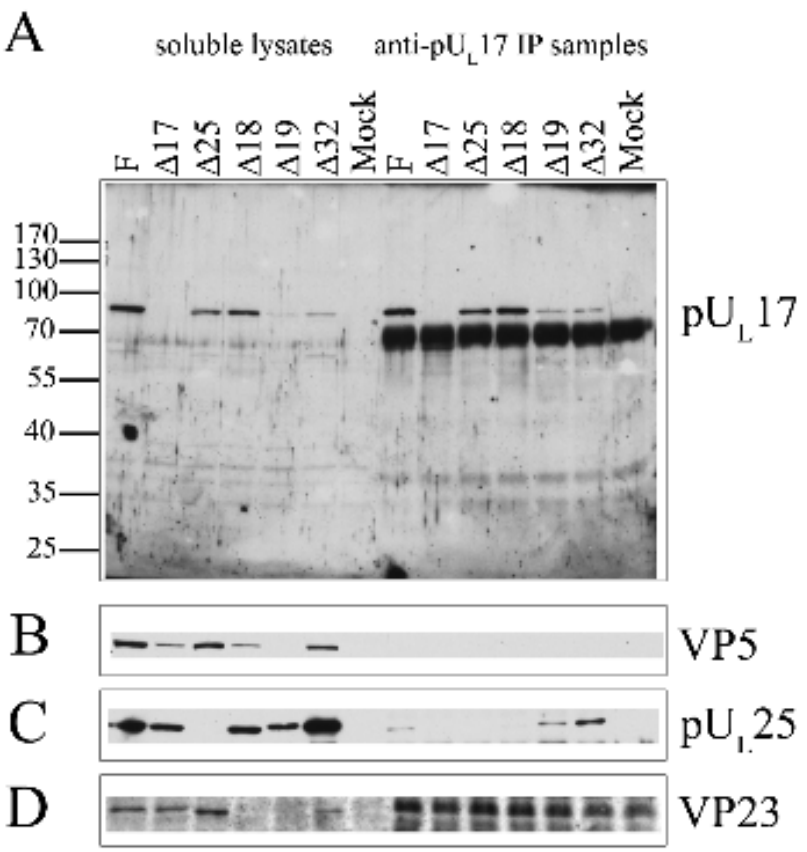

Figure 3.1 Co-immunoprecipitation with pU$_L$17 in F and capsid deletion viruses. Panel A shows immunoblotting with anti-pU$_L$17. Amounts of pU$_L$17 immunoprecipitated (on the right) reflect the relative levels of pU$_L$17 present in the lysates (shown on left). pU$_L$25 immunoblotting indicates that this protein co-immunoprecipitates with pU$_L$17 in F, delta 19, and delta 32 infected cells (Panel C). A barely detectable band of pU$_L$25 was also present in the delta 18 lane (Panel C). Capsid proteins VP5 and VP23 did not co-immunoprecipitate in any sample, including wild-type (F)-infected cell lysates (Panels B and D).

Immunoblotting pU_L17 co-immunoprecipitated material with mouse monoclonal anti-pU_L25 antibody indicated that pU_L25 co-immunoprecipitated with pU_L17 from lysates of cells infected with HSV-1(F), delta 19, and delta 32 (Figure 3.1 C). Lesser amounts of pU_L25 were co-immunoprecipitated from F and delta 19 infected cell lysates compared to that from lysates of cells infected with delta 32. No pU_L25 was immunoprecipitated from lysates of delta 17 infected cells despite high levels of expression in soluble lysates, indicating that pU_L25 was specifically co-immunoprecipitated through interactions with pU_L17 (Figure 3.1 C). These data suggest that pU_L17 and pU_L25 interact independently of assembled capsids and the major capsid protein VP5.

We also noted variable expression of pU_L25 and VP23 in our infections. Higher levels of pU_L25 were noted in delta 32 and HSV-1(F) (to a lesser extent) infected cell lysates compared to levels of pU_L17 and VP23 (Figure 3.1 C vs. Figure 3.1 A, D) . We currently do not understand whether these discrepancies are a specific effect related to each deleted gene or whether they reflect protein expression variation from different viral strains. VP23, in contrast, was specifically decreased to an undetectable level only upon delta 19 infection.

pU_L17 and pU_L25 interaction occurs independently of VP5, the major capsid protein:

We also wanted to determine whether or not the pU_L17/ pU_L25 complex was dependent on major capsid proteins. To address this question we re-probed the pU_L17 immunoprecipitation blot for the capsid protein VP5 (Figure 3.1 B), VP23 (Figure 3.1 D), and VP19c (data not shown). (The triplex

protein VP19C co-migrated with the heavy chain of the rabbit bridging antibody and therefore higher levels of overlapping background signal was observed in immunoblots probed with VP19C-specific antibody.) In all cases, VP5 was not co-immunoprecipitated with pU_L17, suggesting that the pU_L17/ pU_L25 complex forms independently of capsid formation, and of the major component of the outer capsid shell.

Reciprocal immunoprecipitation of pU_L17 with anti- pU_L25:

To confirm the capsid-independent interaction of pU_L17/pU_L25 cells were infected with HSV-1(F), delta 17, delta 25, delta 18, delta 19, and delta 32 viruses, and lysates prepared at 16 hours post-infection were reacted with a pU_L25-specific monoclonal antibody, 25E10. The presence of various proteins in immunoprecipitated material was then determined by immunoblotting with monospecific antibodies. The results are shown in figure 3.2.

Readily detectable amounts of the U_L25 protein were immunoprecipitated from HSV-1(F)-infected lysates, whereas significantly less pU_L25 was detected in delta 18 samples despite the fact that ample pU_L25 was present in the delta 18 infected cell lysate (Figure 3.2 A). Moreover, pU_L25 was not immunoprecipitated with its cognate monoclonal antibody from delta 19 (VP5-null) infected cell lysates to detectable levels. To explain the lack of immunoprecipitated pU_L25 in these samples we hypothesize that pU_L25 adopts at least two conformations, one of which is accessible to reactivity with the monoclonal 25E10 antibody and one that is not. Moreover, the conformational change revealing the epitope recognized by 25E10 requires the major capsid proteins VP5.

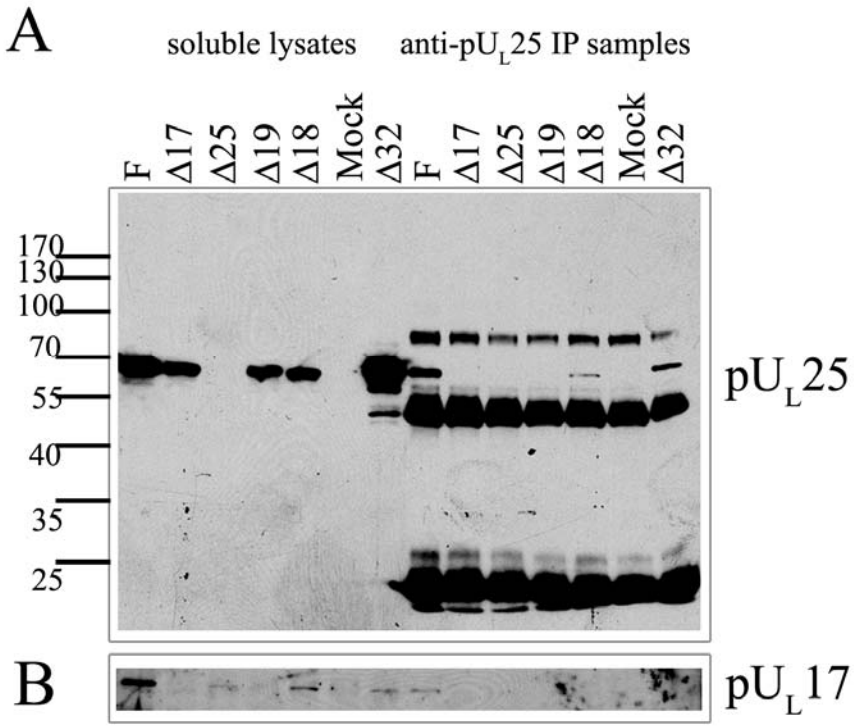

Figure 3.2 Reciprocal immunoprecipitation of pU$_L$17 with anti-pU$_L$25. Panel A shows immunoblotting with anti-pU$_L$25. Despite high concentrations of soluble pU$_L$25 in all lysates except delta 25 and mock, only pU$_L$25 in F, delta 18 and delta 32 is immunoprecipitated. Panel B shows pU$_L$17 co-immunoprecipitates only from F-infected cells.

When the immunoblot of 25E10-immunoprecipitated proteins was reacted with anti-pU_L17 antibody, co-immunoprecipitation of pU_L17 was noted only from HSV-1(F)-infected cell lysates (Figure 3.2 B). These data confirmed the interaction between pU_L17 and pU_L25 from cells infected with wild type virus. Conclusions concerning pU_L17/ pU_L25 interaction in the other cell lysates was hampered by the poor immunoprecipitation of pU_L25 with monoclonal antibody 25E10 in most of these lysates, and the relatively low amounts of pU_L17-specific immunoreactivity detected.

Solubility of pU_L17 in the absence of pU_L25 and capsids:

The above experiment indicated that less pU_L17 was present in lysates of cells infected with viruses lacking U_L19 or U_L18 (see figure 3.2 A). To determine whether this reflected lower levels of pU_L17 in cells infected with these mutant viruses, or a difference in solubility, cells infected with HSV-1(F) or the U_L25, U_L18, or U_L19 null virus infected cell lysates were denatured and subjected to immunoblotting with pU_L17-specific antibodies. As shown in figure 3.3 A , despite the lower levels of these proteins in soluble lysates, steady state levels of pU_L17 in total lysates did not vary significantly in the cells infected with the different viruses. We conclude that at least VP23, VP5, and pU_L25 contribute to the solubility of pU_L17 seen in cells infected with wild type viruses.

Distribution of both pU_L17 and pU_L25 are each altered in the absence of the other:

Having established pU_L17 and pU_L25 association, we next asked whether the distribution of either protein affected the location of the other in

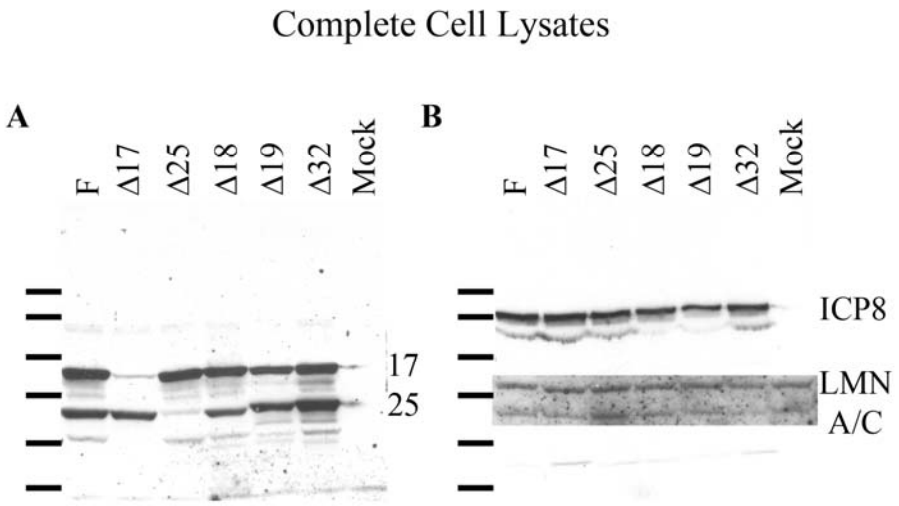

Figure 3.3 Immunoblot of whole cell lysates from infected cells. Panel A, overlaid images of anti-pU_L17 and anti-pU_L25 immunoblots. Panel B overlaid images of immunodetection of anti-ICP8 and Lamin A/C from the same blot.

infected cells. To assess this possibility, we infected Hep2 cells with 5.0 PFU per HSV-1(F), delta17 or delta 25 viruses, fixed and permeabilized the cells at various times after infection, and reacted the cells with chicken polyclonal antibody to pU_L17 and the 25E10 monoclonal antibody directed against pU_L25. After extensive washing, bound immunoglobulins were revealed by reaction with appropriately conjugated antibodies, and the cells were examined by confocal microscopy.

As shown in figure 3.4, upon infection with wild-type HSV-1(F) virus, pU_L17- and pU_L25-specific immunostaining co-localized extensively in nuclei both at 12 and 16 hours post infection (fig 3.4 C, F). Cytoplasmic staining of both pU_L17 and pU_L25 increased slightly by 16 hours after infection, although the great majority of immunoreactivity remained in the nucleus. Of the cytoplasmic signals, very little colocalized.

Immunostaining for either pU_L17 or pU_L25 in the absence of the other was different from that seen in cells infected with wild type HSV-1(F) virus. Specifically, (i) in delta 17-infected cells, pU_L25-specific immunostaining was generally at a much lower intensity (fluorescence intensity in Figure 3.4 G-I was adjusted to illustrate the distribution pattern). (ii) The distribution of pU_L25-specific immunoreactivity in delta 17 infected cells was nearly equal between the nucleus and cytoplasm. (iii) In cells infected with the U_L25 null virus, the majority of pU_L17 was mislocalized to intensely staining foci near the periphery of the nucleus at both 12 and 16 hours post-infection; however, this distribution was more pronounced at the earlier (12 hour) time point, presumably due to increased levels of immunoreactivity at 16 hours that

Figure 3.4 Colocalization of pU_L17/pU_L25 and co-dependent localization. Confocal microscopy of immunofluorescently-stained pU_L17 (Texas Red) and pU_L25 (FITC) in F-infected cells shows extensive co-localization of pU_L17 and pU_L25 in the replication compartment at 12 (A-C) and 16 (D-F) hours post-infection. pU_L25 in the absence of pU_L17 stains diffusely throughout the nucleus and cytoplasm (G-I). pU_L17 is mis-localized into intensely staining aggregates along the periphery of the nucleus in the absence of pU_L25 (J-O) that were more easily observed at 12 hours rather than 16 hours post-infection. Images were captured under 600x magnification with an additional 3x digital zoom.

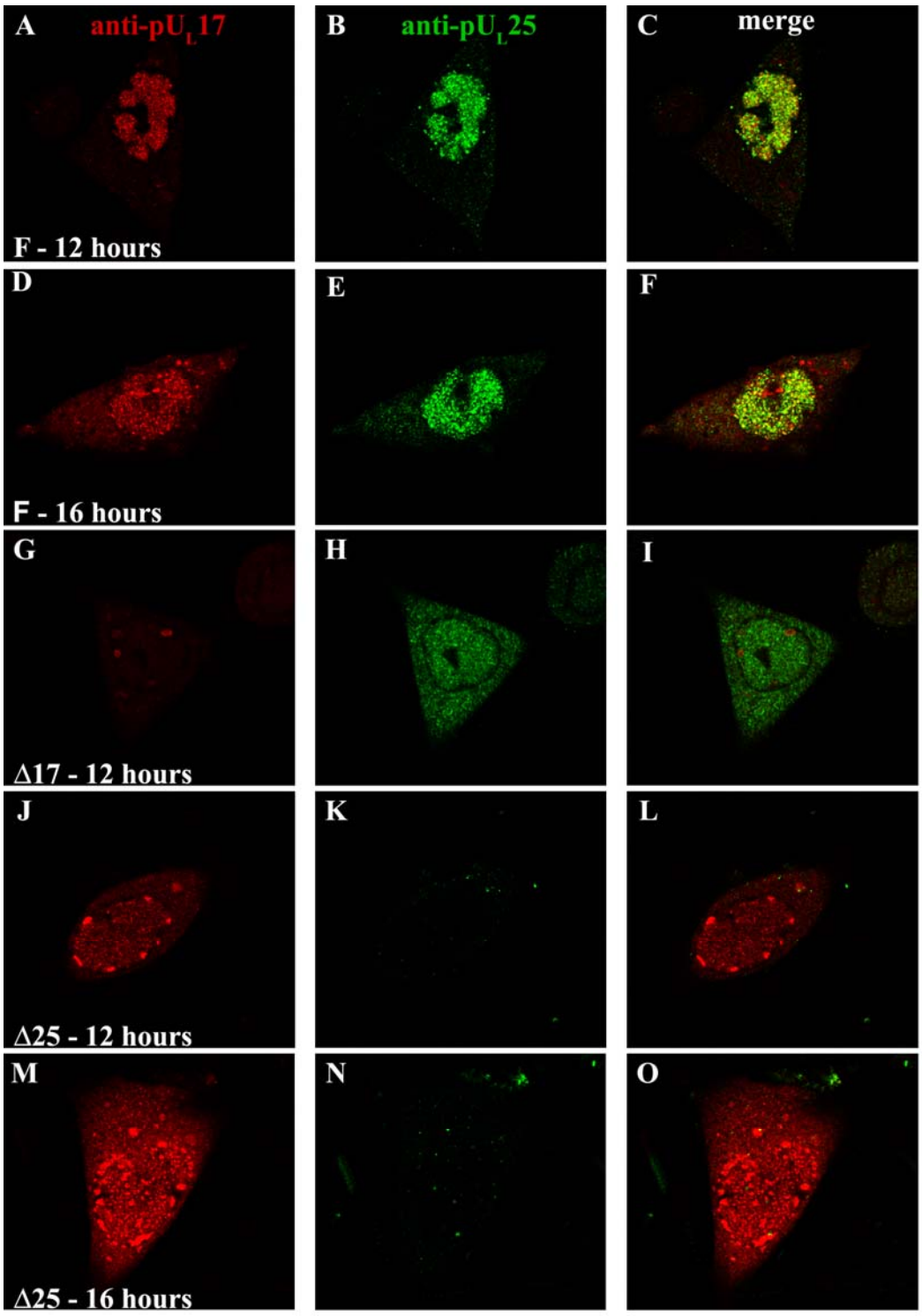
A anti-pU$_L$17
B anti-pU$_L$25
C merge
F - 12 hours
D
E
F
F - 16 hours
G
H
I
Δ17 - 12 hours
J
K
L
Δ25 - 12 hours
M
N
O
Δ25 - 16 hours

obscured the foci (fig 3.4 J, M). We conclude from these data that the proper localization of both pU_L17 and pU_L25 is co-dependent.

pU_L17 colocalizes with capsids in delta 25 infection:

The pU_L17-containing foci at the nuclear periphery of delta 25-infected cells were reminiscent of capsid aggregates observed upon infection with a U_L17 null virus (241). To determine whether the foci containing pU_L17 were also associated with capsids, we immunostained delta 25 infected cells with pU_L17-specific antibody and a monoclonal antibody (8F5), which recognizes VP5 in capsid pentons (253). As shown in figure 3.5, HSV-1(F)-infected cells displayed both pU_L17-specific and capsid-specific staining in the replication compartment as previously observed (figure 3.4 panel A, (241)) (fig 3.5 A-C). However, in delta 25-infected cells, both capsid- and pU_L17-specific immunoreactivity were observed to co-localize at the nuclear periphery (fig. 3.5 D-F, arrows). Examination at higher magnification revealed that pU_L17 and 8F5 immunostaining co-localized not only in the intensely-staining peripheral regions, but also in smaller puncta distributed throughout the central intranuclear replication compartment. The smaller puncta were of a size and distribution similar to those of capsids (Figure 5.2, (82)). This result was expected given the association of pU_L17 and pU_L25 with capsids (254) but was potentially incongruent with the observation that anti-pU_L17 antibody did not co-immunoprecipitate VP5, the major capsid protein (fig 3.1). We favor the hypothesis that pU_L17 interacts with wild type capsids in the presence and absence of pU_L25, but the interaction is of low affinity such that capsid

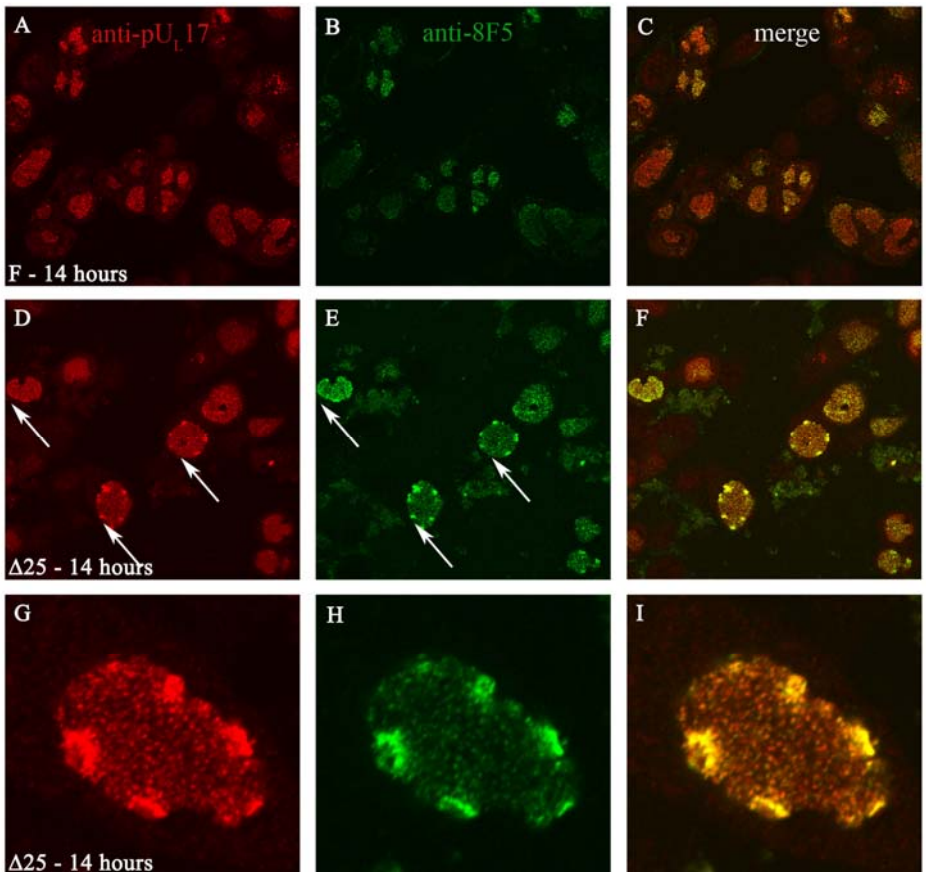

Figure 3.5 Peripheral nuclear aggregates in delta 25 infection contain pU$_L$17 and completely assembled capsids. Fields of wild-type (F) infected cells (A-C) and delta 25 infected cells (D-F) immunostained for assembled capsids and pU$_L$17 with mouse monoclonal 8F5 (FITC) and chicken polyclonal anti-pU$_L$17 (Texas Red) antibodies, respectively. Arrows indicate pU$_L$17 associated with capsids aggregated in the nuclear periphery in delta 25 infection. Panels G-H show high magnification of a single cell to demonstrate co-localization of pU$_L$17 with individual intranuclear capsids as well as capsid in peripheral aggregates upon delta 25 infection. Images A-F were captured under 600x magnification, G-I with an additional 5.33x digital zoom.

proteins do not co-immunoprecipitate with pU_L17 under the conditions employed.

Capsid formation, but not DNA encapsidation, aids nuclear retention of pU_L17 and pU_L25:

Since pU_L17 and pU_L25 are both capsid-associated and necessary for cleavage and packaging, we questioned whether the mislocalization of these proteins in delta 25 and delta 17 infections was a specific effect, or a general effect of either capsid malformation or lack of DNA encapsidation. To distinguish between these possibilities, we determined the distribution of pU_L17 and pU_L25 upon infection with capsid-null and DNA encapsidation-deficient viruses by indirect immunofluorescence.

To address the effect of capsid formation upon pU_L17/pU_L25 localization, we infected cells with delta 18 or delta 19 virus and fixed and stained them to reveal the cellular distribution of pU_L17 and pU_L25 proteins. Cells infected with wild-type HSV-1(F), delta 17, and delta 25 were processed in parallel as controls (fig. 3.6 A, B, M, N, P, Q) and all samples were stained with antibody against ICP8 to indicate that the cells were infected and to mark the DNA replication compartment (fig. 3.6 C, F, I, L, O, R).

Surprisingly, the immunostaining of both pU_L17 and pU_L25 was significantly reduced in cells infected with the delta 18 and delta 19 viruses. Moreover, the relative amount of cytoplasmic staining of both pU_L17 and pU_L25 was increased relative to that seen in cells infected with wild-type virus (fig 3.6 D, E, G, H, and M). Overall, the immunostaining of pU_L25 in cells infected with the U_L17, U_L18 and U_L19 null viruses was similar in distribution

Figure 3.6 Immunostaining of pU_L17 and pU_L25 with cleavage and packaging or capsid mutant viruses. Infected cells were immunostained with anti-pU_L17 (Texas Red) and anti-pU_L25 antibodies (FITC) for cellular localization. ICP8 immunostaining was used as a control for infection. All images were captured under 600x magnification with an additional 3x digital zoom.

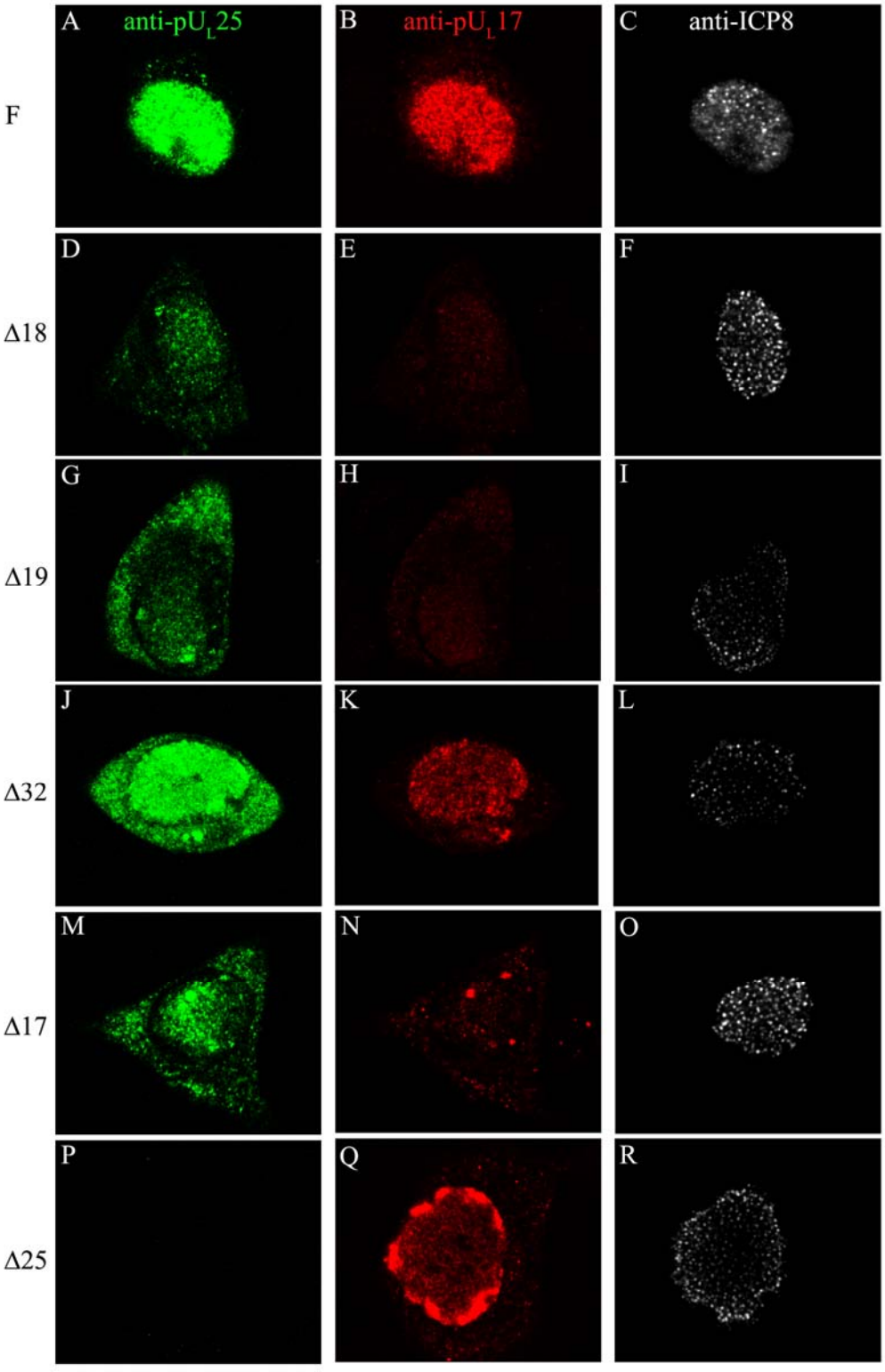
A anti-pU$_L$25
B anti-pU$_L$17
C anti-ICP8
F
D
E
F
Δ18
G
H
I
Δ19
J
K
L
Δ32
M
N
O
Δ17
P
Q
R
Δ25

and intensity (fig. 3.6 D, G and M), thus indicating that appropriate capsid formation is required both for nuclear retention and optimal epitope recognition of pU_L25. In contrast, pU_L17 immunostaining was greatly diminished in cells infected with the U_L18 and U_L19 null viruses whereas the staining was somewhat brighter in cells infected with the U_L25 null virus although this may reflect protein concentration in the aggregates rather than overall levels. Moreover, the mislocalization of pU_L17 into peripheral nuclear aggregates was seen only in delta 25-infected cells (fig. 3.6 Q).

To test the hypothesis that encapsidation of viral DNA was also involved in proper localization of pU_L25 and pU_L17, cells were infected with a virus lacking pU_L32, a protein required for DNA cleavage and packaging (132). In cells infected with delta 32, (figure 3.6 JOKE) the pU_L17-specific signal localized in the intranuclear replication compartment in a pattern similar to that seen in infections with wild type virus. Although pU_L25 specific signals localized primarily in the nucleus, significant levels of pU_L25-specific signal were also present in the cytoplasm. We also noted that pU_L25 immunoreactivity was greater in delta 32 infected cells compared to HSV-1(F) infected cells, whereas pU_L17 immunoreactivity was roughly equal in the two sets of infected cells.

To further test the role of DNA packaging in pU_L25 and pU_L17 localization, these proteins were assayed by indirect immunofluorescence in cells infected with a virus lacking the terminase subunit encoded by U_L15. As shown in figure 3.7, pU_L25 and pU_L17 colocalized within the nuclei of cells infected with the U_L15 null virus in a pattern similar to that of ICP8, a marker of the replication compartment (fig. 3.7 (D-F). The intensity of the

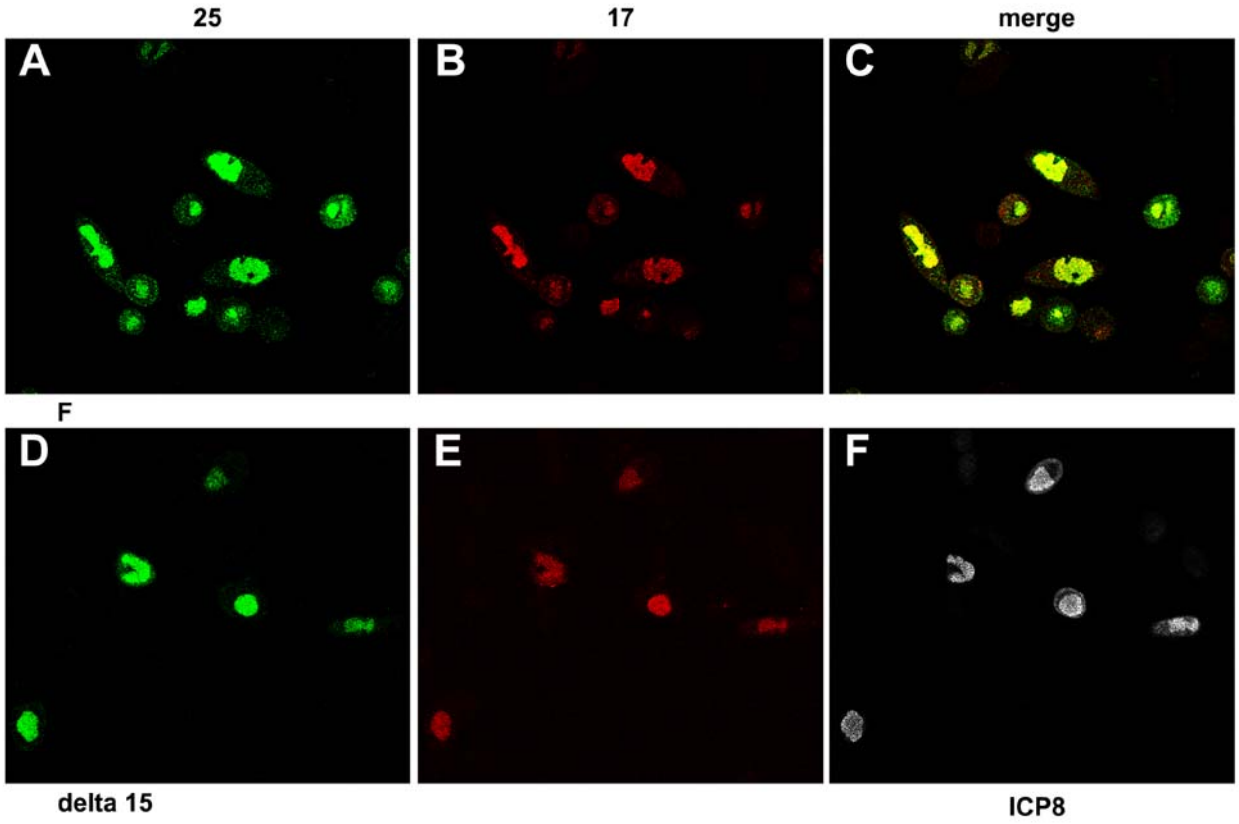

Figure 3.7 Wild-type localization of pU_L17, pU_L25 in delta 15 infected cells. F-infected cells (A-C) are shown as a control. Delta 15 infection does not alter the nuclear retention to pU_L17 (Texas Red) or pU_L25 (FITC). Images were captured under 600x magnification.

immunostaining of both proteins was similar to that in cells infected with wild type virus. We conclude from these studies that proper localization of pU_L17 and pU_L25 does not require the U_L15 protein or the process of viral DNA cleavage and packaging.

Cytoplasmic pU_L25 in cells infected with mutant viruses could be the result of a failure to engage the nuclear import machinery or a failure to retain pU_L25 in the nucleoplasm. In support of the latter possibility, two canonical nuclear export sequences were noted in the U_L25 ORF (data not shown). To further understand the cytoplasmic distribution of pU_L17 and pU_L25, we investigated Crm-1-dependent nuclear export. Previously, HSV was shown to use this cellular mechanism to shuttle the viral proteins VP13/14 (260).

To test the possibility that these motifs were functional, cells infected with HSV-1(F) (data not shown) or the U_L32 null virus were treated at 5 hours post infection with 10 nM leptomycin B, a Crm-1 inhibitor, and were fixed at 13 hours post-infection and immunostained with pU_L25-specific and pU_L17-specific antibodies. As shown in figure 3.8 D, treatment with leptomycin B substantially increased the amount of pU_L25-specific staining in the nuclei of cells infected with the U_L32 null virus, and decreased cytoplasmic staining. This effect was not observed with anti-pU_L17 immunostaining. There was no observable effect of leptomycin B treatment on pU_L25 localization in cells infected with wild type HSV-1(F) (data not shown) which is not surprising since the distribution of pU_L17 and pU_L25 in cells infected with wild-type virus is nearly exclusively nuclear. We conclude that at least one of the Crm-1 motifs in pU_L25 is functional and aids in nuclear retention of pU_L25. Thus the cytoplasmic localization of pU_L25, but not pU_L17, in the absence of pU_L32 is partly dependent on the Crm-1 nuclear export pathway.

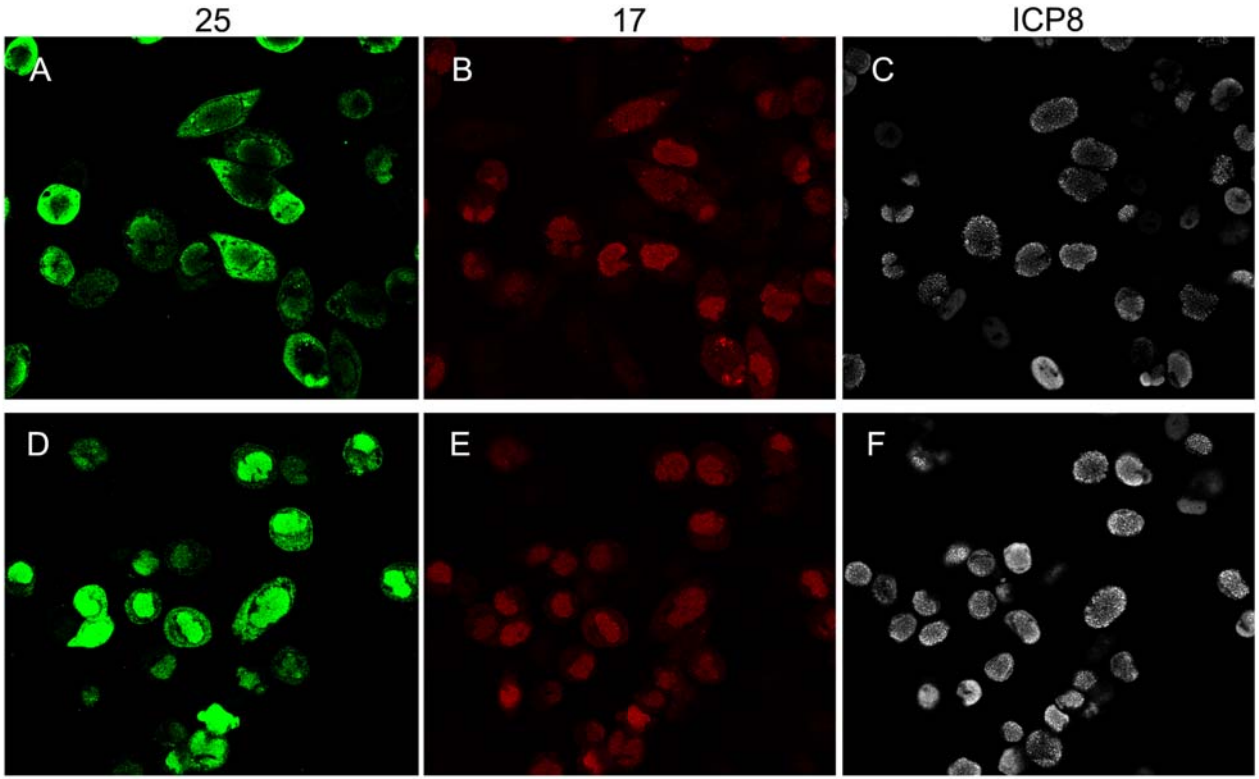

Figure 3.8 The effects of blocking Crm-1 nuclear export in delta 32 infection. Untreated (A-C) and 10 nM Leptomycin-B- treated cells (D-F) were immunostained to reveal effects on cytoplasmic export of pU_L25 (A and D) and pU_L17 (B and E). Cells were also stained with ICP8 (C and F) as an infection control. Images were captured under 600x magnification.

pU_L17 and pU_L25 colocalize in the absence of other viral proteins:

Given that pU_L17 immunoprecipitates with pU_L25 in delta 19 infected cells (and to a small extent in delta 18 infected cells), we conclude that pU_L25 and pU_L17 associate independently of capsid assembly. Next we asked whether expression of any other viral protein was necessary for pU_L17/pU_L25 interaction. For this, we transfected Hep2 cells on glass coverslips with expression constructs, pcDNA3-U_L17 and pcDNA3-U_L25 (pJB71), either alone or together, and 24-36 hours post-transfection cells were fixed and immunostained with anti-pU_L17 and anti-pU_L25 antibodies. In a control experiment, cells were transfected with lipofectamine without plasmid DNA.

Extensive co-localization of the pU_L17 and pU_L25 signals was noted in a mesh-like network throughout the cytoplasm (fig 3.8 C, F) as well as in intensely staining cytoplasmic foci (fig 3.8 C, F, I). pU_L17 was consistently more abundant in the nucleus than pU_L25, although a few cells showed little nuclear pU_L17 staining. These data suggest that pU_L17 and pU_L25 can colocalize in infected cells in the absence of other viral proteins.

Discussion:

As revealed by co-immunoprecipitation and co-localization in the nuclei of infected cells, the presented data indicate the conditions under which pU_L17 and pU_L25 interact. Their interaction can occur independently of capsid formation and in the absence of the major capsid protein VP5 or viral DNA cleavage and packaging. Moreover, VP5 was not co-immunoprecipitated with pU_L17. Because it is known that pU_L17 and pU_L25 associate with capsids the observations suggest that the immunoprecipitation conditions employed in the current studies were stringent and did not detect lower affinity interactions with

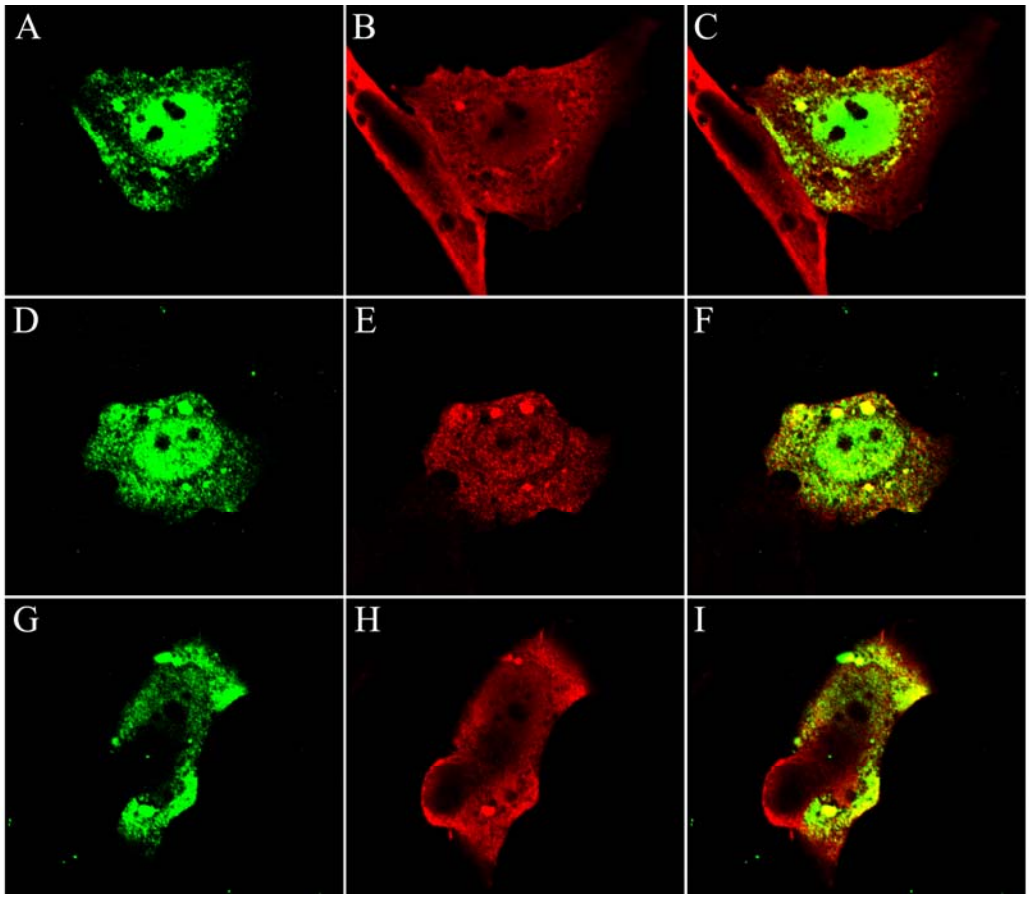

Figure 3.9 Cells co-expressing pU_L17 and pU_L25. Lipofectamine transfected cells stained for pU_L17 (FITC) and pU_L25 (Texas Red) . Extensive cytoplasmic colocalization (yellow) was observed both in aggregates and network-like structures. Images were captured under 600x magnification with an additional 3x digital zoom.

pU_L17. Indeed, we have noted that overnight incubation with pU_L17 antibody can co-immunoprecipitate VP5 and other capsid proteins (data not shown). The studies described here were intended to detect direct rather than indirect interactions.

In contrast to the result with VP5, the triplex protein VP23 was essential for the pU_L17/pU_L25 interaction under the conditions employed. This observation is potentially consistent with the tight association of pU_L17/pU_L25 and triplexes on the capsid surface (254). We also showed that the major capsid proteins, VP5 and VP23, were necessary for normal localization of pU_L17 and pU_L25 in infected cell nuclei, for proficient immunoreactivity with pU_L17 and pU_L25-specific antibodies, and for solubility of pU_L17. Thus the absence of capsid-binding alters immunoreactivity in immunoprecipitation and immunofluoresence, potentially reflecting an altered conformation of pU_L17 and pU_L25. To explain the phenomenon that the pU_L17/ pU_L25 complex requires the presence of capsids for their proper intranuclear localization, we suggest that both proteins when free from capsids may be exported to the cytoplasm but are retained within the nucleus in the presence of capsids. The functional significance of the nuclear export activity during the viral life cycle is unclear. Nuclear export may be involved in capsid egress, or may assist the fidelity of capsid assembly by exporting misfolded complexes to the cytoplasm.

The data presented herein also document unprecedented effects of pU_L32 on the pU_L17/ pU_L25 complex. Because the role of pU_L32 in DNA packaging is unknown, these observations are the first to shed light on its role in the DNA packaging reaction. Perhaps the most striking of the observations was the greatly increased ratio of soluble pU_L25 to pU_L17 in cells infected with the pU_L32 deletion virus. Although pU_L17 and pU_L25 interacted in the

absence of pU_L32, the latter was found to be necessary for retention of pU_L25 in the nucleus, and this role could be rescued by inhibition of the Crm1 nuclear export pathway. The precise mechanism by which pU_L32 mediates its effects is unknown. The possibilities range from effects on pU_L25 expression to chaperone like functions that augment pU_L17 solubility. Further studies will be necessary to distinguish between these and other possibilities.

Finally, the proper nuclear localization of both pU_L17 and pU_L25 requires the expression of the corresponding interacting protein.

These observations suggest that multiple functions are required to mediate the proper behavior, interactions, and localization of the pU_L17/ pU_L25 complex in the infected cell.

CHAPTER IV:

pU_L17 binds a DNA fragment with the HSV packaging site, pac-1

Introduction:

Given that pU_L17 and pU_L25 interact independently and form a heterodimer on the external surface of the capsid (254) (discussed in Chapter III), we hypothesized that these two proteins may share similar functional characteristics. Specifically, evidence suggests that pU_L25 is capable of binding DNA (191) a property that was hypothesized to be important in retaining genomic DNA in the capsid. We wanted to know if pU_L17 has the same property.

Materials and Methods:

Purification of pU_L17-His protein from insect cells - SF21 cells were infected with 5 PFU/cell U_L17-His BacPak-derived virus. Cells were collected, pelleted, and washed once with PBS. The cells were then lysed in 50mM NaH_2PO_4/300mM NaCl/10mM imidazole/1% NP40 pH 8.0 by sonication for 15 seconds on ice. Insoluble material was removed by centrifugation for 10 minutes at 4000 rpm in an Eppendorf 5810R centrifuge with an A-4-62 rotor at 4^0C. A 50% slurry of nickel-nitrilotriacetic acid (Ni-NTA) resin in PBS was added to the solubilized proteins and mixed by rotation at 4^0C for 90 minutes. pU_L17-His-bound Ni-NTA resin was pelleted and washed twice in 50mM NaH_2PO_4/300mM NaCl/20mM imidazole (pH 8.0). Protein was eluted with 50mM NaH_2PO_4/300mM NaCl/250mM imidazole (pH 8.0).

Dialysis of purified pU_L17-His - Eluted proteins were loaded into dialysis tubing and incubated in 1.0 L solutions at 4^0C with rotation. The buffer was changed using step-wise increments from 300 mM to 200 mM, then 150 mM

NaCl while in the constant presence of 50 mM NaH_2PO_4, 10% glycerol, and protease inhibitors.

DNA Binding Assay (EMSA)- U_b upper, GCGCCGCCGCGCTTTAAAGGGCCGCGCGCGACCCCCGGGGGGGTGTGTT TCGGGGGGGGCCCGT and U_b lower ACGGGCCCCCCCCGAAACACACCCCCCGGGGGTCGCGCGCGGCCCTTT AAAGCGCGGCGGCGC oligonucleotide primers were annealed by boiling for 10 minutes followed by slow cooling. Annealed probes were end labeled with γ32 ATP using T4 Polynucleotide Kinase (Promega) per the manufacturer's protocol. On ice, radiolabeled probe and purified, C-His-tagged pU_L17 which was previously dialyzed into 150 mM NaCl, 50 mM NaH_2PO_4 and 10% glycerol were added to binding buffer (50 mM KCl, 10mM Tris-HCl pH 8.0, 0.5 mM EDTA pH 8.0, 0.2 mM DTT, and 12% glycerol) at the molar ratios specified. Samples were mixed and tubes were shifted to 37^{o}C for 30 minutes to let the binding reaction take place. Products were electrophoresed at 65V in non-denaturing 4.5% polyacrylamide gels at 4^{o}C to separate the products. The non-denaturing gels were dried at 80^{o}C for 2 hours and exposed to film.

Results:

Electrophoresis of PNK-labeled, pac-1-containing DNA is altered by purified pU_L17-His:

In parallel to the pU_L25 study, we placed a C-terminal His tag on pU_L17 in a baculovirus expression vector and purified pU_L17-His using Ni-NTA beads. The His tag was previously shown not to cause DNA binding by using a baculovirus-expressed pU_L32-His control that did not bind DNA (191). To

test DNA binding of purified pU_L17-His we P^{32} end-labeled a complementary pair of annealed DNA oligonucleotides using T4 polynucleotide kinase (PNK). This DNA probe contains the pac1 site (U_b region). EMSAs were executed as reported in the Materials and Methods section.

Pilot experiments using various cation-containing buffers were performed to determine the optimal DNA-binding buffer. The migration of DNA-protein complexes was reduced with buffers containing monovalent cations KCl, NaCl, and both KCl and NaCl, but was not significantly altered in the presence of divalent, Zn^{2+} or Mg^{2+} cation-containing buffers (data not shown). The KCl-containing binding buffer (Materials and Methods) was determined to be the most effective and was used in all subsequent mobility shift assays.

Even with the lowest amounts of protein, 250 femtomoles of purified pU_L17-His, mobility shifts were modest yet detectable. We noted that in this assay virtually all free probe was bound by pU_L17-His. Through the addition of more protein up to 2.0 picomoles, DNA migration was even further retarded (fig 4.1). The pU_L17-His/DNA complex was never found to migrate to one or multiple discrete positions in the gel as is customary of a transcription factor binding a single site. At higher concentrations, increasing amounts of pU_L17-His/DNA complexes could be found in the wells (fig 4.1, fig. 4.2). Taken together, these data suggest that pU_L17-His may have multiple occupancy on DNA. Alternatively, some dissociation of pU_L17-His may be occurring during electrophoresis.

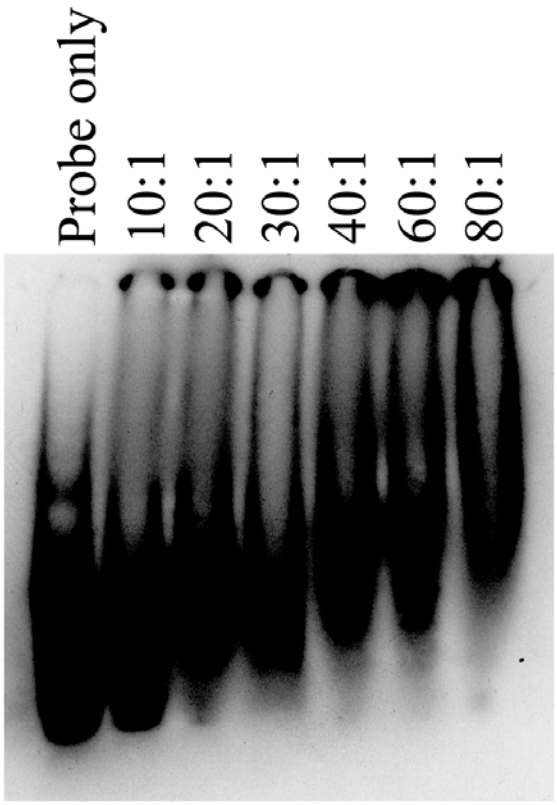

Figure 4.1 Electrophoretic mobility shift assay (EMSA) of pac-1 containing DNA with purified pU_L17-His. Each lane contains 25 femtomoles of γP^{32}-labeled DNA oligonucleotides incubated with increasing amounts of pU_L17-His protein dialyzed into 150mM NaCl, 50mM NaH_2PO_4, with 10% glycerol. Protein:DNA molar ratios are shown at the top of each lane. (1) probe only, no pU_L17-His, (2) 10:1, (3) 20:1, (4) 30:1, (5) 40:1, (6) 60:1, (7) 80:1 such that the minimum pU_L17-His loaded is 250 fmole (lane 2) and the maximum pU_L17-His loaded is 2.0 pmole (lane 7). Complexes were separated on a 4.5% non-denaturing gel and electrophoresed in 0.5x TBE buffer.

Contaminating proteins are reflected in altered migration:

In order to address the specificity of pU_L17-His-DNA binding, uninfected insect cells were processed for Ni-NTA purification in parallel with pU_L17-His. The rationale behind this experiment was to determine if contaminating insect cell proteins and/or imidazole from the elution buffer remaining after dialysis of pU_L17-His were responsible for the DNA-binding effects observed. Insect cell proteins non-specifically binding the nickel matrix were eluted in a volume equal to pU_L17-His and elutions were assayed directly without buffer dialysis in order to more stringently test the effect of imidazole. The results are shown in figure 4.2.

As shown in the previous experiment pU_L17-His again altered the mobility of the pac-1 containing DNA fragment. We observed most protein/DNA complexes at or near the wells of the gel for reasons that are not yet clear. In reactions with proteins eluted from the “purification” from uninfected insect cells altered DNA mobility was detected only in the sample with the highest protein:DNA molar ratio. This shifting of DNA may be caused by imidazole from the elution buffer or from insect cell DNA-binding proteins non-specifically binding to the Ni-NTA matrix. More to the point of this assay, the DNA-binding activity present even in the highest concentrations of uninfected cell lysate samples was significantly less appreciable than that of the lowest concentration of pU_L17-His-containing sample, thus suggesting a role for pU_L17-His in DNA-binding.

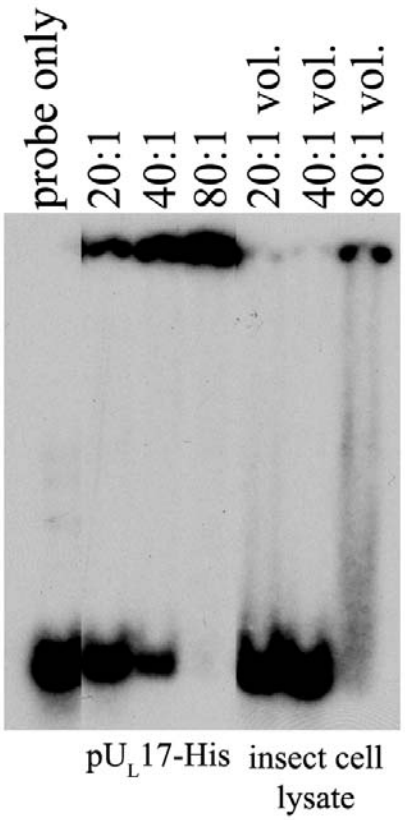

Figure 4.2 Electrophoretic mobility shift assay of pU$_L$17-His and uninfected cell lysate samples. 10 femtomoles of γP^{32}-labeled, pac-1-containing, double-stranded DNA fragment was present in each sample. Probe alone was run in lane 1 as a control. Samples in lanes 2-4 contained non-dialyzed pU$_L$17-His protein, with the molar ratios of protein:DNA indicated at the top of the lane. Equivalent volumes from a parallel "purification" of uninfected insect were also assayed for non-specific DNA binding. Protein/DNA complexes were separated on a 4.5% non-denaturing gel and electrophoresed in 1.0x TAE buffer

Discussion:

The role of pU_L17 DNA-binding activity in the viral life cycle is uncertain. One possibility is that the protein in some way aids association of capsids with DNA pursuant to its eventual cleavage and packaging. Such activities would not be expected to be specific for certain DNA sequences, because the terminase proteins likely provide the recognition of packaging signals. Indeed, the DNA binding activity identified herein was not specific to certain sequences although this was not tested extensively (data not shown).

Another possible role for the DNA binding activity is one of reorganization of nuclear chromatin to augment gene expression, or to mediate heterochromatinization of host cell DNA. Effects of pU_L17 on formation of the DNA replication compartment or architecture of the nucleus might be warranted.

Finally, it is possible that the potential DNA binding activity simply reflects the basic nature of certain regions of pU_L17 that mediate functions other than DNA association in the infected cell. Further mutational analysis to identify DNA binding regions and testing the effects of mutations ablating DNA binding on viral replication, DNA packaging, and interactions with proteins known to interact with pU_L17 would help correlate DNA binding activity to functionality in the infected cell.

CHAPTER V:

The essential protein encoded by U_L17 of herpes simplex virus 1 bridges capsid and tegument proteins

Abstract:

The U_L17 protein (pU_L17) of herpes simplex virus 1 (HSV-1) likely associates with the surfaces of DNA-containing capsids in a heterodimer with pU_L25. pU_L17 is also associated with viral light particles that lack capsid proteins, suggesting its presence in the tegument of the HSV-1 virion. To help determine how pU_L17 becomes incorporated into virions and its functions therein, we identified pU_L17 interacting proteins by immunoprecipitation with pU_L17-specific IgY at 16 hours post infection followed by mass spectrometry. Co-immunoprecipitated proteins included cellular histone proteins H2A, H3 and H4, the intermediate filament protein, vimentin, the major HSV-1 capsid protein, and the HSV tegument proteins VP11/12 (U_L46) and VP13/14 (U_L47). The pU_L17-VP13/14 interaction was confirmed by reciprocal co-immunoprecipitation with a polyclonal anti-VP13/14 antibody, and by affinity co-purification of pU_L17 and VP13/14 from lysates of cells infected with a recombinant virus encoding His-tagged pU_L17. The co-immunoprecipitation from infected cell lysates of VP13/VP14 and VP16, another major HSV-1 tegument protein, required pU_L17. pU_L17 and VP13/14-HA co-localized in the nuclear replication compartment, cytoplasm, and at the plasma membrane between 9 and 18 hours post-infection. The co-expression of pU_L17 and epitope-tagged VP13/14 and VP11/12 caused all three proteins to partially co-localize in cytoplasmic aggregates. Immunoelectron microscopy of cells infected with a virus encoding VP13/14-HA and reacted with HA-specific antibody revealed immunoreactivity distributed in short linear arrays at the nuclear periphery, occasionally with perinuclear virions, and frequently with virions in the cytoplasm and extracellular space. Taken together, these data

suggest that although some VP13/14 associates with perinuclear virions, most becomes incorporated into virions by interaction with pU_L17 in the cytoplasm at the surface of de-enveloped nucleocapsids.

Introduction:

Herpesvirus virions are composed of a double-stranded DNA genome encapsidated into an icosahedral shell, an amorphous proteinaceous network surrounding the capsid termed the tegument, and a glycoprotein-decorated envelope surrounding the tegument [reviewed in (164, 165, 230)]. The predominant model of virion assembly involves primary envelopment of the nucleocapsid at the inner nuclear membrane (INM), fusion of this nascent virion envelope with the outer nuclear membrane (ONM), and subsequent attachment of tegument proteins to the de-enveloped nucleocapsid in a region of the cytoplasm derived from the Golgi apparatus and/or trans-Golgi network (165). That the bulk of the tegument is applied at a step after primary envelopment is consistent with the relatively sparse electron microscopic appearance of the perinuclear virion tegument as opposed to the dense tegument of the extracellular virion (9, 100). This model of virion egress suggests opportunities for a subset of tegument proteins to attach directly or indirectly to the nucleocapsid in either the nucleosol, cytosol, or during budding through nuclear or cytoplasmic membranes. Supporting the idea that at least some tegumentation occurs in the nucleoplasm are the observations that pU_L36 and vhs (the U_L41 gene product) are associated with intranuclear capsids (27, 202). Budding through the INM likely causes incorporation of another set of proteins into the tegument, including the peripheral membrane proteins pU_L11 and pU_L31, the viral kinase encoded by U_S3, and the

nucleoplasmic protein VP16 (the U_L48 gene product) (12, 162, 176, 209). Of these, only the U_L31 gene product is absent from extracellular virions indicating its loss at the de-envelopment step (148, 209).

Major tegument components include the products of the U_L46 gene (VP11/12) and U_L47 gene (VP13/14), present in 400-600 and 1400-1880 copies per virion, respectively (107, 284). Although neither protein is essential for viral replication, they play augmentary roles in VP16-dependent viral transcription (284). Perhaps related to this observation, yeast two hybrid studies detected interactions of VP11/12 with either VP13/14 or VP16 (263). The VP11/12-VP16 interaction was further confirmed in a pull down assay (263). HSV-1 VP13/14 shuttles from the nucleus to cytoplasm during the course of infection (69, 260), a feature shared by the VP13/14 homolog of bovine herpesvirus (261). Localization in both nucleus and cytoplasmic compartments makes it challenging to determine when and where VP13/14 becomes associated with virions. As evidence supporting a cytoplasmic role in tegumentation, cells infected with a pseudorabies virus mutant lacking the homolog of U_L47 contain increased numbers of cytoplasmic capsids lacking electron density attributable to the tegument (126).

The role of VP11/12 in virion assembly is even less clear because viral mutants lacking this protein are unimpaired in virion egress through the nucleus or cytoplasm in all systems studied (13, 70, 126). VP11/12 can associate with membranes, and a VP11/12 /GST fusion protein can associate with capsids purified from infected cell nuclei when added in vitro (174). These data are consistent with functions of VP11/12 in bridging the membrane and capsid in the virion structure, and perhaps during virion budding.

Although the precise contribution of HSV-1 U_L17 protein (pU_L17) to viral replication remains unclear, its role as a structural component of capsids is well documented. Originally classified as a DNA cleavage and packaging protein due to the exclusive production of concatemeric DNA and capsids lacking DNA in cells infected with a U_L17 deletion virus, pU_L17 was found later to be necessary for proper capsid distribution within the intranuclear replication compartment (214, 241). pU_L17 interaction with capsids was further supported by biochemical and electron microscopy studies showing association with the external surfaces of capsids (245, 274). The herpes simplex virus capsid shell is composed of 12 pentons and 150 hexons composed of the major capsid protein VP5 (encoded by U_L19), 375 triplexes made up of two molecules of VP23 (encoded by U_L18) and one molecule of VP19C (encoded by U_L38), and 900 copies of VP26 (U_L35) which localize atop each of 5 VP5 molecules in each hexon. Recent cryoelectron microscopy studies have identified a heterodimer of pU_L25/pU_L17, termed the C Capsid Specific Component (CCSC) that bridges pentons and adjacent hexons in DNA-containing (type C) capsids (254). These observations are consistent with other data indicating that pU_L17 localizes on the capsid surface and enhances association of pU_L25 with capsids (245, 274). In addition to the capsid association studies, pU_L17 is a component of viral light particles, which contain tegument and membrane associated proteins but lack capsids (246). Thus, pU_L17 can become incorporated into tegument-like structures in the absence of capsids.

To clarify specific capsid and tegument protein interactions with pU_L17, we performed co-immunoprecipitations with a pU_L17-specific antibody and have identified interactions with the major capsid protein VP5, as well as

tegument proteins VP11/12 and VP13/14. In light of these and previous data, we suggest two possibly related structural roles for pU_L17 in virion assembly: to ensure that the capsid is competent structurally to package viral DNA, and to serve as sites of attachment for a subset of virion tegument proteins that include pU_L47 and associated proteins.

Materials and Methods:

Cell lines and viruses - Vero and Hep2 cells were obtained from the American Type culture association and were propagated in DMEM supplemented with 10% newborn calf serum (NBCS) and antibiotics as described previously (277).

A novel cell line CV1-17, specifically engineered to support replication of U_L17 null viruses, was created using the Flp-In system from Invitrogen. Briefly, the U_L17 open reading frame was cloned into the FRT-containing expression vector pcDNA5/FRT and verified by DNA sequencing. The pcDNA5/FRT-U_L17 plasmid was co-transfected with pOG44, a Flp recombinase-encoding plasmid, into CV-1 cells previously selected for an integrated FRT locus to support recombination of the transfected DNA. Site-specific recombination resulted in a change of cell line phenotype from Zeocin resistance to Hygromycin (Hyg) B resistance. Hygromycin-resistant colonies resulting from the transfection were amplified and grown into cellular monolayers. Expression of U_L17 in these cells was determined by immunoblotting with anti-pU_L17 antibody, and plaque formation by the U_L17 null virus. One such cell line was designated CV1-17 and was used for further studies. CV1-17 cells were maintained in Dulbecco's modified Eagle's

medium (DMEM) supplemented with 10% fetal bovine serum and 200 μg/ml Hyg B.

The wild type HSV-1(F) strain was used in these studies and has been described previously (72). HSV-1(F) was propagated on Vero (African green monkey kidney) cells.

A new U_L17-null virus was constructed by integration and subsequent selection of a Kanamycin resistance (Kan^R) cassette into the U_L17 open reading frame (ORF) as follows. A gene encoding Kan^R was PCR amplified with the following primers containing sequences homologous to the U_L17 ORF and Kan^R cassette:

(del17F, #11) CAAACTTCCAG GTCGAAATCCAG ACTCGGGCTCATG CCACCGGCGACTG TA CGTGTAGGCTGGAGCTGCTTC; (del17R, #12) TTCCGTAGT GGTGGCGCA GGACCACGGAG ATAGAACGACG GCTCCACAGCC AGTCATTCCGGGGATCCGTCGAC (Kan^R homology underlined). Amplicons were transformed into EL250 cells containing a chloramphenicol–resistant (Cm^R), wild-type HSV-1(F) BAC (238). Cm^R/Kan^R recombinants were selected on agar plates. Extracted BAC DNA was transfected with SuperFect (Qiagen) into CV1-17 cells and after 3 rounds of viral plaque purification, CV1-17 cells grown in 890 cm^2 roller bottles were infected with 0.01 PFU per cell for propagation of viral stocks.

A recombinant HSV-1(F) BAC encoding a U_L17 ORF in frame with 6 histidine codons (His) at the 3' end was created by PCR using the following primers:

(ORF17 3'HisF, #28) GCCGCT GTCCTTAGGTTTT GTCGCA AGGTGTC GTCCGGG AACGGCCGT TCTCGC*CACCAC CACCACCA CCAC***TAG**CGT GTAGGCTGGA GCTGCT TC and (ORF17 3'HisR, #29) CAACGG CGCGG

GGAGGAG TGGATG GGCGAG GTGGCC GGGGGA AGGCGC CCGATT CCGGG GATCC GTCGAC (where the six His codons are italicized, the stop codon indicated in bold, and homology to the Kan^R cassette underlined). PCR amplicons that contained the 6X His tag immediately before U_L17's stop codon, and the Kan^R cassette 3' of the TAG flanked by FRT sites were electroporated into HSV-1(F) BAC-containing EL250 cells. Cm^R/Kan^R clones were identified on selective media. Overnight cultures of Cm^R/Kan^R colonies were grown in the presence of 10% arabinose to induce expression of the FRT recombinase, driving recombination at the FRT sites and resulting in the loss of Kan^R. Purified BAC DNAs from Cm^R/Kan^S clones were transfected by the $CaCl_2/Na_2HPO_4$ method into individual wells containing Vero cells and after 3 rounds of plaque picking, viral stocks were grown on Vero cells inoculated at 0.01 PFU per cell.

Two additional HSV-recombinant viruses, one with DNA encoding a FLAG epitopic tag fused to the 5' end of U_L46 (FLAG-VP11/12) and another encoding an influenza hemagglutinin (HA) tag in frame with the 3' end of U_L47 (VP13/14-HA) were created by en passant mutagenesis, a previously described markerless BAC mutagenesis technique (247). Thus, gel purified primers (EP FLAG46F, #60) GCGGCA TAACTC CGA CCGGCGGGTCCCG ACCGAACGGGCGT CACC**ATG** *GATTACAAGGAT GACGACGATAAG* and (EP FLAG46R, #61) GCACCG CGCCA GCCGCA GGGAGCTCGCG CCGCGCG TCCGGCGCTG *CTTATC GTCGTCA TCCTTG TAATC* **CAT**GGTGA CGCCC GTTCGC AACCA ATTAT CCAAT TCTGAT TAG (FLAG tag italicized, start codon in bold; pEP Kan cassette homology underlined) were used to make FLAG-VP11/12. Primers (EP 47HAF, #62) GTGTCGG GGAGGCG CGCGACC GGGCTGG GAGGCCC GCCACGC CCA*TACC*

*CATACGA CGTCCCA GACTACG CT***TAA**AG GATGA CGACG ATAAGT AGGG and (EP 47HAR, #63) TATGC CGCGT CCAGG GCCATC GGGGCG CTTTTTA TCGGGA GGAGC **TTA***AG CGTAGT CTGGG ACGTC GTATG GGTA*T GGGCG TGGCG GGCCC AACCA ATTAA CCAAT TCTGAT (HA tag italicized, stop codon in bold, pEP Kan cassette homology underlined) were used to generate a VP13/14-HA recombinant BAC. Recombinant BAC DNAs were purified and transfected into Vero cells with SuperFect (Qiagen) for virus propagation.

A recombinant U_L17-His virus was also made by BAC mutagenesis. A carboxy-terminal 6x His tag was added to the U_L17 ORF by PCR with primers (CHis17F, LDS#9) CGGGATCCACCATGAACGCGCACTTGGCCAACGAG and (CHis17R, LDS#10) GGAATTC**CTA***GTGGTGGTGGTGGTGGTG*GCGAGACCGGCCGTTCCCGG A (U_L17 homology underlined, 6xHis tag italicized, stop codon in bold).

Digestion at the flanking BamHI and EcoRI restriction sites allowed for subcloning into the pCR2.1 vector. PCR products were electroporated into HSV BAC containing EL250 cells. Recombinant clones were selected with Chloramphenicol (Cm) and Kan. Overnight cultures of Cm^R/Kan^R were grown in the presence of 10% Arabinose to recombine FRT sites for the loss of Kan. Maxi-preps of Cm^R/Kan^S BAC clones were transfected into Vero cells and after 3 rounds of plaque picking, viral stocks were grown in roller bottles on Vero cells inoculating at an MOI of 0.01.

Immunoprecipitation Assay - A previously described anti-pU_L17 chicken IgY antibody (35) was used to co-immunoprecipitate proteins interacting with

pU_L17 as follows. Approximately 8.0 $x10^8$ rabbit skin cells (RSC) were infected with 5 plaque forming units of HSV-1(F) or U_L17 null virus per cell. Cells were collected at 16 hours post-infection, pelleted by centrifugation, and lysed in NP40 lysis buffer (1.1% NP40, 100 mM Tris pH7.7, 300mM NaCl, 1mM EDTA pH 8.0, 1mM PMSF, 1μg/ml Aprotinin, 1μg/ml Pepstatin, 1μg/ml Leupeptin, Sigma Protease Inhibitor cocktail (P8340), 1mM Na_3VO_4) on ice. Lysates were clarified by a 10 minute, 4000 RPM centrifugation in an Eppendorf 5810R centrifuge with an A-4-62 rotor at 4^0 C 4 times to ensure removal of all cellular debris. In a pre-clearing step, Gamma Bind G beads which contain a recombinant form of streptococcal Protein G covalently bound to Sepharose 4B (GE Healthcare Bio-Sciences AB) were washed with PBS, brought to a 50% slurry in PBS, and reacted with the solubilized cellular proteins for one hour at 4^0C and then were pelleted for 10 minutes at 8000 rpm in a F34-6-38 rotor. The pre-cleared lysates were transferred to new tubes and subsequently reacted for 1.5 hours at 4^0C with rabbit anti-IgY IgG plus Gamma Bind G beads with constant rotation to further remove any non-specific binding. After removal of the bead/rabbit IgG mix by centrifugation at 8000 RPM in a F34-6-38 rotor at 4^0C and transfer to new tubes, the supernatants were reacted with chicken anti-pU_L17 IgY for 2 hours at 4^0C, followed by reaction with rabbit anti-IgY IgG for 2 hours at 4^0C, and finally with Gamma G bind beads overnight. The beads with bound proteins were pelleted, washed 4 times with ice-cold NP40 lysis buffer, and protein was eluted from the beads in 150 μl 2X SDS-PAGE buffer (100mM Tris-HCl pH 6.8, 4.0% SDS, O.2% bromophenol blue, 20% glycerol, 200mM fresh DTT). Samples were separated on both 8% and 15% SDS polyacrylamide gels and stained with Coomassie blue.

MALDI-MS - Proteins of interest were cut from the polyacrylamide gel, digested with trypsin, and the masses of peptides determined by Matrix-Associated Laser Desorption Ionization time of flight mass spectrometry (MALDI-TOF MS). The top 10 scoring peptide matches for each band are reported in table 4.1.

Immunofluorescence Assay (IFA) – Hep2 cells grown on glass coverslips in 6-well dishes to approximately 80-100% confluence were infected by incubation with 5.0 PFU/cell in 199V media (DMEM with 1% NBCS) with rocking for 1 hour, and then returned to stationary incubation. At various times after infection, the cells were fixed in 3% paraformaldehyde in PBS for 15 minutes. Cells infected with virus VP13/14-HA were fixed with ice cold methanol for 10 minutes at 4^0C. Autofluorescence was quenched with 50 mM ammonium chloride for 15 minutes; cells were washed with PBS and permeabilized in 1.0% Triton-X 100 for 5 minutes followed by washing in PBS. PBS supplemented with 1% BSA, 5% donkey serum and 5% human serum was used to block non-specific antibody binding for 20-30 minutes at room temperature. Primary antibodies were diluted in this blocking solution as follows: anti-pU_L17 between 1:1000 and 1:500, anti-acetyl K9 Histone H3 (Upstate) 1:100, anti-ICP5 (VP5) (Virusys) 1:100, anti-ICP8 1:1,000 (a kind gift of Bill Ruyechan), anti-FLAG (M2) 1:200, and anti-HA (Santa Cruz) 1:100. After the 30-60 minute incubation with primary antibody, cover slips were washed at least 3 times with PBST [PBS supplemented with 0.2% Tween-20 (Sigma)] and secondary antibodies were diluted 1:1,000 in blocking solution and reacted for 30-60 minutes. Cover slips were washed at least 4 times in

PBST then briefly in dH_20, mounted on glass slides with Vectashield mounting medium (Vector Laboratories) containing a UV protectant, and sealed with nail polish.

Transfections for transient expression- Adherent Hep2 cells were transfected with the indicated expression plasmids using Lipofectamine 2000 (Invitrogen) according to the protocol of the manufacturer and were processed for indirect immunofluorescence 36-48 hours after transfection as indicated above.

Ni-NTA Protein Purification - Vero cells were infected with 5 PFU/cell U_L17-His virus. Cells were collected, pelleted, and washed once with PBS. The cells were then lysed in 50mM NaH_2PO_4/300mM NaCl/10mM imidazole/1% NP40 pH 8.0 by sonication for 15 seconds on ice. Insoluble material was removed by centrifugation for 10 minutes at 4000 rpm in an Eppendorf 5810R centrifuge with an A-4-62 rotor at 4^0C. A 50% slurry of nickel-nitrilotriacetic acid (Ni-NTA) resin in PBS was added to the solubilized proteins and mixed by rotation at 4^0C for 90 minutes. pU_L17-His-bound Ni-NTA resin was pelleted and washed twice in 50mM NaH_2PO_4/300mM NaCl/20mM imidazole (pH 8.0). Protein was eluted with 50mM NaH_2PO_4/300mM NaCl/250mM imidazole (pH 8.0). Eluted proteins were electrophoretically separated on SDS polyacrylamide gels, transferred electrically to nitrocellulose, and probed with various antibodies as described below.

Immunoblotting – Vero cells were collected and pelleted at 4000 rpm for 10 minutes. Cell pellets were resuspended and lysed in 2x SDS-PAGE sample

buffer. Associated proteins were electrophoretically separated on SDS polyacrylamide gels and transferred to nitrocellulose at 25-30 amps for 5-6 hours at 4^0C. Membranes were blocked in 5% dried milk in PBST, rinsed with PBST, and probed with antibody diluted in PBST supplemented with 1.0% BSA. Primary antibodies were diluted as follows: anti-pU_L17, 1:10,000; anti-VP5, 1:1,000; anti-vimentin, 1:1,000; anti-HA, 1:1,000; anti-VP13/14, 1:1,000; anti-FLAG (M2), 1:2,500; anti-VP22, 1:10,000; anti-VP16, 1:1,000. Excess primary antibody was removed with 3, 10-minute washes in excess PBST. Secondary HRP-conjugated antibodies were diluted 1:5,000 in PBST with 5% milk and rocked for 1 hour at room temperature. Excess antibody was again removed by washing in excess PBST 3 times for 10 minutes each. Bound immunoglobulin was revealed by chemiluminescence using Pierce ECL detection agent exposure to X-ray film for approximately 2 minutes.

Immunogold electron microscopy - Hep2 cells were infected with HSV-1(F) or a recombinant virus bearing a U_L47 gene fused to DNA encoding an HA epitopic tag. At 16 hours after infection the cells were fixed, embedded, and thin sectioned as previously described (3, 24). Thin sections were reacted with rabbit anti-HA antibody diluted 1:50 in PBS supplemented with 0.5% Tween 20 and 1% fish gelatin, followed by extensive washing and reaction with goat anti-rabbit immunoglobulin conjugated to 12 nm gold beads (Jackson ImmunoResearch catalog #111-205-144). Electron microscopy, and photography was performed essentially as described (209).

Results:

Construction of a new U_L17 expressing cell line and viral deletion mutant:

Since pU_L17 is essential for viral replication, propagation of viral null mutants lacking this gene requires complementing cell lines engineered to express U_L17. Because the previously described G5 complementing cells harbored a 16.2 kb fragment of the HSV genome (62), recombination between homologous HSV sequences in the virus and cell line often resulted in genetic reversion of the U_L17 deletion to wild type sequences (data not shown).

To overcome this difficulty, a new cell line, CV1-17, containing only U_L17 was created through the use of the Flp-In system (Invitrogen) as outlined in Materials and Methods. During the course of these efforts, the U_L17 ORF from HSV-1(F) was subcloned and sequenced. This sequence analysis revealed differences between the U_L17 ORFs in HSV-1(F) and the published HSV-1(17) sequences (156). Specifically, a +1 insertion mutation in HSV-1(F) U_L17 was predicted to causes a frame shift relative to HSV-1(17) at codon 11 (Fig. 5.1 A). The open reading frames then realign at codon 21 by a compensatory -1 deletion in U_L17 of HSV-1(F). These mutations are predicted to produce ten distinct amino acids at the N-termini of the two otherwise identical genes. Other silent mutations were observed (data not shown), as well as a single amino acid change at codon 352 (Fig. 5.1B).

After obtaining a U_L17-specific cell line, a novel HSV-1(F) BAC was generated in which a central portion of U_L17 ORF was replaced with a Kanamycin resistance cassette (detailed in Materials and Methods). This deletion of 912 base pairs (bps 212-1,123 with 1 representing the A in the start

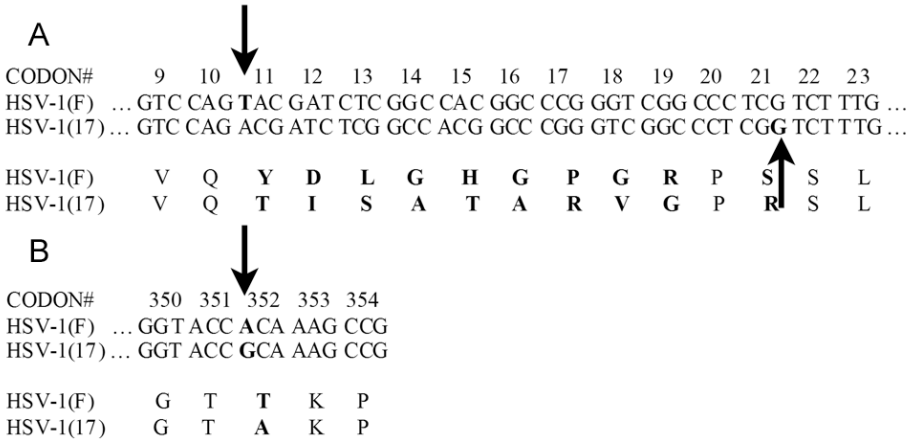

Figure 5.1 U_L17 sequences in different HSV-1 strains. Panel A. An insertion between codons 10 and 11 cause a frameshift in the HSV-1(F) sequence compared to the published HSV-1(17) sequence. A deletion between codons 21 and 22 in the HSV-1(F) bring the two U_L17 genes back into frame. Panel B. A point mutation changes a single amino acid in the HSV-1(F) U_L17 compared to the HSV-1(17) U_L17 sequence.

codon) retained 989 base pairs of the 3' end of the U_L17 coding sequence to preserve the U_L16 promoter region. Transfection of this BAC into supporting CV1-17 cells resulted in a U_L17 deletion virus (designated delta 17) with significantly reduced rates of reversion (data not shown).

Identification of U_L17 interacting proteins: To clarify pU_L17's putative roles in virion assembly as both a tegument and capsid protein, we used co-immunoprecipitation to identify pU_L17 interacting proteins.

In our first approach to discover protein-protein interactions involving pU_L17 we employed ^{35}S metabolic labeling of cells infected with recombinant U_L17-His, F, and delta 17 viruses. Both uninfected and mock infected cells were used as controls. Immunoprecipitation with subsequent autoradiography indicated a substantial amount of two proteins was enhanced specifically in the 17-His-infected sample (Figure 5.2) Of the two the fast migrating species electrophoresed to the expected zone of pU_L17. The slower migrating species, of approximately 160 kDa was presumed to be VP5.

To specifically identify proteins co-immunoprecipitating with pU_L17 we performed an immunoprecipitation with an anti-pU_L17 antibody and identified co-immunoprecipitating proteins by MALDI-TOF MS. Specifically, cells were infected with HSV-1(F) or the novel deletion mutant lacking U_L17. The proteins in each lysate were reacted separately with pU_L17-specific IgY antibody, and immune complexes were purified by reaction with a rabbit anti-IgY bridging antibody that could subsequently be captured with Gamma Bind G Sepharose beads. Immunoprecipitated proteins were eluted and electrophoretically separated on both 8% and 15.0% denaturing polyacrylamide gels to resolve both high and low molecular weight proteins, respectively. The results are shown in figures 5.3 A and 5.3 B.

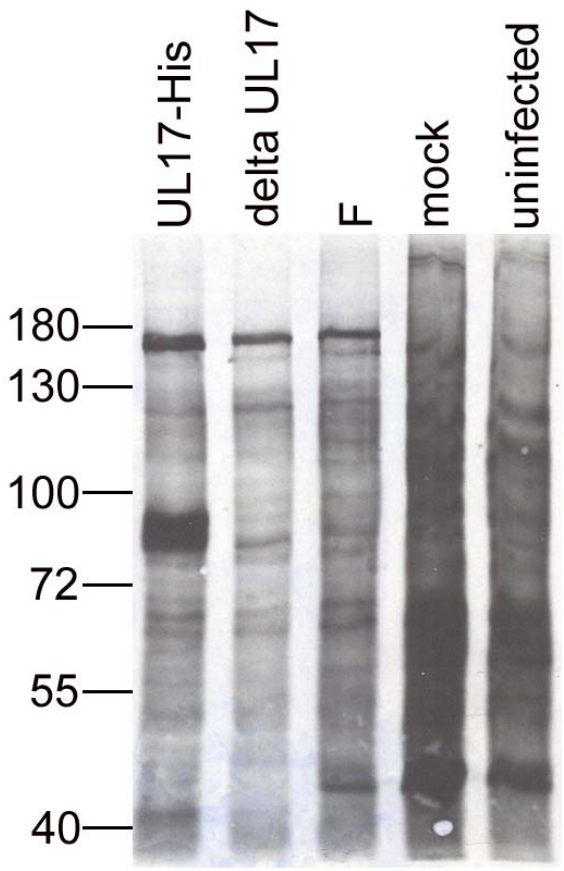

Figure 5.2 Anti-His immunoprecipitation from pU_L17-His-infected cells. Autoradiogram of ^{35}S metabolically labeled cells immunoprecipitated with penta anti-His antibody. Two major species migrating at 160 kDa and 85-90 kDa were immunoprecipitated more efficiently from pU_L17-His infected cells.

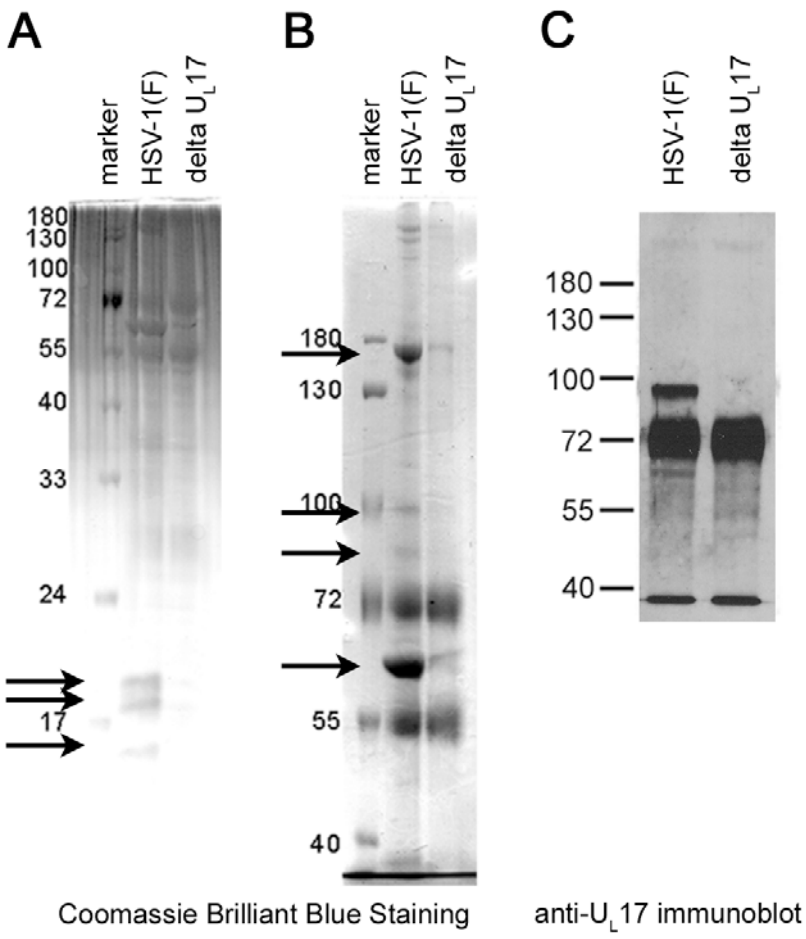

Figure 5.3. Co-immunoprecipitation of proteins with pU_L17-specific antibody. Cells were infected with HSV-1(F) or the U_L17 deletion virus, and pU_L17 was immunoprecipitated. Immunoprecipitated proteins were electrophoretically separated on a 15% (panel A) or 8% SDS polyacrylamide gels (Panels B and C) and were stained with Coomassie brilliant blue (panels A and B), or were subjected to immunoblotting with pU_L17-specific antibody (panel C). Proteins unique to or highly enriched in immunoprecipitations performed with HSV-1(F) infected cells are indicated with arrows, and their identities are indicated in the text.

Four bands in the 8% polyacrylamide gel (indicated in figure 5.2 B and corresponding to apparent M_r's 62,000, 85,000, and 95,000, and 160,000) and three bands from the 15% polyacrylamide gel (Figure 5.3 A; corresponding to apparent M_r's 15,000, 17,500 and 19,000) were exclusive to or greatly enhanced in lanes containing immunoprecipitations from lysates of HSV-1(F), as opposed to immunoprecipitations from lysates of cells infected with the U_L17 deletion virus. These bands were cut from the gel and subjected to trypsin digestion. The masses of the resulting peptides were determined by MALDI- TOF mass spectrometry and were compared to available databases of vertebrate proteins.

As shown in table 5.1, bands from the 8% gel of apparent M_rs 85,000 and 95,000 contained tryptic peptides with masses consistent with the U_L46 and U_L47 gene products of HSV-1 (predicted MW 73,771 and 78,195, respectively). In addition to these species, eight other peptide matches from the 85,000 apparent Mr band matched glycoprotein E peptides. This was not surprising inasmuch as gE/gI complexes have been shown to bind the Fc domain of IgG immunoglobulins (120). Because this complex efficiently binds rabbit immunoglobulins, we expect that the rabbit anti-chicken IgG antibody, used to bridge the IgY and Sepharose beads in this experiment, was responsible for immunoprecipitation of the gE/gI complex. Tryptic peptides from the VP11/12-containing band also included one match to a Zinc-finger protein homolog, and seven other peptides attributable to spindle-like microcephaly-associated proteins (ASMPs).

The three bands from the 15% gel containing proteins of apparent M_rs 15,000, 17,500 and 19,000 most abundantly contained peptides consistent with cellular histone proteins H4 (predicted MW 11,236), H2A (predicted MW

13,927), and H3 (predicted MW 15,498), respectively (Figure 5.3 A and Table 5.1). These masses matched tryptic peptides from a number of animal histones due to the high conservation of these proteins (data not shown).

A predominant band of 62,000 apparent Mr was detected in both the 8% and 15% SDS polyacrylamide gels. This band was much more intense in the HSV-1(F) immunoprecipitation reactions and contained tryptic peptides with masses consistent with those from the human intermediate filament protein vimentin and vimentin homologs, which comprises intermediate filaments in several animal species. The other two most highly ranked matches included unnamed human proteins, both with homology to the N-terminal head region of intermediate filament proteins (data not shown)

The slowest migrating band in this experiment produced tryptic peptides consistent with the major capsid protein from a variety of herpesviruses with human herpesvirus 1 and 2 scoring the highest and second-highest, respectively. This was consistent with pU_L17 association with capsids, which contain abundant amounts of VP5.

Because none of the harvested gel slices contained pU_L17, we transferred the electrophoretically separated proteins immunoprecipitated with anti-pU_L17 antibody to nitrocellulose and probed the proteins with anti-pU_L17 antibody. Bound immunoglobulin was revealed by reaction with horseradish peroxidase conjugated anti-chicken antibody followed by chemiluminescence as detailed in Materials and Methods. As shown in figure 5.3 C, pU_L17 was immunoprecipitated by its cognate antibody inasmuch as it was present in the HSV-1(F) sample. Subsequent experiments demonstrated nearly identical co-migration between pU_L17 and VP13/14 and this is most likely the reason why pU_L17 was not represented in our MALDI-TOF analysis.

Table 5.1 MALDI-TOF MS Results

predicted protein	homologs	SDS-PAGE mass	mol wt	accession no.	protein score	total ion score	best ion score	total C. I. %
histone H4 (mouse)	9 of 10	15,000	12480	gi|27692935	484	334	86	100
histone H2A (human H2Aj)	8 of 10	17,500	13,927.80	gi|7264004	240	187	70	100
histone H3 (human)	7 of 10	19,000	15,498.50	gi|56204740	265	119	92	100
vimentin (human)	7 of 10	62,000	49,623.10	gi|57471646	539	376	115	100
virion protein UL47	2 of 10	85,000	73,771.30	gi|9629428	355	141	52	100
virion protein UL46	2 of 10	95,000	78,195.70	gi|737826	431	263	85	100
major capsid protein HHV1	10 of 10	160,000	148,989.30	gi|9629399	714	464	101	100

To confirm the putative pU_L17 interaction with VP13/14, lysates of cells infected with HSV-1(F) and the U_L17 deletion virus were reacted with polyclonal antibody directed against VP13/14 (a kind gift from the laboratory of David Meredith) and the presence of pU_L17 in immunoprecipitated material was assessed by immunoblotting. As shown in Figure 5.4 C, approximately equal amounts of VP13/14 were immunoprecipitated from cells infected with either the U_L17 deletion or wild type viruses. More important to the purposes of this report, however, pU_L17 was readily co-immunoprecipitated with the VP13/14-specific antibody (fig. 5.4 A). These data therefore confirmed the interaction between pU_L17 and VP13/14.

Because VP13/14 had been reported to interact directly with VP16 in a yeast two-hybrid screen and to enhance VP16-mediated transcription, we were interested to know whether VP16 co-immunoprecipitated with VP13/14 and/or pU_L17. To test this possibility, the immunoblot of VP13/14 immunoprecipitated from lysates of cells infected with wild type and U_L17 deletion viruses was probed with VP16-specific antibody. As shown in figure 5.4 B, VP16 was readily co-immunoprecipitated with VP13/14 from cells infected with HSV-1(F). In contrast to this result, however, VP16 was not co-immunoprecipitated by the VP13/14-specific antibody from lysates of cells infected with the U_L17 deletion mutant. These data indicate that pU_L17 is required for the interaction between VP13/14 and VP16 as detected by immunoprecipitation.

In a second set of experiments to confirm the pU_L17-VP13/14 interaction, we sought to co-purify VP13/14 with pU_L17 by means other than co-immunoprecipitation. Therefore, a novel virus encoding pU_L17 with 6 histidine codons fused to its C-terminus (pU_L17-His) was constructed as

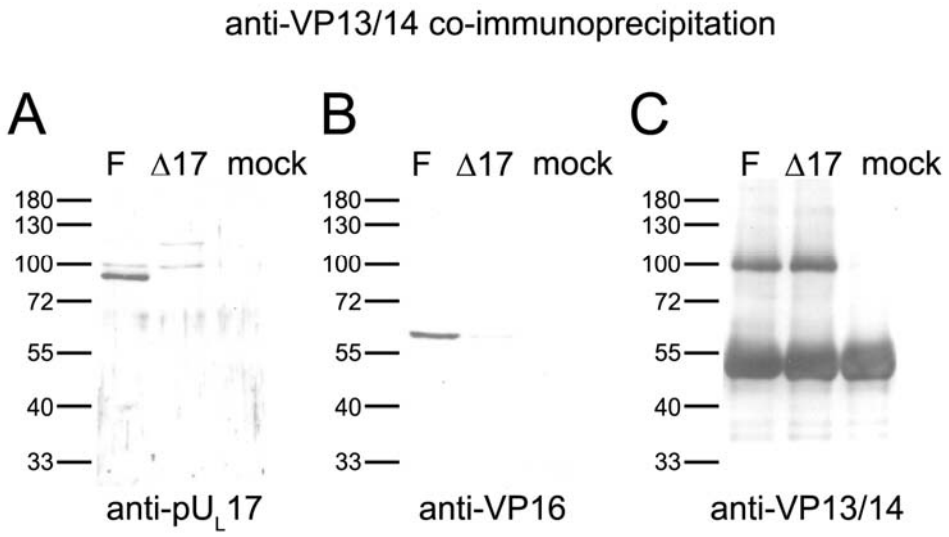

Figure 5.4. Co-immunoprecipitation of proteins with anti-VP13/14 antibody. Cells were mock infected, or were infected with HSV-1(F) or the U_L17 deletion virus and lysates were reacted with VP13/VP14-specific antibody. Immune complexes were purified, electrophoretically separated, subjected to immunoblotting with antibodies against pU_L17 (Panel A), VP16 (Panel B) or VP13/14 (panel C). Bound immunoglobulins were revealed by reaction with appropriately conjugated anti-immunoglobulins, followed by chemiluminescent exposure to X-ray film.

described in Materials and Methods. Cells were infected with this virus and sixteen hours later were lysed in 1% NP40. pU_L17-His was then purified from these lysates by affinity chromatography on Ni^{++}-containing agarose beads. As a negative control, lysates of cells infected with HSV-1(F) were treated identically. Proteins bound to the affinity matrix were eluted sequentially 4 times in the presence of imidazole, denatured in SDS, electrophoretically separated, and transferred to nitrocellulose. As shown in figure 5.5, probing the nitrocellulose with pU_L17-specific antibody revealed pU_L17-His within the eluates from pU_L17-His infected cells but not from eluates derived from cells infected with HSV-1(F). pU_L17 was most concentrated in the first elution, with subsequent elutions diminishing in signal as expected (fig. 5.5 A lane 1, 3).

The same immunoblot was then stripped and re-probed for the presence of VP13/14. As shown in fig. 5.5 B, although a background level of VP13/14 was detectable in the first elution from beads containing HSV-1(F) infected cell proteins, VP13/14 was clearly enriched in eluates derived from cells infected with the U_L17-His virus. Moreover, VP13/14 was readily detectable in the second elution from beads bearing proteins from cells infected with U_L17-His virus, but not from cells infected with HSV-1(F). These data therefore indicate that pU_L17 and VP13/14 can be co-purified via the His tag incorporated into the C-terminus of pU_L17, and further confirm the VP13/14-pU_L17 interaction.

To further investigate the relationship between VP16 and the VP13/14-pU_L17 complex, the affinity purified proteins were also probed with antibody directed against VP16. As shown in figure 5.5 C, lanes 1 and 3, a significantly reduced amount of VP16 was affinity purified from lysates of cells infected with pU_L17-His compared to the amounts eluted from the affinity matrix bearing

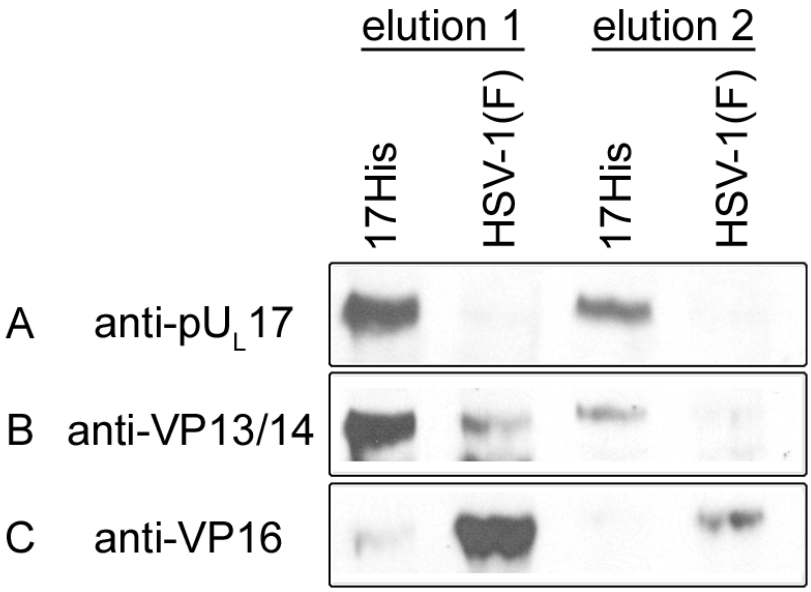

Figure 5.5. Affinity co-purification of VP13/14 and pU$_L$17. Hep2 cells were infected with either HSV-1(F) or a recombinant HSV-1 bearing a histidine tag fused to the C-terminus of pU$_L$17. Lysates of the cells were clarified and soluble proteins subjected to affinity chromatography on Ni++ containing beads. After extensive washing, proteins bound to the beads were eluted in SDS-PAGE sample buffer, electrophoretically separated, transferred to nitrocellulose, and subjected to immunoblotting with antibodies to pU$_L$17 (panel A), VP13/14 (panel B), or VP16 (panel C).

proteins of HSV-1(F) (fig. 5.5 C lanes 2 and 4). Thus, VP16 binds the Ni^{++} beads nonspecifically and does not associate efficiently with the pU_L17- His–VP13/14 complex. Although the reason for nonspecific association of VP16 with the Ni^{++} beads remains unclear, we hypothesize that the presence of pU_L17-His competes for non-specific interactions between VP16 and the charged Ni^{++} beads. Because VP13/14 and VP16 are known to interact, we speculate that the strong binding of VP16 to the affinity matrix might account for the small amount of VP13/14 in the HSV-1(F) eluate (Figure 5.5 B, lane 2). If this were the case, it would argue that relatively few molecules of VP16 associate with VP13/14.

Co-localization of pU_L17, VP11/12 and VP13/14 in infected cells:

Given the results of our immunoprecipitation data, we next asked if VP13/14 and pU_L17 co-localize in infected cells. Because the polyclonal antibody directed against VP13/14 was not useful for indirect immunofluorescence (data not shown), we constructed a recombinant virus placing an HA tag at the C terminus of VP13/14.

Cells were infected with the VP13/14-HA virus, fixed at various times after infection, and immunostained with anti-pU_L17 and anti-HA antibodies. Bound immunoglobulins were revealed by reaction with anti-immunoglobulins conjugated to different fluorescent markers. The results, shown in figure 5.6, indicate that pU_L17 and VP13/14 (as indicated by reaction with the anti-HA antibody) are detectable by 6 hours after infection. At this time point, both pU_L17 and VP13/VP14 co-localized in either the cytoplasm in a perinuclear region of cells or at low levels in the nucleus. By 9 hours, both pU_L17 and VP13/14 were predominantly located in the intranuclear replication

Figure 5.6. Immunofluorescence staining time-course from infection with an HA-tagged VP13/14 virus. At the indicated hours post-infection Hep2 cells were fixed, permeabilized, and reacted with antibodies to pU_L17 (leftmost column), HA (indicating VP13/14 localization; second column to left), or ICP4 (rightmost column). Third column from the left is a merge of the two columns to its left. Arrows indicate regions of the plasma membrane bearing pU_L17 and VP13/14-HA-specific signals. Images were captured under 600x magnification with an additional 3x digital zoom.

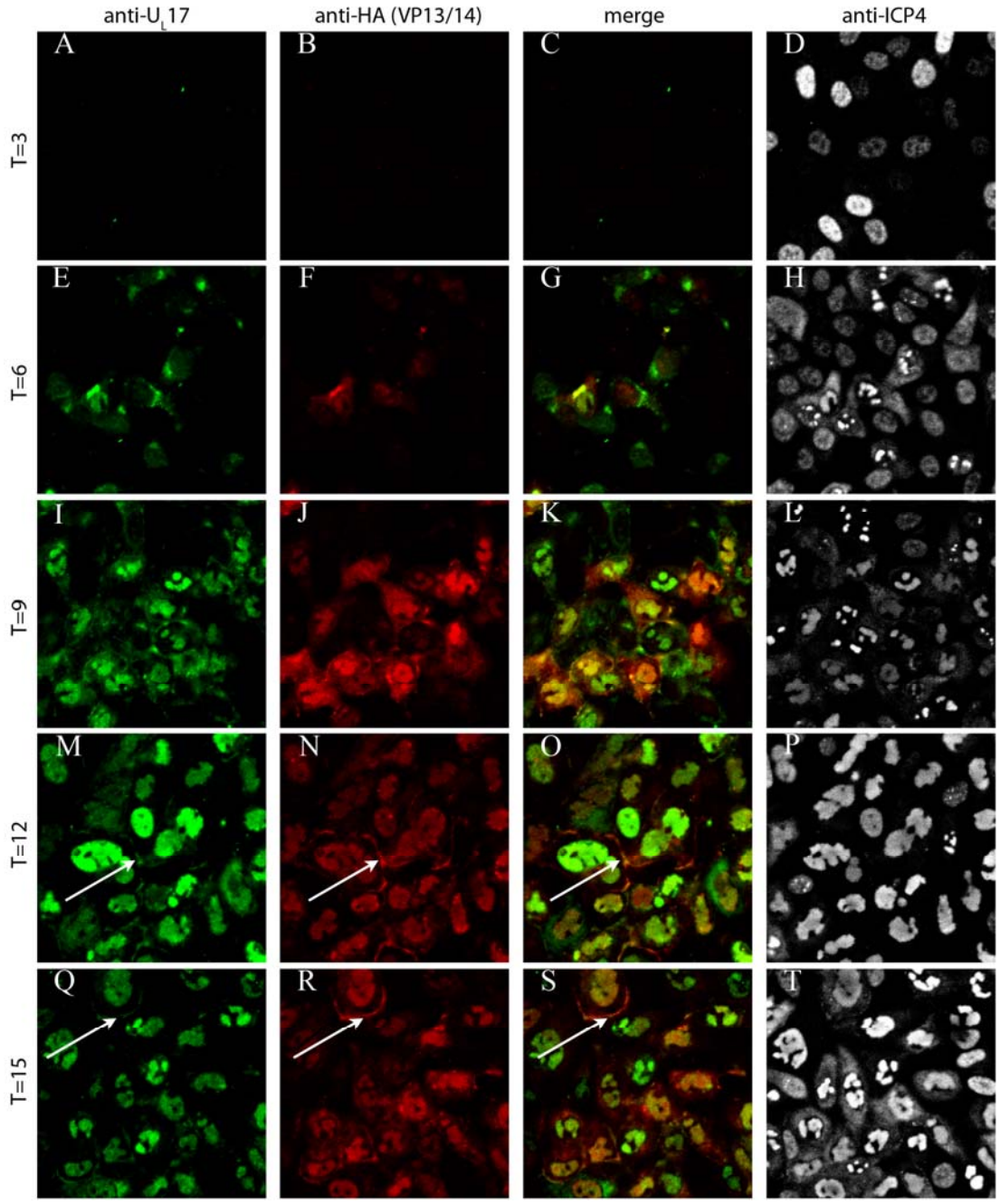
anti-U$_L$17
anti-HA (VP13/14)
merge
anti-ICP4
T=3
T=6
T=9
T=12
T=15
A
B
C
D
E
F
G
H
I
J
K
L
M
N
O
P
Q
R
S
T

compartment as determined by their distribution in a pattern identical to that obtained upon immunostaining with ICP4 specific antibody (57). Some cells contained more pU_L17 specific staining than VP13/14 staining, whereas others contained more VP13/14- than pU_L17-specific immunostaining. Although previous reports indicated that pU_L17 localized to intranuclear aggregates containing VP5 and ICP35, such distribution was seen only rarely in the current study (99). At 12-15 hours post infection, small amounts of immunoreactivity attributable to both VP13/14 and pU_L17 co-localized at the plasma membrane (fig. 5.6 M, N, O, Q, R, S and figure 5.7). These data indicate that, at least as viewed by immunofluorescence, VP13/14 and pU_L17 localize at later times post infection in the replication compartment of the nucleus, and eventually at the plasma membrane.

A recombinant 47HA delta 17 virus was constructed to survey whether the pU_L17 deficiency could alter the distribution of HA-tagged VP13/14. Immunofluorescent studies were repeated with VP13/14-HA and VP13/14-HA delta 17 in parallel and no significant difference was observed in the intensity or distribution of VP13/14 (data not shown). Late in infection, HA staining was still readily apparent in the nucleus, the cytoplasm, and at nuclear and plasma membranes. Thus we conclude that the interaction of pU_L17 with VP13/14 in not necessary to maintain either VP13/14-HA expression or localization.

Co-expression of VP11/12, VP13/14 with pUL17 results in cytoplasmic co-localization:

In order to determine whether pU_L17, VP11/12, and VP13/14 co-localize in the absence of other viral proteins, expression constructs encoding pU_L17, VP13/14-HA and FLAG-VP11/12 were transfected in various

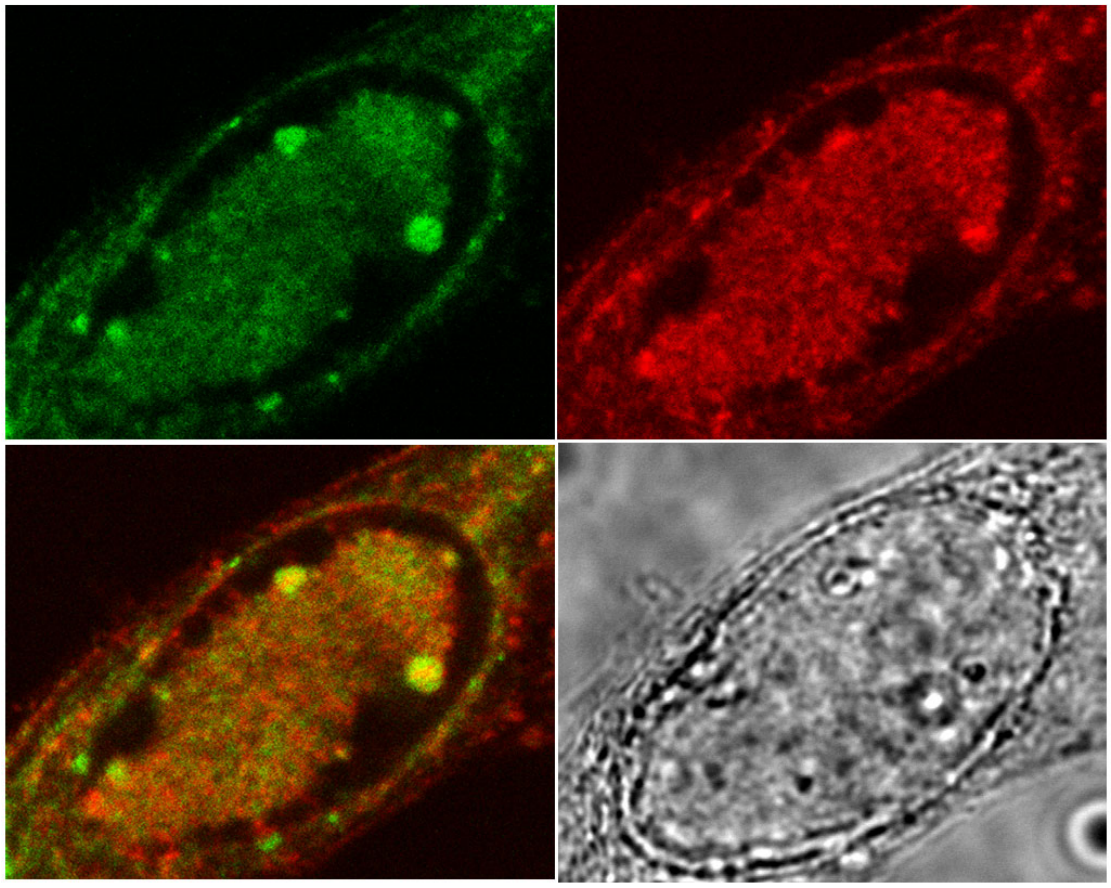

Figure 5.7 Co-localization of pU_L17 and VP13/14. Sixteen hours post-infection co-localization can be seen in the replication compartment, at the nuclear and plasma membrane and in the cytoplasm. pU_L17 (Texas Red), anti-HA (FITC). Images were captured under 600x magnification with an additional 7x digital zoom.

combinations into Hep2 cells. Approximately 36-48 hours later, the cells were reacted with anti-FLAG (M2), anti-pU_L17 and anti-HA antibodies. The results are shown in figure 5.8.

The distribution of pU_L17 expressed in the absence of other viral proteins varied from cell to cell. In some cells, immunoreactivity attributable to pU_L17 accumulated in the cytoplasm almost exclusively, with very light staining in the nucleus (fig. 5.8, panel 1, cell on left). In many cells, pU_L17 was distributed roughly equally in both the cytoplasm and nucleus (fig 5.8, panel 1, cell on right).

Solely expressed VP13/14-HA localized predominantly (although not exclusively) within the nucleoplasm in a smooth pattern exclusive of the nucleolus, with very little immunostaining detectable in the cytoplasm (fig. 5.8, panel 2).

In contrast, FLAG-VP11/12 expressed in the absence of other viral proteins localized exclusively in the cytoplasm and primarily in perinuclear aggregates (fig. 5.8, panel 3). We note that this exclusively cytoplasmic pattern was similar to that expressed by a virus encoding VP11/12-GFP (174, 273) and VP11/12 fused to an HA epitope tag (174). Thus, the punctate distribution of FLAG-VP11/12 in this study was consistent with that seen in previous studies using different fusion partners.

Co-expression of U_L17 and FLAG-VP11/12 caused the encoded proteins to partially co-localize in some perinuclear aggregates (fig. 5.8, panel 6); however, the general pattern of immunostaining of both proteins remained unaltered from that obtained upon expression of the individual proteins. Co-expressed pU_L17 and VP13/14-HA co-compartmentalized (fig. 5.8, panel 9) in the nucleus. Co-expression of FLAG-VP11/12 with VP13/14-HA resulted in a

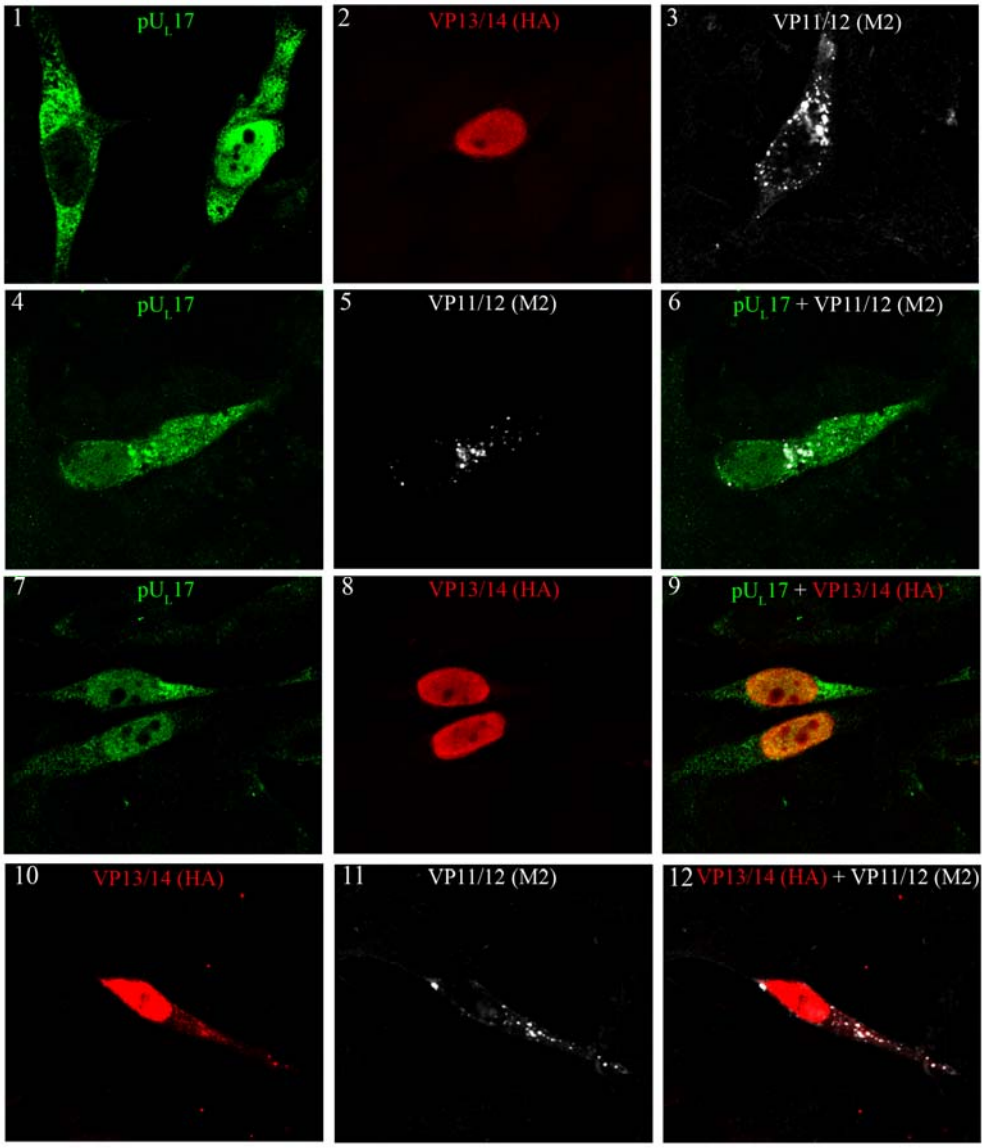

Figure 5.8. Immunofluorescent staining of singly and co-expressed pU$_L$17, VP13/14-HA, and VP11/12-FLAG. Expression of each protein alone is shown (1-3): VP13/14-HA (Texas Red, red), FLAG-VP11/12 (Cy5, white), and pU$_L$17 (FITC, green). Co-transfection indicates cytoplasmic co-localization of pU$_L$17 with FLAG-VP11/12 (6), and FLAG-VP11/12 with VP13/14- HA (12). Images were captured under 600x magnification with an additional 3x digital zoom.

slight increase in the amount of VP13/14-HA immunoreactivity in the cytoplasm (fig. 5.8, panel 10). Although most VP13/14-HA and VP11/12-specific staining did not co-localize, some of the more intensely staining cytoplasmic foci of VP13/14-HA contained FLAG-VP11/12 (fig. 5.8, panel 12).

Lastly, cells receiving all three expression constructs exhibited more cytoplasmic VP13/14-HA, and some cytoplasmic foci contained all three proteins (fig 5.9, panels 4 and 8). Based on these collective data, we conclude that (i) co-expression of VP11/12 and VP13/14 results in a greater cytoplasmic localization of VP13/14 and (iii) co-expressed pU_L17, VP11/12, and VP13/14 co-localize to a limited extent in the cytoplasm.

Assembly of VP13/14 into virions:

Having established collectively in this and previous studies that (i) pU_L17 is located on the surface of nucleocapsids, (ii) VP13/14 and pU_L17 interact and (iii) that both VP13/14 and pU_L17 co-localize in the nucleus and cytoplasm at late times post infection, we wanted to determine at what point during egress VP13/14 becomes incorporated into virions. Preliminary experiments to demonstrate unequivocally the presence of VP13/14-HA in association with intranuclear capsids were unsuccessful because VP13/14-HA migrated throughout sucrose gradients, even when capsid assembly was precluded by deletion of U_L18, which encodes one of the triplex proteins critical to capsid formation (not shown). We therefore used immunogold electron microscopy as an alternative approach. Thus, cells were infected with HSV-1(F) or the VP13/14-HA virus at 5 PFU per cell. Sixteen hours after infection, the cells were fixed, embedded in Epon plastic, and thin sections were reacted with anti-HA antibody. Bound immunoglobulin was revealed by reaction with

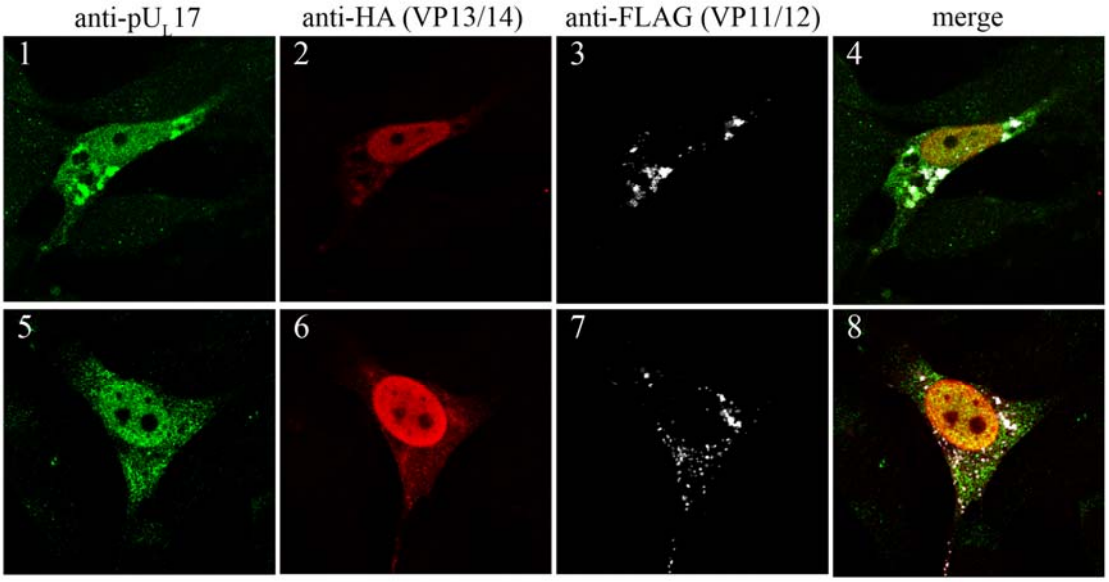

Figure 5.9 VP11/12-FLAG, VP13/14-HA, and pU$_L$17 triple transfection. Co-expression of all three proteins: VP13/14-HA (Texas Red, red), FLAG-VP11/12 (Cy5, white), and pU$_L$17 (FITC, green) and cytoplasmic co-localization. Images were captured under 600x magnification with an additional 3x digital zoom.

goat anti-rabbit immunoglobulin conjugated to 12 nm colloidal gold beads. Representative results are shown in figure 5.10.

Immunoreactivity in thin sections of cells infected with the VP13/14 HA was most intensely associated with virions in the cytoplasm and extracellular space. This was expected inasmuch as VP13/14 is known to accumulate abundantly in virions. In contrast, colloidal gold beads reflecting localization of VP13/14-HA were not associated to an appreciable extent with intranuclear capsids. We also noted many gold beads arranged in short linear or curved arrays at the nuclear periphery. Importantly for the purposes of this study, some perinuclear virions were also decorated with gold beads, but the immunolabeling was not as consistent nor as intense as that of virions in the cytoplasm or extracellular space. In the control experiment performed in parallel, virtually no immunoreactivity was observed in thin sections of cells infected with HSV-1(F) reacted with the HA antibody. This was the case despite the ample presence of virions within these sections (not shown).

We interpret these data as indicating that the bulk of VP13/14-HA is incorporated into de-enveloped virions in the cytoplasm, whereas small amounts may become associated with capsids at the nuclear periphery, presumably at or near the time of budding through the INM.

Discussion:

The main goal of this study was to identify pU_L17 interacting proteins to shed light on its role in tegument and capsid assembly. The studies were initiated by co-immunoprecipitation with pU_L17 antibody, followed by analysis of bands predominantly or exclusively visualized in electrophoretic profiles of proteins immunoprecipitated from lysates of wild type virus as opposed to

Figure 5.10. Immunogold electron microscopy with HA-specific antibody. Cells were infected with a recombinant virus bearing the HA epitopic tag fused to VP13/14, and were embedded 16 hours later. Thin sections of the infected cells were reacted with HA specific antibody and bound antibody was recognized with goat anti-rabbit IgG conjugated to 12 nm colloid gold beads. Panel A. Gold beads arranged in curved linear arrays at the nuclear periphery, and with cytoplasmic virions. Panel B. A single labeled perinuclear virion. Panel C. Gold beads associated with cytoplasmic virions and with the cytosol. Panel D. Gold beads (i) arranged in a curved linear array at the nuclear periphery and (ii) in association with cytoplasmic virions. Onm, outer nuclear membrane; nuc, nucleus; cyto, cytoplasm. As a size standard, HSV-1 capsids are 125 nm in diameter.

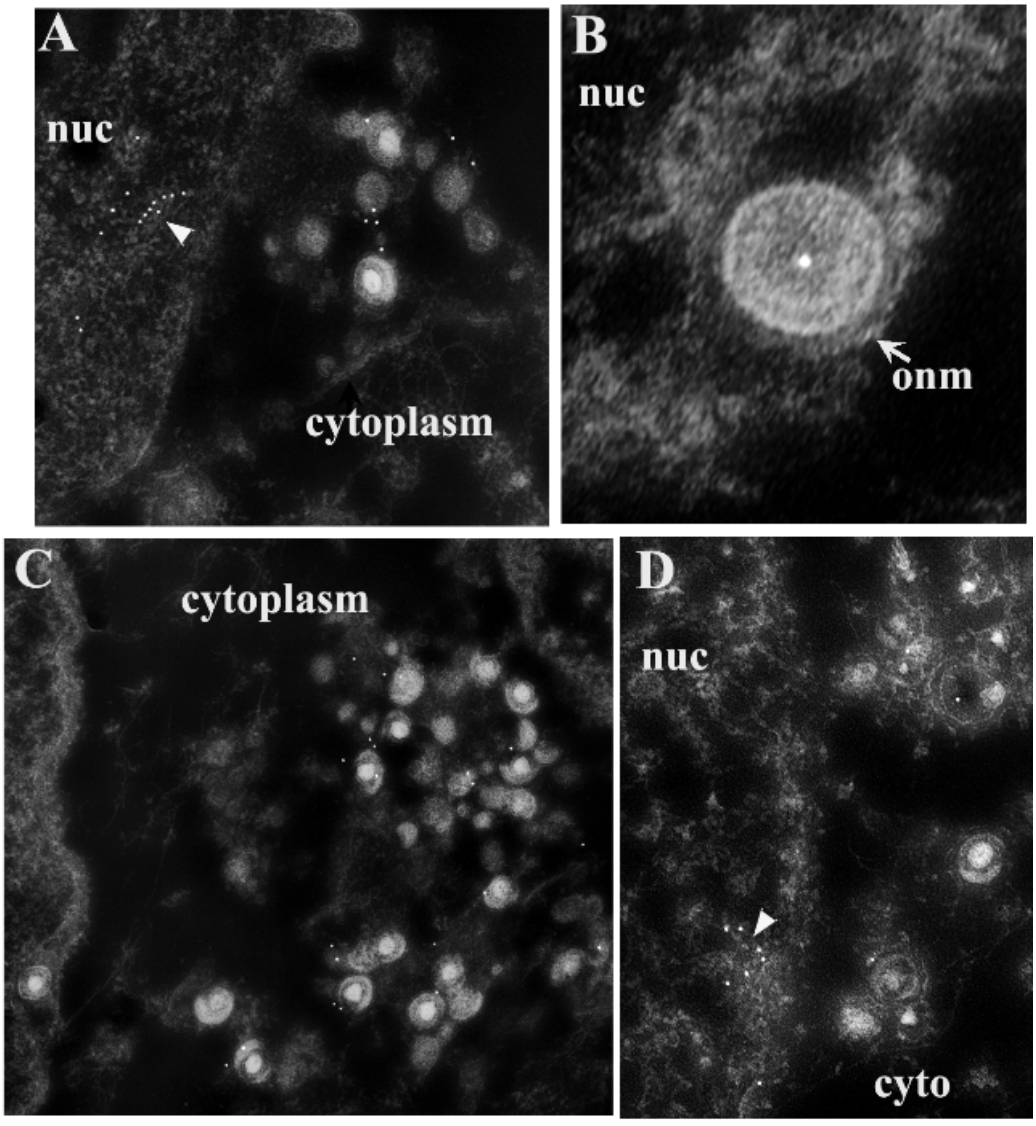
A
nuc
cytoplasm
B
nuc
onm
C
cytoplasm
D
nuc
cyto

those from a U_L17 deletion virus. Although this approach might preclude detection of interesting interacting proteins if they were to co-migrate with (i) proteins immunoprecipitated nonspecifically or (ii) the heavy or light chains of the IgY and IgG antibodies, we were able to identify interactions between pU_L17 and vimentin, cellular histone proteins, the capsid component VP5, and the tegument proteins VP13/14 and VP11/12.

Histone proteins that co-immunoprecipitated with pU_L17 included H4, H2A, and H3, which represent core proteins of the nucleosome. The exclusion of histone H2B from this group may reflect the fact that the encoding gene is transcriptionally down-regulated in lytic HSV infection as a consequence of competition by HSV-1 VP16 for the transcription factor Oct1 (135). Whether the interaction between pU_L17 and histones actually occurs in vivo remains uncertain, however. Such an interaction was not supported by indirect immunofluorescence studies inasmuch as pU_L17 and histone H3 did not co-localize to any appreciable extent in infected cell nuclei (data not shown). We remain similarly skeptical of the pU_L17/vimentin interaction inasmuch as vimentin is a common contaminate of affinity purification and vimentin is mostly cytoplasmic, whereas pU_L17 is largely nuclear in infected cells. Thus, the significance of the histone/pU_L17 and vimentin/pU_L17 co-immunoprecipitations requires further verification.

The co-immunoprecipitation with VP5 is perhaps not surprising given previous observations that pU_L17 localizes on the external surface of the capsid shell, which is largely composed of VP5 (274). It remains unclear, however, whether pU_L17 interacts with monomeric, pentameric or hexameric forms of VP5. The deduced presence of pU_L17 in a heterodimer with pU_L25 atop triplexes bridging capsid pentons to adjacent hexons was observed

exclusively in DNA-containing capsids (i.e. in the CCSC) (254), whereas others using biochemical techniques have detected pU_L17 on all capsid forms including procapsids (246). Reconciling these observations will require further studies, but one possibility is that some triplexes bearing pU_L17 are incorporated into the procapsid, whereas structural changes induced by DNA insertion promote the optimal conformation to promote pU_L17/pU_L25 binding. (We note that although pU_L25 was not detected in these studies, we would expect the protein to co-migrate with the IgY heavy chain and therefore be unapparent in the analysis.) Given that the triplex proteins VP19C and VP23 were also unapparent by Coomassie-staining in the immunoprecipitation with anti- pU_L17 antibody, it is possible that we are detecting pU_L17 interactions with VP5 prior to capsid formation or after lysis of procapsids. Further studies will be required to determine whether other capsid proteins interact directly or indirectly with pU_L17.

It is likely that the tegument is anchored to the capsid by a series of interactions. Previous work to identify such anchoring points on the capsid focused on the pentonic vertices which bear densities of primary tegument when viewed in intact virions (285). The precise identities of the proteins responsible for the penton-associated densities are unknown. pU_L36 has been shown to interact with HSV nucleocapsids and to interact with pU_L25 in the pseudorabies system, suggesting its role as a primary tegument protein (27, 49). The current study suggests another anchoring point of tegument on the capsid, specifically through the interactions between pU_L17 on the capsid surface, and VP11/12 and VP13/14 in the next layer of tegument. Thus, it is possible that the interaction between capsid-associated pU_L17 and tegument proteins VP11/12 and VP13/14 helps capsids engage secondary envelopment

sites in the cytoplasm. That VP11/12 and VP13/14 associate with cytoplasmic capsids primarily is supported by (i) our immunogold study in which cytoplasmic virions were more frequently decorated by gold beads indicative of VP13/14-HA than were intranuclear capsids or perinuclear virions and (ii) the observation that co-localization of co-expressed pU_L17, VP11/12 and VP13/14 only occurs in the cytoplasm.

We also noted that co-immunoprecipitation of VP13/14 and VP16 does not occur in lysates of cells infected with a U_L17 null virus, suggesting that pU_L17 is necessary for the interaction between VP13/14 and VP16 in vivo. Although it is tempting to speculate that this observation reflects pU_L17's effects on the conformation of the tegument, and VP13/14-VP16 in particular, it is unclear whether this is a direct or indirect effect. For example, if engagement of VP16 with VP13/14 required the presence of DNA-containing capsids in the cytoplasm, the absence of such capsids in cells infected with the U_L17 null could explain the failure of VP16 and VP13/14 to interact. Further studies will be required to distinguish between this and other possibilities.

Acknowledgements:

We thank the David Meredith laboratory for the polyclonal antibody to VP13/14. These studies were supported by grants R01GM50741 and T32 AI07618 from the National Institutes of Health.

CHAPTER VI:

Encapsidation of Herpes simplex virus 1 DNA is not responsible for intranuclear movement of capsids

Abstract:

Previous studies indicate that herpes simplex virus (HSV) capsids move in a directed, energy, and actin-dependent fashion in the nuclei of infected cells. Because DNA packaging also requires substantial amounts of energy, we sought to test the hypothesis that energy-dependent movement was linked to DNA packaging. To this end capsid movement of viruses deficient for the essential DNA cleavage and packaging proteins, pU_L6, pU_L15, pU_L17, pU_L25, pU_L28, or pU_L33 was examined by time lapse microscopy. In all cases, capsids moved with similar rates as those of wild type virus. We therefore conclude that capsid movement occurs independently of successful viral DNA cleavage and packaging.

Introduction:

HSV capsid proteins assemble 125 nm shells in the nucleus into which newly replicated HSV DNA is packaged. The precursor capsid type, or procapsid, consists of two shells. The inner shell is composed of scaffold proteins. The outer capsid shell has T=16 symmetry and is mainly composed of the VP5 protein which can form two types of capsomeres of five-fold (termed pentons) and six-fold (termed hexons) symmetry (253, 262). Individual capsomeres are separated by triplexes, which comprise two VP23 molecules and one molecule of VP19C (183, 228, 251). VP26, the 12 kDa capsid protein encoded by U_L35 (160), is external to the core capsid shell (178). The protein is assembled onto the tips of hexons, but is excluded from pentons (25, 287) By analysis of synchronized capsid maturation, it was determined that VP26 is added to the capsid in an ATP-dependent manner

after angularization of the capsid from a spherical precursor or procapsid to more mature forms (45, 184).

After capsid assembly is complete, a group of proteins encoded by U_L6, U_L15, U_L17, U_L25, U_L28, U_L32, and U_L33 mediates packaging of nascent viral genomes. The terminase, comprising subunits encoded by U_L15, U_L28, and U_L33, is the protein complex thought to be responsible for recognizing, binding, and ultimately cleaving HSV DNA at Pac sites in the terminal repeats of the genome (19, 127, 259). In this complex, U_L15 protein (pU_L15) likely encodes the ATPase, pU_L28 contributes specific DNA binding activity, and pU_L33 stabilizes the interaction between pU_L15 and pU_L28 (2, 277, 282). During the packaging reaction, the terminase proteins associate with a specialized portal vertex of the capsid comprising 12 copies of the U_L6 protein (32, 182, 269, 278). The U_L17 and U_L25 genes appear to play a structural role as they encode minor capsid proteins that are added to the external surface and border hexons and pentons (245, 254, 274). pU_L25 is dispensable for cleavage of genomes of less than full length, but in full length genomes is essential for maintenance of one end of the packaged genome. This indicates that either pU_L25 (i) is required for accuracy of the final DNA cleavage event that releases the genome from the concatemer or (ii) ensures proper capsid conformation to ensure that the genome stays in the capsid to avoid degradation (158, 231). Potentially consistent with either role is the observation that pU_L25 is present in greater amounts on DNA-containing capsids.

GFP from the bioluminescent jellyfish, *Aequorea Victoria*, has been used extensively in both prokaryotic and eukaryotic systems as a molecular reporter for gene expression and cellular localization (reviewed in (37)).

Because its fluorescence is independent of other co-factors, GFP facilitates live-cell analysis of proteins and organelle dynamics (38). This characteristic of GFP and other chromophore derivatives (RFP, YFP etc) has been useful in labeling and monitoring HSV capsids (58, 63, 82) tegument proteins (58, 76), and glycoproteins (10, 18) by live cell microscopy.

In HSV infection, VP26 is not essential for viral replication or proper tegumentation (42) and thus can be tagged and used to track capsids in living infected cells without substantially disturbing virion assembly. Baculoviruses co-expressing the triplex proteins, scaffold protein, and the major capsid protein of HSV or Marek's disease virus (another alphaherpesvirus) have been shown to produce large-cored B capsids in the absence of VP26 although assembly is facilitated in the presence of VP26 (130, 239, 244).

Previous studies have shown that intranuclear capsids produced by HSV-1 strain KOS labeled with GFP-VP26 move in a directed but erratic manner, and that this movement is both energy- and actin-dependent (82). The motor responsible for movement in the nucleus has yet to be identified. Although capsid movement was halted with myosin inhibitor 2,3-butanedione monoxime (BDM), this drug has effects on the cell other than myosin inhibition (82). It is also unclear what advantage, if any, such movement serves in the viral life cycle.

A simple hypothesis is that intranuclear capsid movement is driven by the HSV DNA packaging motor. The packaging motor must be sufficiently powerful to encapsidate viral DNA under extreme pressure, at near liquid crystalline density, thus it is a good candidate to support capsid movement. It is conceivable that the terminase motor could be used to move capsids along bound DNA in search for packaging signals prior to DNA cleavage/packaging.

As an approach to address whether DNA packaging can account for capsid movement, we characterized the nuclear movement of GFP-labeled capsids in cells infected with a variety of DNA cleavage and packaging mutants. Intranuclear capsids were observed to move in cells infected with all the mutant viruses tested. We therefore conclude that intranuclear capsid movement can occur independently of the DNA encapsidation process.

Materials and methods:

Production of a novel VP26-GFP expressing cell line - A GFP-U_L35-expressing pcDNA3 clone was created through an intermediate pCR2.1-U_L35 subclone derived from a KOS GFP-VP26 virus previously reported by Desai et al (63). This fusion was formed by ligating a 711 base pair NcoI/BsrGI fragment of EGFP from pEGFP-N1 (Clontech) into the U_L35 open reading frame such that EGFP started at the fifth codon of U_L35 (63). A GFP-U_L35 DNA fragment and linear pcDNA3 vector were obtained by EcoRI digestion and ligated to yielded a GFP-U_L35 expression clone. Hep2 cells were transfected with GFP-U_L35-pcDNA3 and GFP positive clones were sorted by an ExCalibur FACS (fluorescence activated cell sorter) to enrich for FITC+ cells. Cells were pooled and selected for stable expression of GFP-U_L35.

Production of a novel UL17 expressing cell line - A novel cell line CV1-17, specifically engineered to support replication of U_L17 null viruses, was created using the Flp-In system from Invitrogen. Briefly, the U_L17 open reading frame was cloned into the FRT-containing expression vector pcDNA5/FRT and verified by DNA sequencing. The pcDNA5/FRT-U_L17 plasmid was co-transfected with pOG44, a Flp recombinase-encoding plasmid, into CV-1 cells

previously selected for an integrated FRT locus to support recombination of the transfected DNA. Site-specific recombination resulted in a change of cell line phenotype from Zeocin resistance to Hygromycin (Hyg) B resistance. Hygromycin-resistant colonies were amplified and grown into cellular monolayers. Expression of U_L17 in these cells was determined by immunoblotting with anti-pU_L17 antibody, and plaque formation by the U_L17 null virus. One such cell line was designated CV1-17 and was used for further studies. CV1-17 cells were maintained in Dulbecco's modified Eagle's medium (DMEM) supplemented with 10% fetal bovine serum and 200 μg/ml Hyg B.

Live-cell microscopy of GFP-VP26 cells infected with DNA packaging-deficient viruses - GFP-VP26 Hep2 cells were infected with viruses deleting individual DNA cleavage and encapsidation proteins. Nine hours post-infection the glass cover slips containing infected cells were mounted into a Bioptics flow cell and the intranuclear movement of GFP-labeled capsids was assayed by confocal time-lapse microscopy as was done previously (82). Multiple cells were analyzed for each infection. Scan zones were cropped to isolate individual nuclei allowing for higher laser scanning frequencies ranging from 0.366 to 1.08 seconds per frame.

Production of a BAC derived GFP-VP26 virus - Since our assay of infecting GFP-VP26 cells with deletion viruses results in two populations of VP26, non-labeled and GFP-labeled, reporting capsid dynamics by GFP only represents a portion of total VP26. In order to ensure that we were not missing an effect on capsid dynamics in our unlabeled population, we recreated a GFP-VP26

virus through recombinant BAC technology. This virus was engineered to mimic the K26GFP virus (63) including the previously reported 50 base pair deletion of non-coding sequence upstream of U_L35 (175) leaving only a small FRT scar upstream of the GFP-U_L35 coding region. Briefly, primers LDS #36 CCATGGTGAGCAAGGGCGAGGAG and TF #79 GCGTTATCCGCCGATGA with EGFP and VP26 homology, respectively, were used to amplify the GFP-VP26 fusion protein from K26GFP viral DNA. In an independent reaction, primers LDS #38 GCACCGCCGCCCTAATCGCCAGTGCGTTCCGGACGCCTTCGCCCCACTC GACCCGTGTAGGCTGGAGCTGCTTC (Kan homology underlined) with flanking oligonucleotides homologous to sequence upstream of U_L35 and LDS#39 AGCTCGACCAGGATGGGCACCACCCCGGTGAACAGCTCCTCGCCCTTG CTCACCATATTCCGGGGATCCGTCGAC (Kan homology underlined) with flanking oligonucleotides homologous to the N terminus of GFP were used to amplify a FRT-KAN-FRT cassette. In a subsequence stitching PCR reaction, products were annealed and the complete construct: upstream U_L35 sequence / FRT-KAN-FRT / GFP–U_L35 was amplified with LDS #38 and TF #79 primers. This construct was sub-cloned into pCR2.1 and sequenced to ensure proper junctions. EcoRI digestion of subclones released the KAN / GFP-U_L35 fusion fragment with flanking U_L35 sequence which was transformed into EL250 cells with a chloramphenicol-resistant, HSV-containing, bacterial artificial chromosome (BAC) (238) and recombinants were selected on Kan/Cm agar plates. DNA extracted from resulting colonies was verified by electrophoresis of restriction digest. Overnight cultures were grown in the presence of 0.1% arabinose to induce FRT-mediated recombination resulting in release of the

Kan gene and the following day bacteria was struck on Cm plates for single colonies. A selected group of resulting single colonies were replica-plated, first inoculating a Kan/Cm plate and subsequently a Cm only plate. All selected colonies grew only on the Cm plate, indicating induction was complete and the Kan gene was lost through recombination. These results were verified through successful colony PCR with upstream U_L35 and internal U_L35 primers [LDS #31 GAACGACAAACGGTGAATAGGTG (internal) and LDS #32 TATTTGGTGGGTGGTTGGTGCTGGCG (upstream)]. Three colonies were chosen for further analysis by BAC DNA extraction and BamHI digestion. DNA from one clone, 38-2-11, was co-transfected by SuperFect (Qiagen) into rabbit skin cells with pCAGGS, a Cre recombinase-containing plasmid, to excise the BAC backbone. Three rounds of plaque purification on Vero cells produced our GFP-VP26 virus. The GFP-VP26 recombinant virus demonstrated wild-type growth properties.

To knock-out one of the proteins essential for cleavage and packaging, U_L17, in the context of this novel GFP-VP26 virus, electrocompetent EL250 cells harboring the GFP-VP26 BAC were electroporated with a Kanamycin resistance cassette (Kan^R). A gene encoding Kan^R was PCR amplified with the following primers containing sequences homologous to the U_L17 ORF and Kan^R cassette:

(del17F, #11) CAAACTTCCAG GTCGAAATCCAG ACTCGGGCTCATG CCACCGGCGACTG TA CGTGTAGGCTGGAGCTGCTTC; (del17R, #12) TTCCGTAGT GGTGGCGCA GGACCACGGAG ATAGAACGACG GCTCCACAGCC AGTCATTCCGGGGATCCGTCGAC (Kan^R homology underlined). Amplicons were transformed into EL250 cells containing a chloramphenicol–resistant

(Cm^R) GFP-VP26 BAC (238). Cm^R/Kan^R recombinants were selected on agar plates. BAC DNA isolated from selected recombinants was co-transfected with pCAGGS into CV1-17 cells to yield GFP-VP26 delta 17 virus.

Capsid purification - Two roller bottles of Vero cells (approximately 4.0 $x10^8$) were infected with GFP-VP26 virus at an MOI of 5 and collected at 16 hours post-infection. Cells were pelleted at 4000 rpm for 10 minutes, and pellets were resuspended in 16 mls dH_20 and stored at -80^0C overnight. Infected cell pellets were thawed, dounce homogenized with 15 strokes to lyse, and nuclei were pelleted at 4000 rpm for 15 minutes. Pellets were resuspended in 8 mls of 1.0% TritonX100 in dH_20 and sonicated for 45 seconds, before pelleting debris for 10 minutes again. The supernatant was transferred to new tubes and returned to -80^0C. Capsid containing supernatents were thawed and sedimented by ultracentrifugation at 20K rpm for 1 hour through a 35% (w/v) sucrose cushion. After capsid were pelleted the cushion was carefully discarded and capsids were resuspended in 500 μl of STE buffer, sonicated for 3 seconds, and loaded onto the top of a 20% to 50% continuous sucrose gradient. Capsid bands were formed upon ultracentrifugation at 23-25K for 1 hour. The entire sucrose gradient was fractioned into 500 ml aliquots with number 1 and number 22 representing the top and bottom fractions, respectively. Aliquots of each of the 22 fractions were mixed with 2X SDS-PAGE sample buffer, electrophoretically separated on an 8% SDS polyacrylamide gel, and transferred to nitrocellulose. The membrane was blocked with 5% milk in PBST (PBS with 0.2% Tween-20) for 30 minutes and reacted with a 1:2,000 dilution of rabbit anti-GFP antibody (Molecular Probes A-11122) for 2 hours, washed 3 times with PBST for 5-10 minutes each, and

incubated with a 1:5,000 dilution of HRP-conjugated anti-rabbit secondary antibody. Excess secondary was washed from the membrane with another 3 PBST washes and bound antibody was detected with a 1 minute incubation of (Pierce) ECL. Fluorescence was captured on film.

ATPase Assay: C-His-tagged pU_L17 expressed in insect cells was purified with Qiagen Ni-NTA beads as previously described (Chapter 4). 500 nM or 1μM pUL17 were incubated with γP32-labeled ATP in BTR buffer (50 mM Tris pH 7.5, 10 mM $MgCl_2$, 0.5 mM EDTA, 0.02% β-mercaptoethanol) at 37°C for 60 minutes. Samples were spotted on Whatman paper and dried with heat. Chromatography proceeded in a TLC chamber using a 50 ml solution containing 1.05g of lithium chloride and 2.6 mls of formic acid as a solvent. Chromatography was stopped before the migration front reached the end of the paper. The paper was dried and exposed to film.

Results:

Verification of the GFP-VP26 virus:

A recombinant BAC was generated that encoded GFP-VP26 virus in place of the U_L35 gene. To ensure that GFP-VP26 was able to bind to capsids, capsids were purified and subjected to immunoblotting with GFP-specific antibody. An identical peak in signal from fractions 13-15 was also seen with VP5 immunoblotting. As shown in figure 1A, a band containing GFP immunoreactivity was detected that contained protein with a relative molecular weight (M_r) of 34.6 kDa in capsid fractions 10-22, with peak intensities in fractions 13-15 (fig 6.1). This was in close agreement with the calculated molecular weight, 38,170 of the GFP/VP26 fusion protein. Bound IgG was

removed chemically, and the nitrocellulose was re-probed with a 1:1,000 dilution of anti-VP5 antibody (Virusys) followed by reaction with an HRP-linked anti-mouse secondary conjugate (Pierce) and fluorography. As shown in figure 6.1, the capsid-containing fractions as revealed by those with intense VP5 immunostaining corresponded to those containing VP26/GFP (fig 6.1).

To determine whether GFP labeling was uniform among capsids, and that the observed capsids were consistent in fluorescent intensity compared to those reported in our previous studies, ten microliter aliquots of sucrose gradient fractions, 2, 7, 10, 14, 16, 18, 20, and 22 were spotted on glass slides and covered with coverslips. Capsid fraction aliquots were analyzed on an Olympus confocal microscope at 600x and representative fields of capsids were photographed. Fraction 14, corresponding to the fraction with the most

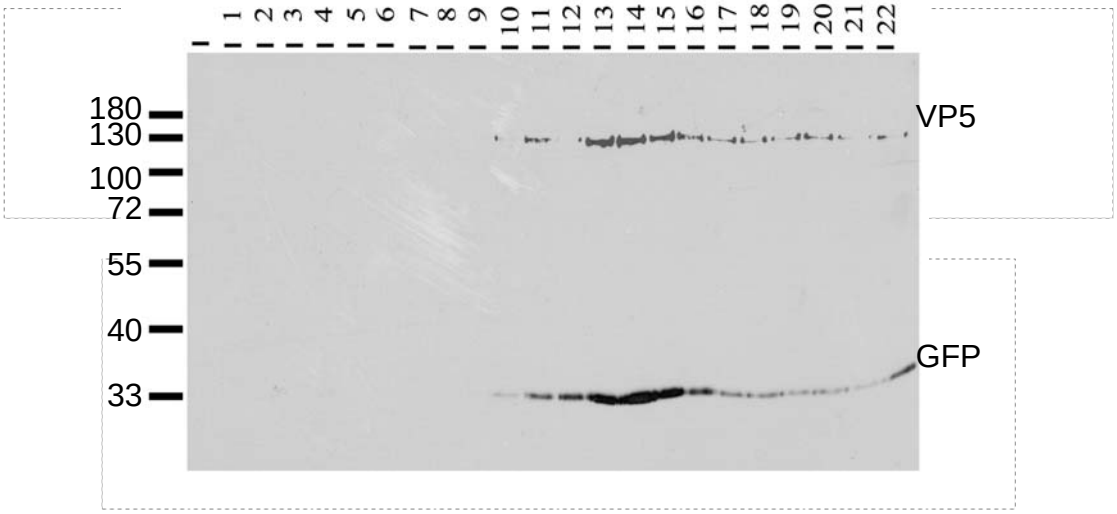

Figure 6.1 GFP-VP26 capsid isolation. GFP-VP26 purified from infected cell nuclei was separated in a sucrose gradient that was fractioned into 500 μl aliquots numbered 1-22 with #1 and #22 representing the top and bottom of the gradient, respectively. Separate immunoblotting with anti-GFP and anti-VP5 antibodies each shows a peak of capsids in fractions 13-15. (Images are overlaid) The M_r of GFP-VP26 was calculated to be 34.6 kDa.

VP26/GFP immunoreactivity, demonstrated the highest density of GFP foci (fig. 6.2). Labeled foci were determined to be fundamentally uniform in size and GFP intensity. These were approximately equal in fluorescence intensity compared to labeled capsids seen in previous live-cell microscopy experiments (78, 82, 150). Larger fluorescent foci, which have been termed assemblons, were not detected in any sampled fraction including the bottom-most fraction, #22, where cell debris might accumulate (fig 6.2).

Live-cell microscopic analysis of GFP-U_L35 infection indicates different phases of capsid movement during the course of infection:

Initial experiments to characterize intranuclear movement of capsids revealed multiple phases of capsid dynamics upon infection. Specifically, most cells assayed prior to 8 hours post infection showed diffuse, hazy GFP staining without obvious single bright foci. Subsequent to this, and starting around 9 hours post-infection, bright foci could be distinguished within the infected cell nucleus. These foci moved very rapidly in a seemingly random pattern (fig. 6.3). Measuring the rate of movement was hampered by the diffuse signal, high rate of movement, and the fact that individual foci moved in and out of the focal plane very rapidly, precluding tracking of individual foci for significant lengths of travel. By 10 hours post-infection additional larger fluorescent areas because apparent. These were relatively immobile compared to the smaller foci. The large fluorescent areas corresponded in size and position to previously identified assemblons (as shown in movies below Figures 6.4, 6.5, 6.6, 6.7, 6.8 , 6.9) and referred to as assemblons hereafter). The assemblons remained essentially static during observation periods on the order of minutes, and only occasionally merged. Smaller foci

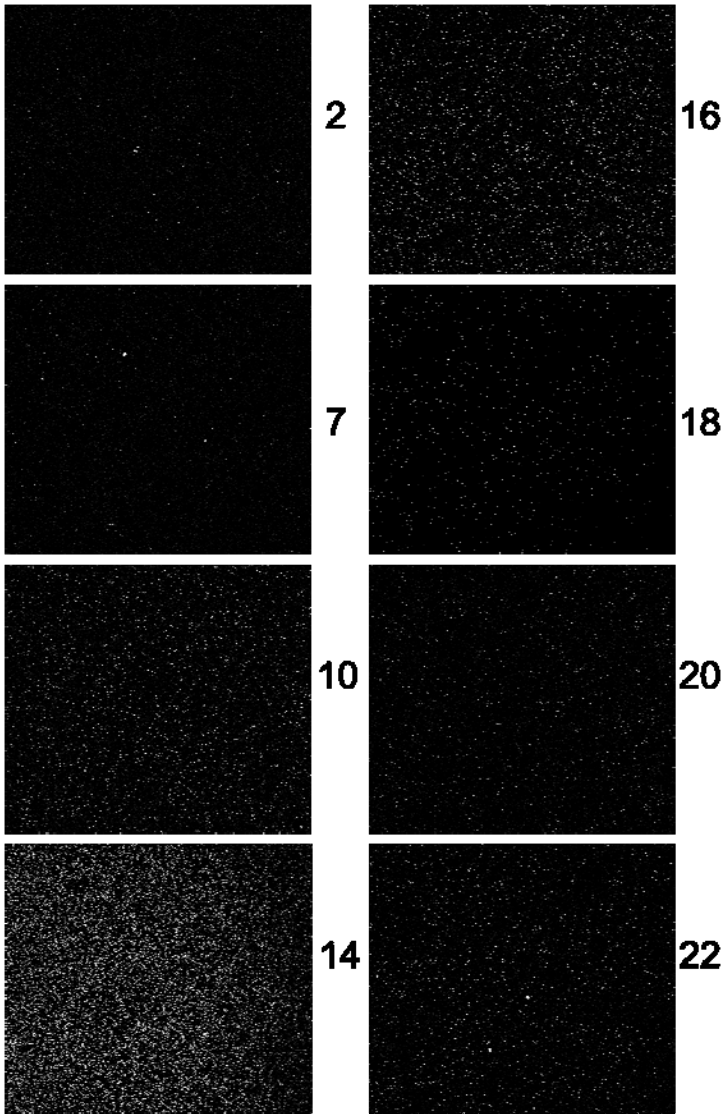

Figure 6.2 Confocal immunofluorescence of purified GFP-VP26 capsids. Numbers along the side represent the gradient fraction from which the sample was taken. Note the uniform size and intensity of particles. Images were captured under 600x magnification.

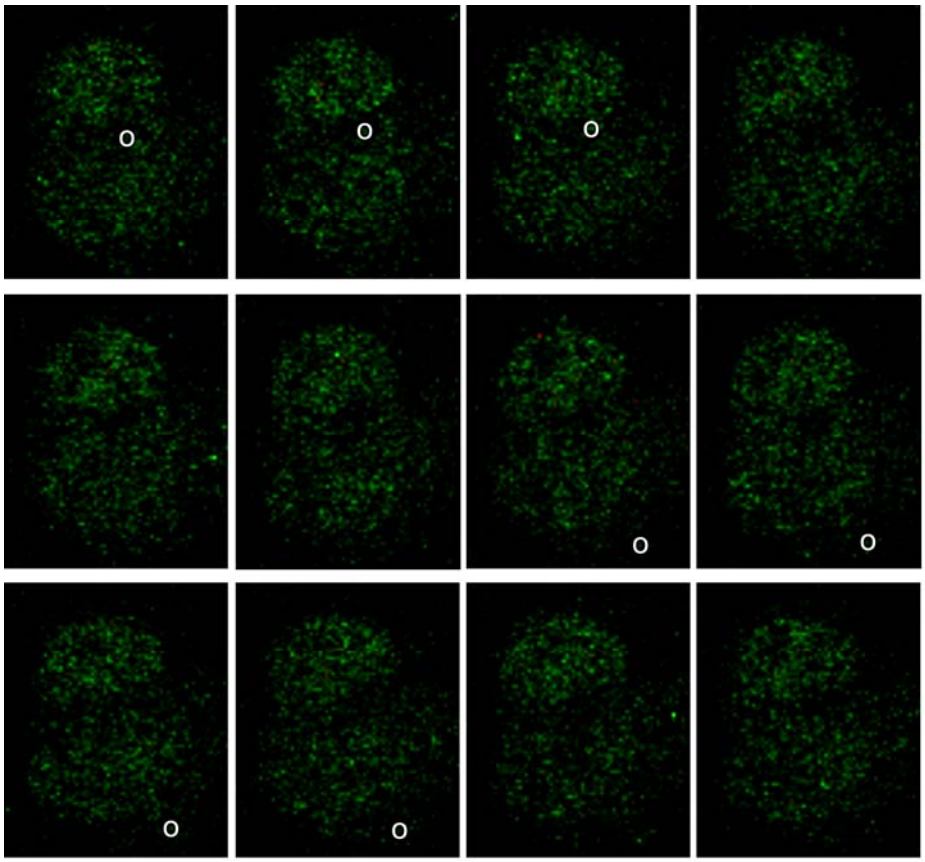

Figure 6.3 Confocal time-lapse microscopy of BAC-derived GFP-VP26 recombinant virus. At earlier times in infection capsids displayed rapid movement in the absence of assemblons. Images were cropped to 3.6771 μm x 4.5057 μm and captured at 0.60 frames/second under 600x magnification. Dynamics were such that only short paths of movement from individual particles could be traced, as indicated by white circles.

indicative of capsids were observed both entering and exiting the assemblon like structures, but entering was observed more frequently. At later times after infection starting at 15 hours, movement of the small foci slowed considerably and became traceable over longer trajectories, with individual capsids moving at rates similar to those reported previously (82). This type of movement was previously shown to be dependent on both energy and intact actin inasmuch as it was inhibited by depletion of ATP and depolymerization of F-actin with latrunculin B (82).

Movement of capsids without DNA cleavage and packaging:

To analyze movement of capsids in the absence of DNA cleavage and packaging, Hep 2 cells were infected with a recombinant virus bearing a deletion in U_L17 and in which U_L35 was replaced with a fused gene encoding GFP-VP26. Similar to observations of wild type capsids tagged with GFP, fluorescent U_L17-null capsids were first observed at 9 hours post infection. Much like wild-type capsids, rapid migration of labeled capsids and virtual stasis of assemblons was observed, thus indicating that, at least with respect to the U_L17 deletion mutant, capsid movement could still occur in the absence of DNA packaging (fig 6.4).

To ensure that DNA packaging proteins other than pU_L17 are not involved in the intranuclear movement of viral particles, we sought to examine the movement of capsids in cells infected with viruses lacking other DNA packaging proteins. To expediently address this issue, a cell line expressing GFP-VP26 was constructed and infected with various mutant and wild type viruses. At 9-10 hours post-infection many assemblons and hundreds of individual capsids were discernable in individual nuclei in all infected cells.

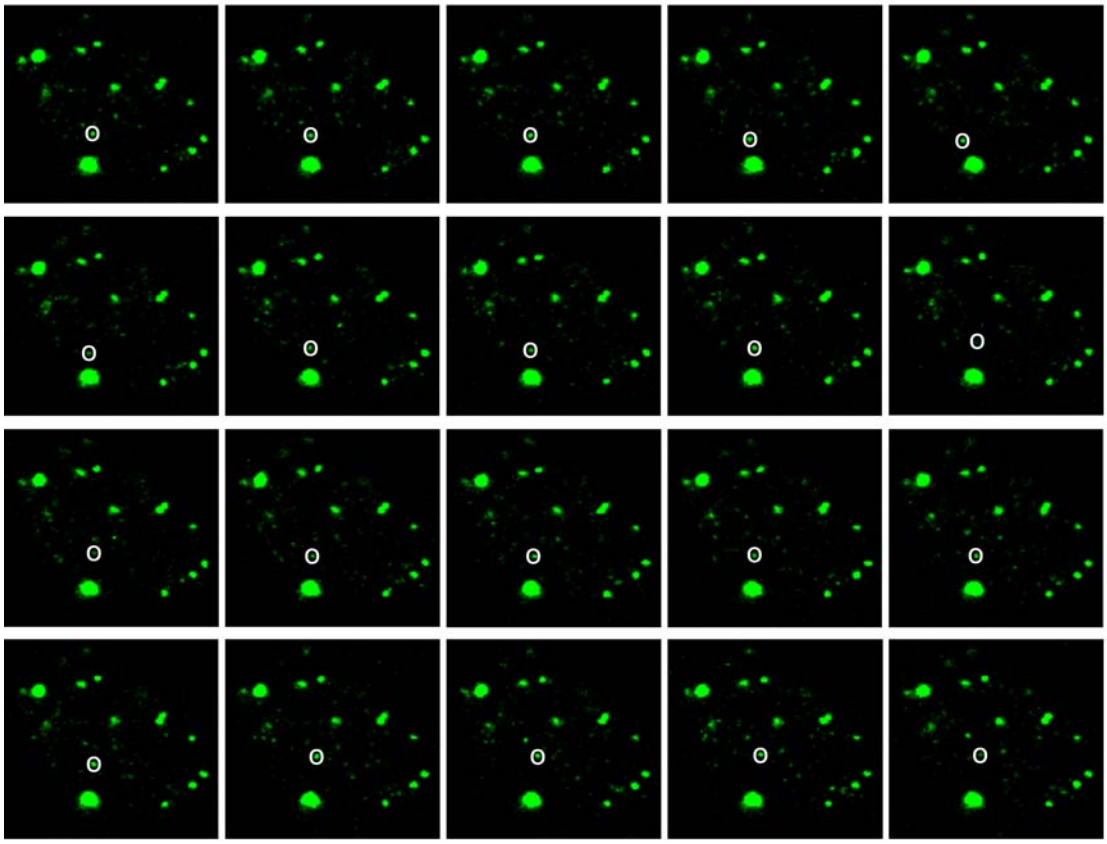

Figure 6.4 Confocal time-lapse microscopy of GFP-VP26 delta 17 infection. Between 9-10 hours post-infection many dynamic capsids were discernable as well as the large assemblons. Images were cropped to 5.3344 μm x 4.9201 μm and captured at 0.50 frames/second under 600x magnification. An individual capsid moving within the focal plane is indicated in circles.

The movement of individual capsids of each virus could be traced and was found to be similar to wild type virus, despite the fact that DNA cleavage and packaging were precluded (Figures 6.5 – 6.10). Intranuclear capsid movement was maintained even in the absence of the U_L15 gene that encodes the ATPase subunit of the terminase, and in capsids that lacked the portal protein pU_L6 (Figures 6.8, 6.7). These observations suggest that capsids move through the nucleus by a mechanism that is completely independent of the individual viral proteins necessary to cleave and package the HSV genome as well as the action of DNA encapsidation mechanism.

In contrast to individual capsid movement, the brightly fluorescent assemblon-like structures were found to be relatively static during the course of both wild-type and DNA packaging-deficient infections. Capsids were observed to migrate towards and enter assemblons (Figure 6.9). However, only rarely were capsids observed leaving assemblons. This suggests assemblons may be inactive depots where capsids accumulate; alternatively, capsids may have exited assemblons in focal planes other than those observed. Only once were two assemblons observed to merge over a longer period of observation of a delta 17 infection (fig. 6.11). When the same cell was assayed two minutes later the assemblons still remained merged. Examination of these bright foci by electron microscopy revealed that only some contained capsids (data not shown), indicating that the aggregates mostly represent accumulation of VP26/GFP.

ATP hydrolysis with purified pU_L17-His:

Although our data clearly show that cleavage and packaging proteins are not needed for capsid movement, we hypothesized that in addition to the

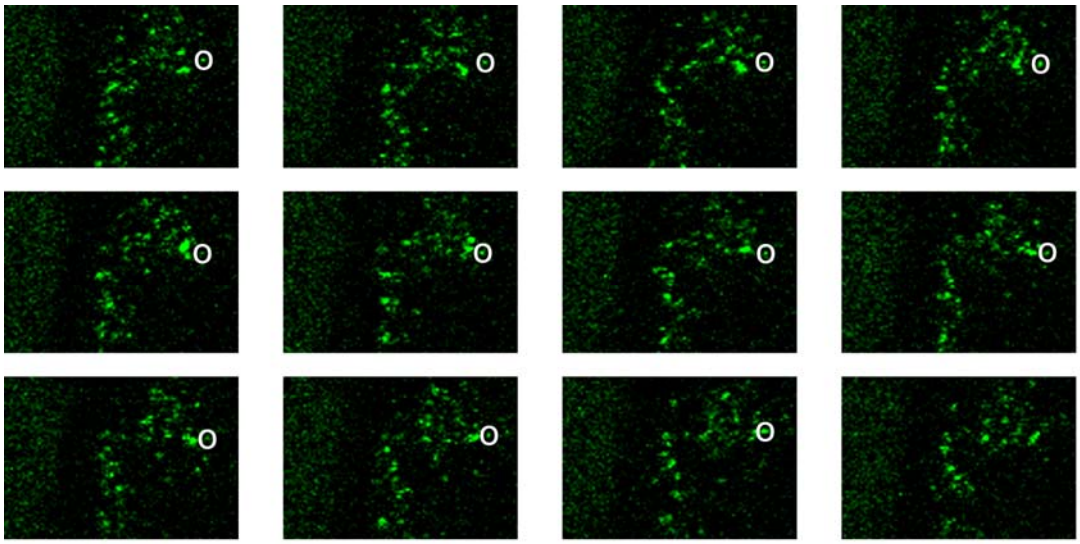

Figure 6.5 Confocal time-lapse microscopy of delta 17 infection in pJB193 cells. Images were cropped to 6.5773 μm x 3.6771 μm and captured at 0.29 frames/second under 600x magnification. An individual capsid moving within the focal plane is indicated in circles.

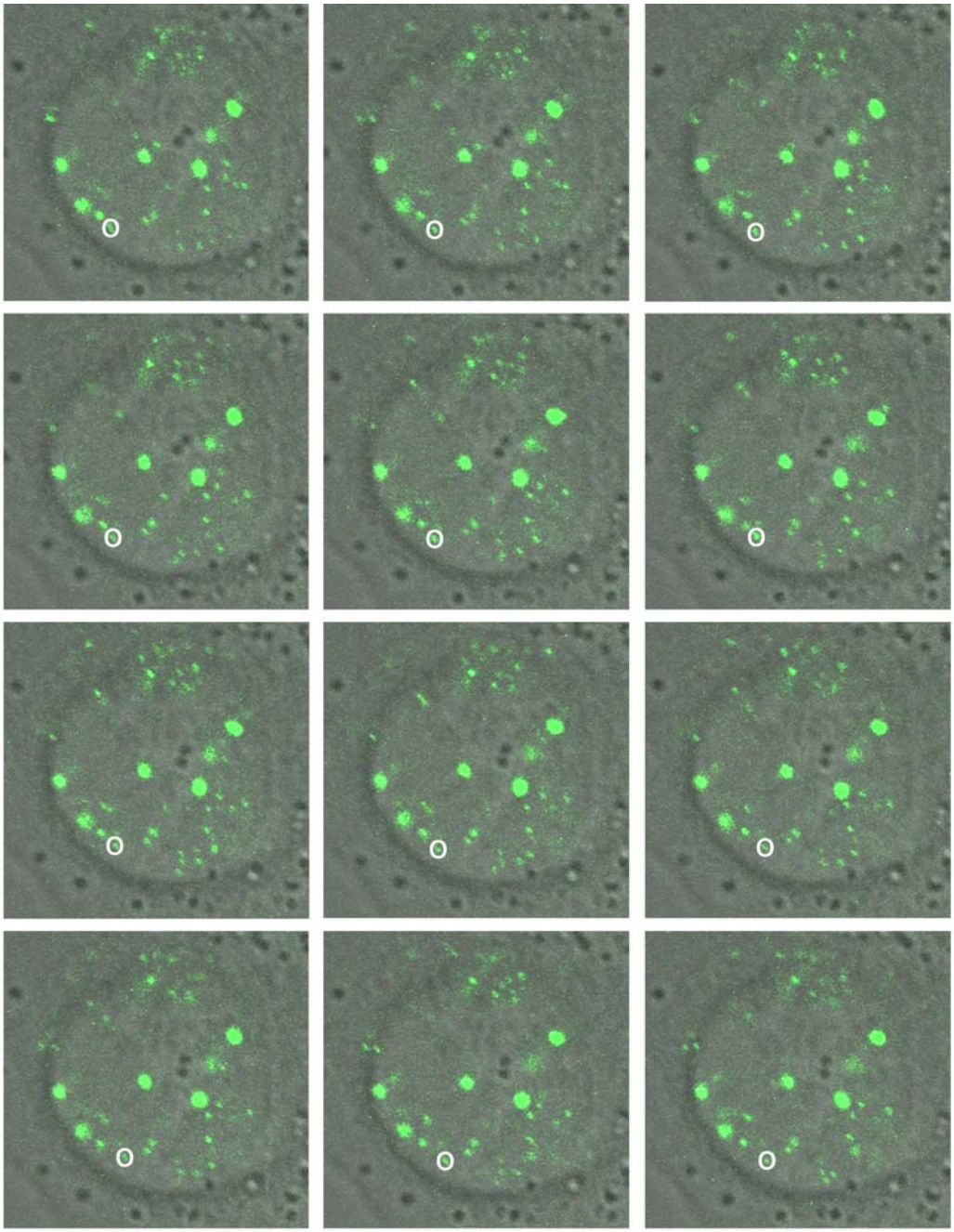

Figure 6.6 Confocal time-lapse microscopy of delta 25 infection in pJB193 cells. Images were cropped to 14.657 μm x 14.242 μm and captured at 0.92 frames/second under 600x magnification. An individual capsid moving within the focal plane is indicated in circles.

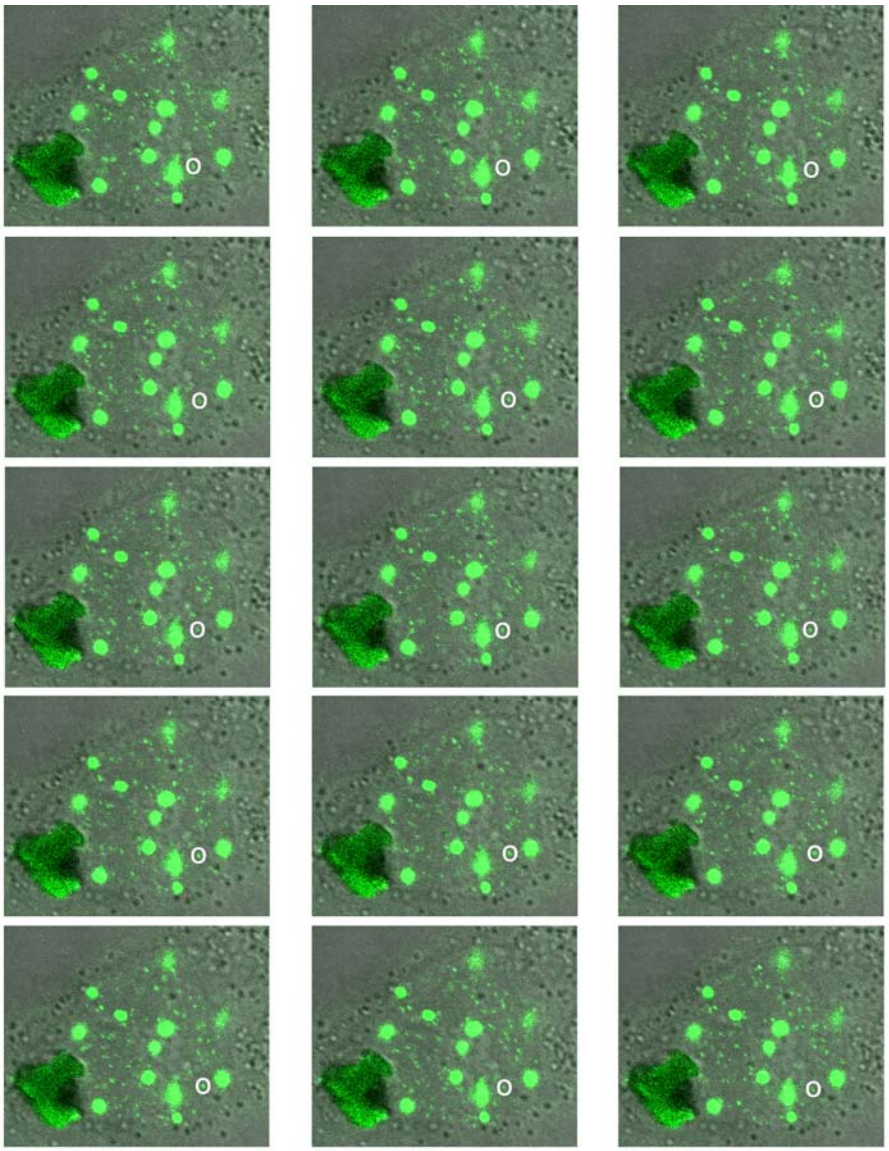

Figure 6.7 Confocal time-lapse microscopy of delta 6 infection in pJB193 cells. Images were cropped to 18.593 μm x 15.485 μm and captured at 0.99 frames/second under 600x magnification. An individual capsid moving within the focal plane is indicated in circles.

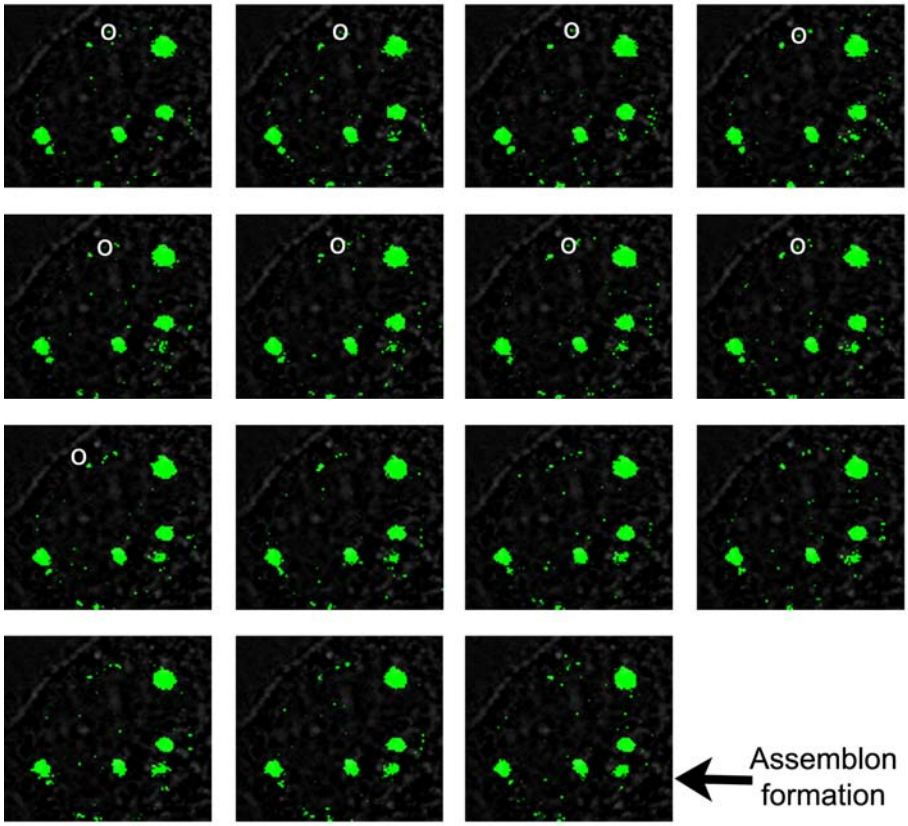

Figure 6.8 Confocal time-lapse microscopy of delta 15 infection in pJB193 cells. Images were cropped to 5.5415 μm x 4.9201 μm and captured at 0.38 frames/second under 600x magnification. An individual capsid moving within the focal plane is indicated in circles. An assemblon which was not detected at the start of the movie was observed to appear within these frames.

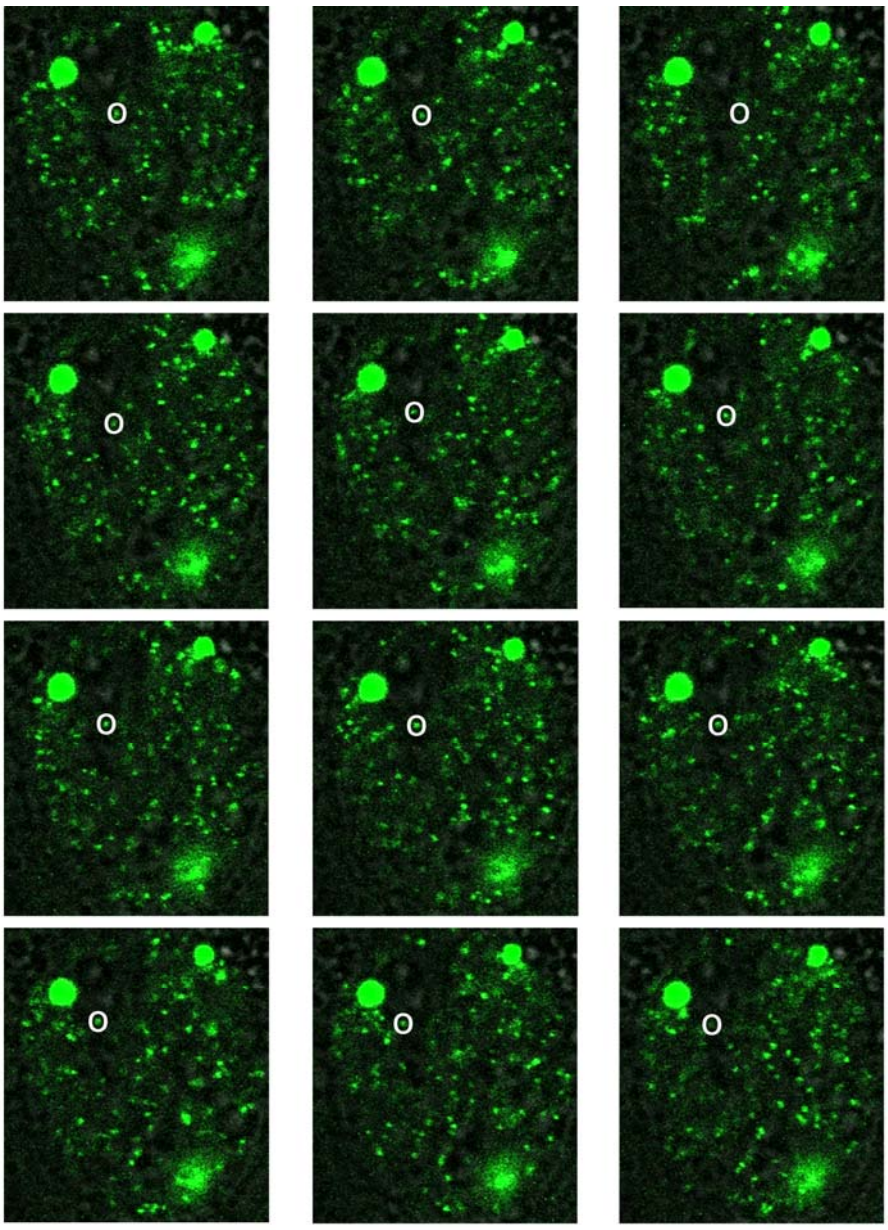

Figure 6.9 Confocal time-lapse microscopy of delta 28 infection in pJB193 cells. Images were cropped to 12.585 μm x 14.035 μm and captured at 0.91 frames/second under 600x magnification. An individual capsid moving within the focal plane is indicated in circles.

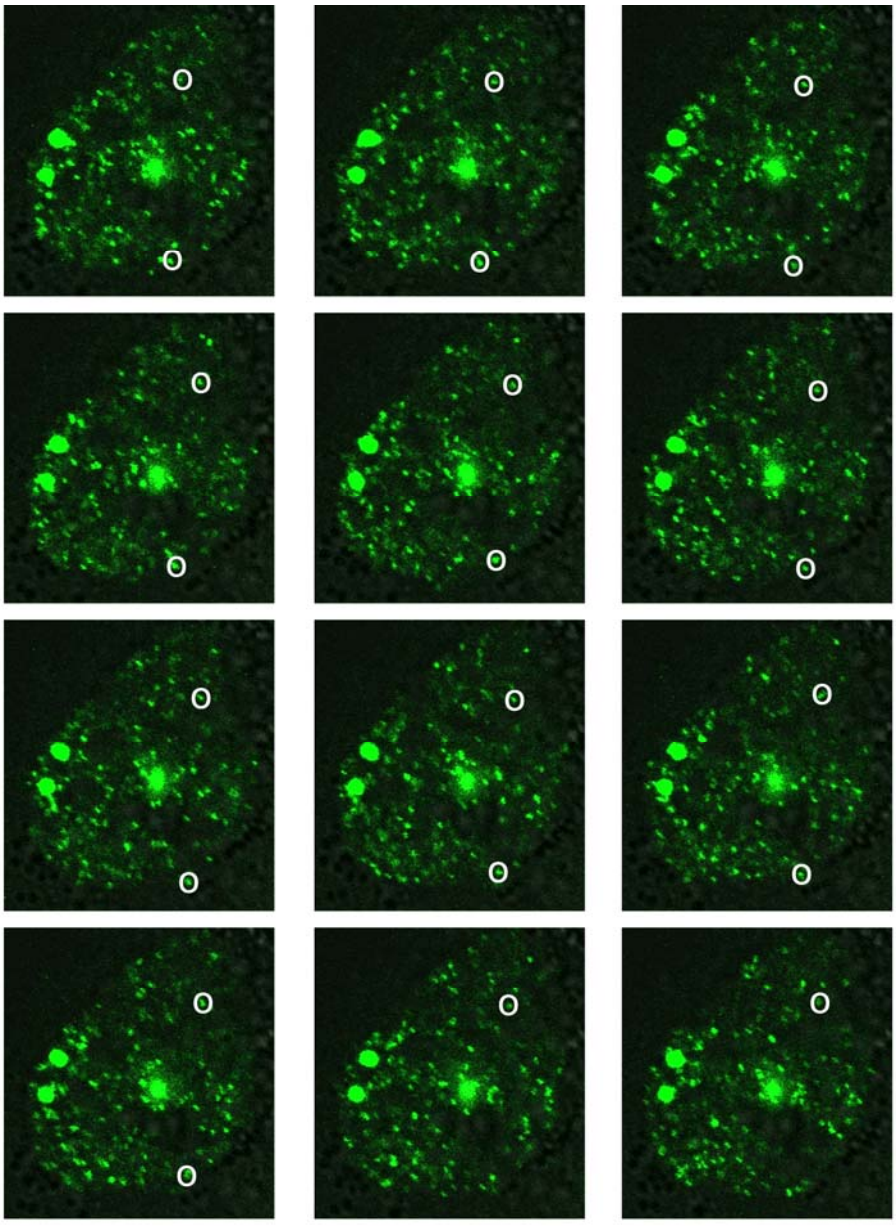

Figure 6.10 Confocal time-lapse microscopy of delta 33 infection in pJB193 cells. Images were cropped to 15.692 μm x 16.935 μm and captured at 1.08 frames/second under 600x magnification. Individual capsids moving within the focal plane are indicated in circles.

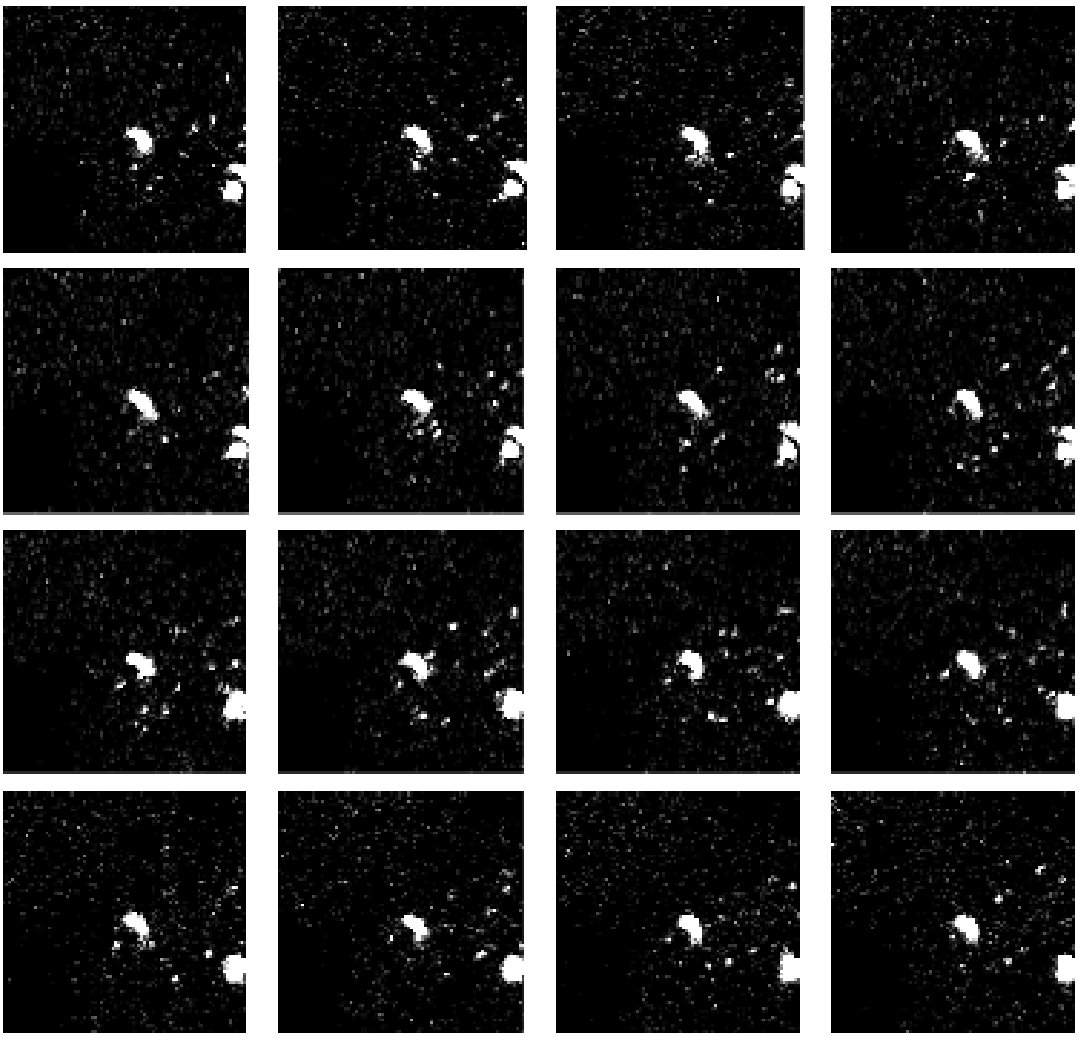

Figure 6.11 Converging assemblons in delta 17 infection of pJB193 cells. Individual time-lapse microscopy frames from delta 17 movie show two assemblons in close proximity that appear to merge (frame 9 of this panel), into one, larger assemblon (lower right corner). The field was cropped to 6.5773 μm x 4.7129 μm and imaged at 0.37 frames/second under 600x magnification.

putative ATPase, pU_L15, other cleavage and packaging proteins may have the ability to hydrolyze ATP which may aid in genomic encapsidation. Specifically, we tested whether or not one of the outer capsid proteins, pU_L17 has the ability to hydrolyze ATP. A recombinant baculovirus was used to express pU_L17 with a C-terminal 6x-(His) tag in SF21 insect cells. Soluble pU_L17-His was purified by affinity chromatography with Ni-NTA beads, eluted in 50mM NaH_2PO_4/300mM NaCl/250mM imidazole (pH 8.0), dialyzed into 50mM NaCl /50 mM NaH_2PO4 and stored briefly at 4^oC before use. Purified protein was mixed with γP^{32}-radiolabeled ATP at modest concentrations, 0.5-1.0 μM, and thin layer chromatography (TLC) was used to separate hydrolyzed free γP^{32} phosphate from γP^{32}-labeled ATP.

Assays comparing pU_L17-containing samples to buffer only controls in the presence or absence of HSV-1(F) BAC DNA indicated hydrolysis was taking place specifically in the presence of pU_L17 and independent of HSV DNA (Figure 6.12). Hydrolysis of ATP was readily apparent in all pU_L17-containing samples. Quantitative analysis of these data was performed using the Storm phosphoimager. The percentage of free phosphate compared to the total radioactivity of the lane ranged from 31.9% - 39.2% in lanes 3, 4, 7 and 8. Quantization of negative samples (buffer only and buffer + DNA) ranged from 3.8% - 5.9%.

Having established that pU_L17-containing samples were capable of hydrolyzing ATP, we next wanted to show that this activity was specific to pU_L17. To specifically block the hydrolysis of ATP we employed two antibodies that recognize purified pU_L17-His, a commercial monoclonal anti-penta His antibody (Qiagen) and a polyclonal chicken anti-pU_L17-His (Figure 6.13). The assay was performed with 500 nM pU_L17 as it proved sufficient for

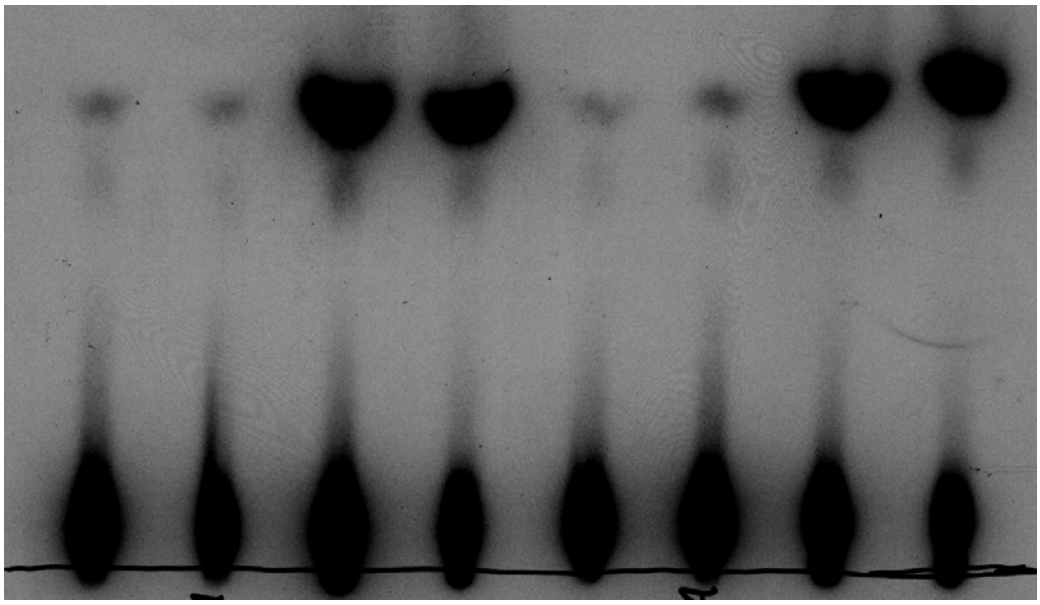

1 2 3 4 5 6 7 8

Figure 6.12 ATPase assay of purified pU_L17-(His). The drawn line indicates the point of origin before TLC separation was applied. Lower migrating species are indicative of γP^{32} labeled ATP whereas the upper species represents free phosphate. Lanes 1-4 are as follows, (1) buffer only, (2) buffer + HSV BAC DNA, (3) buffer + 500 nM purified pU_L17, (4) buffer + 500 nM purified pU_L17 + HSV BAC DNA. Lanes 5-8 repeat these samples, only pU_L17 was added at 1.0 μM where applicable.

hydrolysis in preceding experiments. The result of this assay was that neither antibody was capable of inhibiting ATP hydrolysis of pU_L17; ATP hydrolysis occurred in all pU_L17-containing samples.

There are a number of reasons why the inclusion of antibody did not preclude ATP-hydrolysis. It is not surprising that the anti-His antibody did not inhibit ATPase activity because it is a monoclonal antibody and thus directed at only a single epitope of the pU_L17 protein. In addition, the effective concentration of anti-His used was nearly 50-fold less than the anti-pU_L17 antibody. Thus, it is possible that either an insufficient amount was added, or more likely that the His epitope is distinct from any putative ATPase domain on pU_L17.

The anti-pU_L17 chicken polyclonal antibody was also incapable of inhibiting ATPase activity in pU_L17-containing samples. Since (i) ample antibody (>10 ug) was added to the pU_L17 + anti-pU_L17 Ab reaction and (ii) this antibody has the potential to bind multiple epitopes on pU_L17, the lack of an effect with its addition was unexpected. Therefore, we must address the possibility that this hydrolytic function may be coming from another contaminating protein in our purification of pU_L17.

To address the issue of protein purity we processed uninfected SF21 cells and cells infected with another baculovirus expressing an unrelated His-tagged protein (Stu2) with no known ATPase activity (a kind gift from T. Huffaker) in parallel with pU_L17-His . Elutions of Stu2 yielded 3- fold lower protein concentrations than that of pU_L17. ATPase assays were then performed with 500 nM concentrations of pU_L17-His and Stu2-His. No concentration could be assigned for the proteins binding non-specifically to the

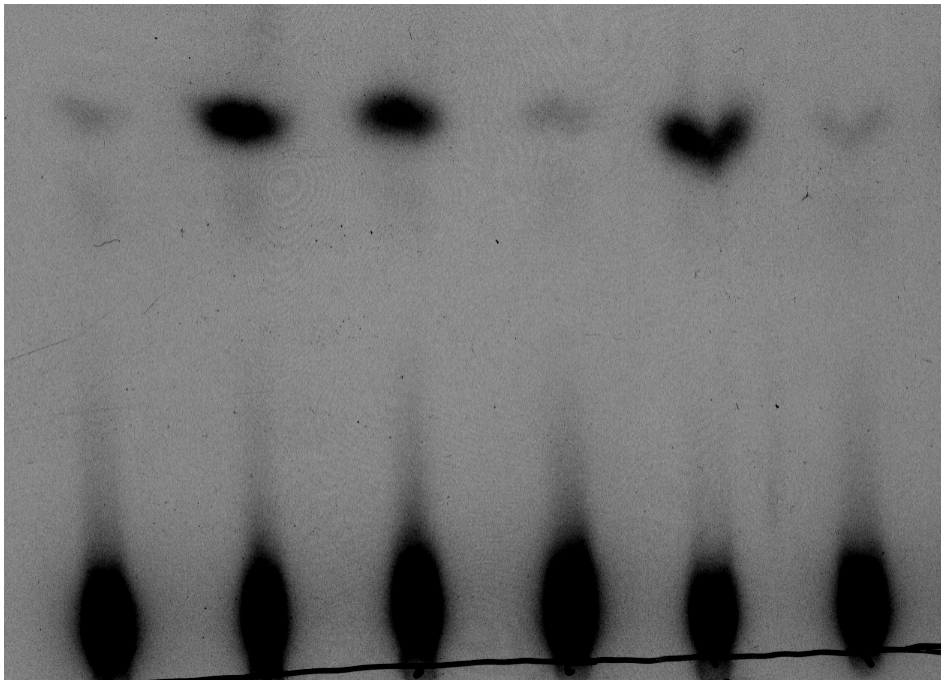

1 2 3 4 5 6

Figure 6.13 ATP hydrolysis in the presence of pU_L17-His antibodies. Lanes are as follows: buffer only (1), pU_L17 (2), pU_L17 + α-His Ab (3), α-His Ab (4), pU_L17 + α-pU_L17 Ab (5), α-pU_L17 Ab (6). Hydrolysis of ATP is not inhibited by either antibody; instead, hydrolysis is observed in all pU_L17-containing samples.

Ni-NTA matrix from the uninfected sample, so to be conservative we used the same volume of uninfected “purification” elution as was used for the less concentrated Stu2-His protein. The results are shown in Figure 6.14.

As previously shown, pU_L17-His hydrolyzed ATP; however, levels of ATPase activity in both Stu2-His and uninfected purification samples exceeded that of pU_L17. Although it is likely that the pU_L17-His extraction contains a contaminating protein with ATPase activity, this may not account for all activity observed. Due to the lower concentration of Stu2-His recovered from purification, 3-4 fold larger volume of both Stu2-His and proteins eluted from uninfected-cell lysate was added compared to that of pU_L17-His. The intensities of free phosphate species in Stu2-His and uninfected samples do not appear to have a 3-4-fold increase over hydrolyzed phosphate in the pU_L17-His, which suggests pU_L17-His maybe be contributing to the ATPase activity observed.

Discussion:

The HSV DNA packaging motor must be powerful enough to overcome charge effects as it packages viral DNA into the capsid at near liquid crystalline density. In order for the genome to be inserted, either the DNA moves into a relatively stationary capsid, the capsid moves along fixed DNA, or both relationships occur at different stages. Since intranuclear capsid dynamics had already been observed, we chose to address the hypothesis that these capsid dynamics were linked to DNA encapsidation. We found that precluding DNA cleavage and packaging did not stop the motility of capsids, indicating that the movement of capsids does not reflect activity of the DNA packaging reaction. Additionally, none of the essential encapsidation

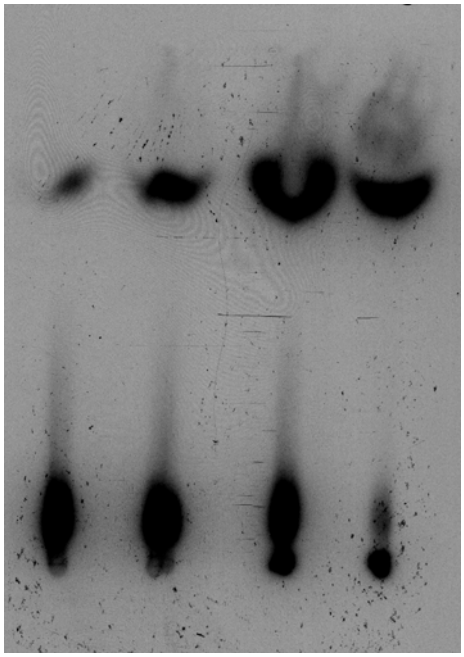

1 2 3 4

Figure 6.14 ATP hydrolysis with pU_L17-His, Stu-2, and non-specific purified proteins. Lanes are as follows: buffer only (1), pU_L17-His (2), Stu2-His (3), “uninfected” (non-specific binding proteins) (4).

proteins tested, including the ATPase-containing terminase complex, was individually required for capsid movement.

In our assays in both wild-type and mutant-infected cells, assemblons were readily observed. These large aggregates were nearly static during the course of infection. Rarely, perceptible but slow movement of these structures was observed. Due to their intensity which precluded detection of labeled capsids within them, no conclusions could be made about the dynamics of capsids within these structures.

The role of assemblons in viral assembly is controversial (132, 266). The relatively uncommon detection of capsids within these structures indicates that they mostly represent deposition of GFP-VP26, rather than capsids, a conclusion consistent with the notion that DNA packaging occurs elsewhere in the nucleus.

We extended our investigation of the mechanisms underlying cleavage and packaging by assaying for energy production from pU_L17, a minor capsid protein that is essential for cleavage and packaging. Purified pU_L17 samples were consistently able to hydrolyze the third phosphate of ATP into free phosphate in γP^{32} ATPase assays. This function was shown to be independent of HSV DNA. However, a monoclonal and polyclonal antibody against the His tag and pU_L17-His, respectively, were unable to preclude the reaction, and non-specifically purified proteins were also shown to have the same activity. Thus, pU_L17 may function as an ATPase but the possibility that a contaminating protein in the purification is responsible for the hydrolysis of ATP has not been eliminated.

CHAPTER VII:

CONCLUSION

Implications and Future Studies:

In probing for protein interactions this work establishes pU_L17's relationship to both capsid and tegument proteins. The first clues to a structural role for pU_L17 were revealed by immunoelectron microscopy studies presented in Chapter II which suggested that pU_L17 lies on the external face of the capsid. To address this question, a high-affinity anti-pU_L17 serum was generated which has proved to be invaluable to further studies.

More precise capsid interactions between pU_L17 and pU_L25, which form a heterodimeric complex, were discussed in Chapter III. Immunoprecipitation assays suggest that these two proteins dimerize even in the absence of capsids. Additionally, each protein requires its partner for proper distribution in infected cells. Our results also suggest that pU_L25 and pU_L17 may undergo a conformational change independent of other capsid proteins.

Many avenues of novel investigation of the pU_L17/pU_L25 heterodimer are opening Future studies involving monoclonal antibodies or structure determination may pin-point the exact physical changes in these proteins, the timing of these conformational changes, and any functional implications. Although this complex is essential for DNA packaging, it is unclear if pU_L17/pU_L25 play only a structural role in preparing or in stabilizing capsid conformation, or if they are active participants in the encapsidation process.

Recent studies are beginning to investigate the role this heterodimer plays in acquisition of tegument . It also remains to be seen if the heterodimer may also be important in selection of C capsids for primary envelopment.

The observations described here also suggest that pU_L17 makes contact with tegument proteins, specifically VP11/12 and VP13/14, to bridge the capsid and tegument layers. Chapter IV investigates the requirements for the interaction of pU_L17 and VP13/14. Although pU_L17 is not necessary for localization of VP13/14, the two proteins were observed to co-localize in the cytoplasm when in the presence of VP11/12. The question remains whether these cytoplasmic aggregates represent tegumentation sites, or are artifacts of enhanced protein expression.

In addition to establishing a structural role for pU_L17, this work investigates potential functional roles pU_L17 may play. We clearly demonstrated that pU_L17, along with other cleavage and packaging proteins, was not responsible for intranuclear capsid movement. However, other functional assays, such as DNA-binding and ATP hydrolysis show indications of pU_L17 activity in preliminary experiments. To perform these *in vitro* assays, a baculovirus expressing pU_L17-His was engineered. Upon infection of insect cells pU_L17 was highly expressed and soluble protein was readily purified, a tool that no doubt will prove beneficial in subsequent functional assays. As Chapter V illustrates pU_L17 may posses the ability to hydrolyze ATP, although more stringent purification perhaps through TAP will be necessary before this can be concluded. In electrophoretic mobility-shift assays, purified pU_L17 also showed potential to bind both single and double-stranded DNA in a concentration dependent manner. Difficulties in resolving a discrete migrating species most likely indicate that pU_L17 has multiple binding sites on DNA.

Further studies will be needed to determine if the 6x-Histidine tag allows electrostatic interactions with DNA or if pU_L17 binds DNA independently of the epitope tag. Also, chromatin immunoprecipitation assays may prove useful as a survey to find if pU_L17 binds specifically to a region of the HSV genome.

To conclude, although no precise functional role for pU_L17 was determined, these investigations have illuminated specific associations between pU_L17 and capsid structure, tegumentation, and intranuclear capsid transport.

REFERENCES

1. **Abbotts, A. P., V. G. Preston, M. Hughes, A. H. Patel, and N. D. Stow.** 2000. Interaction of the herpes simplex virus type 1 packaging protein UL15 with full-length and deleted forms of the UL28 protein. J Gen Virol **81:**2999-3009.
2. **Adelman, K., B. Salmon, and J. D. Baines.** 2001. Herpes simplex virus DNA packaging sequences adopt novel structures that are specifically recognized by a component of the cleavage and packaging machinery. Proc Natl Acad Sci U S A **98:**3086-91.
3. **al-Kobaisi, M. F., F. J. Rixon, I. McDougall, and V. G. Preston.** 1991. The herpes simplex virus UL33 gene product is required for the assembly of full capsids. Virology **180:**380-8.
4. **Alam, T. I., B. Draper, K. Kondabagil, F. J. Rentas, M. Ghosh-Kumar, S. Sun, M. G. Rossmann, and V. B. Rao.** 2008. The headful packaging nuclease of bacteriophage T4. Mol Microbiol **69:**1180-90.
5. **Alam, T. I., and V. B. Rao.** 2008. The ATPase domain of the large terminase protein, gp17, from bacteriophage T4 binds DNA: implications to the DNA packaging mechanism. J Mol Biol **376:**1272-81.
6. **Amici, C., A. Rossi, A. Costanzo, S. Ciafre, B. Marinari, M. Balsamo, M. Levrero, and M. G. Santoro.** 2006. Herpes simplex virus disrupts NF-kappaB regulation by blocking its recruitment on the IkappaBalpha promoter and directing the factor on viral genes. J Biol Chem **281:**7110-7.
7. **Atanasiu, D., J. C. Whitbeck, T. M. Cairns, B. Reilly, G. H. Cohen, and R. J. Eisenberg.** 2007. Bimolecular complementation reveals that glycoproteins

gB and gH/gL of herpes simplex virus interact with each other during cell fusion. Proc Natl Acad Sci U S A **104:**18718-23.

8. **Baines, J. D., C. Cunningham, D. Nalwanga, and A. Davison.** 1997. The U(L)15 gene of herpes simplex virus type 1 contains within its second exon a novel open reading frame that is translated in frame with the U(L)15 gene product. J Virol **71:**2666-73.
9. **Baines, J. D., C. E. Hsieh, E. Wills, C. Mannella, and M. Marko.** 2007. Electron tomography of nascent herpes simplex virus virions. J Virol **81:**2726-35.
10. **Baines, J. D., A. P. Poon, J. Rovnak, and B. Roizman.** 1994. The herpes simplex virus 1 UL15 gene encodes two proteins and is required for cleavage of genomic viral DNA. J Virol **68:**8118-24.
11. **Baines, J. D., and B. Roizman.** 1991. The open reading frames UL3, UL4, UL10, and UL16 are dispensable for the replication of herpes simplex virus 1 in cell culture. J Virol **65:**938-44.
12. **Baines, J. D., and B. Roizman.** 1992. The UL11 gene of herpes simplex virus 1 encodes a function that facilitates nucleocapsid envelopment and egress from cells. J Virol **66:**5168-74.
13. **Barker, D. E., and B. Roizman.** 1990. Identification of three genes nonessential for growth in cell culture near the right terminus of the unique sequences of long component of herpes simplex virus 1. Virology **177:**684-91.
14. **Batterson, W., D. Furlong, and B. Roizman.** 1983. Molecular genetics of herpes simplex virus. VIII. further characterization of a temperature-sensitive mutant defective in release of viral DNA and in other stages of the viral reproductive cycle. J Virol **45:**397-407.

15. **Batterson, W., and B. Roizman.** 1983. Characterization of the herpes simplex virion-associated factor responsible for the induction of alpha genes. J Virol **46:**371-7.

16. **Baumann, R. G., J. Mullaney, and L. W. Black.** 2006. Portal fusion protein constraints on function in DNA packaging of bacteriophage T4. Mol Microbiol **61:**16-32.

17. **Beard, P. M., and J. D. Baines.** 2004. The DNA cleavage and packaging protein encoded by the UL33 gene of herpes simplex virus 1 associates with capsids. Virology **324:**475-82.

18. **Beard, P. M., C. Duffy, and J. D. Baines.** 2004. Quantification of the DNA cleavage and packaging proteins U(L)15 and U(L)28 in A and B capsids of herpes simplex virus type 1. J Virol **78:**1367-74.

19. **Beard, P. M., N. S. Taus, and J. D. Baines.** 2002. DNA cleavage and packaging proteins encoded by genes U(L)28, U(L)15, and U(L)33 of herpes simplex virus type 1 form a complex in infected cells. J Virol **76:**4785-91.

20. **Bender, F. C., J. C. Whitbeck, H. Lou, G. H. Cohen, and R. J. Eisenberg.** 2005. Herpes simplex virus glycoprotein B binds to cell surfaces independently of heparan sulfate and blocks virus entry. J Virol **79:**11588-97.

21. **Bender, F. C., J. C. Whitbeck, M. Ponce de Leon, H. Lou, R. J. Eisenberg, and G. H. Cohen.** 2003. Specific association of glycoprotein B with lipid rafts during herpes simplex virus entry. J Virol **77:**9542-52.

22. **Bhattacharyya, S. P., and V. B. Rao.** 1993. A novel terminase activity associated with the DNA packaging protein gp17 of bacteriophage T4. Virology **196:**34-44.

23. **Bjerke, S. L., and R. J. Roller.** 2006. Roles for herpes simplex virus type 1 UL34 and US3 proteins in disrupting the nuclear lamina during herpes simplex virus type 1 egress. Virology **347:**261-76.

24. **Boehmer, P. E., and I. R. Lehman.** 1997. Herpes simplex virus DNA replication. Annu Rev Biochem **66:**347-84.

25. **Bowman, B. R., M. L. Baker, F. J. Rixon, W. Chiu, and F. A. Quiocho.** 2003. Structure of the herpesvirus major capsid protein. EMBO J **22:**757-65.

26. **Browne, H., S. Bell, and T. Minson.** 2004. Analysis of the requirement for glycoprotein m in herpes simplex virus type 1 morphogenesis. J Virol **78:**1039-41.

27. **Bucks, M. A., K. J. O'Regan, M. A. Murphy, J. W. Wills, and R. J. Courtney.** 2007. Herpes simplex virus type 1 tegument proteins VP1/2 and UL37 are associated with intranuclear capsids. Virology **361:**316-24.

28. **Bullough, P. A., F. M. Hughson, J. J. Skehel, and D. C. Wiley.** 1994. Structure of influenza haemagglutinin at the pH of membrane fusion. Nature **371:**37-43.

29. **Cai, W. Z., S. Person, S. C. Warner, J. H. Zhou, and N. A. DeLuca.** 1987. Linker-insertion nonsense and restriction-site deletion mutations of the gB glycoprotein gene of herpes simplex virus type 1. J Virol **61:**714-21.

30. **Campadelli-Fiume, G., M. Amasio, E. Avitabile, A. Cerretani, C. Forghieri, T. Gianni, and L. Menotti.** 2007. The multipartite system that mediates entry of herpes simplex virus into the cell. Rev Med Virol **17:**313-26.

31. **Campbell, S. M., S. M. Crowe, and J. Mak.** 2001. Lipid rafts and HIV-1: from viral entry to assembly of progeny virions. J Clin Virol **22:**217-27.

32. **Cardone, G., D. C. Winkler, B. L. Trus, N. Cheng, J. E. Heuser, W. W. Newcomb, J. C. Brown, and A. C. Steven.** 2007. Visualization of the herpes

simplex virus portal in situ by cryo-electron tomography. Virology **361:**426-34.

33. **Carfi, A., S. H. Willis, J. C. Whitbeck, C. Krummenacher, G. H. Cohen, R. J. Eisenberg, and D. C. Wiley.** 2001. Herpes simplex virus glycoprotein D bound to the human receptor HveA. Mol Cell **8:**169-79.
34. **Casjens, S., and M. Hayden.** 1988. Analysis in vivo of the bacteriophage P22 headful nuclease. J Mol Biol **199:**467-74.
35. **Casjens, S., L. Sampson, S. Randall, K. Eppler, H. Wu, J. B. Petri, and H. Schmieger.** 1992. Molecular genetic analysis of bacteriophage P22 gene 3 product, a protein involved in the initiation of headful DNA packaging. J Mol Biol **227:**1086-99.
36. **Catalano, C. E., D. Cue, and M. Feiss.** 1995. Virus DNA packaging: the strategy used by phage lambda. Mol Microbiol **16:**1075-86.
37. **Chalfie, M.** 1995. Green fluorescent protein. Photochem Photobiol **62:**651-6.
38. **Chalfie, M., Y. Tu, G. Euskirchen, W. W. Ward, and D. C. Prasher.** 1994. Green fluorescent protein as a marker for gene expression. Science **263:**802-5.
39. **Chang, Y. E., A. P. Poon, and B. Roizman.** 1996. Properties of the protein encoded by the UL32 open reading frame of herpes simplex virus 1. J Virol **70:**3938-46.
40. **Chang, Y. E., and B. Roizman.** 1993. The product of the UL31 gene of herpes simplex virus 1 is a nuclear phosphoprotein which partitions with the nuclear matrix. J Virol **67:**6348-56.
41. **Chang, Y. E., C. Van Sant, P. W. Krug, A. E. Sears, and B. Roizman.** 1997. The null mutant of the U(L)31 gene of herpes simplex virus 1: construction and phenotype in infected cells. J Virol **71:**8307-15.

42. **Chen, D. H., J. Jakana, D. McNab, J. Mitchell, Z. H. Zhou, M. Dougherty, W. Chiu, and F. J. Rixon.** 2001. The pattern of tegument-capsid interaction in the herpes simplex virus type 1 virion is not influenced by the small hexon-associated protein VP26. J Virol **75:**11863-7.

43. **Cheshenko, N., and B. C. Herold.** 2002. Glycoprotein B plays a predominant role in mediating herpes simplex virus type 2 attachment and is required for entry and cell-to-cell spread. J Gen Virol **83:**2247-55.

44. **Chi, J. H., C. A. Harley, A. Mukhopadhyay, and D. W. Wilson.** 2005. The cytoplasmic tail of herpes simplex virus envelope glycoprotein D binds to the tegument protein VP22 and to capsids. J Gen Virol **86:**253-61.

45. **Chi, J. H., and D. W. Wilson.** 2000. ATP-Dependent localization of the herpes simplex virus capsid protein VP26 to sites of procapsid maturation. J Virol **74:**1468-76.

46. **Cines, D. B., A. P. Lyss, M. Bina, R. Corkey, N. A. Kefalides, and H. M. Friedman.** 1982. Fc and C3 receptors induced by herpes simplex virus on cultured human endothelial cells. J Clin Invest **69:**123-8.

47. **Cockrell, S. K., M. E. Sanchez, A. Erazo, and F. L. Homa.** 2009. Role of the UL25 protein in herpes simplex virus DNA encapsidation. J Virol **83:**47-57.

48. **Cohen, G. H., M. Ponce de Leon, H. Diggelmann, W. C. Lawrence, S. K. Vernon, and R. J. Eisenberg.** 1980. Structural analysis of the capsid polypeptides of herpes simplex virus types 1 and 2. J Virol **34:**521-31.

49. **Coller, K. E., J. I. Lee, A. Ueda, and G. A. Smith.** 2007. The capsid and tegument of the alphaherpesviruses are linked by an interaction between the UL25 and VP1/2 proteins. J Virol **81:**11790-7.

50. **Connolly, S. A., D. J. Landsburg, A. Carfi, J. C. Whitbeck, Y. Zuo, D. C. Wiley, G. H. Cohen, and R. J. Eisenberg.** 2005. Potential nectin-1 binding site on herpes simplex virus glycoprotein d. J Virol **79:**1282-95.

51. **Connolly, S. A., J. J. Whitbeck, A. H. Rux, C. Krummenacher, S. van Drunen Littel-van den Hurk, G. H. Cohen, and R. J. Eisenberg.** 2001. Glycoprotein D homologs in herpes simplex virus type 1, pseudorabies virus, and bovine herpes virus type 1 bind directly to human HveC(nectin-1) with different affinities. Virology **280:**7-18.

52. **Cross, T., G. Griffiths, E. Deacon, R. Sallis, M. Gough, D. Watters, and J. M. Lord.** 2000. PKC-delta is an apoptotic lamin kinase. Oncogene **19:**2331-7.

53. **Cunningham, C., and A. J. Davison.** 1993. A cosmid-based system for constructing mutants of herpes simplex virus type 1. Virology **197:**116-24.

54. **Davison, A. J.** 1992. Channel catfish virus: a new type of herpesvirus. Virology **186:**9-14.

55. **Davison, M. D., F. J. Rixon, and A. J. Davison.** 1992. Identification of genes encoding two capsid proteins (VP24 and VP26) of herpes simplex virus type 1. J Gen Virol **73 (Pt 10):**2709-13.

56. **de Bruyn Kops, A., and D. M. Knipe.** 1988. Formation of DNA replication structures in herpes virus-infected cells requires a viral DNA binding protein. Cell **55:**857-68.

57. **de Bruyn Kops, A., S. L. Uprichard, M. Chen, and D. M. Knipe.** 1998. Comparison of the intranuclear distributions of herpes simplex virus proteins involved in various viral functions. Virology **252:**162-78.

58. **de Oliveira, A. P., D. L. Glauser, A. S. Laimbacher, R. Strasser, E. M. Schraner, P. Wild, U. Ziegler, X. O. Breakefield, M. Ackermann, and C.**

Fraefel. 2008. Live visualization of herpes simplex virus type 1 compartment dynamics. J Virol **82:**4974-90.

59. **Deckman, I. C., M. Hagen, and P. J. McCann, 3rd.** 1992. Herpes simplex virus type 1 protease expressed in Escherichia coli exhibits autoprocessing and specific cleavage of the ICP35 assembly protein. J Virol **66:**7362-7.

60. **Deiss, L. P., and N. Frenkel.** 1986. Herpes simplex virus amplicon: cleavage of concatemeric DNA is linked to packaging and involves amplification of the terminally reiterated a sequence. J Virol **57:**933-41.

61. **del Rio, T., C. J. DeCoste, and L. W. Enquist.** 2005. Actin is a component of the compensation mechanism in pseudorabies virus virions lacking the major tegument protein VP22. J Virol **79:**8614-9.

62. **Desai, P., N. A. DeLuca, J. C. Glorioso, and S. Person.** 1993. Mutations in herpes simplex virus type 1 genes encoding VP5 and VP23 abrogate capsid formation and cleavage of replicated DNA. J Virol **67:**1357-64.

63. **Desai, P., and S. Person.** 1998. Incorporation of the green fluorescent protein into the herpes simplex virus type 1 capsid. J Virol **72:**7563-8.

64. **Desai, P., G. L. Sexton, E. Huang, and S. Person.** 2008. Localization of herpes simplex virus type 1 UL37 in the Golgi complex requires UL36 but not capsid structures. J Virol **82:**11354-61.

65. **Desai, P. J.** 2000. A null mutation in the UL36 gene of herpes simplex virus type 1 results in accumulation of unenveloped DNA-filled capsids in the cytoplasm of infected cells. J Virol **74:**11608-18.

66. **Dohner, K., A. Wolfstein, U. Prank, C. Echeverri, D. Dujardin, R. Vallee, and B. Sodeik.** 2002. Function of dynein and dynactin in herpes simplex virus capsid transport. Mol Biol Cell **13:**2795-809.

67. **Dolan, A., M. Arbuckle, and D. J. McGeoch.** 1991. Sequence analysis of the splice junction in the transcript of herpes simplex virus type 1 gene UL15. Virus Res **20:**97-104.

68. **Dolin, R., F. A. Gill, and A. J. Nahmias.** 1975. Genital herpes simplex virus type 1 infection--variability in modes of spread. J Am Vener Dis Assoc **2:**13-6.

69. **Donnelly, M., and G. Elliott.** 2001. Nuclear localization and shuttling of herpes simplex virus tegument protein VP13/14. J Virol **75:**2566-74.

70. **Dorange, F., B. K. Tischer, J. F. Vautherot, and N. Osterrieder.** 2002. Characterization of Marek's disease virus serotype 1 (MDV-1) deletion mutants that lack UL46 to UL49 genes: MDV-1 UL49, encoding VP22, is indispensable for virus growth. J Virol **76:**1959-70.

71. **Duffy, C., E. F. Mbong, and J. D. Baines.** 2009. VP22 of herpes simplex virus 1 promotes protein synthesis at late times in infection and accumulation of a subset of viral mRNAs at early times in infection. J Virol **83:**1009-17.

72. **Ejercito, P. M., E. D. Kieff, and B. Roizman.** 1968. Characterization of herpes simplex virus strains differing in their effects on social behaviour of infected cells. J Gen Virol **2:**357-64.

73. **Elliott, G., G. Mouzakitis, and P. O'Hare.** 1995. VP16 interacts via its activation domain with VP22, a tegument protein of herpes simplex virus, and is relocated to a novel macromolecular assembly in coexpressing cells. J Virol **69:**7932-41.

74. **Elliott, G., and P. O'Hare.** 1998. Herpes simplex virus type 1 tegument protein VP22 induces the stabilization and hyperacetylation of microtubules. J Virol **72:**6448-55.

75. **Elliott, G., and P. O'Hare.** 1997. Intercellular trafficking and protein delivery by a herpesvirus structural protein. Cell **88:**223-33.

76. **Elliott, G., and P. O'Hare.** 1999. Live-cell analysis of a green fluorescent protein-tagged herpes simplex virus infection. J Virol **73:**4110-9.

77. **Ellis, J. A., M. Craxton, J. R. Yates, and J. Kendrick-Jones.** 1998. Aberrant intracellular targeting and cell cycle-dependent phosphorylation of emerin contribute to the Emery-Dreifuss muscular dystrophy phenotype. J Cell Sci **111 (Pt 6):**781-92.

78. **Enquist, L. W., M. J. Tomishima, S. Gross, and G. A. Smith.** 2002. Directional spread of an alpha-herpesvirus in the nervous system. Vet Microbiol **86:**5-16.

79. **Farnsworth, A., T. W. Wisner, and D. C. Johnson.** 2007. Cytoplasmic residues of herpes simplex virus glycoprotein gE required for secondary envelopment and binding of tegument proteins VP22 and UL11 to gE and gD. J Virol **81:**319-31.

80. **Fields, B. N., D. M. Knipe, and P. M. Howley.** 2007. Fields' virology, 5th ed. Wolters Kluwer Health/Lippincott Williams & Wilkins, Philadelphia.

81. **Foisner, R., and L. Gerace.** 1993. Integral membrane proteins of the nuclear envelope interact with lamins and chromosomes, and binding is modulated by mitotic phosphorylation. Cell **73:**1267-79.

82. **Forest, T., S. Barnard, and J. D. Baines.** 2005. Active intranuclear movement of herpesvirus capsids. Nat Cell Biol **7:**429-31.

83. **Franklin, J. L., D. Haseltine, L. Davenport, and G. Mosig.** 1998. The largest (70 kDa) product of the bacteriophage T4 DNA terminase gene 17 binds to single-stranded DNA segments and digests them towards junctions with double-stranded DNA. J Mol Biol **277:**541-57.

84. **Friedman, H. M., G. H. Cohen, R. J. Eisenberg, C. A. Seidel, and D. B. Cines.** 1984. Glycoprotein C of herpes simplex virus 1 acts as a receptor for the C3b complement component on infected cells. Nature **309:**633-5.

85. **Fuchs, W., H. Granzow, B. G. Klupp, M. Kopp, and T. C. Mettenleiter.** 2002. The UL48 tegument protein of pseudorabies virus is critical for intracytoplasmic assembly of infectious virions. J Virol **76:**6729-42.

86. **Fuchs, W., H. Granzow, and T. C. Mettenleiter.** 2003. A pseudorabies virus recombinant simultaneously lacking the major tegument proteins encoded by the UL46, UL47, UL48, and UL49 genes is viable in cultured cells. J Virol **77:**12891-900.

87. **Fuchs, W., B. G. Klupp, H. Granzow, C. Hengartner, A. Brack, A. Mundt, L. W. Enquist, and T. C. Mettenleiter.** 2002. Physical interaction between envelope glycoproteins E and M of pseudorabies virus and the major tegument protein UL49. J Virol **76:**8208-17.

88. **Fuller, A. O., and P. G. Spear.** 1987. Anti-glycoprotein D antibodies that permit adsorption but block infection by herpes simplex virus 1 prevent virion-cell fusion at the cell surface. Proc Natl Acad Sci U S A **84:**5454-8.

89. **Fusco, D., C. Forghieri, and G. Campadelli-Fiume.** 2005. The pro-fusion domain of herpes simplex virus glycoprotein D (gD) interacts with the gD N terminus and is displaced by soluble forms of viral receptors. Proc Natl Acad Sci U S A **102:**9323-8.

90. **Gaffney, D. F., J. McLauchlan, J. L. Whitton, and J. B. Clements.** 1985. A modular system for the assay of transcription regulatory signals: the sequence TAATGARAT is required for herpes simplex virus immediate early gene activation. Nucleic Acids Res **13:**7847-63.

91. **Garner, J. A.** 2003. Herpes simplex virion entry into and intracellular transport within mammalian cells. Adv Drug Deliv Rev **55:**1497-513.

92. **Geraghty, R. J., C. Krummenacher, G. H. Cohen, R. J. Eisenberg, and P. G. Spear.** 1998. Entry of alphaherpesviruses mediated by poliovirus receptor-related protein 1 and poliovirus receptor. Science **280:**1618-20.

93. **Gianni, T., R. Fato, C. Bergamini, G. Lenaz, and G. Campadelli-Fiume.** 2006. Hydrophobic alpha-helices 1 and 2 of herpes simplex virus gH interact with lipids, and their mimetic peptides enhance virus infection and fusion. J Virol **80:**8190-8.

94. **Gianni, T., C. Forghieri, and G. Campadelli-Fiume.** 2006. The herpesvirus glycoproteins B and H.L are sequentially recruited to the receptor-bound gD to effect membrane fusion at virus entry. Proc Natl Acad Sci U S A **103:**14572-7.

95. **Gianni, T., P. L. Martelli, R. Casadio, and G. Campadelli-Fiume.** 2005. The ectodomain of herpes simplex virus glycoprotein H contains a membrane alpha-helix with attributes of an internal fusion peptide, positionally conserved in the herpesviridae family. J Virol **79:**2931-40.

96. **Gianni, T., L. Menotti, and G. Campadelli-Fiume.** 2005. A heptad repeat in herpes simplex virus 1 gH, located downstream of the alpha-helix with attributes of a fusion peptide, is critical for virus entry and fusion. J Virol **79:**7042-9.

97. **Gianni, T., A. Piccoli, C. Bertucci, and G. Campadelli-Fiume.** 2006. Heptad repeat 2 in herpes simplex virus 1 gH interacts with heptad repeat 1 and is critical for virus entry and fusion. J Virol **80:**2216-24.

98. **Gibson, W., and B. Roizman.** 1972. Proteins specified by herpes simplex virus. 8. Characterization and composition of multiple capsid forms of subtypes 1 and 2. J Virol **10:**1044-52.

99. **Goshima, F., D. Watanabe, H. Takakuwa, K. Wada, T. Daikoku, M. Yamada, and Y. Nishiyama.** 2000. Herpes simplex virus UL17 protein is associated with B capsids and colocalizes with ICP35 and VP5 in infected cells. Arch Virol **145:**417-26.

100. **Granzow, H., B. G. Klupp, W. Fuchs, J. Veits, N. Osterrieder, and T. C. Mettenleiter.** 2001. Egress of alphaherpesviruses: comparative ultrastructural study. J Virol **75:**3675-84.

101. **Granzow, H., B. G. Klupp, and T. C. Mettenleiter.** 2005. Entry of pseudorabies virus: an immunogold-labeling study. J Virol **79:**3200-5.

102. **Granzow, H., F. Weiland, A. Jons, B. G. Klupp, A. Karger, and T. C. Mettenleiter.** 1997. Ultrastructural analysis of the replication cycle of pseudorabies virus in cell culture: a reassessment. J Virol **71:**2072-82.

103. **Gross, S. T., C. A. Harley, and D. W. Wilson.** 2003. The cytoplasmic tail of Herpes simplex virus glycoprotein H binds to the tegument protein VP16 in vitro and in vivo. Virology **317:**1-12.

104. **Hampar, B.** 1966. Persistent cyclic herpes simplex virus infection in vitro. 3. Asynchrony in the progression of infection and cell regrowth. J Bacteriol **91:**1965-70.

105. **Hannah, B. P., T. M. Cairns, F. C. Bender, J. C. Whitbeck, H. Lou, R. J. Eisenberg, and G. H. Cohen.** 2009. Herpes simplex virus glycoprotein B associates with target membranes via its fusion loops. J Virol **83:**6825-36.

106. **Heald, R., and F. McKeon.** 1990. Mutations of phosphorylation sites in lamin A that prevent nuclear lamina disassembly in mitosis. Cell **61:**579-89.

107. **Heine, J. W., R. W. Honess, E. Cassai, and B. Roizman.** 1974. Proteins specified by herpes simplex virus. XII. The virion polypeptides of type 1 strains. J Virol **14:**640-51.

108. **Heldwein, E. E., and C. Krummenacher.** 2008. Entry of herpesviruses into mammalian cells. Cell Mol Life Sci **65:**1653-68.

109. **Hendrix, R. W.** 1978. Symmetry mismatch and DNA packaging in large bacteriophages. Proc Natl Acad Sci U S A **75:**4779-83.

110. **Herold, B. C., R. J. Visalli, N. Susmarski, C. R. Brandt, and P. G. Spear.** 1994. Glycoprotein C-independent binding of herpes simplex virus to cells requires cell surface heparan sulphate and glycoprotein B. J Gen Virol **75 (Pt 6):**1211-22.

111. **Herold, B. C., D. WuDunn, N. Soltys, and P. G. Spear.** 1991. Glycoprotein C of herpes simplex virus type 1 plays a principal role in the adsorption of virus to cells and in infectivity. J Virol **65:**1090-8.

112. **Herold, M., and G. Spiteller.** 1996. Enzymatic production of hydroperoxides of unsaturated fatty acids by injury of mammalian cells. Chem Phys Lipids **79:**113-21.

113. **Higgins, R. R., and A. Becker.** 1995. Interaction of terminase, the DNA packaging enzyme of phage lambda, with its cos DNA substrate. J Mol Biol **252:**31-46.

114. **Higgins, R. R., and A. Becker.** 1994. The lambda terminase enzyme measures the point of its endonucleolytic attack 47 +/- 2 bp away from its site of specific DNA binding, the R site. EMBO J **13:**6162-71.

115. **Holaska, J. M., K. L. Wilson, and M. Mansharamani.** 2002. The nuclear envelope, lamins and nuclear assembly. Curr Opin Cell Biol **14:**357-64.

116. **Homa, F. L., and J. C. Brown.** 1997. Capsid assembly and DNA packaging in herpes simplex virus. Rev Med Virol **7:**107-122.

117. **Hutchinson, L., H. Browne, V. Wargent, N. Davis-Poynter, S. Primorac, K. Goldsmith, A. C. Minson, and D. C. Johnson.** 1992. A novel herpes

simplex virus glycoprotein, gL, forms a complex with glycoprotein H (gH) and affects normal folding and surface expression of gH. J Virol **66:**2240-50.

118. **Igarashi, K., R. Fawl, R. J. Roller, and B. Roizman.** 1993. Construction and properties of a recombinant herpes simplex virus 1 lacking both S-component origins of DNA synthesis. J Virol **67:**2123-32.

119. **Jardine, P. J., and D. L. Anderson.** 2006. DNA packaging in Double-Stranded DNA Phages. *In* R. Calendar and S. T. Abedon (ed.), The Bacteriophages. Oxford University Press.

120. **Johnson, D. C., M. C. Frame, M. W. Ligas, A. M. Cross, and N. D. Stow.** 1988. Herpes simplex virus immunoglobulin G Fc receptor activity depends on a complex of two viral glycoproteins, gE and gI. J Virol **62:**1347-54.

121. **Jovasevic, V., L. Liang, and B. Roizman.** 2008. Proteolytic cleavage of VP1-2 is required for release of herpes simplex virus 1 DNA into the nucleus. J Virol **82:**3311-9.

122. **Kato, A., M. Yamamoto, T. Ohno, H. Kodaira, Y. Nishiyama, and Y. Kawaguchi.** 2005. Identification of proteins phosphorylated directly by the Us3 protein kinase encoded by herpes simplex virus 1. J Virol **79:**9325-31.

123. **Klupp, B. G., W. Fuchs, H. Granzow, R. Nixdorf, and T. C. Mettenleiter.** 2002. Pseudorabies virus UL36 tegument protein physically interacts with the UL37 protein. J Virol **76:**3065-71.

124. **Klupp, B. G., H. Granzow, G. M. Keil, and T. C. Mettenleiter.** 2006. The capsid-associated UL25 protein of the alphaherpesvirus pseudorabies virus is nonessential for cleavage and encapsidation of genomic DNA but is required for nuclear egress of capsids. J Virol **80:**6235-46.

125. **Klyachkin, Y. M., K. D. Stoops, and R. J. Geraghty.** 2006. Herpes simplex virus type 1 glycoprotein L mutants that fail to promote trafficking of

glycoprotein H and fail to function in fusion can induce binding of glycoprotein L-dependent anti-glycoprotein H antibodies. J Gen Virol **87:**759-67.

126. **Kopp, M., B. G. Klupp, H. Granzow, W. Fuchs, and T. C. Mettenleiter.** 2002. Identification and characterization of the pseudorabies virus tegument proteins UL46 and UL47: role for UL47 in virion morphogenesis in the cytoplasm. J Virol **76:**8820-33.

127. **Koslowski, K. M., P. R. Shaver, J. T. Casey, 2nd, T. Wilson, G. Yamanaka, A. K. Sheaffer, D. J. Tenney, and N. E. Pederson.** 1999. Physical and functional interactions between the herpes simplex virus UL15 and UL28 DNA cleavage and packaging proteins. J Virol **73:**1704-7.

128. **Kosturko, L. D., E. Daub, and H. Murialdo.** 1989. The interaction of E. coli integration host factor and lambda cos DNA: multiple complex formation and protein-induced bending. Nucleic Acids Res **17:**317-34.

129. **Krummenacher, C., A. V. Nicola, J. C. Whitbeck, H. Lou, W. Hou, J. D. Lambris, R. J. Geraghty, P. G. Spear, G. H. Cohen, and R. J. Eisenberg.** 1998. Herpes simplex virus glycoprotein D can bind to poliovirus receptor-related protein 1 or herpesvirus entry mediator, two structurally unrelated mediators of virus entry. J Virol **72:**7064-74.

130. **Kut, E., and D. Rasschaert.** 2004. Assembly of Marek's disease virus (MDV) capsids using recombinant baculoviruses expressing MDV capsid proteins. J Gen Virol **85:**769-74.

131. **Lam, Q., C. A. Smibert, K. E. Koop, C. Lavery, J. P. Capone, S. P. Weinheimer, and J. R. Smiley.** 1996. Herpes simplex virus VP16 rescues viral mRNA from destruction by the virion host shutoff function. EMBO J **15:**2575-81.

132. **Lamberti, C., and S. K. Weller.** 1998. The herpes simplex virus type 1 cleavage/packaging protein, UL32, is involved in efficient localization of capsids to replication compartments. J Virol **72:**2463-73.

133. **Lander, G. C., L. Tang, S. R. Casjens, E. B. Gilcrease, P. Prevelige, A. Poliakov, C. S. Potter, B. Carragher, and J. E. Johnson.** 2006. The structure of an infectious P22 virion shows the signal for headful DNA packaging. Science **312:**1791-5.

134. **Laquerre, S., R. Argnani, D. B. Anderson, S. Zucchini, R. Manservigi, and J. C. Glorioso.** 1998. Heparan sulfate proteoglycan binding by herpes simplex virus type 1 glycoproteins B and C, which differ in their contributions to virus attachment, penetration, and cell-to-cell spread. J Virol **72:**6119-30.

135. **Latchman, D. S., J. F. Partidge, J. K. Estridge, and L. M. Kemp.** 1989. The different competitive abilities of viral TAATGARAT elements and cellular octamer motifs, mediate the induction of viral immediate-early genes and the repression of the histone H2B gene in herpes simplex virus infected cells. Nucleic Acids Res **17:**8533-42.

136. **Leach, N., S. L. Bjerke, D. K. Christensen, J. M. Bouchard, F. Mou, R. Park, J. Baines, T. Haraguchi, and R. J. Roller.** 2007. Emerin is hyperphosphorylated and redistributed in herpes simplex virus type 1-infected cells in a manner dependent on both UL34 and US3. J Virol **81:**10792-803.

137. **Lee, G. E., J. W. Murray, A. W. Wolkoff, and D. W. Wilson.** 2006. Reconstitution of herpes simplex virus microtubule-dependent trafficking in vitro. J Virol **80:**4264-75.

138. **Lee, J. H., V. Vittone, E. Diefenbach, A. L. Cunningham, and R. J. Diefenbach.** 2008. Identification of structural protein-protein interactions of herpes simplex virus type 1. Virology **378:**347-54.

139. **Leffers, G., and V. B. Rao.** 2000. Biochemical characterization of an ATPase activity associated with the large packaging subunit gp17 from bacteriophage T4. J Biol Chem **275:**37127-36.

140. **Leuzinger, H., U. Ziegler, E. M. Schraner, C. Fraefel, D. L. Glauser, I. Heid, M. Ackermann, M. Mueller, and P. Wild.** 2005. Herpes simplex virus 1 envelopment follows two diverse pathways. J Virol **79:**13047-59.

141. **Liang, L., and J. D. Baines.** 2005. Identification of an essential domain in the herpes simplex virus 1 UL34 protein that is necessary and sufficient to interact with UL31 protein. J Virol **79:**3797-806.

142. **Lidholt, K., J. L. Weinke, C. S. Kiser, F. N. Lugemwa, K. J. Bame, S. Cheifetz, J. Massague, U. Lindahl, and J. D. Esko.** 1992. A single mutation affects both N-acetylglucosaminyltransferase and glucuronosyltransferase activities in a Chinese hamster ovary cell mutant defective in heparan sulfate biosynthesis. Proc Natl Acad Sci U S A **89:**2267-71.

143. **Ligas, M. W., and D. C. Johnson.** 1988. A herpes simplex virus mutant in which glycoprotein D sequences are replaced by beta-galactosidase sequences binds to but is unable to penetrate into cells. J Virol **62:**1486-94.

144. **Lin, H., V. B. Rao, and L. W. Black.** 1999. Analysis of capsid portal protein and terminase functional domains: interaction sites required for DNA packaging in bacteriophage T4. J Mol Biol **289:**249-60.

145. **Lin, H., M. N. Simon, and L. W. Black.** 1997. Purification and characterization of the small subunit of phage T4 terminase, gp16, required for DNA packaging. J Biol Chem **272:**3495-501.

146. **Liu, J., Z. Shriver, R. M. Pope, S. C. Thorp, M. B. Duncan, R. J. Copeland, C. S. Raska, K. Yoshida, R. J. Eisenberg, G. Cohen, R. J. Linhardt, and R. Sasisekharan.** 2002. Characterization of a heparan sulfate

octasaccharide that binds to herpes simplex virus type 1 glycoprotein D. J Biol Chem **277:**33456-67.

147. **Liu, X., K. Fitzgerald, E. Kurt-Jones, R. Finberg, and D. M. Knipe.** 2008. Herpesvirus tegument protein activates NF-kappaB signaling through the TRAF6 adaptor protein. Proc Natl Acad Sci U S A **105:**11335-9.

148. **Loret, S., G. Guay, and R. Lippe.** 2008. Comprehensive characterization of extracellular herpes simplex virus type 1 virions. J Virol **82:**8605-18.

149. **Lundberg, M., and M. Johansson.** 2001. Is VP22 nuclear homing an artifact? Nat Biotechnol **19:**713-4.

150. **Luxton, G. W., S. Haverlock, K. E. Coller, S. E. Antinone, A. Pincetic, and G. A. Smith.** 2005. Targeting of herpesvirus capsid transport in axons is coupled to association with specific sets of tegument proteins. Proc Natl Acad Sci U S A **102:**5832-7.

151. **Lycke, E., B. Hamark, M. Johansson, A. Krotochwil, J. Lycke, and B. Svennerholm.** 1988. Herpes simplex virus infection of the human sensory neuron. An electron microscopy study. Arch Virol **101:**87-104.

152. **Mardberg, K., E. Trybala, J. C. Glorioso, and T. Bergstrom.** 2001. Mutational analysis of the major heparan sulfate-binding domain of herpes simplex virus type 1 glycoprotein C. J Gen Virol **82:**1941-50.

153. **Mardberg, K., E. Trybala, F. Tufaro, and T. Bergstrom.** 2002. Herpes simplex virus type 1 glycoprotein C is necessary for efficient infection of chondroitin sulfate-expressing gro2C cells. J Gen Virol **83:**291-300.

154. **Maurer, U. E., B. Sodeik, and K. Grunewald.** 2008. Native 3D intermediates of membrane fusion in herpes simplex virus 1 entry. Proc Natl Acad Sci U S A **105:**10559-64.

155. **McClain, D. S., and A. O. Fuller.** 1994. Cell-specific kinetics and efficiency of herpes simplex virus type 1 entry are determined by two distinct phases of attachment. Virology **198:**690-702.

156. **McGeoch, D. J., M. A. Dalrymple, A. J. Davison, A. Dolan, M. C. Frame, D. McNab, L. J. Perry, J. E. Scott, and P. Taylor.** 1988. The complete DNA sequence of the long unique region in the genome of herpes simplex virus type 1. J Gen Virol **69 (Pt 7):**1531-74.

157. **McKnight, J. L., T. M. Kristie, and B. Roizman.** 1987. Binding of the virion protein mediating alpha gene induction in herpes simplex virus 1-infected cells to its cis site requires cellular proteins. Proc Natl Acad Sci U S A **84:**7061-5.

158. **McNab, A. R., P. Desai, S. Person, L. L. Roof, D. R. Thomsen, W. W. Newcomb, J. C. Brown, and F. L. Homa.** 1998. The product of the herpes simplex virus type 1 UL25 gene is required for encapsidation but not for cleavage of replicated viral DNA. J Virol **72:**1060-70.

159. **McNabb, D. S., and R. J. Courtney.** 1992. Analysis of the UL36 open reading frame encoding the large tegument protein (ICP1/2) of herpes simplex virus type 1. J Virol **66:**7581-4.

160. **McNabb, D. S., and R. J. Courtney.** 1992. Identification and characterization of the herpes simplex virus type 1 virion protein encoded by the UL35 open reading frame. J Virol **66:**2653-63.

161. **Menotti, L., M. Lopez, E. Avitabile, A. Stefan, F. Cocchi, J. Adelaide, E. Lecocq, P. Dubreuil, and G. Campadelli-Fiume.** 2000. The murine homolog of human Nectin1delta serves as a species nonspecific mediator for entry of human and animal alpha herpesviruses in a pathway independent of a detectable binding to gD. Proc Natl Acad Sci U S A **97:**4867-72.

162. **Mettenleiter, T. C.** 2004. Budding events in herpesvirus morphogenesis. Virus Res **106:**167-80.

163. **Mettenleiter, T. C.** 2002. Herpesvirus assembly and egress. J Virol **76:**1537-47.

164. **Mettenleiter, T. C.** 2006. Intriguing interplay between viral proteins during herpesvirus assembly or: the herpesvirus assembly puzzle. Vet Microbiol **113:**163-9.

165. **Mettenleiter, T. C., B. G. Klupp, and H. Granzow.** 2006. Herpesvirus assembly: a tale of two membranes. Curr Opin Microbiol **9:**423-9.

166. **Mettenleiter, T. C., and T. Minson.** 2006. Egress of alphaherpesviruses. J Virol **80:**1610-1; author reply 1611-2.

167. **Milne, R. S., A. V. Nicola, J. C. Whitbeck, R. J. Eisenberg, and G. H. Cohen.** 2005. Glycoprotein D receptor-dependent, low-pH-independent endocytic entry of herpes simplex virus type 1. J Virol **79:**6655-63.

168. **Mocarski, E. S., and B. Roizman.** 1982. Structure and role of the herpes simplex virus DNA termini in inversion, circularization and generation of virion DNA. Cell **31:**89-97.

169. **Monier, K., J. C. Armas, S. Etteldorf, P. Ghazal, and K. F. Sullivan.** 2000. Annexation of the interchromosomal space during viral infection. Nat Cell Biol **2:**661-5.

170. **Montgomery, R. I., M. S. Warner, B. J. Lum, and P. G. Spear.** 1996. Herpes simplex virus-1 entry into cells mediated by a novel member of the TNF/NGF receptor family. Cell **87:**427-36.

171. **Morrison, E. E., Y. F. Wang, and D. M. Meredith.** 1998. Phosphorylation of structural components promotes dissociation of the herpes simplex virus type 1 tegument. J Virol **72:**7108-14.

172. **Mou, F., T. Forest, and J. D. Baines.** 2007. US3 of herpes simplex virus type 1 encodes a promiscuous protein kinase that phosphorylates and alters localization of lamin A/C in infected cells. J Virol **81:**6459-70.

173. **Mouzakitis, G., J. McLauchlan, C. Barreca, L. Kueltzo, and P. O'Hare.** 2005. Characterization of VP22 in herpes simplex virus-infected cells. J Virol **79:**12185-98.

174. **Murphy, M. A., M. A. Bucks, K. J. O'Regan, and R. J. Courtney.** 2008. The HSV-1 tegument protein pUL46 associates with cellular membranes and viral capsids. Virology **376:**279-89.

175. **Nagel, C. H., K. Dohner, M. Fathollahy, T. Strive, E. M. Borst, M. Messerle, and B. Sodeik.** 2008. Nuclear egress and envelopment of herpes simplex virus capsids analyzed with dual-color fluorescence HSV1(17+). J Virol **82:**3109-24.

176. **Naldinho-Souto, R., H. Browne, and T. Minson.** 2006. Herpes simplex virus tegument protein VP16 is a component of primary enveloped virions. J Virol **80:**2582-4.

177. **Nemecek, D., G. C. Lander, J. E. Johnson, S. R. Casjens, and G. J. Thomas, Jr.** 2008. Assembly architecture and DNA binding of the bacteriophage P22 terminase small subunit. J Mol Biol **383:**494-501.

178. **Newcomb, W. W., and J. C. Brown.** 1991. Structure of the herpes simplex virus capsid: effects of extraction with guanidine hydrochloride and partial reconstitution of extracted capsids. J Virol **65:**613-20.

179. **Newcomb, W. W., F. L. Homa, and J. C. Brown.** 2006. Herpes simplex virus capsid structure: DNA packaging protein UL25 is located on the external surface of the capsid near the vertices. J Virol **80:**6286-94.

180. **Newcomb, W. W., F. L. Homa, D. R. Thomsen, F. P. Booy, B. L. Trus, A. C. Steven, J. V. Spencer, and J. C. Brown.** 1996. Assembly of the herpes simplex virus capsid: characterization of intermediates observed during cell-free capsid formation. J Mol Biol **263:**432-46.

181. **Newcomb, W. W., F. L. Homa, D. R. Thomsen, and J. C. Brown.** 2001. In vitro assembly of the herpes simplex virus procapsid: formation of small procapsids at reduced scaffolding protein concentration. J Struct Biol **133:**23-31.

182. **Newcomb, W. W., R. M. Juhas, D. R. Thomsen, F. L. Homa, A. D. Burch, S. K. Weller, and J. C. Brown.** 2001. The UL6 gene product forms the portal for entry of DNA into the herpes simplex virus capsid. J Virol **75:**10923-32.

183. **Newcomb, W. W., B. L. Trus, F. P. Booy, A. C. Steven, J. S. Wall, and J. C. Brown.** 1993. Structure of the herpes simplex virus capsid. Molecular composition of the pentons and the triplexes. J Mol Biol **232:**499-511.

184. **Newcomb, W. W., B. L. Trus, N. Cheng, A. C. Steven, A. K. Sheaffer, D. J. Tenney, S. K. Weller, and J. C. Brown.** 2000. Isolation of herpes simplex virus procapsids from cells infected with a protease-deficient mutant virus. J Virol **74:**1663-73.

185. **Nicholson, P., C. Addison, A. M. Cross, J. Kennard, V. G. Preston, and F. J. Rixon.** 1994. Localization of the herpes simplex virus type 1 major capsid protein VP5 to the cell nucleus requires the abundant scaffolding protein VP22a. J Gen Virol **75 (Pt 5):**1091-9.

186. **Nicola, A. V., J. Hou, E. O. Major, and S. E. Straus.** 2005. Herpes simplex virus type 1 enters human epidermal keratinocytes, but not neurons, via a pH-dependent endocytic pathway. J Virol **79:**7609-16.

187. **Nicola, A. V., A. M. McEvoy, and S. E. Straus.** 2003. Roles for endocytosis and low pH in herpes simplex virus entry into HeLa and Chinese hamster ovary cells. J Virol **77:**5324-32.

188. **Nicola, A. V., and S. E. Straus.** 2004. Cellular and viral requirements for rapid endocytic entry of herpes simplex virus. J Virol **78:**7508-17.

189. **O'Hare, P., and C. R. Goding.** 1988. Herpes simplex virus regulatory elements and the immunoglobulin octamer domain bind a common factor and are both targets for virion transactivation. Cell **52:**435-45.

190. **O'Regan, K. J., M. A. Murphy, M. A. Bucks, J. W. Wills, and R. J. Courtney.** 2007. Incorporation of the herpes simplex virus type 1 tegument protein VP22 into the virus particle is independent of interaction with VP16. Virology **369:**263-80.

191. **Ogasawara, M., T. Suzutani, I. Yoshida, and M. Azuma.** 2001. Role of the UL25 gene product in packaging DNA into the herpes simplex virus capsid: location of UL25 product in the capsid and demonstration that it binds DNA. J Virol **75:**1427-36.

192. **Park, R., and J. D. Baines.** 2006. Herpes simplex virus type 1 infection induces activation and recruitment of protein kinase C to the nuclear membrane and increased phosphorylation of lamin B. J Virol **80:**494-504.

193. **Pasdeloup, D., D. Blondel, A. L. Isidro, and F. J. Rixon.** 2009. Herpesvirus Capsid Association To The Nuclear Pore Complex And Viral DNA Release Involve The Nucleoporin CAN/Nup214 And The Capsid Protein pUL25. J Virol.

194. **Patel, A. H., and J. B. MacLean.** 1995. The product of the UL6 gene of herpes simplex virus type 1 is associated with virus capsids. Virology **206:**465-78.

195. **Patel, A. H., F. J. Rixon, C. Cunningham, and A. J. Davison.** 1996. Isolation and characterization of herpes simplex virus type 1 mutants defective in the UL6 gene. Virology **217:**111-23.

196. **Perdue, M. L., J. C. Cohen, C. C. Randall, and D. J. O'Callaghan.** 1976. Biochemical studies of the maturation of herpesvirus nucleocapsid species. Virology **74:**194-208.

197. **Poon, A. P., and B. Roizman.** 1993. Characterization of a temperature-sensitive mutant of the UL15 open reading frame of herpes simplex virus 1. J Virol **67:**4497-503.

198. **Preston, C. M., M. C. Frame, and M. E. Campbell.** 1988. A complex formed between cell components and an HSV structural polypeptide binds to a viral immediate early gene regulatory DNA sequence. Cell **52:**425-34.

199. **Preston, V. G., J. Murray, C. M. Preston, I. M. McDougall, and N. D. Stow.** 2008. The UL25 gene product of herpes simplex virus type 1 is involved in uncoating of the viral genome. J Virol **82:**6654-66.

200. **Randall, R. E., and N. Dinwoodie.** 1986. Intranuclear localization of herpes simplex virus immediate-early and delayed-early proteins: evidence that ICP 4 is associated with progeny virus DNA. J Gen Virol **67 (Pt 10):**2163-77.

201. **Read, G. S., B. M. Karr, and K. Knight.** 1993. Isolation of a herpes simplex virus type 1 mutant with a deletion in the virion host shutoff gene and identification of multiple forms of the vhs (UL41) polypeptide. J Virol **67:**7149-60.

202. **Read, G. S., and M. Patterson.** 2007. Packaging of the virion host shutoff (Vhs) protein of herpes simplex virus: two forms of the Vhs polypeptide are associated with intranuclear B and C capsids, but only one is associated with enveloped virions. J Virol **81:**1148-61.

203. **Rentas, F. J., and V. B. Rao.** 2003. Defining the bacteriophage T4 DNA packaging machine: evidence for a C-terminal DNA cleavage domain in the large terminase/packaging protein gp17. J Mol Biol **334:**37-52.

204. **Reske, A., G. Pollara, C. Krummenacher, B. M. Chain, and D. R. Katz.** 2007. Understanding HSV-1 entry glycoproteins. Rev Med Virol **17:**205-15.

205. **Reuven, N. B., A. E. Staire, R. S. Myers, and S. K. Weller.** 2003. The herpes simplex virus type 1 alkaline nuclease and single-stranded DNA binding protein mediate strand exchange in vitro. J Virol **77:**7425-33.

206. **Reynolds, A. E., Y. Fan, and J. D. Baines.** 2000. Characterization of the U(L)33 gene product of herpes simplex virus 1. Virology **266:**310-8.

207. **Reynolds, A. E., L. Liang, and J. D. Baines.** 2004. Conformational changes in the nuclear lamina induced by herpes simplex virus type 1 require genes U(L)31 and U(L)34. J Virol **78:**5564-75.

208. **Reynolds, A. E., B. J. Ryckman, J. D. Baines, Y. Zhou, L. Liang, and R. J. Roller.** 2001. U(L)31 and U(L)34 proteins of herpes simplex virus type 1 form a complex that accumulates at the nuclear rim and is required for envelopment of nucleocapsids. J Virol **75:**8803-17.

209. **Reynolds, A. E., E. G. Wills, R. J. Roller, B. J. Ryckman, and J. D. Baines.** 2002. Ultrastructural localization of the herpes simplex virus type 1 UL31, UL34, and US3 proteins suggests specific roles in primary envelopment and egress of nucleocapsids. J Virol **76:**8939-52.

210. **Roizman, B., and D. Furlong.** 1972. The replication of herpesviruses, p. 229-403. *In* H. Fraenkel-Conrat and R. R. Wagner (ed.), Comprehensive Virology. Plenum Press, New York.

211. **Roller, R. J., Y. Zhou, R. Schnetzer, J. Ferguson, and D. DeSalvo.** 2000. Herpes simplex virus type 1 U(L)34 gene product is required for viral envelopment. J Virol **74:**117-29.

212. **Rubinchik, S., W. Parris, and M. Gold.** 1994. The in vitro endonuclease activity of gene product A, the large subunit of the bacteriophage lambda terminase, and its relationship to the endonuclease activity of the holoenzyme. J Biol Chem **269:**13575-85.

213. **Salmon, B., and J. D. Baines.** 1998. Herpes simplex virus DNA cleavage and packaging: association of multiple forms of U(L)15-encoded proteins with B capsids requires at least the U(L)6, U(L)17, and U(L)28 genes. J Virol **72:**3045-50.

214. **Salmon, B., C. Cunningham, A. J. Davison, W. J. Harris, and J. D. Baines.** 1998. The herpes simplex virus type 1 U(L)17 gene encodes virion tegument proteins that are required for cleavage and packaging of viral DNA. J Virol **72:**3779-88.

215. **Schmelter, J., J. Knez, J. R. Smiley, and J. P. Capone.** 1996. Identification and characterization of a small modular domain in the herpes simplex virus host shutoff protein sufficient for interaction with VP16. J Virol **70:**2124-31.

216. **Schrag, J. D., B. V. Prasad, F. J. Rixon, and W. Chiu.** 1989. Three-dimensional structure of the HSV1 nucleocapsid. Cell **56:**651-60.

217. **Sheaffer, A. K., W. W. Newcomb, M. Gao, D. Yu, S. K. Weller, J. C. Brown, and D. J. Tenney.** 2001. Herpes simplex virus DNA cleavage and packaging proteins associate with the procapsid prior to its maturation. J Virol **75:**687-98.

218. **Sherman, G., and S. L. Bachenheimer.** 1988. Characterization of intranuclear capsids made by ts morphogenic mutants of HSV-1. Virology **163:**471-80.

219. **Shieh, M. T., D. WuDunn, R. I. Montgomery, J. D. Esko, and P. G. Spear.** 1992. Cell surface receptors for herpes simplex virus are heparan sulfate proteoglycans. J Cell Biol **116:**1273-81.

220. **Shinder, G., and M. Gold.** 1989. Integration host factor (IHF) stimulates binding of the gpNu1 subunit of lambda terminase to cos DNA. Nucleic Acids Res **17:**2005-22.

221. **Shukla, D., J. Liu, P. Blaiklock, N. W. Shworak, X. Bai, J. D. Esko, G. H. Cohen, R. J. Eisenberg, R. D. Rosenberg, and P. G. Spear.** 1999. A novel role for 3-O-sulfated heparan sulfate in herpes simplex virus 1 entry. Cell **99:**13-22.

222. **Simpson-Holley, M., J. Baines, R. Roller, and D. M. Knipe.** 2004. Herpes simplex virus 1 U(L)31 and U(L)34 gene products promote the late maturation of viral replication compartments to the nuclear periphery. J Virol **78:**5591-600.

223. **Simpson-Holley, M., R. C. Colgrove, G. Nalepa, J. W. Harper, and D. M. Knipe.** 2005. Identification and functional evaluation of cellular and viral factors involved in the alteration of nuclear architecture during herpes simplex virus 1 infection. J Virol **79:**12840-51.

224. **Sodeik, B., M. W. Ebersold, and A. Helenius.** 1997. Microtubule-mediated transport of incoming herpes simplex virus 1 capsids to the nucleus. J Cell Biol **136:**1007-21.

225. **Spear, P. G.** 1993. Membrane fusion induced by herpes simplex virus, p. 201-232. *In* J. Bentz (ed.), Viral Fusion Mechanisms. CRC Press, Boca Raton.

226. **Spear, P. G., R. J. Eisenberg, and G. H. Cohen.** 2000. Three classes of cell surface receptors for alphaherpesvirus entry. Virology **275:**1-8.

227. **Spear, P. G., M. T. Shieh, B. C. Herold, D. WuDunn, and T. I. Koshy.** 1992. Heparan sulfate glycosaminoglycans as primary cell surface receptors for herpes simplex virus. Adv Exp Med Biol **313:**341-53.

228. **Spencer, J. V., W. W. Newcomb, D. R. Thomsen, F. L. Homa, and J. C. Brown.** 1998. Assembly of the herpes simplex virus capsid: preformed triplexes bind to the nascent capsid. J Virol **72:**3944-51.

229. **Stackpole, C. W.** 1969. Herpes-type virus of the frog renal adenocarcinoma. I. Virus development in tumor transplants maintained at low temperature. J Virol **4:**75-93.

230. **Steven, A. C., P.G. Spear.** 1997. Herpesvirus capsid assembly and envelopment, p. 312-351. *In* W. Chiu, M. Burnett, R. Garcea. (ed.), Structural Biology of Viruses. Oxford University Press, New York, N.Y.

231. **Stow, N. D.** 2001. Packaging of genomic and amplicon DNA by the herpes simplex virus type 1 UL25-null mutant KUL25NS. J Virol **75:**10755-65.

232. **Stow, N. D., E. C. McMonagle, and A. J. Davison.** 1983. Fragments from both termini of the herpes simplex virus type 1 genome contain signals required for the encapsidation of viral DNA. Nucleic Acids Res **11:**8205-20.

233. **Strand, S. S., and D. A. Leib.** 2004. Role of the VP16-binding domain of vhs in viral growth, host shutoff activity, and pathogenesis. J Virol **78:**13562-72.

234. **Stylianou, J., K. Maringer, R. Cook, E. Bernard, and G. Elliott.** 2009. Virion incorporation of the herpes simplex virus type 1 tegument protein VP22 occurs via glycoprotein E-specific recruitment to the late secretory pathway. J Virol **83:**5204-18.

235. **Subak-Sharpe, J. H., and D. J. Dargan.** 1998. HSV molecular biology: general aspects of herpes simplex virus molecular biology. Virus Genes **16:**239-51.

236. **Sun, S., K. Kondabagil, P. M. Gentz, M. G. Rossmann, and V. B. Rao.** 2007. The structure of the ATPase that powers DNA packaging into bacteriophage T4 procapsids. Mol Cell **25:**943-9.

237. **Taddeo, B., M. T. Sciortino, W. Zhang, and B. Roizman.** 2007. Interaction of herpes simplex virus RNase with VP16 and VP22 is required for the accumulation of the protein but not for accumulation of mRNA. Proc Natl Acad Sci U S A **104:**12163-8.

238. **Tanaka, M., H. Kagawa, Y. Yamanashi, T. Sata, and Y. Kawaguchi.** 2003. Construction of an excisable bacterial artificial chromosome containing a full-length infectious clone of herpes simplex virus type 1: viruses reconstituted from the clone exhibit wild-type properties in vitro and in vivo. J Virol **77:**1382-91.

239. **Tatman, J. D., V. G. Preston, P. Nicholson, R. M. Elliott, and F. J. Rixon.** 1994. Assembly of herpes simplex virus type 1 capsids using a panel of recombinant baculoviruses. J Gen Virol **75 (Pt 5):**1101-13.

240. **Taus, N. S., and J. D. Baines.** 1998. Herpes simplex virus 1 DNA cleavage/packaging: the UL28 gene encodes a minor component of B capsids. Virology **252:**443-9.

241. **Taus, N. S., B. Salmon, and J. D. Baines.** 1998. The herpes simplex virus 1 UL 17 gene is required for localization of capsids and major and minor capsid proteins to intranuclear sites where viral DNA is cleaved and packaged. Virology **252:**115-25.

242. **Taylor, T. J., E. E. McNamee, C. Day, and D. M. Knipe.** 2003. Herpes simplex virus replication compartments can form by coalescence of smaller compartments. Virology **309:**232-47.

243. **Tengelsen, L. A., N. E. Pederson, P. R. Shaver, M. W. Wathen, and F. L. Homa.** 1993. Herpes simplex virus type 1 DNA cleavage and encapsidation require the product of the UL28 gene: isolation and characterization of two UL28 deletion mutants. J Virol **67:**3470-80.

244. **Thomsen, D. R., L. L. Roof, and F. L. Homa.** 1994. Assembly of herpes simplex virus (HSV) intermediate capsids in insect cells infected with recombinant baculoviruses expressing HSV capsid proteins. J Virol **68:**2442-57.

245. **Thurlow, J. K., M. Murphy, N. D. Stow, and V. G. Preston.** 2006. Herpes simplex virus type 1 DNA-packaging protein UL17 is required for efficient binding of UL25 to capsids. J Virol **80:**2118-26.

246. **Thurlow, J. K., F. J. Rixon, M. Murphy, P. Targett-Adams, M. Hughes, and V. G. Preston.** 2005. The herpes simplex virus type 1 DNA packaging protein UL17 is a virion protein that is present in both the capsid and the tegument compartments. J Virol **79:**150-8.

247. **Tischer, B. K., J. von Einem, B. Kaufer, and N. Osterrieder.** 2006. Two-step red-mediated recombination for versatile high-efficiency markerless DNA manipulation in Escherichia coli. Biotechniques **40:**191-7.

248. **Tiwari, V., C. Clement, M. B. Duncan, J. Chen, J. Liu, and D. Shukla.** 2004. A role for 3-O-sulfated heparan sulfate in cell fusion induced by herpes simplex virus type 1. J Gen Virol **85:**805-9.

249. **Tiwari, V., C. O'Donnell, R. J. Copeland, T. Scarlett, J. Liu, and D. Shukla.** 2007. Soluble 3-O-sulfated heparan sulfate can trigger herpes simplex

virus type 1 entry into resistant Chinese hamster ovary (CHO-K1) cells. J Gen Virol **88:**1075-9.

250. **Tomka, M. A., and C. E. Catalano.** 1993. Physical and kinetic characterization of the DNA packaging enzyme from bacteriophage lambda. J Biol Chem **268:**3056-65.

251. **Trus, B. L., F. P. Booy, W. W. Newcomb, J. C. Brown, F. L. Homa, D. R. Thomsen, and A. C. Steven.** 1996. The herpes simplex virus procapsid: structure, conformational changes upon maturation, and roles of the triplex proteins VP19c and VP23 in assembly. J Mol Biol **263:**447-62.

252. **Trus, B. L., N. Cheng, W. W. Newcomb, F. L. Homa, J. C. Brown, and A. C. Steven.** 2004. Structure and polymorphism of the UL6 portal protein of herpes simplex virus type 1. J Virol **78:**12668-71.

253. **Trus, B. L., W. W. Newcomb, F. P. Booy, J. C. Brown, and A. C. Steven.** 1992. Distinct monoclonal antibodies separately label the hexons or the pentons of herpes simplex virus capsid. Proc Natl Acad Sci U S A **89:**11508-12.

254. **Trus, B. L., W. W. Newcomb, N. Cheng, G. Cardone, L. Marekov, F. L. Homa, J. C. Brown, and A. C. Steven.** 2007. Allosteric signaling and a nuclear exit strategy: binding of UL25/UL17 heterodimers to DNA-Filled HSV-1 capsids. Mol Cell **26:**479-89.

255. **Trybala, E., T. Bergstrom, B. Svennerholm, S. Jeansson, J. C. Glorioso, and S. Olofsson.** 1994. Localization of a functional site on herpes simplex virus type 1 glycoprotein C involved in binding to cell surface heparan sulphate. J Gen Virol **75 (Pt 4):**743-52.

256. **Trybala, E., B. Svennerholm, T. Bergstrom, S. Olofsson, S. Jeansson, and J. L. Goodman.** 1993. Herpes simplex virus type 1-induced hemagglutination:

glycoprotein C mediates virus binding to erythrocyte surface heparan sulfate. J Virol **67:**1278-85.

257. **Turcotte, S., J. Letellier, and R. Lippe.** 2005. Herpes simplex virus type 1 capsids transit by the trans-Golgi network, where viral glycoproteins accumulate independently of capsid egress. J Virol **79:**8847-60.

258. **van Genderen, I. L., R. Brandimarti, M. R. Torrisi, G. Campadelli, and G. van Meer.** 1994. The phospholipid composition of extracellular herpes simplex virions differs from that of host cell nuclei. Virology **200:**831-6.

259. **Varmuza, S. L., and J. R. Smiley.** 1985. Signals for site-specific cleavage of HSV DNA: maturation involves two separate cleavage events at sites distal to the recognition sequences. Cell **41:**793-802.

260. **Verhagen, J., M. Donnelly, and G. Elliott.** 2006. Characterization of a novel transferable CRM-1-independent nuclear export signal in a herpesvirus tegument protein that shuttles between the nucleus and cytoplasm. J Virol **80:**10021-35.

261. **Verhagen, J., I. Hutchinson, and G. Elliott.** 2006. Nucleocytoplasmic shuttling of bovine herpesvirus 1 UL47 protein in infected cells. J Virol **80:**1059-63.

262. **Vernon, S. K., M. Ponce de Leon, G. H. Cohen, R. J. Eisenberg, and B. A. Rubin.** 1981. Morphological components of herpesvirus. III. Localization of herpes simplex virus type 1 nucleocapsid polypeptides by immune electron microscopy. J Gen Virol **54:**39-46.

263. **Vittone, V., E. Diefenbach, D. Triffett, M. W. Douglas, A. L. Cunningham, and R. J. Diefenbach.** 2005. Determination of interactions between tegument proteins of herpes simplex virus type 1. J Virol **79:**9566-71.

264. **Wagenaar, F., J. M. Pol, B. Peeters, A. L. Gielkens, N. de Wind, and T. G. Kimman.** 1995. The US3-encoded protein kinase from pseudorabies virus affects egress of virions from the nucleus. J Gen Virol **76 (Pt 7):**1851-9.

265. **Walker, J. E., M. Saraste, M. J. Runswick, and N. J. Gay.** 1982. Distantly related sequences in the alpha- and beta-subunits of ATP synthase, myosin, kinases and other ATP-requiring enzymes and a common nucleotide binding fold. EMBO J **1:**945-51.

266. **Ward, P. L., W. O. Ogle, and B. Roizman.** 1996. Assemblons: nuclear structures defined by aggregation of immature capsids and some tegument proteins of herpes simplex virus 1. J Virol **70:**4623-31.

267. **Warner, M. S., R. J. Geraghty, W. M. Martinez, R. I. Montgomery, J. C. Whitbeck, R. Xu, R. J. Eisenberg, G. H. Cohen, and P. G. Spear.** 1998. A cell surface protein with herpesvirus entry activity (HveB) confers susceptibility to infection by mutants of herpes simplex virus type 1, herpes simplex virus type 2, and pseudorabies virus. Virology **246:**179-89.

268. **Whitbeck, J. C., Y. Zuo, R. S. Milne, G. H. Cohen, and R. J. Eisenberg.** 2006. Stable association of herpes simplex virus with target membranes is triggered by low pH in the presence of the gD receptor, HVEM. J Virol **80:**3773-80.

269. **White, C. A., N. D. Stow, A. H. Patel, M. Hughes, and V. G. Preston.** 2003. Herpes simplex virus type 1 portal protein UL6 interacts with the putative terminase subunits UL15 and UL28. J Virol **77:**6351-8.

270. **White, J. M., S. E. Delos, M. Brecher, and K. Schornberg.** 2008. Structures and mechanisms of viral membrane fusion proteins: multiple variations on a common theme. Crit Rev Biochem Mol Biol **43:**189-219.

271. **Wild, P., M. Engels, C. Senn, K. Tobler, U. Ziegler, E. M. Schraner, E. Loepfe, M. Ackermann, M. Mueller, and P. Walther.** 2005. Impairment of nuclear pores in bovine herpesvirus 1-infected MDBK cells. J Virol **79:**1071-83.

272. **Wild, P., C. Senn, C. L. Manera, E. Sutter, E. M. Schraner, K. Tobler, M. Ackermann, U. Ziegler, M. S. Lucas, and A. Kaech.** 2009. Exploring the nuclear envelope of herpes simplex virus 1-infected cells by high-resolution microscopy. J Virol **83:**408-19.

273. **Willard, M.** 2002. Rapid directional translocations in virus replication. J Virol **76:**5220-32.

274. **Wills, E., L. Scholtes, and J. D. Baines.** 2006. Herpes simplex virus 1 DNA packaging proteins encoded by UL6, UL15, UL17, UL28, and UL33 are located on the external surface of the viral capsid. J Virol **80:**10894-9.

275. **Wu, H., L. Sampson, R. Parr, and S. Casjens.** 2002. The DNA site utilized by bacteriophage P22 for initiation of DNA packaging. Mol Microbiol **45:**1631-46.

276. **WuDunn, D., and P. G. Spear.** 1989. Initial interaction of herpes simplex virus with cells is binding to heparan sulfate. J Virol **63:**52-8.

277. **Yang, K., and J. D. Baines.** 2006. The putative terminase subunit of herpes simplex virus 1 encoded by UL28 is necessary and sufficient to mediate interaction between pUL15 and pUL33. J Virol **80:**5733-9.

278. **Yang, K., F. Homa, and J. D. Baines.** 2007. Putative terminase subunits of herpes simplex virus 1 form a complex in the cytoplasm and interact with portal protein in the nucleus. J Virol **81:**6419-33.

279. **Yeo, A., and M. Feiss.** 1995. Specific interaction of terminase, the DNA packaging enzyme of bacteriophage lambda, with the portal protein of the prohead. J Mol Biol **245:**141-50.

280. **York, I. A., C. Roop, D. W. Andrews, S. R. Riddell, F. L. Graham, and D. C. Johnson.** 1994. A cytosolic herpes simplex virus protein inhibits antigen presentation to CD8+ T lymphocytes. Cell **77:**525-35.

281. **Yu, D., A. K. Sheaffer, D. J. Tenney, and S. K. Weller.** 1997. Characterization of ICP6::lacZ insertion mutants of the UL15 gene of herpes simplex virus type 1 reveals the translation of two proteins. J Virol **71:**2656-65.

282. **Yu, D., and S. K. Weller.** 1998. Genetic analysis of the UL 15 gene locus for the putative terminase of herpes simplex virus type 1. Virology **243:**32-44.

283. **Yu, D., and S. K. Weller.** 1998. Herpes simplex virus type 1 cleavage and packaging proteins UL15 and UL28 are associated with B but not C capsids during packaging. J Virol **72:**7428-39.

284. **Zhang, Y., and J. L. McKnight.** 1993. Herpes simplex virus type 1 UL46 and UL47 deletion mutants lack VP11 and VP12 or VP13 and VP14, respectively, and exhibit altered viral thymidine kinase expression. J Virol **67:**1482-92.

285. **Zhou, Z. H., D. H. Chen, J. Jakana, F. J. Rixon, and W. Chiu.** 1999. Visualization of tegument-capsid interactions and DNA in intact herpes simplex virus type 1 virions. J Virol **73:**3210-8.

286. **Zhou, Z. H., W. Chiu, K. Haskell, H. Spears, Jr., J. Jakana, F. J. Rixon, and L. R. Scott.** 1998. Refinement of herpesvirus B-capsid structure on parallel supercomputers. Biophys J **74:**576-88.

287. **Zhou, Z. H., J. He, J. Jakana, J. D. Tatman, F. J. Rixon, and W. Chiu.** 1995. Assembly of VP26 in herpes simplex virus-1 inferred from structures of wild-type and recombinant capsids. Nat Struct Biol **2:**1026-30.

288. **Zhou, Z. H., B. V. Prasad, J. Jakana, F. J. Rixon, and W. Chiu.** 1994. Protein subunit structures in the herpes simplex virus A-capsid determined from 400 kV spot-scan electron cryomicroscopy. J Mol Biol **242:**456-69.